



LUND UNIVERSITY

Reliability-based evaluation of concrete dams

Westberg, Marie

2007

[Link to publication](#)

Citation for published version (APA):

Westberg, M. (2007). *Reliability-based evaluation of concrete dams*. [Licentiate Thesis, Division of Structural Engineering].

Total number of authors:

1

General rights

Unless other specific re-use rights are stated the following general rights apply:

Copyright and moral rights for the publications made accessible in the public portal are retained by the authors and/or other copyright owners and it is a condition of accessing publications that users recognise and abide by the legal requirements associated with these rights.

- Users may download and print one copy of any publication from the public portal for the purpose of private study or research.
- You may not further distribute the material or use it for any profit-making activity or commercial gain
- You may freely distribute the URL identifying the publication in the public portal

Read more about Creative commons licenses: <https://creativecommons.org/licenses/>

Take down policy

If you believe that this document breaches copyright please contact us providing details, and we will remove access to the work immediately and investigate your claim.

LUND UNIVERSITY

PO Box 117
221 00 Lund
+46 46-222 00 00

Report TVBK-1033
ISSN 0349-4969
ISRN:LUTVDG/TVBK-1033/07-SE(228)

Reliability-based evaluation of concrete dams

Marie Westberg

Licentiate Thesis

Lund University
Division of Structural Engineering
P.O. Box 118
SE-221 00 Lund, Sweden

Telephone: +46 46 222 9503
Telefax: +46 46 222 4212
www: <http://www.kstr.lth.se>

Preface

The project in which the work of this thesis has been carried out is part of the research consortium VBT (Road/Bridge & Dam/Tunnel, Väg/ bro & damm/tunnel). Funding was provided by Elforsk AB, Vinnova and Lund University. The main part of the work has been carried out at Vattenfall AB Vattenkraft, but with regular visits and supervision at the Division of Structural Engineering, Lund University.

Many people have earned my gratitude during the past years;

My supervisor Professor Sven Thelandersson (Structural Engineering, Lund University), my co-supervisors Professor Jan Alemo (Structural Engineering, Lund University, former Vattenfall Utveckling AB) and Lic. Eng. Stefan Berntsson (Vattenfall AB Vattenkraft) for encouragement, discussions and help

Those involved in different parts, giving ideas and help; Dr Christian Bernstone (Vattenfall Research and Development), Professor Georg Lindgren (Mathematical Statistics, Lund University) and master thesis students Lucas Ahlsén Farell and Jill Holmberg are especially worth mentioning

Those helping with comments on written material, special thanks to Dr Martin Hansson (Carl Bro AB), M.Sc. Malte Cederström (Vattenfall AB Vattenkraft) and Dr. Des N. D. Hartford (BC Hydro, Canada)

My colleagues at Vattenfall AB Vattenkraft and at the Division of Structural Engineering, Lund University, for support, for amusement, for answering lots of questions and for help in everyday-life

My friends and family, for everything.

The Water Genie in *Haroun and the Sea of Stories* by Salman Rushdie states that there is a something called P2C2E. In the beginning of my work P2C2E's were a common thing. Now I know that there is no such thing as a Process Too Complicated To Explain, but a whole lot of PC2E still 2bE:ed, and that is what I will try to continue doing.

Stockholm, March 2007

Marie Westberg

Abstract

Swedish concrete dams are designed and assessed based on deterministic design using safety factors. The combination of increasing age, new methods for calculation of design floods and increasing demands by society to ensure a high level of safety, has resulted in upgrading and rebuilding needs for dams. When safety is re-evaluated it is important that evaluation is based on modern safety concepts. The objective of this thesis is to describe how reliability based methodology can be used for assessment of concrete dams, how it fits into the dam safety risk management process and the present state of knowledge of relevant statistic information of resistance and load parameters.

Risk management is becoming more frequently used in dam safety all over the world and structural reliability analysis can be used for safety assessment of existing dams. Since object specific information, monitoring results, known loads etcetera can be included in the analysis it gives more reliable results than a more general assessment procedure based on traditional dam safety design guidelines.

In this thesis the sliding and overturning failure modes are used for analysis, but there are reasons to further analyse the failure mode formulation. Overturning is not considered in several guidelines, instead resultant location is used as an indicator, and failure is associated with sliding or overstressing. The Swedish guideline on dam safety, RIDAS, does not, unlike guidelines used elsewhere in the world, take account to cohesion when the sliding stability is estimated. Even so, cohesion is included in the sliding criterion used for analysis in this thesis.

In structural reliability analysis the failure mode of interest is described by a limit state function, which is a function of a number of basic variables, described by their statistical distribution. For a concrete dam the basic variables for the sliding failure mode are self-weight (G), cohesion (c), base area (A), friction angle (ϕ), uplift pressure (U), hydrostatic water pressure (H) and ice load (I) and the limit state function becomes

$$g(G, U, H, I, \phi, c, A) = c \cdot A + (G - U) \cdot \tan \phi - (H + I)$$

Limit state functions for overturning or other failure modes can be defined in the same way.

When statistical distributions are known for the basic variables, the safety index, β , can be calculated. β is related to the probability of failure by $p_f = \Phi(-\beta)$, where Φ is the standardized normal distribution function.

For safety evaluation, β is compared to a target safety index, β_T . For dams no such target value exists. There are different approaches how to set a target and the most straightforward is calibration to existing practice, but there are also reasons to believe that target safety for dams should be based also on tolerable risk concepts.

The basic variables affecting concrete dam stability are described and special attention is given to uplift, where a thorough state-of-the art is given, as it has been shown in previous research to have a large influence on dam stability. Uplift varies depending on temperature (higher uplift during cold periods), due to loads (increasing water levels may give rise to uplift pressure to increase more than the linear design assumption), is highly dependant on foundation treatment and drainage and is difficult to monitor (uplift in one point represent only a local area). A promising approach on how to use geostatistical modelling to derive statistical distribution for uplift is shown. The hydraulic conductivity beneath the dam is assumed to have certain properties (mean value and variance) and is quantified by a spatial correlation structure. Flow and uplift pressure distribution is then solved by use of a finite element program. A large number of simulations is used to obtain a statistical distribution of uplift force and moment on the whole dam base area. The uplift force active on the dam is described as

$$U_L = u \cdot C$$

where u is the uplift force, calculated from the linear uplift reduction assumption used in design, and C is a random variable based on the simulations. The treatment of moment of uplift is similar. This concept can and should be further developed, e.g. by investigating real rock properties and analyzing 3-D modelling of hydraulic conductivities. Even though there are questions to be solved, this approach gives useful results.

In the first of two examples, the capacity of a wall in a spillway chute is analyzed. The result is that the wall can withstand approximately 20 % higher water levels than that resulting from design according to RIDAS. In the second example a dam, fulfilling the requirements in RIDAS, is analysed. The results reveal that the cohesion and the friction coefficient gives the largest contribution to the uncertainty of β for sliding failure, whereas self-weight, followed by uplift and ice load, dominates the uncertainty for overturning failure.

The main conclusions are that structural reliability analysis can be used as a tool in the dam safety risk management process and that the most important factors for further analysis are cohesion, friction coefficient, ice load, uplift and self-weight. The examples shown, and the results of a master thesis, indicates that today's guideline (RIDAS) results in a number of "problems", among them that the safety index seems to be dependant on dam type and dam height and that cross-sectional design is, at least in one example, conservative.

Keywords: uplift, structural reliability analysis, concrete dam, assessment, spatial correlation, existing structure

Sammanfattning

Svenska betongdammar dimensioneras och utvärderas på basis av deterministiska principer baserade på säkerhetsfaktorer. Kombinationen av dammarnas ökande ålder, nya beräkningsmetoder för dimensionerande flöden samt ökande samhällskrav på säkerhet, leder till att dammar behöver uppgraderas och byggas om. När stabiliteten utvärderas är det viktigt att detta sker på basis av moderna säkerhetskoncept. Målet med denna avhandling är att beskriva hur tillförlitlighetsbaserad metodik kan användas för utvärdering av betongdammars stabilitet, hur detta passar in i riskhanteringsprocessen för dammar samt sammanställa nuvarande kunskapsnivå gällande relevant statistisk information om bärförmåga och lastparametrar.

Formaliserad riskhantering används alltmer i dammsäkerhetsarbetet över hela världen och tillförlitlighetsanalys kan användas för säkerhetsutvärdering av befintliga dammar. Eftersom objektspecifik information, mätresultat, kända laster, med mera, kan inkluderas i analysen ger den mer tillförlitliga resultat än en utvärdering baserad på en mer generell dimensioneringsriktlinje/norm.

I denna avhandling används felmoderna glidning och stjälpning, men det finns anledning att ytterligare analysera formuleringen av felmoder. I ett antal utländska riktlinjer analyseras inte stjälpningsfallet och istället analyseras lastresultantens läge, där ett läge utanför kärngränsen ses som en indikator på problem. Brott associeras istället med glidning eller överskriden hållfasthet. I Riktlinjer för dammsäkerhet, RIDAS, tas, till skillnad från riktlinjer som används på andra ställen i världen, ej hänsyn till kohesionens inverkan på glidstabiliteten. I denna avhandling tas, trots det, hänsyn till kohesion när kriteriet för glidstabilitet formuleras.

I en tillförlitlighetsanalys beskrivs den aktuella felmoden av en gränsfunktion som beror av ett antal variabler, beskrivna av sina respektive statistiska fördelningar. För en betongdamm är variablerna i glidningsfallet egentynghet (G), kohesion (c), basarea (A), friktionsvinkel (ϕ), upptryck (U), hydrostatiskt tryck (H) samt islast (I). Gränsfunktionen kan skrivas som

$$g(G, U, H, I, \phi, c, A) = c \cdot A + (G - U) \cdot \tan \phi - (H + I)$$

Gränsfunktioner för stjälpning och andra felmoder definieras på liknande sätt.

När de statistiska fördelningarna är kända för de ingående variablerna kan säkerhetsindex β beräknas. β kan relateras till brottsannolikhet via $p_f = \Phi(-\beta)$, där Φ är den standardiserade normalfördelningen.

Vid säkerhetsutvärdering jämförs β med ett godkänt värde, β_T , för att bedöma om konstruktionen är tillräckligt säker. För dammar finns inget sådant godkänt värde angivet. Det finns olika tillvägagångssätt för att bestämma vilket gränsvärde som är lämpligt och det enklaste är kalibrering mot existerande praxis. Det finns skäl att anta att gränsvärdet för dammar även bör återspegla vad som anses som en tolerabel risk.

I avhandlingen beskrivs de variabler som påverkar stabiliteten hos en betongdamm och upptryck ägnas särskild uppmärksamhet, eftersom det i tidigare studier visat sig ha stor betydelse. En omfattande litteraturstudie kring upptryck visar bland annat att det varierar beroende på temperatur (högre upptryck under kalla perioder), är beroende av de laster som verkar på dammen (ökande vattennivåer kan ge upptryck som ökar snabbare än det linjära antagande som brukar användas), är beroende av grundläggningsåtgärder och dränage, samt är svårt att mäta (trycket i en punkt återspeglar endast trycket lokalt). Ett lovande tillvägagångssätt där geostatistisk modellering används för att ta fram statistiska fördelningar för upptrycket visas. Den hydrauliska konduktiviteten i grunden antas ha vissa egenskaper (medelvärde och varians) och kvantifieras med hjälp av en korrelationsstruktur. Flöde och upptryck kan sedan lösas ut med hjälp av ett finit elementprogram. En stor mängd simuleringar används för att få fram en statistisk fördelning för upptryckskraften och upptrycksmomentet för hela dammen. Upptryckskraften kan beskrivas som

$$U_L = u \cdot C$$

där u är den kraft som fås i det fall som normalt används vid dimensionering (linjär upptrycksreduktion) och C är en stokastisk variabel baserad på simuleringsresultaten. Momentet behandlas på liknande sätt. Detta koncept kan och bör utvecklas vidare, tex. genom undersökning av bergegenskaper och 3-D analys av hydraulisk konduktivitet. Detta tillvägagångssätt ger, trots att vissa frågor återstår, värdefulla och användbara resultat.

I det första av två exempel analyseras bärförmågan hos en mur i en utskovskanal. Resultatet visar att muren klarar ca 20 % högre vattennivå än vad utvärderingen enligt RIDAS ger. I det andra exemplet analyseras en damm som uppfyller kraven enligt RIDAS. Resultatet visar att kohesionen och friktionskoefficienten ger störst bidrag till osäkerheten hos β i glidningsfallet, medan egentygden, följd av upptryck och islast, dominerar osäkerheten i stjälpningsfallet.

De viktigaste slutsatserna är att tillförlitlighetsanalys kan användas som ett verktyg i dammsäkerhetsarbetet och att de viktigaste variablerna för vidare analys är kohesion, friktion, islast, upptryck och egentygnd. Exemplet och resultatet av ett examensarbete visar att dagens riktlinje (RIDAS) resulterar i ett antal problem, bland annat att säkerhetsindex blir beroende av dammtyp och dammhöjd och att tvärsnittsdimensioneringen, åtminstone i ett exempel, är konservativ.

Sökord: Upptryck, tillförlitlighetsanalys, betongdamm, säkerhetsutvärdering, korrelationsstruktur, befintlig konstruktion.

Nomenclature

Abbreviations

BBK	Swedish design code for concrete structures (Boverkets handbok om betongkonstruktioner)
BKR	Swedish design regulations (Boverkets Konstruktionsregler)
CIB	International council for research and innovation in building and construction
COMREL	Computer software for reliability analysis
COV	Coefficient of variation, $COV = \sigma/\mu$
ENV, Eurocode	European design guidelines
ETA	Event tree analysis
FE	Finite element
FMEA	Failure modes and effect analysis
FMECA	Failure modes, effect and criticality analysis
FORM	First order reliability method
FTA	Fault tree analysis
HSE	Health & Safety Executive, Great Britain
ICOLD	International commission on large dams
IEC	International Electrotechnical Commission
IRGC	International Risk Governance Council
JCSS	Joint committee on structural safety
MATLAB	Computer software for technical computing
NKB	Nordic Committee on building regulations (Nordiska kommittén för byggbestämmelser)
RIDAS	Swedish guidelines for dam safety (Riktlinjer för dammsäkerhet)
SORM	Second order reliability method

Definitions

Design point	Point on limit state surface giving the safety index
Failure criteria	Criteria in guideline/design code to account for a failure mode, when fulfilled the structure is considered safe enough
Failure mode	The manner in which a failure can occur
Limit state	A set of performance criteria (e.g. stability) that must be met when the structure is subject to loads. Can be either ultimate limit state or serviceability limit state.
Limit state function	Function describing the limit state of interest.
Risk	A measure of the probability and severity of an adverse effect to health, property or the environment (Probability · consequence of unwanted event).
Risk assessment	Process of deciding if present risk is tolerable or not (risk analysis and risk evaluation)
Risk analysis	Process of identifying and estimating the risk to individuals, population, environment, society etc from hazards
Risk evaluation	Process to examine and judge the significance of risk
Risk management	Complete process of risk assessment and risk control
Safety factor	A multiplier applied to the calculated maximum load to which a structure will be subjected

Symbols

A	Area
a	Parameter describing Beta-distribution of uplift
b	Parameter describing Beta-distribution of uplift
c	Cohesion
C	Random variable describing uplift force
$C(h)$	Covariance function
C_m	Random variable describing uplift moment
d	Water depth above retention water level
E	Expected value
E_d	Effectiveness of drainage
$F(x)$	Cumulative distribution function (cdf)
$f(x)$	Probability density function (pdf)
g	Gravity acceleration
G	Self weight
G_M	Moment of self weight
$G(x\dots)$	Limit state function
H	Hydrostatic load
H_M	Moment of hydrostatic load
h	Separation distance
h_w	Head water level
I	Moment of inertia
I	Ice load
I_M	Moment of ice load
K	Hydraulic conductivity
K_d	Effectiveness of drainage
M_L	Moment of uplift
M_R	Resisting moment

M_S	Overturning moment
m	Moment of uplift when pressure drop is linear (design assumption)
N	Loads normal to sliding surface
owl	Known water level above rwl
$P(X \leq x)$	Probability of $X \leq x$
p_f	Probability of failure
Q	Flow
R	Resistance
r	Parameter describing Beta-distribution of uplift
rwl	Retention water level
S	Load action (Sollicitation)
sf	Safety factor
T	Loads parallel to sliding surface
t	Parameter describing Beta-distribution of uplift
U_L	Uplift force
u	Uplift force when pressure drop is linear (according to design assumption)
V, Var	Variance
X_k	Characteristic value of X

α	Sensitivity factor
β	Safety index
β_T	Target safety index
ϕ	Friction angle
Φ	Standard normal cdf
γ_x	Partial safety factor
$\gamma(h)$	Semi-variogram
λ	Parameter of the exponential distribution
μ	Mean value
ρ_c	Concrete density
ρ_w	Density of water
σ	Standard deviation
ξ	Parameter accounting for voluntariness of risk

Table of contents

PREFACE	I
ABSTRACT	III
SAMMANFATTNING	V
NOMENCLATURE	VII
1. INTRODUCTION	1
1.1 Background	1
1.2 Objectives of research and future aim	2
1.3 Limitations	2
1.4 Outline	3
2. CONCRETE DAMS, FAILURE MODES AND DESIGN	5
2.1 Concrete dams in Sweden	5
2.2 Failure modes for concrete dams	8
2.2.1 Sliding	9
2.2.1.1. Models describing shear strength	9
2.2.1.2. Size effects	12
2.2.1.3. Shear strength description for concrete dams	13
2.2.2 Overstressing	15
2.2.3 Overturning	16
2.2.3.1. Cracked base analysis	16
2.2.4 Observed failure modes	16
2.2.5 Causes of failure	17
2.3 Failure criteria in codes and literature	18
2.3.1 Literature	18
2.3.2 Federal Energy Regulatory Commission (FERC, 2002), USA	18
2.3.3 Bureau of Reclamation (BUREC), USA	19
2.3.4 U.S. Army Corps of Engineers (USACE), USA	20
2.3.5 China Electricity Council, China	20
2.3.6 CDA, Canada	21
2.3.7 RIDAS, Sweden	22
2.4 Discussion of failure mode definition	22
2.4.1 Failure modes in structural reliability analysis	23
3. SAFETY CONCEPTS	25
3.1 Structural reliability analysis	26
3.1.1 Basic reliability problem	26
3.1.2 Failure probability and safety index	27
3.1.3 First and second order methods	29
3.2 Bayesian updating	32
3.3 Target safety index	33
3.3.1 Calibration to existing practice	33

3.3.2 Target safety index in different structural codes	34
3.4 Methods for reliability design	39
3.4.1 Method and calibration of partial factors	39
4. RISK MANAGEMENT AND DAM SAFETY RISK MANAGEMENT	43
4.1 General risk management of technical systems	43
4.1.1 Risk analysis	44
4.1.2 Risk evaluation process	47
4.1.2.1. Tolerable risk	47
4.1.3 Risk reduction	52
4.2 Dam Safety in Sweden	52
4.2.1 Dam safety today	55
4.2.2 Comments	56
4.3 Risk management in Dam Safety	56
4.4 Structural reliability analysis in dam safety	59
4.4.1 Target safety index for dams	59
4.4.1.1. Calibration of target safety index	61
4.4.2 Structural reliability in the dam safety in the near future	63
4.4.3 Structural reliability in the dam safety of tomorrow	63
4.5 Dam safety at Vattenfall	64
4.5.1 Risk management process	64
4.5.1.1. Deficiencies and valuation	66
4.5.1.2. Prioritization or risk reduction measures	71
5. RANDOM VARIABLES AFFECTING DAM STABILITY	73
5.1 Self-weight of concrete	75
5.1.1 Distribution used	76
5.2 Shear strength	77
5.2.1 Ruggeri et al & EPRI	77
5.2.2 Chinese standards	82
5.2.3 Distributions used	85
5.3 Hydrostatic pressure	87
5.3.1 Flow in unregulated and regulated rivers	87
5.3.2 Calculation of design flow	88
5.3.3 Treatment of headwater level	89
5.3.3.1. Head water at retention water level	90
5.3.3.2. Head water above retention water level	90
5.3.3.3. Operational or functional failures	92
5.3.4 Example	93
5.4 Ice loads	94
5.4.1 Reason for ice loads	94
5.4.2 Creep	96
5.4.3 Time of peak loads	96
5.4.4 Other considerations	98
5.4.5 Testing and modelling	98
5.4.5.1. Laboratory tests	98

5.4.5.2. Field measurement	98
5.4.5.3. Theoretical modelling	99
5.4.6 Load values	99
5.4.7 Distribution used	101
5.5 Uplift	103
5.5.1 State-of-the-art	103
5.5.1.1. Flow through soil	104
5.5.1.2. Uplift design assumptions	106
5.5.1.3. Water flow in rock and influence for dams on rock	112
5.5.1.4. Modelling water flow in rock mass	122
5.5.1.5. Cracking	125
5.5.2 Uplift modelling by geostatistical approach	125
5.5.2.1. Geostatistics	126
5.5.2.2. Uplift simulation using geostatistics	128
5.5.2.3. Results	134
5.5.2.4. Discussion and conclusions of modelling	147
5.5.3 Use of uplift monitoring	149
5.5.4 Distributions used	153
5.6 Conclusions of chapter	154
6. EXAMPLES	157
6.1 Example 1: Stability calculation of dividing wall in Ajaure spillway chute	157
6.1.1 Information about Ajaure	157
6.1.2 Background of assessment	161
6.1.3 Calculation model and assumptions	165
6.1.3.1. Loads	165
6.1.3.2. Water depth and velocity in canal	167
6.1.3.3. Material properties	170
6.1.3.4. Reinforcement	170
6.1.3.5. Concrete	171
6.1.4 Assessment according to RIDAS	171
6.1.4.1. Resistance of wall	171
6.1.4.2. Results	172
6.1.5 Structural reliability analysis	173
6.1.5.1. Target safety index	173
6.1.5.2. Reliability analysis	176
6.1.6 Results	177
6.1.7 Cracking of concrete	179
6.1.8 Discussion and conclusions of example	182
6.2 Example 2: Reliability analysis of theoretical dam	183
6.2.1 Stability according to RIDAS	184
6.2.2 Reliability analysis of dam	185
6.2.2.1. Results	187
6.2.3 Discussions and conclusion of example	193
6.2.3.1. Overturning	193

6.2.3.2. Sliding	194
6.2.3.3. Conclusions of example	194
6.3 Conclusions of chapter	195
7. CONCLUDING REMARKS	197
7.1 General safety considerations	197
7.2 Conclusions	198
7.2.1 Target safety	198
7.2.2 Failure modes definition	198
7.2.3 Loads and resistance	198
7.2.4 General	199
7.3 Suggestions for further research	199
8. REFERENCES	201
APPENDIX A1	209
APPENDIX A2	210

1. Introduction

1.1 Background

Sweden has a large number of dams of increasing age. They represent a considerable value in terms of fixed capital assets and of future generation profits. The consequences of a dam failure could be significant, in casualties and/or in economic and environmental damage, and safety is therefore given highest priority.

Design of infrastructures (dams, bridges, house etc) has been based on safety factors. During the 1970's new design guidelines, based on partial factors, were developed and later introduced in e.g. bridge and house design. By applying larger partial factors for loads of large uncertainty than those with smaller uncertainty, the safety level was made more independent of load case and material (NKB 55, 1987). This resulted in better material use and more uniform, but sustained, safety level. Design guidelines based on partial factors are e.g. BKR (1998) and Eurocode (ENV 1990, 2001).

Dam design is, in Sweden as well as most of the world, still based on safety factors. One reason is that the dam building era was coming to an end when the new design concepts were developed.

Partial factors in other areas were calibrated from existing design standards by use of reliability-based, or probabilistic, methodology. Reliability-based methodology is particularly useful for evaluation of existing structures and offers the possibility of rational integration of specific information concerning a certain object. It also offers good possibilities to implement successively additional information available, from e.g. investigations, testing and monitoring. Design codes are formulated from a general point of view. High randomness in loads is difficult to handle, and simplifications are made to be on the safe side. This means that, in some cases, a more refined statistical description of loads and resistances can be used to verify that the safety is sufficient in the existing state, so that expensive and unnecessary reconstruction measures can be avoided and resources be used more efficiently.

The combination of increasing age, with its associated problems, new methods for calculation of design floods and increasing demands by society to ensure a high level of safety has resulted in upgrading and rebuilding needs for dams. When safety is re-evaluated it is important that evaluation is based on modern safety concepts.

Several projects where probability based evaluation of existing road bridges for upgrading of load-bearing capacity was performed have been undertaken, see e.g. Jeppson (2003), Carlsson et al (2002), Carlsson (2006). In this type of applications the results from testing of material properties in existing structures and data from measurement of traffic loads as well as other loads, can be used. Jeppson (2003) also analyzed a dam and found that more research was needed to better define several factors of large uncertainty.

1.2 Objectives of research and future aim

The objectives of this thesis is to

- Describe and demonstrate the capability of applying reliability-based methodology for assessment of concrete dams and how this fits into the dam risk management process.
- Compile and document present knowledge of relevant statistic information of resistance and load parameters for concrete dams.

To do this it is necessary to describe how dam safety assessment is performed today, what is meant by reliability-based evaluation and how this can be used in dam safety and, evidently, what further development is needed to implement it in this area.

The future aims, given the above background and if this is what the hydropower business wants, are to

- Present a reliability based methodology to be used as part of the assessment phase when an existing structure does not fulfil general safety standards. This methodology should also be possible to use for design of new dams
- Formulate a new basis of design for assessment of existing dams and design of new dams. To end up with a consistent handling of safety the design should be based on one safety concept only. This could be the partial factor concept, or if more appropriate, a reliability-based methodology.

1.3 Limitations

In dam context the use of reliability-based methods is virgin soil. At the same time, dam safety is a complex and very interesting area, and the result is that one can easily find oneself drifting away in an un-intended direction. In some aspects the area I have tried to grip may be considered too vast, but the intention has been to give background of both safety concepts and dam safety and by doing so show how structural reliability fits into dam safety. Those areas are both huge and for this reason the summaries given does not claim to be complete in any way.

Further limitations are that only ultimate limit state of concrete dams have been considered and that after a state-of-the art of concrete dam failure modes the “standard” ones were chosen for use in the structural reliability analysis, even though there are reasons to believe that they are not appropriate.

Concerning the load bearing capacity and loads, this thesis is limited to describe self-weight of concrete, shear strength of concrete to rock interface, uplift, hydrostatic water pressure and ice loads.

Failure in the foundation rock is not taken to account. For a complete analysis, failure of foundation is of major importance.

To be able to give some examples of reliability analysis, calculation, statistical descriptions were needed and chosen, even in cases where the background information was to scarce. This is clearly mentioned where relevant.

1.4 Outline

Chapter 2 describes concrete dams in general and the failure modes generally applied in concrete dam design.

In Chapter 3 different safety concepts are discussed. Focus is on structural reliability analysis, but partial factor design is briefly described. Target safety values in design guidelines are given.

Chapter 4 gives a summary of technical risk management in general and a discussion on tolerable risk. Dam safety risk management in general, in Sweden and in the hydropower owning company Vattenfall is described with the objective to place structural reliability of concrete dams in its right context.

In Chapter 5 resistance parameters and the main loads acting on concrete dams are described more in detail. The objective here is to present distribution functions for stochastic variables to be used in future re-assessment situations. The main focus is on uplift, where an extensive state-of-art is given and an approach to model the possible uplift is presented.

Chapter 6 gives examples of the applicability of structural reliability analysis in dam safety. A simple example of a dividing wall in a spillway chute is analysed and a schematic example of a concrete dam is given.

Chapter 7 includes a brief discussion, conclusions and suggestions to further research.

2. Concrete dams, failure modes and design

The purpose of this chapter is to give a general background of concrete dams, mainly on the types common in Sweden. Failure modes are described and a short summary of failure causes is given. Failure criteria in some codes are summarized. The purpose is to give an introduction to concrete dam behaviour and to, as is done in the last section, discuss the appropriate definition of failure modes, as it should be used in the structural reliability analysis to follow.

2.1 Concrete dams in Sweden

In principle dams can be divided into three groups, characterized by building material: earth or rock fill dams, masonry dams and concrete dams.

Concrete dams are, in turn, divided into three groups: gravity dams, buttress dams and arch dams. There are also hybrids, like arch-gravity dams, concrete faced rock fill dams etc, but in Sweden those are not represented. Arch dams are mainly built in narrow, steep valleys where the hydrostatic force from the reservoir can be transmitted horizontally to rock on the banks. Only a few arch dams have been built in Sweden, mainly because this is not the common type of Swedish valley as mentioned in Bernstone (2006). Instead, Swedish concrete dams are in general gravity or buttress dams, see Figure 2-1 and Figure 2-2. For gravity dams, see Figure 2-3, the self-weight of the dam is sufficient to withstand the hydrostatic forces and transmit them to the ground.

Buttress dams, see Figure 2-4, consists of an inclined or vertical front plate supported by columns that transfer the hydrostatic forces to the ground. This design significantly reduces the concrete volume compared to gravity dams.



Figure 2-1 - Gravity dam at Stadsforsen.



Figure 2-2 - Buttress dam at Stornorrfors.

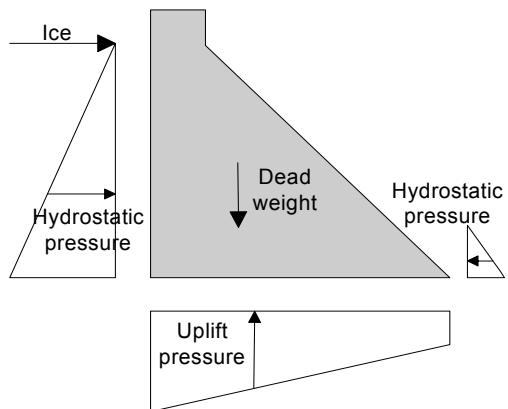


Figure 2-3 – Main forces of concrete gravity dam.

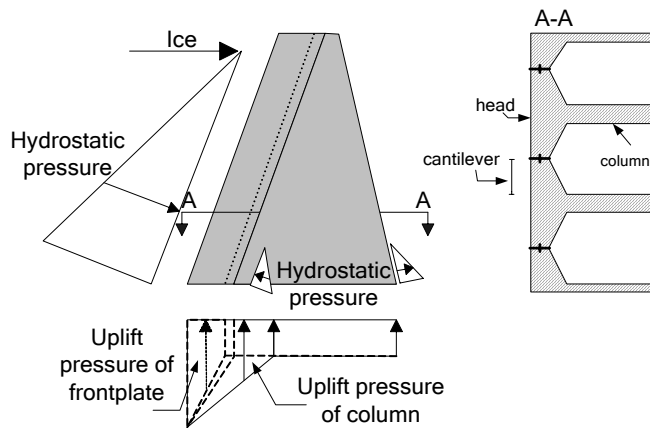


Figure 2-4 – Main forces of buttress dam.

Figure 2-5 is from Bernstone (2006) and show year of completion of 212 Swedish concrete dams (dams with > 80 % concrete parts). This figure includes both high dams (dams of height > 15 m according to ICOLD), and low dams. Sweden has few high dams, mainly because of the topography with wide valleys, as mentioned above. In addition to these concrete dams most dam sites dominated of earth or rock fill dams has intake and discharge facilities in concrete. The behaviour of these are similar to that of concrete gravity or buttress dams, but geometries and loading conditions may be more complicated.

The situation in Sweden is, and has been during the last decade, that no new establishments of dams are under consideration. Instead focus has mainly been on maintaining the ageing dam portfolio at an acceptable safety level or to make improvements to reach this level, and building and construction of new dams has been essentially zero. This situation is now slowly changing, as some of the oldest dams have to be improved or completely rebuilt to fulfil today's safety requirements. It must be pointed out that the vision in the Swedish design guidelines RIDAS (2002, will be further discussed in chapter 4) is continuous dam safety improvements, and thus the sufficiently safe level can change with time.

The resistance of a concrete dam is due to its self-weight and to shear, compressive and tensile strength of concrete, foundation and, where relevant, reinforcement. The most important forces are hydrostatic force, ice load and uplift pressure. These factors will be treated more in detail later. Forces from sediment and earthquakes are of importance in many parts of the world, but not in Sweden. Earth pressure and traffic load can be of importance and loads of temperature, shrinkage and creep are often substantial, but neither is treated in this thesis.

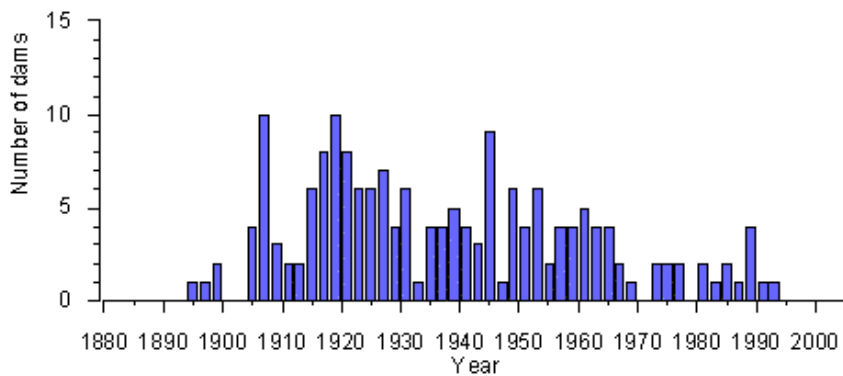


Figure 2-5 - Year of completion of Swedish concrete dams (from Bernstone, 2006).

2.2 Failure modes for concrete dams

The failure modes of concrete dams, described in literature and design guidelines, are:

- Sliding. Sliding of the whole dam section or a monolith, or part thereof along the concrete to rock interface, lift joints (construction joint) in the dam body or along weak planes in the foundation.
- Overstressing. Ultimate stresses exceed ultimate strength in foundation or dam body.
- Overturning. Overturning of the whole monolith or part thereof. This failure mode is not explicitly accounted for in some guidelines, as will be shown later in this chapter.

The failure modes are of major importance in dam design and assessment. The failure of a structure can be seen as a series system where the reliability is defined by the weakest link. Figure 2-6 shows an example for a concrete dam. If the failure modes identified are not the most essential, meaning that there are unidentified or neglected modes which will occur with higher probability, the outcome of the analysis will not reflect reality – no matter the refinement of calculation methods or knowledge of input parameters. In most design and assessment of concrete dams the dam is treated as a rigid body when calculating stresses. This is an idealization with limitations and not considering these may lead to erroneous results.

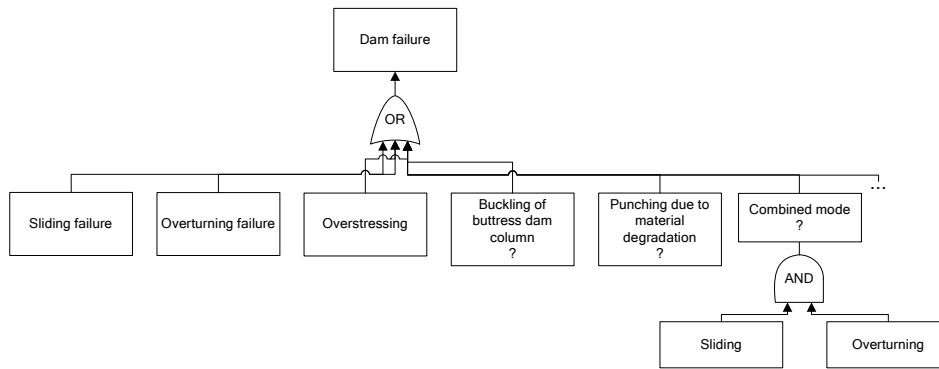


Figure 2-6 - Example of theoretical series system of failure modes for concrete dams.

2.2.1 Sliding

The most used and accepted methods to evaluate safety against sliding regard the dam as a rigid body allowed to slide along its base or lift joints, or along critical surfaces in the foundation. Sliding surfaces are defined based on judgement of the most probable ones and occur when the resisting force (shear strength) is insufficient compared to the driving forces. Swedish dams are mainly founded on rock and this is in focus here.

There are different approaches how to evaluate the shear strength; some methods use forces along the entire sliding surface, others differentiate the area of the sliding surface where normal stresses are compressive from that where tensile stresses exceed the tensile strength (cracked base analysis, which will be further discussed in 2.2.3.1) (Ruggeri et al, 2004).

2.2.1.1. Models describing shear strength

The Mohr-Coulomb constitutive model describe the maximum allowed tangential stress τ for each point of the sliding surface as

$$\tau \leq c + \sigma_n \cdot \tan \phi \quad \text{Eqn. 2-1}$$

where c is the cohesion, σ_n is the normal stress to the sliding surface and ϕ the friction angle.

The Mohr-Coulomb failure criterion approximates the failure envelope with a linear approximation as shown in Figure 2-7a), but the failure envelope for rock masses is not linear but slightly curved. If high confining pressures exist, the cohesion becomes high and the friction angle low. If, on the other hand, the confining pressure is low the friction angle becomes high and the cohesion low. This is due to the curved failure envelope, the approximation thus depends on around which point the linearization is performed. An example is shown in Figure 2-7c), where approximation of the failure envelope is performed for a range of high normal stresses (r_1) and one for low (r_2). For shallow foundations this linear approximation is only acceptable if the parameters are

evaluated within the range of stresses that are present in the foundation (Johansson, 2005).

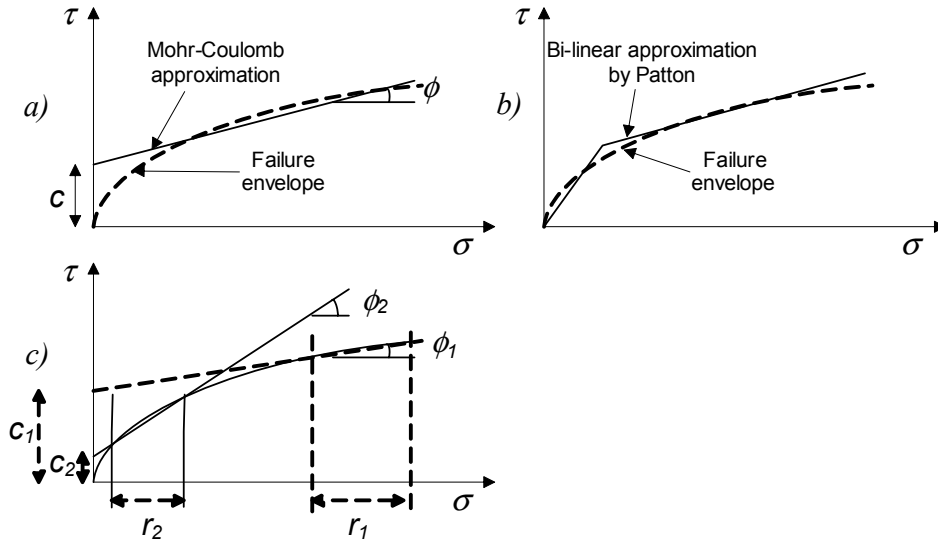


Figure 2-7 - a) Mohr-Coulomb approximation b) Patton's approximation c) Mohr_c.

The Hoek and Brown failure criterion describes the failure envelope of rock masses better than the Mohr-Coulomb failure criteria but is more cumbersome to use. It is empirical and applicable for both intact rock and rock masses with a curved failure envelope.

The Hoek and Brown criteria is expressed as

$$\sigma'_1 = \sigma'_3 + \sigma'_{ci} \left(m_b \frac{\sigma'_3}{\sigma'_{ci}} + s \right)^a \quad \text{Eqn. 2-2}$$

where σ'_1 and σ'_3 are the major and minor effective principal stress at failure, m_b , s and a are material constants depending on characteristics of the rock mass and σ'_{ci} is the uniaxial compressive strength of the intact rock. The material constants are linked to GSI (Geological Strength Index) and a disturbance factor D , representing the degree of disturbance in the rock mass of blast damage and stress relaxation (Ruggeri et al, 2004).

For estimation of the shear strength of discontinuities Patton (according to Johansson, 2005) proposed two equations,

- for low normal stresses σ'_n

$$\tau_f = \sigma'_n \cdot \tan(\phi_b + i) \quad \text{Eqn. 2-3}$$

where ϕ_b is the basic friction angle and i the angle of the “saw-tooth” of the discontinuity.

- For higher normal stresses the effect of the “saw-tooth” will disappear due to asperity override, failure through the asperities or by a combination of them and the above equation reduces to

$$\tau_f = \sigma'_n \cdot \tan(\phi_b) \quad \text{Eqn. 2-4}$$

The result is a bi-linear failure envelope, see Figure 2-7b).

Barton (according to Ruggeri et al, 2004) developed the work by Patton to an empirical curved failure criterion which estimates the peak shear strength of discontinuities. It accounts for roughness and compressive strength of the discontinuity surface and is written as

$$\tau_f = \sigma'_n \cdot \tan \left(JRC \log_{10} \left(\frac{JCS}{\sigma'_n} \right) + \phi_b \right) \quad \text{Eqn. 2-5}$$

where JRC is the joint roughness coefficient and JCS the joint wall compressive strength. For this failure criterion to be valid a minimum normal stress has to be applied, as described by e.g. Johansson (2005).

The shear stress-strain curve of rock masses, concrete to rock interface or for concrete itself is shown in Figure 2-8. It is necessary to define on which point of the stress-strain curve failure will occur. If the failure is brittle and associated with small deformations the peak strength defines the strength, for large deformations or post-earthquake load cases the residual strength should be used and for some cases it is the point before large deformations occur, denoted ultimate strength, that is of interest (Johansson, 2005, Ruggeri et al, 2004).

USACE (1994) point out that with proper interpretation, failure envelopes over most design stress ranges can be closely approximated by the linear Coulomb equation.

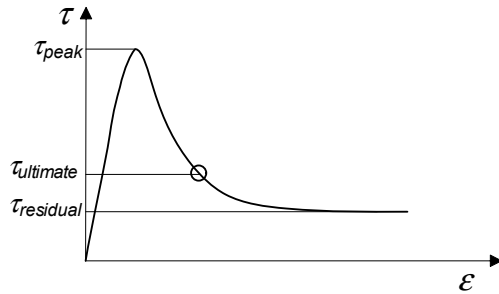


Figure 2-8 - Shear stress - strain curve.

2.2.1.2. Size effects

Concrete and rock properties are scale dependant and knowledge of this is necessary when results from small-scale testing are to be used in larger scale.

Bandis et al (1981) performed experiments to study the scale effect on the shear behaviour of rock joints. Their results show that increasing block size or length of joints leads to a gradual increase in the peak shear displacement and transition from brittle to plastic failure mode, as shown in Figure 2-9. As mentioned in Ruggeri et al (2004) the scale effect is treated in the shear strength model by Barton described above.

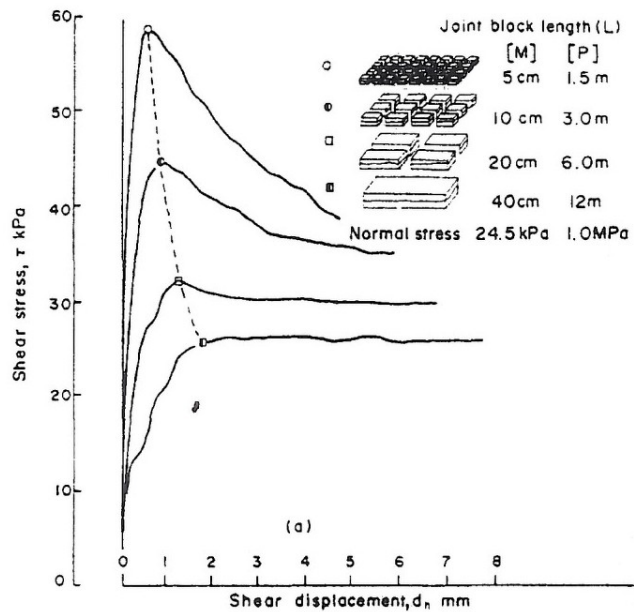


Figure 2-9 - Cumulative mean shear stress - shear displacement (from Bandis et al (1981)).

2.2.1.3. Shear strength description for concrete dams

For gravity dams the Mohr-Coulomb criterion is often used, and σ_n and τ then has to be integrated over the sliding plane which result in the safety condition to be

$$T \leq \frac{cA + N \cdot \tan \phi}{sf} \quad \text{Eqn. 2-6}$$

where T is the resultant forces parallel to the sliding plane, N the resultant forces normal to it, ϕ the friction angle, c the cohesion and A the contact area. Dams are in general assessed and designed with safety factors and sf is the safety factor applied. As mentioned in Ruggeri et al this expression considers that, at failure, the ultimate capacity is reached at each point on the sliding surface, hence the integration. This is, however, true for ductile materials, but sliding planes can often be considered semi-brittle.

Ruggeri et al investigated the regulatory rules and guidelines concerning sliding stability of existing dams and found that only two of fourteen countries in the investigation (Sweden and Italy) apply the simple criteria where the safety assessment is based on the ratio T/N between the resultant of the forces parallel (T) and perpendicular (N) to the sliding surface.

In the Swedish design guidelines, RIDAS TA (2003), the safety condition of sliding is expressed as

$$\frac{\tan \phi}{sf} \geq \frac{T}{N} \quad \text{Eqn. 2-7}$$

where ϕ is the friction angle, T and N are as described above and sf is a safety factor.

The safety factors in RIDAS are shown in Table 2-1 for different cases.

Table 2-1 - safety factors for sliding stability of concrete dams according to RIDAS TA (2003).

Foundation	Normal load case	Exceptional load case	Accidental load case
Rock	1,35	1,1	1,05
Morain, coarse sand, gravel	1,5	1,35	1,25
Silt	1,5	1,35	1,25

Of the countries investigated, six applied one safety factor for both friction angle and cohesion, whereas six differentiate them from each other, applying larger safety factors

for cohesion. In many countries it is not explicitly stated if peak or residual values are to be used for the shear strength parameters. Where it is, the safety factors used vary depending on if peak or residual strength is used. Differentiation is also made depending on if the strength values are based on laboratory or in-situ testing or on values given in the code.

As pointed out in ICOLD bulletin 88 (1993) the most critical case for sliding stability in the rock mass are flat, smooth surfaces of large area that are filled with soft materials. Under these circumstances shear strength is developed through friction alone and is not influenced by the scale effect. Due to possible shear displacements in the geological past, that may have reduced the cohesion to zero, the residual strength is the only reliable factor for the strength of the rock mass.

Ruggeri et al (2004) describe different approaches to evaluate safety against sliding:

- Limit equilibrium (rigid body).
Either evaluation of the tangential forces along the entire sliding surface or differentiating the part of the sliding surface where compressive stresses are present from that where they are not (cracked-base analysis).
- Deformable body approach.
Dam and foundation are described as deformable bodies. Material properties and straining range of interest is used to decide if linear or non-linear models are to be used. Such methods are well suited to incorporate many details of the actual loading sequence and the geometrical layout and allow for many refinements in constitutive modelling. As monitoring data, gathered within operational limits, is used as validation tool, “extrapolation” of data outside of the associated displacement ranges has to be overcome to get reliable solutions for ultimate states.
- Constitutive behaviour and models of joints/interfaces.
Elastoplastic approaches use tensile strength, cohesion and friction angle whereas *linear fracture mechanics* use fracture toughness and *nonlinear fracture mechanics* uses fracture energy.
- Coupled response.
Modelling of crack growth and the development of the associated water penetration and pore pressure growth are specific aspects of these models, taking into account the full coupling of stress and hydraulic response (for more information see Ruggeri et al (2001)).
- Numerical models
Finite element, finite differences or boundary elements are used for numerical analysis or discrete crack models or smeared crack models. In a benchmark using a number of different numerical models many conclusions were made, among those:

- Results significantly depend on meshing strategy (type of elements and refinement)
- For updating of uplift pressure to follow joint opening *ad hoc* procedures had to be used since this is not available in standard finite element codes
- The ultimate capability to resist sliding was dependant on peak strengths rather than residual ones.
- Different scenarios of uplift pressure distribution had a strong influence on the result

2.2.2 Overstressing

Overstressing will occur if the stresses induced in the dam body or foundation exceeds the material capacity. For buttress dams the front plate (head) will function as a cantilever beam, see Figure 2-4, and one possible failure mode is overstressing of the cantilever beam. This case is, however, not a global failure mode and will not be further discussed here.

Stresses are often calculated based on “beam model” analysis using Navier’s equation:

$$\sigma = \frac{V}{A} \pm \frac{M_c \cdot y_p}{I} \quad \text{Eqn. 2-8}$$

where V is the vertical force, A the base area, M_c the moment around the centre of gravity of the base area, axis, y_p the distance from the centre of gravity to the point of interest and I the moment of inertia.

Finite element analysis can also be used to determine stresses. This is especially true when the beam idealisation is inadequate.

As pointed out by Reinius (1962) the basic requirement behind Navier’s equation, that plane cross-sections remain plane, is not fulfilled and larger stress concentrations will therefore occur at the heel and toe of the dam. Stresses from finite element analysis will represent the behaviour more accurately.

It is usually assumed (cracked base analysis) that if tensile stresses calculated by rigid body analysis occur at the dam toe, a crack will form and water will percolate the crack, causing full uplift pressure along the whole crack length.

As pointed out in ICOLD bulletin 88 (1993), the concrete to rock interface has tensile strength that, for all practical purposes, is assumed to be zero. This is since joints or fractures may be located directly below the concrete/rock interface and the rock mass will then not be able to develop any tensile capacity (FERC, 2002).

In RIDAS TA (2003) allowable stresses are determined case-specifically and there is no recommendations regarding safety factors.

2.2.3 Overturning

Overturning may occur if the stabilizing forces, mainly the self-weight, are less than the overturning forces. The criterion, where used, is usually given as:

$$\frac{M_R}{M_S} > sf \quad \text{Eqn. 2-9}$$

where sf is the safety factor, M_R is the resisting moment and M_S is the overturning moment. The overturning moments are calculated around the dam toe or some other relevant point, i.e. for lift joints in the dam body or other weak planes.

In RIDAS TA, safety factors according to Table 2-2 are used to ensure the overturning stability.

Table 2-2 - Safety factors of overturning according to RIDAS TA (2003).

Normal load case	1.5
Exceptional load case	1.35
Accidental load case	1.1

2.2.3.1. Cracked base analysis

According to RIDAS TA (2003) two criterions shall be fulfilled to ensure the overturning stability; the one described above, and that “resultant forces fall within the mid third of the base area (normal load case) or within the mid 3/5th of the base area. (exceptional load cases)”.

This criterion actually comes from the “cracked base criteria” mentioned above: if the resultant falls outside the mid third of the base area, tensile forces will occur in the upstream heel of the dam, resulting in full uplift pressure in the cracks thus appearing.

2.2.4 Observed failure modes

It is difficult to know if the failure modes described above are the “true” failure modes and if it is all possible failure modes. One possibility is to analyse known dam failures, but those does not necessarily cover all possible failure modes (the number of concrete dam failures is, luckily, not large enough to assume that all possible failure modes has been experienced). It can also be difficult to know the exact failure mode, especially long time after failure has occurred and for combined failure modes. It is still worth analysing but is not further discussed here.

ICOLD bulletin 109 (1997) mention two types of failure:

- Piping in the foundation. Occurred for dams on gravel or clay with no grout curtain.
- Overturning of blocks or sliding in the foundation.

No further details are given to describe those failure modes.

2.2.5 Causes of failure

As summarised by FEMA (2006) concrete dams fail for one or combinations of i.a. the following factors:

- Overtopping caused by floods that exceed the discharge capacity.
- Deliberate acts of sabotage.
- Structural failure of materials used in dam construction.
- Movement and/or failure of the foundation supporting the dam.
- Settlement and cracking of concrete dams.
- Inadequate maintenance and upkeep

ICOLD Bulletin 99 (1995) gives a summary of dam failures and Figure 2-10 shows the reasons for concrete dam failures. Foundation problems are the most common cause, internal erosion and insufficient shear strength of the foundation each account for 21 percent of the failures. Of all concrete dam failures insufficient capacity of spillways during passage of maximum floods was the primary cause of about 22 percent of the dam failures and secondary cause in about 39 percent of the failures.

According to ICOLD Bulletin 111 (1998) a concrete dam may withstand significant overtopping and the limiting factor in such conditions is the erosion of the foundation or abutments. Structural failure is usually due to weak foundation, structural deficiencies or sabotage. The failure of arch and buttress dams is usually assumed to be instantaneous. Gravity dams are assumed to have relatively short but not instantaneous failure time. The frequency of dam failures is approximately the same for all dam heights. The largest number of failure is among new dams, failures frequently occur within the first 10 years after construction and especially during first fill.

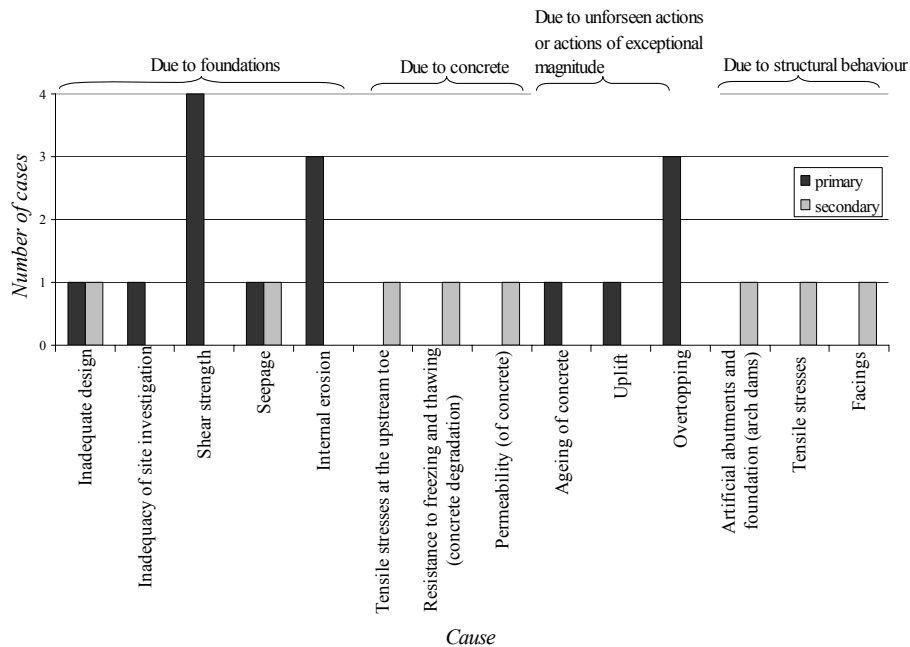


Figure 2-10 - Cause of dam failures, after ICOLD Bulletin 99.

2.3 Failure criteria in codes and literature

2.3.1 Literature

Ajaújo et al (1998) made a probabilistic finite element analysis of concrete gravity dams subjected to earthquakes and mention, in passing, that safety verification of concrete gravity dams can be based on three criteria: cracking, concrete crushing and sliding at the dam-foundation interface.

2.3.2 Federal Energy Regulatory Commission (FERC, 2002), USA

In Federal Energy Regulatory Commission (2002) – *Engineering guidelines for the evaluation of Hydropower projects. Chapter III Gravity dams* the acceptance criterions are:

- *The basic requirement for stability of a gravity dam* subjected to static loads is that force and moment equilibrium be maintained without exceeding the allowed limits of concrete, foundation or concrete/foundation interface strength.

- *The internal concrete stresses should not exceed the strength.* It is pointed out that in most cases, the stresses in the body of a gravity dam are quite low but situations arise in which stress is a concern and then the
 - Shear stress on pre-cracked failure plane should be less than $1.4 \cdot \sigma_n$ and
 - Principal axis tension within intact concrete be less than $1.7 \cdot (f'_c)^{2/3}$. The tensile strength of the rock-concrete interface should be assumed 0 (see section 2.2.2).
- *The sliding safety should follow the recommended safety factors.* Safety factors are given for the case of cohesion, but since this is very difficult to quantify and typically exhibit extreme variability, alternative safety factors are offered for sliding stability calculations without cohesion.

Theoretical cracked base is allowed for all loading conditions for existing structures as long as the resultant of forces remains within the base of the dam and adequate sliding safety is obtained. Cohesion may not be assumed in the cracked part of the base.

2.3.3 Bureau of Reclamation (BUREC), USA

The following is from Bureau of Reclamation (1987) *Design of Small Dams*. It applies to dams of all sizes, but focus is on dams with height up to 50 ft (approximately 15m).

A concrete dam must be designed to resist, with ample safety factor, internal stresses and sliding failure within the dam and foundation.

- The maximum allowable compressive stress for concrete in a gravity dam should not be greater than the compressive strength divided by a safety factor of 3.0 (usual load combinations).
- In order to not exceed the allowable tensile stress, the minimum allowable compressive stress computed without internal water pressure should be determined from $\sigma_{zu} = pwh - \frac{f_t}{s}$

where σ_{zu} = minimum allowable stress at the face, p = reduction factor to account for drains, w = unit weight of water, h = depth below water surface, f_t = tensile strength of concrete at lift surfaces and s = safety factor = 3.0 for usual loading conditions.

- The shear-friction safety factor, Q , should for usual loading conditions, be 3.0 within the dam or along concrete-rock interface, and 4.0 for any plane of weakness in the rock mass. Q is the safety factor according to Eqn. 2-6.

For most gravity dams, internal stresses can be adequately determined for a cross section using the gravity method of analysis.

2.3.4 U.S. Army Corps of Engineers (USACE), USA

From *Gravity dam design – Engineering guideline* (2003).

“For sliding and bearing, the stability requirements have been expressed deterministically in terms of an explicit factor of safety that sets the minimum acceptable ratio of foundation strength along the most critical failure plane to the design loads applied. The analysis for determination of the resultant location in prior guidance has been termed an *overturning stability analysis*. This is a misnomer since a foundation bearing, crushing of the structure toe, and/or sliding failure will occur before the structure overturns.” In the USACE manual overturning stability analysis is replaced with resultant location.

Stability is ensured by:

- Providing an adequate factor of safety against sliding at all possible failure planes
- Providing specific limitations on the magnitude of the foundation bearing pressure.
- Providing constraints on the permissible location of the resultant force on any plane.
- Providing an adequate factor of safety against flotation of the structure.

The sliding stability is defined according to Eqn. 2-6.

Rotational behaviour is evaluated by determining the location of the resultant of all applied forces. This location can be determined through static analysis. The entire base must be in compression for usual load condition, for the unusual case higher uplift pressure may develop in a relatively short crack (75 % of base should be in compression), but this would only cause minor nonlinear behaviour. For extreme loading conditions a shear or bearing failure will occur before overturning occur and the resultant is permitted to be anywhere within the base.

2.3.5 China Electricity Council, China

The Standards Compilation of Water Power in China was worked out in order to unify basic principles and standards for the design of reliable hydraulic China Electricity Council took out engineering structures and the English version to the ICOLD congress in Beijing 2000. The design is based on limit state design using partial safety factors. For the limit state of load bearing capacity the dam section, structure and dam foundation should be checked for sliding stability and, if necessary, floating and overturning stability. The limit states considered are:

- Strength of dam body and foundation. Stresses are calculated using Navier’s equation, assuming rigid body movements. The action effect function is:

$$S(\bullet) = \left[\frac{\sum W_R}{A_R} - \frac{\sum M_R T_R}{J_R} \right] (1 + m_2^2)$$

and the limit state compressive strength reactive function is:
 $R(\bullet) = f_c$ or $R(\bullet) = f_R$

where $\sum W_R$ is the sum of all normal actions on dam foundation/calculated section, M_R is the sum of moment by all actions with respect to the centroid of the dam foundation, A_R is the area of dam foundation/, J_R is the moment of

inertia of the dam foundation with respect to the centroidal axis, T_R is the distance from the centroidal axis of the dam foundation to the downstream toe, m_2 is the downstream slope of dam, f_c is the compressive strength of concrete, f_R is the compressive strength of dam foundation

- Sliding stability along contact surface between dam body and foundation. The action effect function is:

$$S(\bullet) = \sum P_R$$

where $\sum P_R$ is the sum of all tangential actions on the dam foundation. The sliding stability resistance function is:

$$R(\bullet) = f'_R \sum W_R + c'_R A_R$$

where $\sum W_R$ is the sum of all normal actions on dam foundation, f'_R is the shearing rupture-friction factor on foundation surface, c'_R is the shearing rupture cohesion on foundation surface

- Sliding stability along dam body lifts joints. The limit state equation is similar to that above but actions and resistance are calculated for lift joints.
- Sliding stability along soft structural plane in deep foundation.

2.3.6 CDA, Canada

The following is taken from the CDA guidelines from 1995, which were updated in 1999 and are currently under revision.

Acceptance criteria for concrete dams: concrete gravity, buttress and arch dams and their foundations shall have adequate sliding resistance to withstand all reasonable loads and load combinations that could occur.

The concrete must have sufficient strength so that the loads will not result in excessive deformations or overstressing.

Concrete dams and other water-retaining structures shall be assessed on the basis of performance indicators such as:

- Position of resultant force (for the usual loading case the resultant of all forces should be in the middle third of the surface being analyzed. Dam designers

have recognized that this performance indicator is more useful than the “overturning factor” which does not provide any indication of the state of normal stress on the section being analyzed).

- Normal stresses at the heel and the toe.
- Average shear stresses acting on the surface. The net calculated driving force is considered to be uniformly distributed over the zone of calculated compression. These stresses are compared with the available shear strengths of the foundation, or the joint in consideration.
- Calculated sliding factors and strength factors. The resistance of a gravity dam against sliding on any surface is assessed by comparing the Net Driving Force with its Available Shear Strength. The ratio of the Available Shear Strength and the Net Driving Force is referred to as the Sliding Factor (SF):
$$sf = \frac{\text{Available Shear Strength}}{\text{Net Driving Force}}$$
. The available shear strength can be based on peak strength (function of angle of internal friction and cohesion) or residual strength (function of angle of sliding friction and residual cohesion). Different safety factors are applied for these different cases.

2.3.7 RIDAS, Sweden

The stability criteria in RIDAS TA (2003) has already been mentioned:

- Sliding stability according to the simplified criterion in Eqn. 2-7 and safety factors according to Table 2-1.
- Concrete and foundation strength. Allowed stresses are determined case-specific based on testing or engineering judgement of the concrete and foundation strength. Stresses are determined by Navier’s equation (or by finite element analysis). Safety factors for allowed stresses are not given.
- Overturning stability with safety factors according to Table 2-2 and force resultant within the mid third (mid 3/5th) of the base area

2.4 Discussion of failure mode definition

It must be pointed out that the summary given above is for a very small number of design guidelines and for general conclusions this is insufficient. What is obvious, based on the report by Ruggeri et al (2004) is that the sliding stability criterion in RIDAS does not, unlike many other codes, take advantage of cohesion. This is a conservative assumption that is justified when uncertainties are large and design and assessment is based on the safety factor method, but for the structural reliability analysis this is too conservative. As pointed out by Ruggeri et al, even a small cohesion gives significant contribution to the sliding stability. For assessment of an existing structures *a priori* assumption of shear strength could be made based on previous experience of similar foundation conditions or on the basis of engineering judgement. By taking

samples from the dam the *a priori* distribution of cohesion and friction angle could be updated to a *posteriori* distribution.

As for the overturning failure mode it can be noted that it is not explicitly stated in some of the guidelines. In the USACE manual (2003) it is explained that shear or bearing failure will occur before overturning does and therefore the position of resultant requirement is more important. However, penetrating this requirement, what is actually sought is that the whole base area should be in compression in the usual load case. The reason why the requirement does not explicitly consider stresses is not clear, but one explanation could be that, as mentioned, stress concentrations occur at the heel and toe of the dam, making stress definition difficult. Requiring that there should be no “tensile” stresses at the heel would likely result in over-conservative structures. Stress distributions derived by FE-analysis will result in different result than the beam idealization analysis, which is important to note.

The overturning criterion given in RIDAS, as well as other guidelines, can be questioned; first of all – does overturning really occur? To answer this question substantially more literature review and an analysis of reported failure modes of concrete dam failures is needed. Secondly, the cracked base assumption is only mentioned for the overturning case, not for the sliding case. This may, however not be a problem in the current guideline, since tensile stresses at the heel will automatically induce remedial works, such as anchoring, and the uplift is thus reduced. Some dam geometries could be especially sensitive to overturning failure of parts of the structure.

2.4.1 Failure modes in structural reliability analysis

It must be noted that the criterions above are derived for practical use and has been proven useful during a long period of time. When it comes to finite element analysis or structural reliability analysis the formulation is, however, less fitted for its purpose.

The procedure to use the position of resultant forces as a stability criterion may be appropriate in safety factor analysis, but in a structural reliability analysis it is not feasible, especially when compared to sliding stability. The probability of limit state violation of the sliding limit state can be considered as the probability of failure. The probability of limit state violation for the position of resultant force, on the other hand, is not directly comparable to failure but rather to cracking of the heel.

Safety factors are not possible to determine for the overturning failure mode if a finite element analysis is performed. The result of such analysis is stress and/or deformation distributions. If what is sought is really sufficient safety against tensile stresses or cracking of the heel, this should be reflected in the guideline.

In the project behind this thesis the failure modes used in RIDAS was at first assumed to be the “true” failure modes and focus was on defining loads and resistance. During the whole time questions like “can overturning really happen” have been asked to me, and slowly my opinion on the formulation of failure conditions has changed. At first for the sliding failure mode, where RIDAS does not account for cohesion, and later also for the overturning failure mode.

It is my opinion that a broader discussion of the formulation of failure modes to define the limit states in the structural reliability analysis is necessary. For now, and in this thesis, the limit states used for structural reliability analysis are:

- Overturning:

$$G = M_R - M_S \quad \text{Eqn. 2-10}$$

where G is the limit state, M_R is the resisting moment and M_S is the overturning moment.

- Sliding:

$$G = cA + N \cdot \tan \phi - T \quad \text{Eqn. 2-11}$$

where G is the limit state, c the cohesion, A the base area, N the normal force, ϕ the friction angle and T the forces parallel to the sliding plane.

3. Safety concepts

In the basic structural reliability problem, verification that the structure does not exceed a specified limit state is performed. This requires an analytical model describing the limit state and the model must include all the relevant basic variables. Basic variables are:

- Actions
- Material parameters
- Geometrical parameters

In the most simple case a load effect (action) S is resisted by the load bearing capacity R .

The traditional method to define structural safety is through a *factor of safety*, sf , where the resistance R and the action S shall fulfil the following requirement:

$$S \leq \frac{R}{sf} \quad \text{Eqn. 3-1}$$

The factor of safety is selected on the basis of experimental observations, past experience, economical and political considerations and should be large enough to provide sufficient safety towards the unwanted event that is assumed to occur if

$$S \geq R.$$

The *partial factor method* is a development of the factor of safety implying that the permissible actions (or required resistance) shall fulfil the relation

$$\frac{R}{\gamma_R} \geq \gamma_{Di} \cdot S_{Di} + \gamma_{Li} \cdot S_{Li} + \dots \quad \text{Eqn. 3-2}$$

where R is the resistance, S_D is the dead loads, S_L the live loads and γ_R , γ_D , γ_L partial factors. Actions with high variability can with this formulation be given greater partial factors than those with low variability, and thus allows for better representation of the uncertainties associated with actions and resistance (Melchers, 2001). Calibration of partial factors will be briefly discussed in chapter 3.4.1.

This thesis deals mainly with the structural reliability analysis described below, but the connection between the different safety concepts will be further described later (in chapter 3.4). There is substantial literature on structural reliability analysis, see e.g. Melchers (2001), Thoft-Christensen & Baker (1982) and Schneider (1997).

3.1 Structural reliability analysis

3.1.1 Basic reliability problem

The basic variables describing R and S may be random variables, including the special case deterministic variables, or stochastic processes or random fields (JCSS, 2001). All essential sources of uncertainties must be integrated in the basic variable model. Those are e.g.

- Physical or mechanical uncertainty
- Statistical uncertainty due to small sample of observations
- Model uncertainties.

A *limit state function* $G(x_1, \dots, x_n)$ describing the failure mode of interest is defined, where x_1, \dots, x_n are the basic variables. The *limit state* is defined to occur when

$$G(x_1, \dots, x_n) = 0 \quad \text{Eqn. 3-3}$$

and can be either a serviceability limit state (e.g. concerning the deformations or crack widths of a beam) or an ultimate limit state (e.g. material failure or structural failure) depending on the problem at hand.

If $G(x_1, \dots, x_n) > 0$ the limit state is not reached, e.g. failure will not occur. If $G(x_1, \dots, x_n) \leq 0$ the limit state is violated, e.g. failure will occur. (Schneider, 1997).

The probability, p_f , of limit state violation can be expressed as

$$p_f = P(G(R, S) \leq 0) \quad \text{Eqn. 3-4}$$

p_f is usually called the probability of failure.

For independent R and S the failure probability becomes

$$p_f = P(R - S \leq 0) = \iint_D f_{RS}(r, s) dr ds = \int_{-\infty}^{\infty} \int_{-\infty}^{s \geq r} f_R(r) f_S(s) dr ds \quad \text{Eqn. 3-5}$$

where f_{RS} is the joint density function and f_R and f_S are density functions of R and S , as shown in Figure 3-1a), and D is the failure domain where $G < 0$.

As the cumulative distribution function is given by

$$F_X(x) = P(X \leq x) = \int_{-\infty}^x f_X(y) dy \quad \text{Eqn. 3-6}$$

eqn. (2) can be written as

$$p_f = \int_{-\infty}^{\infty} F_R(x) f_S(x) dx \quad (\text{the convolution integral}) \quad \text{Eqn. 3-7}$$

where $F_R(x)$ is the probability that $R \leq x$ or the probability that the actual resistance R of the member is less than some value x . Let this represent failure. The term $f_S(x)$ represents the probability that the load effect S acting in the member has a value between x and $x+\Delta x$ in the limit as $\Delta x \rightarrow 0$. By considering all possible values of x , i.e. by taking the integral over all x , the total failure probability is obtained. This is also shown in Figure 3-2a) where f_R and f_S are drawn on the same axis. (Melchers, 2001).

Examples of possible failure modes in the ultimate limit state for concrete dams is overturning and sliding where the limit state functions, as discussed in chapter 2, are

$$G(R, S) = M_R - M_S \quad \text{Eqn. 3-8}$$

And

$$G(N, \phi, c, A, T) = N \cdot \tan \phi + c \cdot A - T \quad \text{Eqn. 3-9}$$

respectively.

3.1.2 Failure probability and safety index

For independent normal random variables and linear limit state functions it is possible to make an analytical integration of the convolution integral and in this case

$$p_f = P(R - S \leq 0) = P(Z \leq 0) = \Phi\left(\frac{0 - \mu_Z}{\sigma_Z}\right) \quad \text{Eqn. 3-10}$$

where $\mu_Z = \mu_R - \mu_S$ and $\sigma_Z = \sigma_R - \sigma_S$ and Φ is the standardized normal distribution function. μ_R and μ_S mean values of R and S , and σ_R and σ_S standard deviation of R and S . (Thoft-Christensen & Baker, 1982).

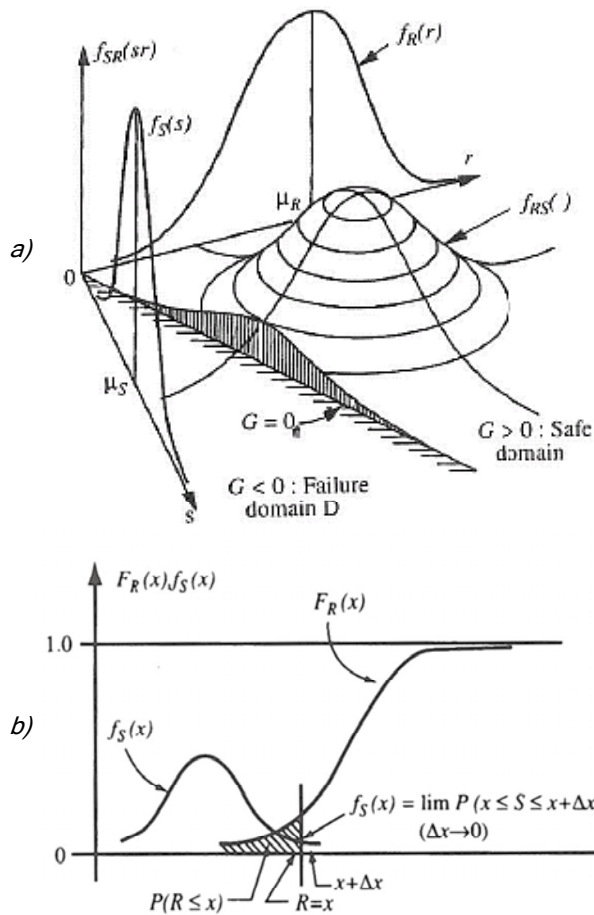


Figure 3-1 - a) joint density function b) basic R-S problem (from Melchers)

The Cornell safety index, β_C , is defined as

$$p_f = \Phi \left[\frac{-(\mu_R - \mu_S)}{(\sigma_S^2 + \sigma_R^2)^{1/2}} \right] = \Phi(-\beta_C) \quad \text{Eqn. 3-11}$$

A low value of β_C thus corresponds to a large probability of failure (small margin $\mu_R - \mu_S$ and/or large uncertainty $\sigma_R^2 + \sigma_S^2$). For normally distributed variables Eqn. 3-11 yields the exact failure probability. The Cornell safety index is, however, not unique. Non-

linear failure functions have to be linearized to calculate the safety index and the result will then depend on the choice of linearization point. This leads to different safety index depending on how the safety margin Z is defined.

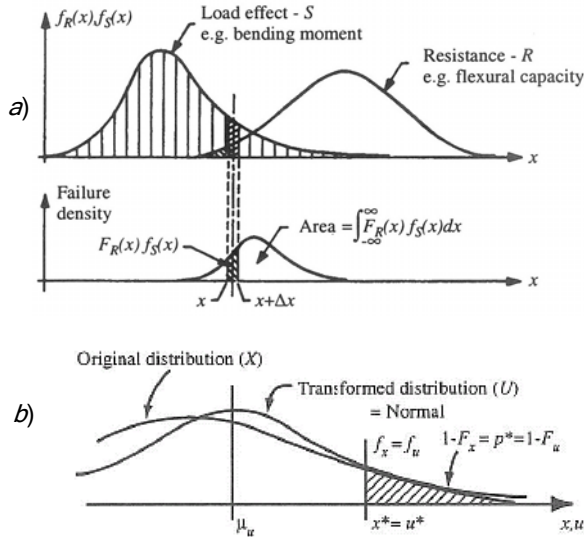


Figure 3-2 - a) f_R and f_S and integral giving the failure probability b) normal tail transformation.

3.1.3 First and second order methods

The linearization can be performed by expanding $G(x_1, \dots, x_n)$ as a first order Taylor-series about some point \mathbf{x}^* (see e.g. Melchers). Approximations which linearize the failure function are called ‘first order’ methods. If the original limit state function is concave around the origin p_f is underestimated.

In *first order-second moment methods*, FOSM, also safety index of limit state functions including non-normal variables can be calculated using their first two moments, mean value and standard deviation. The non-normal variables are then transformed into normal space. For uncorrelated variables, x_i , this is done using the transformation

$$Y_i = \frac{X_i - \mu_{X_i}}{\sigma_{X_i}} \quad \text{Eqn. 3-12}$$

where Y_i has $\mu_{Y_i} = 0$ and $\sigma_{Y_i} = 1$. A set of correlated variables first has to be transformed to a set of uncorrelated variables.

The safety index can then be calculated (after possibly linearizing the limit state function). The safety index now corresponds to the shortest distance from the origin to the failure surface in standard-normal space. Since all equivalent failure functions result in the same failure surface the result is a safety index invariant to choice of failure function. A schematic picture of a transformation from non-normal variables with a non-linear limit state function to linear limit state function in standard normal space is shown in Figure 3-3.

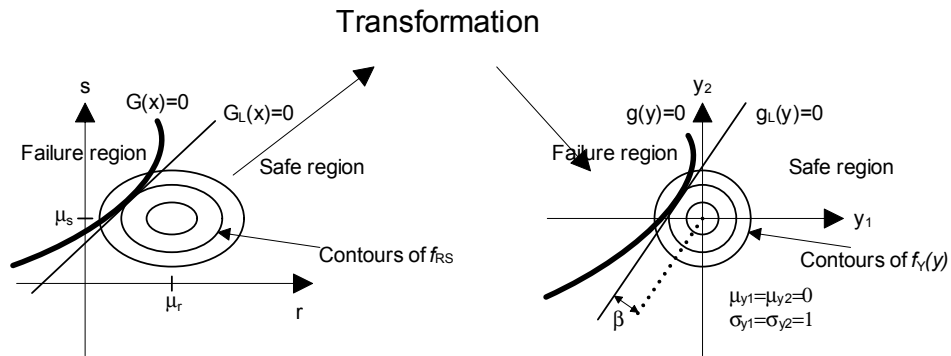


Figure 3-3 - Transformation of non-normal variable to standard normal space and linearization of limit state function.

The safety index is now given by

$$\beta_{HL} = \min \left(\sum_{i=1}^n y_i^2 \right)^{1/2} \quad \text{Eqn. 3-13}$$

where y_i represent the coordinates of any point on the limit state surface and the point giving the lowest β_{HL} is the “design point”, y^* . The safety index is called the Hasofer-Lind safety index (Hasofer & Lind, 1973).

In the special case when $M = R - S$, R and S are normally distributed and un-correlated, the safety index β can also be given a geometrical interpretation with reference to Figure 3-4, where it represents the number of standard deviations from the origin to the design point in the transformed system.

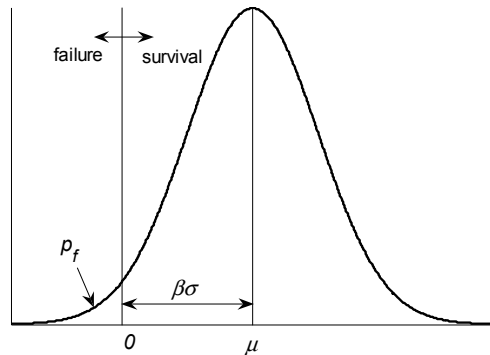


Figure 3-4 - geometric interpretation of β .

The design point represents the point of greatest probability density for the failure domain and the zone of the failure surface closest to y^* gives the greatest contribution to the total probability content in the failure region.

If α_i are the direction cosines, the coordinates of the y^* the coordinates can be written

$$y_i = -\alpha_i \beta \quad \text{Eqn. 3-14}$$

α_i represent the sensitivity of the standardized limit state function to changes in y_i and

$$\left(\alpha_1^2 + \dots + \alpha_n^2\right)^{1/2} = 1 \quad \text{Eqn. 3-15}$$

A low α_i indicates that the limit state function is not sensitive to changes in y_i and y_i might even be treated as a deterministic rather than random variable. High values of α_i indicate high sensitivity and that even a small change in y_i would result in considerable changes in β .

For non-normal distributions the failure probability is no longer exact but nominal, and it is therefore not useful to refer to failure probability, but more convenient to use the safety index β exclusively.

In the *first-order reliability method (FORM)* the random variables are no longer approximated by its first two moments (mean value and standard deviation). In transforming a non-normal variable Y to an equivalent normal variable U different choices of U can be made. In the “normal tail approximation” the probability density and the cumulative distribution function for U should be set equal to those of Y in the design point. This transformation is focused on fitting the tail of the equivalent normal distribution to that of the original non-normal one, as shown schematically in Figure 3-2b).

The reason that this is a useful transformation is that for the ultimate limit state of a common structure the probability of failure is very low and only the highest or lowest values of a parameter give contribution, hence the tail is of major importance.

There are a number of transformation methods, besides the normal tail approximation e.g. the Rosenblatt transformation and Nataf transformation (useful if only marginal distribution functions and correlation data is available).

Finding the safety index is an iterative process, for more information, see e.g. Melchers (2001).

The first order reliability method, often referred to as FORM, is one of the most frequently used for calculation of the safety index.

If the limit state surface has a significant curvature first-order methods may not be satisfactory. Higher order methods deal with the non-linear limit state functions, e.g. by attempting to fit parabolic, quadratic or higher order surface to the actual surface, centered on the design point. The most commonly used second order method is *second-order reliability method*, SORM, which is basically the same as FORM but with second order treatment of the limit state surface. The approximation with linear limit state surface becomes more accurate as the joint probability function gets “flatter” and thus as $\beta \rightarrow \infty$. For results with high β , FORM (first order reliability methods) and SORM (second order reliability method) will be the same.

The integrals of Eqn. 3-5 can also be solved by simulation techniques, e.g. by Monte Carlo simulation. This is a sampling technique where values for all variables are randomly drawn from their respective cumulative probability function and the probability of failure is given by

$$p_f = \frac{n(G(x_i) \leq 0)}{N_{trial}} \quad \text{Eqn. 3-16}$$

where $n(G(x_i) \leq 0)$ is the number of simulations which resulted in violation of the limit state and N_{trial} is the total number of simulations.

3.2 Bayesian updating

In the assessment of existing structures knowledge of the actual behaviour, loads and material properties can be used as input in the reliability analysis, by the use of Bayesian updating.

General information of material properties can often be obtained from building documentation and it is often also possible to estimate the COV from knowledge of the material (information of this is available in e.g. JCSS probabilistic model code (2001)). This information is however generic in nature and not connected to a specific structure.

The generic information can be used as so called *a priori* information. In an existing structure material properties can be measured (e.g. by testing of samples) and by use of

this new information and the *a priori* distribution an *a posteriori* distribution of the material property can be obtained. More information of Bayesian updating of material properties can be found in e.g. Thelandersson (2004), Melchers (2001) and JCSS (2001).

Knowledge of past good performance for a long period of time can also be used. This is however more difficult, as a long service time does not necessarily imply that the structure has withstood large forces and these are the most likely to cause failure. Even so, it may be of importance to include such information (Melchers, 2001)

Loads can be measured and updated in the same way as the material properties, but this is also a more cumbersome task. Time-varying loads will have to be measured for at least a number of years to be used as input.

3.3 Target safety index

In order to determine if the safety index calculated for a specific structure is sufficient, i.e. if the structure is safe enough, comparison to a target safety index is necessary. The safety of the structures is expressed in terms of the accepted minimum safety index or the accepted maximum failure probability.

The derivation of a target safety index is very complex and should be made by scientists, designers and politicians in cooperation. This may be a utopian dream, but it must be emphasized that decisions on tolerable risk and target safety have impact on society as a whole and should not be performed solely on the basis of engineering judgement. Derivation of target safety index could be performed on the basis of tolerable risks, but this is a difficult and controversial approach. This will be briefly discussed in the chapter 4.

3.3.1 Calibration to existing practice

According to Schneider (1997) target safety index can be calibrated to existing practice, assuming that existing practice is optimal. There are reasons to believe that this is true, as practice would change quickly if design of structures often resulted in failure. A way to proceed in the calibration of target safety index is to design a set of typical structures or structural elements according to existing codes with random parameters (loads and resistance) and uncertainties fixed. From these assumptions the reliability index β of each of the elements with respect to their requirements can be calculated. Iteration back and forth will result in a set of β -values within acceptable bounds and within these bounds a target reliability level β_0 can be found. This procedure has been used to calibrate national codes in many countries as well as the Eurocodes (European design guidelines, see e.g. ENV 1990, 2001) and BKR (Swedish design guidelines, 2003).

In the Chinese guidelines (China Electricity Council, 2000) a procedure for calibration of the target safety index is suggested and in short this is to

-
- Select typical structures or structural elements and divide into three groups in accordance with their safety grade (consequence class).
 - For each structure or structural element a coefficient ω_i is assigned, according to frequency of use, cost and experience of the structural type, and for each group
 - $$\sum_{i=1}^n \omega_i = 1 .$$
 - The typical structures are designed according to current codes and the amount of material used is minimized.
 - Statistic parameters and probability distributions of actions and resistance are used as input to determine β_{ii} for each of the typical structures.
 - The weighted reliability index, β_I , of a group of structures with the same safety level is determined. This reliability index is an index calibrated at this safety level according to relevant codes.
 - Existing typical structures are grouped according to safety level and the reliability index is determined for each structure. For each group of structures of the same safety level, a weighted reliability index β_2 is determined.
 - The target reliability index β_T is determined for each safety level according to β_I , β_2 (i.e. taking account to both existing structures, β_2 , and typical “designed” ones, β_I) and taking account of the optimal balance of safety and economy.

In NKB 55 (1987) the determination of the target safety index was based on comparative calculations carried out for more or less specific structures chosen from among structures of common occurrence. The result is normally a number of values varying within relatively wide limits, as the safety level is non-uniform, and the final choice of β_T must therefore be based on assessment of the calculation results.

It is important to note that the probability of failure (corresponding to the safety index) does not account for human error and human intervention effects and includes approximations. The result is that the failure probability becomes a nominal one. This is not a problem as long as it is used in a comparative manner between components. When it is used as a measure of the safety of a structure against more general societal risk criteria, human error and other effects may have significant influence and the comparison is thus not straightforward (Melchers, 2001).

3.3.2 Target safety index in different structural codes

For civil structures (house, bridge etc) in Sweden, the EU and other parts of the world target safety indices are specified, but this is not so for Swedish dams (there is for Chinese dams, but this appears to be the only exception throughout the world). Two

major arguments against the use of probability based evaluation of dams in Sweden are related to the lack of target safety index:

- The safety format used is based on safety factors and target safety index has thus not been needed
- The authorities does not specify the safety level, partly due to the strict responsibility of the dam owner discussed in chapter 4.

The most common way to find a target safety index for structural design is by calibration to existing practice as will be discussed.

Target safety index given in Schneider (1997), BKR (2000), ENV1990 (2001) and JCSS (2001) will be compared here and those according to China Electricity Council (2000) are shown in chapter 4. Only values for the ultimate limit state are discussed. The purpose of this part is to give an apprehension of the possible region of the target safety index, and to describe variables that influence it.

The relation between safety index and probability of failure for normal variables is given by

$$p_f = \Phi(-\beta) \quad \text{Eqn. 3-17}$$

where Φ is the cumulative distribution function of the standard normal distribution and Table 3-1 show the relation.

Table 3-1 - Relation between safety index and p_f .

p_f	0.5	10^{-1}	10^{-2}	10^{-3}	10^{-4}	10^{-5}	10^{-6}	10^{-7}	10^{-8}	10^{-9}
β	0	1.28	2.33	3.09	3.72	4.26	4.75	5.20	5.61	6.0

In JCSS (2001) it is pointed out that risk-benefit (cost-benefit) analyses should be applied when expected casualties are of importance.

Since risk is a product of the probability and consequence of failure, different failure probabilities are tolerated for high and low consequences. From Schneider (1997) the following table of target safety index depending on type of structure and type of failure has been taken.

Table 3-2 - Target safety index β /year, from Schneider (1997).

		Type of failure			
		Type A - serviceability	Type B - ductile	Type C - ductile, non-redundant	Type D - brittle, non-redundant
Consequences	Class 1 - no consequences	1	1.5	2	2.5
	Class 2 - minor consequences	1.5	2	2.5	3
	Class 3 - moderate consequences	2	2.5	3.5	4
	Class 4 - large consequences, medium hazards to life (bridges etc)	2.5	3	4.5	5
	Class 5 - Extreme consequences, high hazards to life (large dams etc)	3	4	5	6

Large dams often fall into the class 5 as the consequences can be extreme, either to human life or in economic consequences. Swedish dams are often placed in so called cascades, and the result of one dam breach can thus be the failure of several downstream dams as well. It must be pointed out, however, that this is not always the case. In many cases failure of a concrete dam would result “only” in loss of part of the dam and emptying of the reservoir (but still this might cause damage to downstream area). Emergency plans are available for most dams and consequences in human lives as well as in downstream consequences for other dams can thus be mitigated. Dams do not have redundancy and will in many cases (e.g. sliding of a concrete dam) exhibit brittle behaviour with no or very short warning. If consequences are large the resulting required β value is thus around 6, corresponding approximately to a probability of failure of 10^{-9} /year.

In Swedish design guidelines (for bridge and buildings, dams not included) the required safety level is given in Table 3- 3 below. The highest safety class, 3, is for structures where failure could result in loss of human lives.

Table 3- 3 - Target safety index from BKR (2003).

Safety Class	β /year
1	3.7
2	4.3
3	4.8

In Eurocode 0 (ENV-1990, 2001) target values for the reliability index β for the ultimate limit state is given for reference periods of 1 year and 50 years. Consequence classes CC1-CC3 are defined according to xx and the reliability classes RC1 to RC 3 of Table 3-5 are associated with those consequence classes.

When the main uncertainty comes from actions that have statistically independent maxima in each year, the values of β for a reference period of n years can be calculated according to

$$\Phi(\beta_n) = [\Phi(\beta_1)]^n \quad \text{Eqn. 3-18}$$

where β_n is the reliability index for a reference period of n years and β_1 is that for a reference period of 1 year. This can also be expressed as

$$p_{fn} = 1 - (1 - p_{f1})^n \quad \text{Eqn. 3-19.}$$

where p_{fn} is the probability of failure during the n year reference period and p_{f1} that during 1 year.

Table 3-4 - Definition of consequences classes. From Eurocode 0.

Consequences class	Description	Examples of buildings and civil engineering works
CC3	High consequence for loss of human life, or economic, social or environmental consequences very great	Grandstands, public buildings where consequences of failure are high (e.g. A concert hall)
CC2	Medium consequence for loss of human life, economic, social or environmental consequences considerable	Residential and office buildings, public buildings where consequences of failure are medium (e.g. An office building)
CC1	Low consequence for loss of human life, and economic social or environmental consequences small or negligible	Agricultural buildings where people do not normally enter (e.g. Storage buildings, greenhouses)

Table 3-5 - Target safety index, from Eurocode 0.

Reliability class	Minimum value for β	
	1 year reference period	50 years reference period
RC3	5.2	4.3
RC2	4.7	3.8
RC1	4.2	3.3

JCSS (2001) proposes target reliability values for ultimate limit states as shown in Table 6. These were obtained based on cost benefit analysis for the public at characteristic and representative, but simple, example-structures and are compatible with calibration studies and statistical observations. In this table ρ is defined as the ratio between total costs (construction costs plus direct failure costs) and construction costs.

It is pointed out that the type of failure is also of importance; a structural element that could collapse suddenly without warning should be designed for a higher level of reliability than an element where collapse is preceded by warning enabling consequence-reduction measures.

For most structures target values of the moderate consequences can be applied.

The relative cost of safety measures are given classes A-C. If large uncertainties (COV > 40 %) are associated with loading or resistance the additional costs to achieve a high reliability are prohibitive, the structure is in class A, and lower reliability class should be used. For low uncertainties (COV < 10 %) higher reliability class should be used as the increase of reliability can be achieved by very little effort, giving class C. The normal class B is associated with medium variability, normal design life and normal obsolescence rate.

For existing structures the costs of achieving a higher reliability level are high compared to the costs for a structure under design and therefore the target level should be lower. For structures designed for short service life, the safety index can be lowered by one or half a class. Quality assurance and inspections have an increasing effect on costs giving lower class, but at the same time uncertainties will be reduced, and a higher class therefore becomes more economically attractive.

Table 6 - Target safety index β /year, from JCSS. ρ = total costs/construction costs.

Relative cost of safety measure	Minor consequences of failure $\rho < 2$	Moderate consequences of failure $2 < \rho < 5$	Large consequences of failure $5 < \rho < 10$
Large (A)	$\beta = 3.1$	$\beta = 3.3$	$\beta = 3.7$
Normal (B)	$\beta = 3.7$	$\beta = 4.2$	$\beta = 4.4$
Small (C)	$\beta = 4.2$	$\beta = 4.4$	$\beta = 4.7$

As is seen in the above comparison, a number of different target safety indices exist. Most systems define different target safety indices depending on safety level. Only JCSS (2001) specifically gives different target index if the structure is already existing or meant to be built.

Obviously there are many different variables that may be included when target safety index is defined; consequences of failure, type of failure, uncertainties in input parameters, if the structure is an existing one or to be built etc. Target safety index can

be derived on the basis of calibration to existing practice or on the basis of cost-benefit, but as will be discussed in chapter 4 it could also be derived from tolerable risk, though this approach is not easily applicable.

3.4 Methods for reliability design

Often in the discussion of reliability analysis three categories are distinguished:

- Level 3 methods: attempt to obtain the best estimate of the probability of failure, making use of a full probabilistic description of the joint occurrence of various quantities and taking the true nature of the failure domain into consideration. These methods are not useful in practise.
- Level 2 methods: methods involve approximate iterative calculation procedure to receive the nominal probability of failure, using simplified representation of the joint probability distribution and idealisation of the failure domain. Structural reliability analysis as described above falls into this category.
- Level 1 method: the partial factor approach; a semi-probabilistic version of the traditional safety factor, commonly used in design.

The factor of safety is not included in this categorization as it is deterministic.

Traditionally, safety factors were selected largely on the basis of intuition and experience, but level 2 methods (e.g. structural reliability analysis) made it possible to relate the partial factors of the level 1 methods to the safety index β or the failure probability p_f (Melchers, 2001).

3.4.1 Method and calibration of partial factors

Design of structures according to e.g. BKR and Eurocode is performed on basis of the method of partial factors. This method is based on characteristic values and partial factors. For calculation of limit states, load combinations are defined. Account is taken to the probability of one or more actions occurring simultaneously with high values. Strongly correlated actions are regarded as one action, whereas actions supposed to be mutually exclusive are not combined (NKB 55E, 1987).

In Eurocode 0 the general format of effects of actions, E_d , is described as

$$E_d = \gamma_{Sd} E \left\{ \sum \gamma_{G,j} G_{k,j} + \gamma_P P + \gamma_{Q,1} Q_{k,1} + \sum G_{Q,i} \psi_{0,i} Q_{k,i} \right\} \quad \text{Eqn. 3-20}$$

where γ_{Sd} is the partial factor associated with the uncertainty of the action and/or action effect model, E is the “effect of actions”, $\gamma_{G,j}$ is the partial factor for permanent action j , $G_{k,j}$ is the characteristic value of permanent action j , γ_P is the partial factor for prestressing actions, P is the prestressing action, $\gamma_{Q,1}$ is the partial factor of for variable

action 1, $Q_{k,1}$ is the characteristic value of the leading action 1, $\gamma_{Q,i}$ is the partial factor of the leading variable action i , $Q_{k,i}$ is the characteristic value of the accompanying action i , $\psi_{0,i}$ is the combination value of variable action i .

The design value, R_d , of a resistance variable is given as

$$R_d = \frac{R \left\{ \frac{\eta X_k}{\gamma_m}; a_d \dots \right\}}{\gamma_{Rd}} \quad \text{Eqn. 3-21}$$

where R is the resistance, η is a conversion factor, X_k is the characteristic value of a material property, γ_m is the partial factor for a material property, a_d is design values of geometrical data and γ_{Rd} is the partial factor associated with the uncertainty of the resistance model.

The characteristic value is defined so that it has a certain probability of being exceeded, i.e. the $x\%$ -fractile.

- For resistance parameters the value of x depend on i.e. the variability, but is typically around 5 % for variables with significant variability.
- For action effect the characteristic value, in BKR (Boverket, 2003), is defined as the mean value (i.e. 50%-fractile) for permanent actions and the 98%-fractile of annual maximum for variable loads.

When the characteristic value of a variable action, $Q_{k,j}$ is combined with $\psi_{0,i}$ a frequent value is received (Melchers (2001), Eurocode 0 (2001), NKB 55E (1987), Boverket (2003)).

The procedure to calibrate the partial factors can be described by the flowchart shown in Figure 3-5. The boxes in grey are where structural reliability analysis is performed. More information is found in e.g. Melchers (2001), NKB 55E (1987), NKB 1995:02 (1995) and Thoft-Christenssen & Baker (1982).

The aim is to end up with

- An acceptable probability of failure and which is, as far as possible, independent of the kind of load, type of structure and material,
- Partial coefficients of loads independent of type of structure and material, partial coefficients of strength values independent of the type of load.

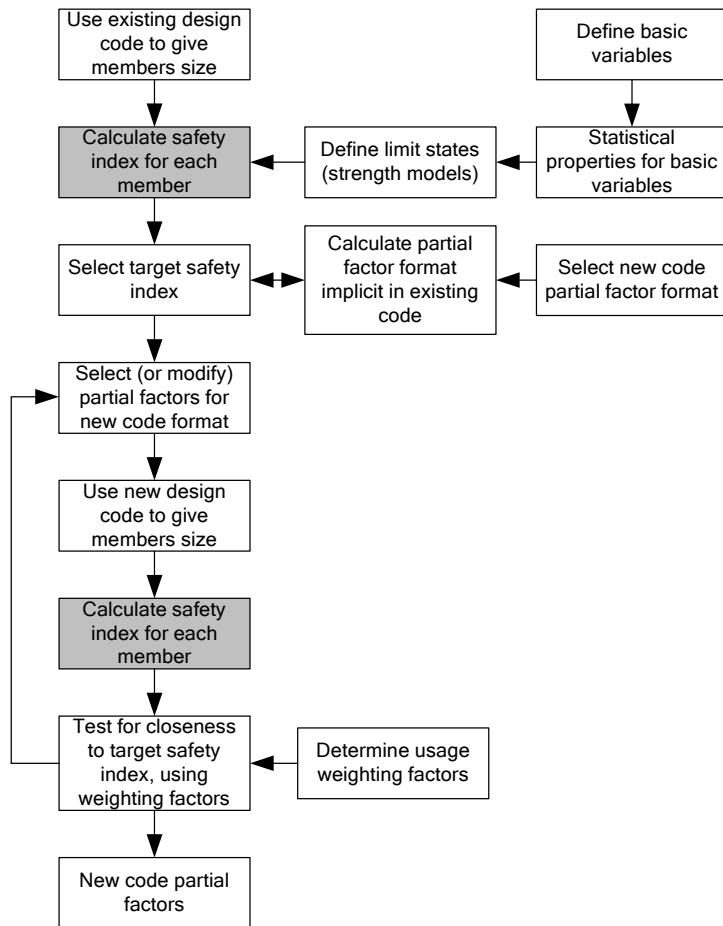


Figure 3-5 - Flow chart of code calibration, partly after Melchers (2001). Structural reliability analysis is indicated with gray.

Structural reliability analysis, definition of relevant limit states, definition of basic variables and statistical properties for basic variables are all essential elements needed if calibration is to be performed for concrete dams.

4. Risk management and dam safety risk management

In this chapter the general risk management process is briefly described in order to show how it can be, and to some extent is, used in dam safety. Approaches to derive tolerable risk are briefly discussed and a short introduction to the dam safety work in Sweden is given. The advantages of risk management in dam safety are described. The possibilities to use structural reliability analysis in the dam safety risk assessment process will be shown. In the last section the dam safety work performed at Vattenfall is described and it is shown how results from structural reliability analysis can be used as input in the prioritization of safety measures.

4.1 General risk management of technical systems

Absolute safety is neither possible nor desirable to attain, as it would be achieved only by use of infinite resources. Instead a tolerable level of *risk* must be found. Risk is the result of uncertainty; when no uncertainties are involved we can say with complete confidence what will be the outcome of a certain event and thus avoid the dangers imposed. On the other hand, as mentioned in Hansson (2002), for the uncertainty to constitute a risk something must be known about it - otherwise it will not be regarded as a risk. In many technical contexts, dam safety included, *risk* is defined as the product of *probability* of occurrence and the associated *consequence* of an unwanted event. There are several other definitions of risk but those are not discussed here. A *hazard* is a condition with the potential for an undesirable consequence, while risk describes the potential effect that hazard is likely to cause on a specific target.

Humans perform risk analyses intuitively in every day life. The use of formal risk analysis in “risky” business has been developed in areas such as human health, nuclear power, space engineering and for chemical industries. In dam safety, risk analysis is finding increasing acceptance.

Risk management is generally used for the whole process of identifying, estimating and evaluating risk, and decisions, implementation and monitoring of risk reducing measures (Ljungqvist, 2005). According to IRGC (2006) risk management can suggest alternatives for the same need so that the hazard is removed, isolate activities so that exposure is prevented or make risk targets less vulnerable to potential harm (prevent, control, mitigate). Figure 4-1 shows the general risk management process (IEC:1995), similar to that by Kemikontoret (2001), Hartford and Baecher (2004), SS-EN 1050:1996 and Kolluru (1996)).

Risk assessment has at least two different definitions. In this thesis it is defined in accordance with i.e. ICOLD bulletin 130 (2005), Ljungqvist (2005) and Hartford & Baecher (2004) and includes *risk analysis* (estimation of likelihood of unwanted events, estimation of their consequences and the uncertainties involved) and *risk evaluation* (consideration of the tolerability of the risk), see also Figure 4-1. This is however, not

the only definition of risk assessment and there are important issues of interpretation that has to be taken into account by risk managers before definition of the risk assessment process is made.

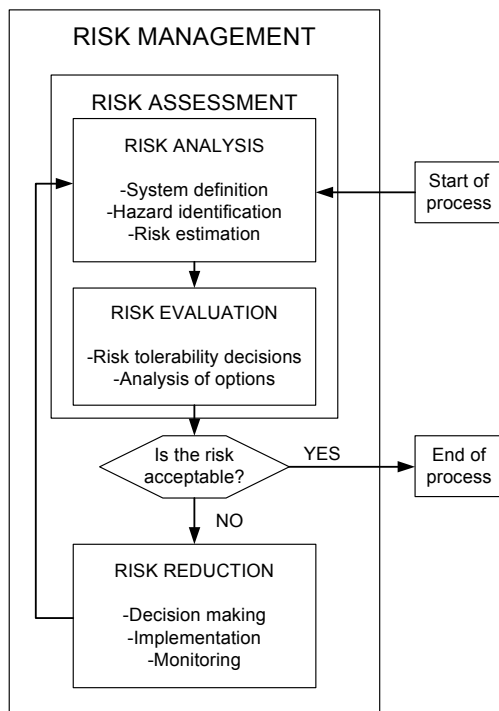


Figure 4-1 - Risk management process (IEC:1995).

4.1.1 Risk analysis

The purpose of risk analysis is to describe and estimate the risks that a system poses on its environment. The fundamentals of risk analysis are to de-aggregate the system into subsystems and reveal the connections and functions in order to understand the sources and magnitude of risk.

The risk analysis process should, according to IEC:1995 and Hartford & Baecher (2004), be performed according to the following procedure (also shown in Figure 4-2):

- Scope definition
- Hazard identification and initial consequence evaluation
- Risk estimation
- Verification
- Documentation

- Analysis update

The hazards should be identified together with the ways in which they could be realized. Known hazards should be stated and formal methods (as those described below) should be used to identify potential hazards.

The hazard identification may give rise to a very large number of possible scenarios and, in such case they can be qualitatively ranked, and quantification of the risk can sometimes be limited to those hazards giving the highest level of risk (Kolluru, 1996).

The risk estimation should “examine the initiating events or circumstances, the sequence of events that are of concern, any mitigating features and the nature and frequency of the possible deleterious consequences of the identified hazards to produce a measure of the level of the risks being analysed” (IEC:1995).

The list below gives short descriptions of some methods used for hazard identification and risk estimation. More information is found in e.g. Hartford & Baecher (2004), Bertsson (2001), Melchers (2001), Kemikontoret (2001).

- FMEA – Failure Modes and Effect Analysis.

A type of reliability analysis used to map out effects or consequences of individual component failure in the whole system. The system is broken down to component level, failure modes of each component are identified and effects of these on the system as a whole are systematically identified. If criticality of the considerations can be included the result is an FMECA. For analysis of failure modes FTA and ETA are useful.

- ETA – Event tree analysis.

Identifies the possible outcomes, and if required their probabilities, given the occurrence of an initiating event. The basic question is “What happens if...”. ETA reveals the relationship between functioning or failure of mitigating systems and are useful for identifying events that require further analysis by e.g. FTA. Figure 4-3 shows a simple example of an analysis where an event tree branch becomes the top event of the fault tree.

- FTA – Fault tree analysis.

A logic method focusing on an undesirable event (i.e. accident or malfunction of a system), called the top event. The fault tree is a graphical model showing the combinations of events that can result in the top event. It may also include human failures.

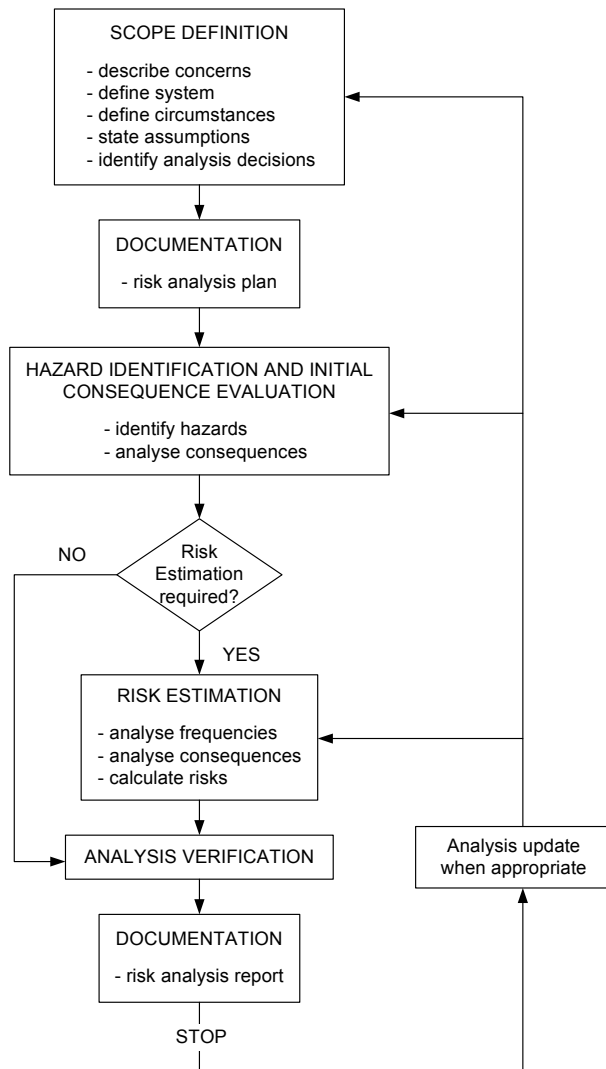


Figure 4-2 - The risk analysis process (adopted from IEC:1995).

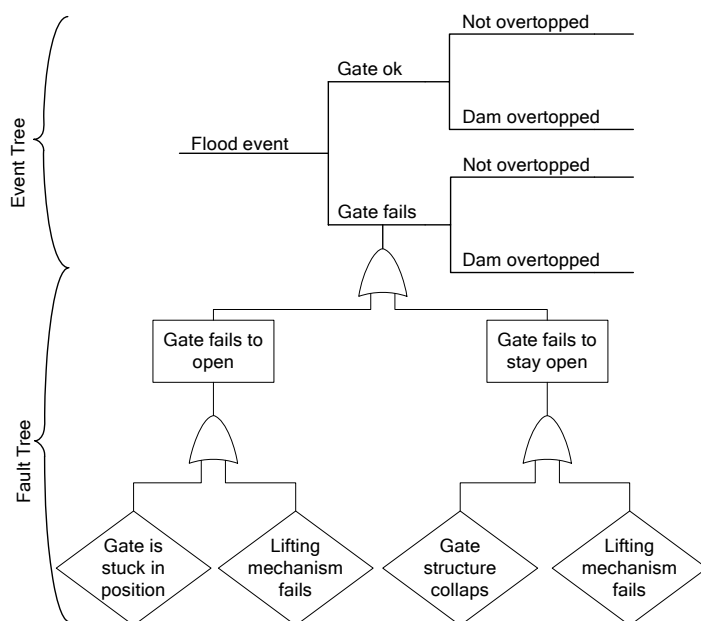


Figure 4-3 – Example of Event tree with Fault tree analysis of branch (incomplete chain).

4.1.2 Risk evaluation process

Risk evaluation is “the process of examining and judging the significance of risk” (ICOLD bulletin 130, 2005). In order to take decisions regarding the necessity to reduce risks a tolerable level of risk has to be defined. The last step in the risk assessment process is to compare the risk resulting from the risk analysis with the tolerable risk from the risk evaluation process to judge if risk reduction is necessary.

4.1.2.1. Tolerable risk

This section is a short summary and does not in any way claim to be complete. The aim is to give some knowledge of the difficulties inherent in decisions of tolerability for some further discussions on tolerable levels and target safety index for dams.

The HSE (2001) carefully distinguishes between *acceptable risk*, which is the risk everyone who might be impacted is prepared to accept, and *tolerable risk*, the risk within a range that society can live with, that might not be regarded as negligible or something we might ignore, but something we need to keep under review and reduce if and when we can. IRGC (2006) add that “acceptable” refer to a situation where risks are so low that additional efforts for risk reduction are not seen as necessary.

4.1.2.1.1. *Perception of risk*

The idea of tolerable risk is rather novel and aims at protection or risk minimizing when risks are felt to be high. The way people perceive risks and apply value judgement is complex and an important basis for risk decision-making and risk evaluation criteria. Among many factors influencing or apprehension of risk can be mentioned (see e.g. Kemikontoret, 2001) :

- Degree of benefit. Larger risks are accepted if an activity is beneficial. An industry can, e.g., be accepted in one area but not in another depending on the unemployment rate and thus benefit.
- Voluntary or involuntary. Risks which we can not influence are less accepted than voluntary risks, we are willing to go skiing or mountaineering, but less willing to accept risks, orders of magnitude smaller, from e.g. industries near our home.
- Potential of societal catastrophe. Relatively frequent small accidents are more easily accepted than one single rare accident with large consequences, even if the total number of casualties in the small accidents is equal or greater. This phenomenon is called risk aversion.
- Possibility to control. If the person bearing a risk also controls the risk, it will be more easily accepted than if someone else is in control of the risk.
- Known or unknown sources. Unknown sources are less accepted. New technology is often treated more strictly than already established technology.

Historically, protective measures were not taken until the hazard had shown its consequences. Vrijling et al (1998) points out that the public and political opinion of risk is to a large extent influenced by sudden and spectacular accidents (e.g. the Chernobyl catastrophe), and then not only by the accident itself but also by the attention paid to it by media and politicians.

4.1.2.1.2. *Principles and approaches to address tolerable risk*

As pointed out in Vrouwenvelder et al (2001) (a summary of a larger study by working group 32 within CIB) it is not the engineer who makes the decision about acceptance of risk from civil engineering activities, but politicians. They are, in turn, influenced by e.g. media, public opinion and lobby groups. Vrijling et al (1998) argue that decisions of acceptable risk should, in a modern and highly technological society, be based not only on historical and subjective ideas but on outcome of risk analysis and probabilistic computations based on an objective set of rules. Ramsberg (1999) points out that current societal decision-making about risk is most likely wasting resources and that potential gains from reducing the irrationality and arbitrariness are very large.

Hansson (2002), on the other hand, writes “the risk issues of different social sectors always have important aspects that connect them to other issues in these respective sectors. The technocratic dream, with its unified calculation for all social sectors, is insensitive to the concerns and the decision procedures of the various social sectors”.

IRGC (2006) is of the opinion that for society to make prudent choices about risks the scientific process (in risk assessment) should include both the natural/technical and social sciences, including economics. The process should be that, first, technical scientists produce the best estimate of the physical harm that a risk source induce and, secondly social scientists and economists identify and analyse the issues that individuals or society as a whole link with a certain risk.

As summarised by ICOLD (ICOLD Bulletin 130, 2005) the top principles to find a tolerable level of risk, from which sub-ordinate principles and the associated tolerability of risk criteria are derived, are:

- Equity – the right of individuals and society to be protected, and the right that the interests of all are treated with fairness;
- Efficiency – the need for society to distribute and use available resources so as to achieve the greatest benefit.

According to Vrouwenvelder et al (2001) acceptance limits originate from three different angles:

- Individual acceptable level of risk.
- Societal acceptable level of risk.
- Economic criteria

Individual acceptable level

The individual concern (HSE, 2001) is that of how a risk affects individuals, their family and things they value.

The tolerable level for individual risk can be derived from comparison with the overall risk of dying and can be approximated by

$$P(\text{casualty}) < \xi \cdot 10^{-4} \qquad \text{Eqn. 4-1}$$

where ξ depends on the voluntariness and profit. Involuntary risks of little benefit result in low ξ of 0.01-0.1 (Vrouwenvelder et al, 2001).

On individual level, Vrijling et al (1998) note a tolerance of 1000 times greater risks for voluntary than for involuntary activities with the same benefit.

Societal acceptable level of risk

Unlike the individual risk tolerability, where the risk is weighted against direct and indirect personal benefits, the societal risk tolerability must consider risk-benefit trade-off for the whole population. In the individual sphere, decisions can be amended if risks exceed the expected benefit, but in the societal sphere individuals can only choose their own risk acceptability to a limited extent. From the societal point of view the total damage in terms of casualties, material, environmental and economic damage must be considered. On a national level it is also important that the total risk is acceptable,

implying that for a large number of locations of a hazardous activity the acceptable probability of accidents for each of the locations is lower than in a case of few locations (Vrijling et al, 1998).

The societal risk is often presented by F-N curves as that shown in Figure 4-4. The requirement is $P(N_d > n) < A \cdot n^{-k}$, where N_d is the number of people being killed in one year in one accident, A ranges from 0.001-1/year and k is from 1 to 2. High values of k express the social aversion to large disasters.

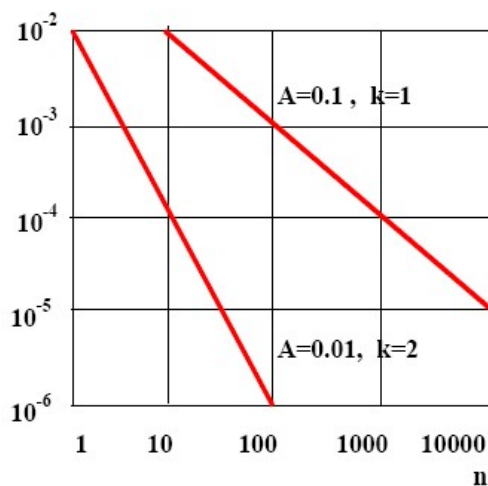


Figure 4-4 - FN-curve, from Vrouwenvelder et al (2001)

Economic criteria

Vrijling et al (2000) are convinced that the acceptance of risk can only be understood in a cost-benefit framework in the widest sense, where personal and national gain, capital and running costs, damage to environment as well as the risk play a part in the weighing process. A regulation where no attention is given to benefits of the activity is useless, as the weighing process between alternatives then become distorted. The risk of a large hydropower dam and the damage it does to the environment (in the building and operation phase or in case of failure) cannot be discussed apart from the benefit it brings to the national and local economy.

There are different descriptions on how an economic criteria should be formulated, but should include investments (and net capitalised profits), direct and indirect costs of failure (direct damage, cost of repair, future failure costs of the repaired structure), as well as probability of failure (Vrouwenvelder et al, 2001, JCSS, 2001, Vrijling et al, 1998). Difficulties are to determine the cost of failure, where, in some approaches, the value of a human life has to be defined. This can be defined in a number of ways; the net national product per inhabitant, the amount of money the individual would earn, one's value to oneself etc. Vatn (1998).

Vrijling (1998) suggest the economically optimal level of safety given as

$$\min(Q) = \min(I(P_f) + PV(P_f \cdot S)) \quad \text{Eqn. 4-2}$$

where Q is the total cost, I is the investment, PV is the present value, S is the total damage and if human life is involved the amount of damage is increased to $P_{dfi} \cdot N_{pi} \cdot s + S$

where P_{dfi} is the probability of being killed in case of the event, N_{pi} is the number of participants in activity i and s is the value of a human life.

One point to be made here is that, even though this approach is conceptually possible, it is not so easily applied and, above all, it is a matter of society (government) to decide which approach is to be used and, in case of this approach to be chosen, to put a value on human lives.

4.1.2.1.3. ALARP

A principle not discussed so far is the “As Low As Reasonably Practicable” (ALARP). This principle, states that only if further risk reduction measures (in time, money, etc) are GROSSLY disproportional to the risk reduction achieved, it is considered to be unreasonable (HSE, 2001, Ale, 2005). The ALARP principle is applied in the UK, where it is a matter for court to decide if the ALARP principle has been followed, and thus it can only be judged whether or not the ALARP demonstration is acceptable after the consequences has been incurred.

With reference to Figure 4-4, it can be said that if risks fall above the upper line risks are unacceptable, and below the lower line they are acceptable (no risk reduction needed). Between those lines the ALARP principle is valid.

Whether or not the ALARP principle should be applied is a governmental decision, or perhaps, if not prescribed by government, that of a company (for use within the company) to go beyond minimum legal requirements.

Unlike the UK, where the ALARP principle is applied and “everything that is not explicitly allowed is forbidden, unless it can be justified, where necessary in court”, the Netherlands has (according to ICOLD bulletin 130) the only known example of legislatively approved risk criteria. In the Netherlands “everything that is not explicitly forbidden is allowed” and risk reductions are weighted against risk in a much finer balancing act (Ale, 2005). In the Netherlands the onus is on the duty holder to get the risk modelling and numerical elements of analysis right and quantify the risk acceptability, and the political judgements are built into the risk acceptability criteria. Surety is provided by getting the numbers right (Hartford, 2006). In the UK acceptable risk is defined in terms of “not un-acceptable”, “not reducible”, and “worth taking”.

4.1.2.1.4. Tolerable risk in Sweden

In a report (Räddningsverket, 1997) is mentioned that several European countries have criteria for what is considered a tolerable risk. Risk analysis where tolerable risks are

needed as input are increasingly used in Sweden as well, but common criteria or guidelines does not exist.

4.1.3 Risk reduction

When the risk analysis has resulted in an estimate of risk and the risk evaluation has given tolerable levels it is up to managers to decide if risk reduction is necessary. If the ALARP principle is applied, risk reduction when risks fall in the “ALARP-area” (between unacceptable and acceptable) has to be decided upon. No further discussion on this matter is given here.

4.2 Dam Safety in Sweden

In 1990 the Swedish Committee for Design Flood Determination published their Guidelines on flood determination (Flödeskommitténs riktlinjer, 1990). After this, work to upgrade the dams for the new design flood criteria started. This work was made river by river, and since the discharge capacity needed for one reservoir is dependant on the retention and discharge of water of the dam upstream (and inflow to the river from the area between the dams), it was evident that there would be many possible solutions. The simplest would be just to build new spillways to pass the water on, but this would give severe damages along the river, especially to the cities near the Baltic sea.

Building of new spillways, or modification of old, would be necessary and dams would have to be heightened. Thus, it was agreed to use some larger reservoirs for retention of the water and in this way reduce the flow in the river. To do this, the first calculation was made assuming the dams to be infinitely high and the spillways to have the “real” width but to be as high as needed. After this consequences were analysed and some changes made - for example the effect of a new spillway could be tested and this would decrease the water level in the reservoir. The effects were studied and new modifications tested. At the same time the total cost for upgrading of the river was approximated and the consequences were studied and, finally, an optimal design for the river system was found and agreed upon by the stakeholders.

Projects to upgrade or rebuild dams for the new design floods should give a result that fulfils modern criteria also in other respects. In order to avoid mistakes and to pinpoint problem areas, especially those connected with the increased discharges or temporary water levels above the legal water retention level, many studies were started by the power industry and resulted in 26 VASO-reports. It is important to point out that in Sweden the dam owners has the full responsibility and there has been no authority defining dam safety requirements (besides what was decided in the permit for the dam, and supervision of maintenance by County Administrative Board). The appointment of Svenska Kraftnät (in 2004) to guide Länsstyrelserna (the County Administrative Boards) in their task to follow the dam safety work indicates an increased interest in the area. Several investigations have been initiated by the government (usually after periods with inundation problems due to high floods), but the conclusions have been that the dam safety situation is good and that the system is well functioning.

4. Risk management and dam safety risk management

According to Mill (2002) the Swedish model for dam safety can be separated into three parts:

- Demands by society expressed in comprehensive and general rules in Miljöbalken (the Environmental Act). Each dam owner has strict responsibility for all consequences resulting from a dam failure, meaning that the owner is liable to pay compensation (except in the case of war actions).
- RIDAS (2002), see explanation below.
- Supervision by authorities (Svenska Kraftnät and the County Administrative Boards (Länsstyrelserna)). This task will be developed to support dam owners ability to take their responsibility. RIDAS

RIDAS is the Swedish Guidelines for Dam Safety (Kraftföretagens riktlinjer för dammsäkerhet). The guidelines shall not be considered as law or directions but Swedish dam owners who are members of the SwedEnergy (Svensk Energi) are committed to follow the guidelines.

The overall objectives of the guidelines are to

- Define requirements and give guidance to sufficient and uniform dam safety
- Form a basis for uniform assessment of dam safety and for identification of upgrading needs due to dam safety issues
- Support governmental dam safety supervision.

RIDAS is formulated as two parts; *guidelines* and *application guideline*, where the application guideline gives detailed information and guidance on how to use the guidelines in practice.

The level of dam safety prescribed in RIDAS shall be achieved. Since the guidelines does not have the binding status of a law, and their purpose is to provide objective support for dam safety work, deviations from the guideline are allowed if the same or higher dam safety is achieved, as long as motives and documentation is clear and RIDAS can be said to specify the minimum safety level (RIDAS, 2002, Berntsson, 2001). Dam safety shall be carried on with good quality in planning, design, building, operation, monitoring, maintenance and emergency preparedness.

One of the most important fundamentals in RIDAS is the *consequence classification*, where dams are classified according to the consequences if dam failure should occur. The consequences (more specific, the incremental consequences, i.e. the incremental impacts which would not have occurred under the same natural conditions (e.g. flood)) are evaluated in terms of probability for loss of human lives and probability of damage on environment, infrastructure and other economic values. Table 4-1 shows the consequence classes in terms of human lives and Table 4-2 the consequences of damage. The highest number resulting from any of the tables is the actual consequence class. Safety requirements are differentiated, with higher demands for higher consequence classes (the highest class is 1A and the lowest 3).

Table 4-1 – Consequence classes according to RIDAS (2002). Classification with respect to probability of loss of human life or serious personal injury.

Consequence class	Consequence of a postulated dam-breach
1A	High probability of loss of many human lives
1B	Probability of loss of human lives or serious personal injury is not negligible
2	

Table 4-2 – Consequence classes according to RIDAS (2002). Classification with respect to probability of environmental, infrastructural or economic damage

Consequence class	Consequence of a postulated dam-breach
1A	High probability for very serious damage on - important urban infrastructure - considerable environmental values or very large economic damage
1B	noteworthy probability of damage on/to - important urban infrastructure - considerable environmental values or high probability of large economic damage
2	not negligible probability of noteworthy damage to - urban infrastructure - environmental values or economic damage
3	

According to RIDAS a dam owner shall perform dam safety inspections and reviews at the following levels and intervals:

Table 4-3 – Intervals of dam safety review according to RIDAS (2002).

Dam safety review	1A	1B	2
Operational inspections	Continuously	Continuously	Continuously
Dam monitoring	Continuously	Continuously	Continuously
Inspection	2/year	2/year	1/year
3-year inspection	1/3 years	1/3 years	1/6 years
Periodic Dam Safety Review (FDU)	1/15 years	1/24 years	1/30 years

In the Periodic Dam Safety Review a comprehensive and systematic analysis and valuation of the safety of the dam, based on a complete analysis of the whole system, is performed.

During all types of dam safety inspections and reviews, deviations from required or desired level of performance are noted. These have to be taken care of so that the dam fulfils required safety. For an owner of a large dam portfolio the dam safety work has to include some kind of prioritization of remediation works to use available resources in the best way possible. This prioritization can be designed in different ways and is at present under development by some of the Swedish dam owners.

During the period from 2000 to present times, dams are redesign and upgrades or rebuilt for the new design floods and also in other RIDAS aspects. The process of determining design floods for dams and the process of upgrading/rebuilding is quite complicated and the rebuilding/upgrading process will continue many more years.

4.2.1 Dam safety today

At present the majority of dams with insufficient discharge capacity has been rebuilt or upgraded and focus is shifting to other areas such as (Cederström, 2006):

- Risk management/Risk analysis Under development. Bench-mark studies have been performed and risk analysis is becoming increasingly used.
- Monitoring and surveillance. Historically this area was not well-developed in Sweden but recent research has come up with several new methods and these together with traditional methods and monitoring equipment will be installed and used at a great number of dams for continuous or periodic surveillance.
- PTO – People Technology Organisation. Dam safety operation, especially during complex situations, is to great extent influenced by uncertainties in human behaviour. Badly defined organization or complex technology can become critical during those conditions.
- Emergency preparedness. One of the areas pointed out in the VASO-reports. A pilot project by the power industry in cooperation with the authorities involved to improve the emergency preparedness plans have been completed and new technique with digital maps is being increasingly used.
- Ensuring human resources/competence.
- Security and Public safety. These areas are to some extent connected to dam safety but does only partly influence it.
- Debris

From a general point of view it is also important to notice the gradual shift from analysis of details to systems analysis.

4.2.2 Comments

As the dam owner is strictly responsible, the government and authorities does not specify any target safety for dams. Instead it is up to the owners to decide what is safe enough, and RIDAS is used as guidance. Ultimately, however, it is up to each company to decide if further risk reduction should be applied, and if e.g. the ALARP principle is to be used.

4.3 Risk management in Dam Safety

Dams are used for water e.g. irrigation and energy production all over the world. Their contribution to economic and societal development and welfare is substantial. At the same time dams is a potential threat to the society due to the remote, but still real, possibility that a dam might fail. A dam failure could have huge impacts; considerable numbers of people could lose their lives, most of the property in the threatened area would be damaged, heritage and works of art could vanish and the environment would be threatened directly by the water and indirectly by the release of toxic substances from installations damaged by the flood waters (ICOLD bulletin 130, 2005). As pointed out in (ICOLD bulletin 59,1987) even a smaller dam failure resulting only in operational loss will have serious economic consequences. Dam engineers have known of this since the first dams were built and dam safety is a very important area.

In ICOLD bulletin 59 (1987) a safe dam is defined as “a dam with appropriate reserves, taking into account all reasonably imaginable scenarios of normal utilization and exceptional hazard which it may have to withstand during its life”. In RIDAS (2002) the concept dam safety refers to “safety towards emergence of uncontrolled discharge of water from reservoir, which might cause damages in the vicinity or downstream area of the dam. It is also a conception of a qualified, interdisciplinary activity aiming at reducing risk of accidents and minimizing their effects”.

During the history of dams, risks have been considered and taken care of, but by an engineering standards-based approach using large safety factors, conservatism and engineering judgement.

Figure 4-5 shows an example of the risk decision framework. Typically civil engineering activities fall into the upper part (A); codes and standards are extensively used and deal with most uncertainties, good practice and engineering judgement supplements where necessary. The risk analysis is thus made implicitly. In more complex situations risk-based analysis is used.

Dam safety decision-making, on the other hand, falls into the mid part. This is since in dam safety, codes and standards are not as well-developed and used and consequently decisions have to large extent been based on good practice and engineering judgement. Decisions based on risk analysis or assessment is now becoming increasingly used. In cases where uncertainties or economic implications are large, decisions may even be dominated by company or societal values (Hartford & Baecher, 2004). The result is that

decisions in dam safety are to larger extent than in other civil engineering activities influenced by the complex risk apprehension and acceptance of the public.

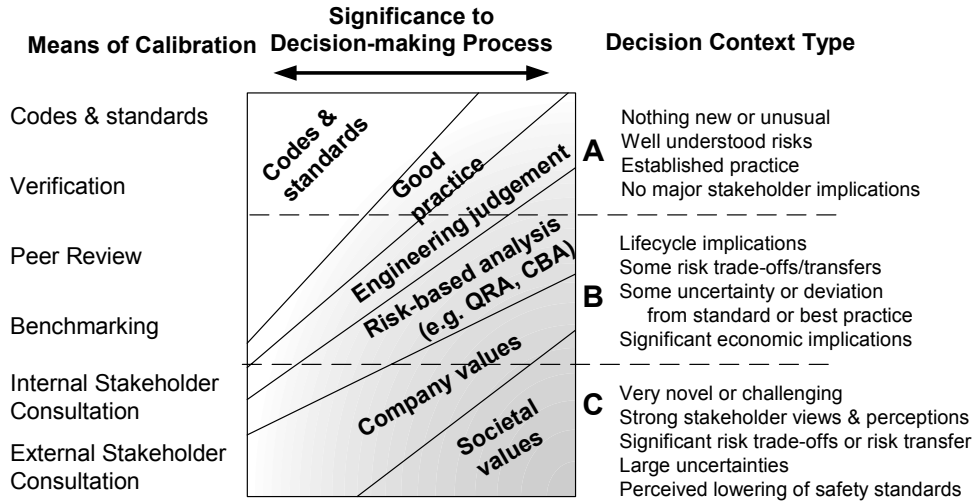


Figure 4-5 - Risk decision framework (from Hartford & Baecher, 2004, referring to UK Offshore Association, Brinded, 2000).

The use of risk analysis and assessment in dam engineering is still in its infancy, but becoming increasingly used worldwide. As pointed out by ICOLD bulletin 130 (2005) uncertainties are all-present in dam design, but dealing with uncertainty is such an intrinsic part of work that managers and designers do not give this conscious consideration and overlook the fact that the main part of their work is risk management. This means that risk analysis is, and has been, performed at all times, but that this is often not performed in the structured and reflective way described in the preceding sections.

The application of risk analysis in dam safety management is, among other things used to (ICOLD bulletin 130, 2005):

- Determine the consequence category of a dam,
- Assist in developing more effective surveillance processes,
- Improve conventional dam safety assessment processes,
- Demonstrate a sound understanding of the sources of risk and their relative contributions,
- Determine resource requirements for investigations,
- Determine how analysis and surveillance should be allocated to a particular dam,

- Prioritise dam safety modifications and improvements across a portfolio of dams,
- Communicate dam safety recommendations and/or decisions to financial planners, senior management, regulatory bodies and the public.

It has been mentioned already, but the importance of considering the whole system when performing the risk analysis must not be underestimated. When analysing a particular dam this usually means that the whole river system has to be seen as the system, as shown in Figure 4-6.

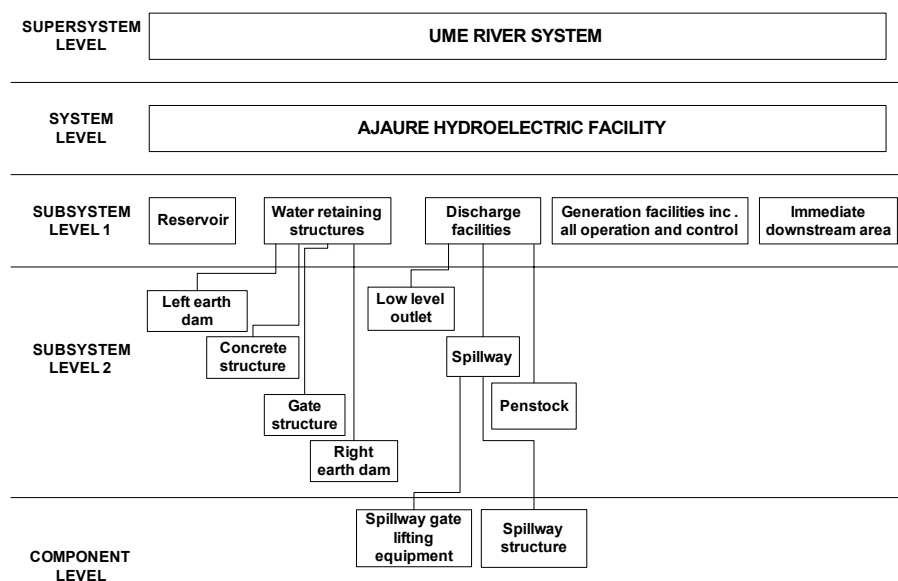


Figure 4-6 – Example of a block diagram (Vattenfall AB, 2000. By courtesy of Vattenfall).

The limitations of risk assessment for dams are among others the difficulty to reliably quantify the probability of failure or an incident that are not amenable to analysis, the difficulty to estimate the consequences of dam failure, the lack of widely recognised and accepted methodology for determining tolerable risks and the lack of acceptance in society of the concept of tolerable risk (ICOLD bulletin 130, 2005).

Risk reduction includes activities such as ensuring the structural integrity of the dams for all possible events, that operation of the dam does not endanger it in any way and that the operational personnel can deal with all possible situations, ensuring that discharge capacity is sufficient for design floods etc. Consequence reduction includes activities such as early warning and emergency preparedness plans, cooperation with

rescue corps, etc. All of these activities include uncertainty, sometimes to great extent, which make it difficult to know when safety is sufficient and when it is not.

4.4 Structural reliability analysis in dam safety

4.4.1 Target safety index for dams

A risk assessment includes both risk analysis and risk evaluation. The structural reliability analysis can be used to give an estimate of the risk (in terms of the safety index or probability of failure), but for the risk estimation a target safety index is needed.

From the discussion of chapter 3 and section 4.1.2.1 different approaches to derive a target safety index can be distinguished, but the only straightforward is that of calibration towards existing practice. Derivation based on tolerable risk, as that shown in Vrijling et al (1998) may give hints on acceptable levels but is a matter for governmental decisions. It should also be pointed out that, as discussed by Melchers (2001) the probability of failure (correspondent to the safety index) does not account for human error and human intervention effects and include approximations. The result is that the failure probability becomes a nominal one. This is not a problem as long as it is used in a comparative manner between components. When it is used as a measure of the safety against more general societal risk criteria, human error and other effects may have significant influence and the comparison is thus not straightforward.

If the ALARP principle is applied, the target safety index would give the lowest allowable safety index (maximum allowable failure probability) and any further risk reduction would be decided upon based on the ALARP.

As pointed out by JCSS (2002), for existing structures the costs of achieving a higher reliability level are high compared the costs for higher reliability of a structure under design. Therefore the target level could be lower for existing structures. This is also pointed out by R ddningsverket (1997) “risks related to new activities should be lower than those tolerated for existing activities for the following reasons:

- The aim of society is, and has been, to continuously improve the safety level
- It is easier to achieve risk reduction during design of new construction than by making changes in existing ones
- Choice of location can be used to reduce the risk level for the public in new activities (perhaps not applicable to dams, but rather to industries).

As described in chapter 3 the way to set target safety index for civil structures has been by calibration to existing practice. The target safety values for other structures can not be “just” used for dams, the reasons are that

- The calculated safety index is a nominal one and comparison between components is helpful, but comparison between structures of different types

(especially when failure modes and loading conditions differ) may not be correct

- Consequences might not be comparative
- Dam safety risk management is, as pointed out in section 4.3 to larger extent than other civil structures affected by value judgement and this should be reflected.

Based on calibration and judgement by experts, the target reliability index of bearing capacity of concrete gravity dams and reinforced concrete hydraulic structures are listed in “The standards compilation of water power in China” (China Electricity Council, 2000), shown in Table 4-4. It is, however, not defined what reference period this table refer to. A reference period of 100 years for Grade I structures and 50 years for Grade II and III is mentioned. Use of equation 3-18 (Eurocode) in chapter 3 then gives $\beta_T = 4.75$ for the first type of failure and $\beta_T = 5.15$ for the second type of failure of grade I structures.

As pointed out in ICOLD bulletin 130 comparisons between risk tolerability in different countries is not straightforward. “Since the risk evaluation stage is where societal, regulatory, legal, owners and other values and value judgements enter the decision process it should not be surprising that country to country variations, and indeed within country variations, will be more evident in risk evaluation than in any other risk assessment process” (ICOLD bulletin 130, 2005). This means that the target safety index from Table 4-4 can not be immediately used for Swedish conditions.

Table 4-4 - Target safety index of in Chinese “The standards compilation of water power in China”.

Safety grade of structures		Grade III	Grade II	Grade I (highest importance/conseq. of failure)
Type of failure	First type (failure with "warning")	2,7	3,2	3,7
	Second type (sudden failure without apparent signs)	3,2	3,7	4,2

If a target value is to be specified for dams a broad discussion among government and dam owners is necessary. It must be pointed out that the setting of a target safety value should not be performed by engineers alone, but economists, politicians and social scientists should also be involved. There are a number of questions that need be discussed: Is the target value to be calibrated to existing practice? Is it to be based on societal values as well? Are new dams (or parts of dams) supposed to have higher safety index than existing ones? Are dams to be separated into different consequence classes (as in RIDAS) with different target safety index?

But perhaps the setting of a target does not have to be very complicated: RIDAS is today used as a guideline and dams fulfilling the safety “requirements” are considered

“safe enough”. This means that they should be considered safe even by use of structural reliability analysis, and thus a target safety index can be derived.

4.4.1.1. Calibration of target safety index

An attempt to derive target safety index for Swedish dams has been performed as a master’s thesis by undergraduate students Jill Holmberg and Lucas Ahlsén under supervision by the author of this thesis.

The procedure was to

- Choose “typical” dam structures. Based on some data from Vattenfall “typical” dimensions of gravity and buttress dams were chosen. Gravity dams were defined to have a crest of certain width, the downstream side was considered to have a slope of 50 degrees and two types of buttress dams (one with vertical and one with inclined front) was tested. All dams were considered to have a freeboard of 1.3-1.7 m (depending on height).
- Design according to current practice. RIDAS application guideline was used to set the requirements. A dam with certain dimensions (height, crest width, etc) was given a width so that the safety factors of RIDAS (sliding and overturning) were fulfilled.
- Define basic variables. This is the most difficult part, as the information is scarce. Also this is the most important part as the input affects the safety index. Sensitivity analysis of the basic variables was performed, but for the most part the basic variables are taken according to that shown in chapter 6 of this thesis. For exact information, see Ahlsén & Holmberg (2007).
- Calculate the safety index. This was done using the computer software COMREL (RCP, 1997).

The results indicate that for gravity dams the safety index (thus safety) decreases with increasing height as shown in Figure 4-7, whereas the safety of buttress dams increases with increasing height in case of overturning and decreases in case of sliding. The failure modes considered was that of sliding and overturning, and this might be questioned. In the sliding case cohesion was taken into account (even though this is not considered in RIDAS). The results indicate that the current guideline does not result in a uniform safety level.

The analysis of the results is all but simple, as many factors come into play. Here only some short notes are summarized:

- For the overturning of a gravity dam the chosen geometry has impact. When the same calculations were performed for a triangular-shaped geometry, the result is a more uniform overturning stability. However, completely triangular-shaped does not exist, which indicates that the design guideline is not very well fitted for “typical” dams.

- Sliding of a gravity dam is heavily influenced by the cohesion. As cohesion is not taken into account in RIDAS, a triangular-shaped geometry without cohesion gives a steady safety level with $\beta = 1.5-1.4$ (for $h = 15-30$ m), whereas if cohesion is taken into account the same geometry gives $\beta = 7.6-6.2$ for the same heights. This is since the base area (at which the cohesion is active) increases by only a factor of 2, while the vertical and horizontal forces increases with a factor of 4. If the “safe” dams had safety index of only 1.4 (corresponding to approximately $p_f = 0.07$, i.e. extremely high) they would have to be rebuilt and we would probably have seen dam failures due to sliding.
- For buttress dams the explanation of the sliding case is the same as for gravity dams.

Non-uniformity of the safety level of guidelines means that resources are likely to be used inefficiently – if the design code imply that a structure is unsafe, when in fact it is safe enough, and remedial works are performed, that would have better been spent on another structure, which might have in fact been deemed safe according to the code, but was not.

More information of procedure and findings are given in Ahlsén & Holmberg (2007).

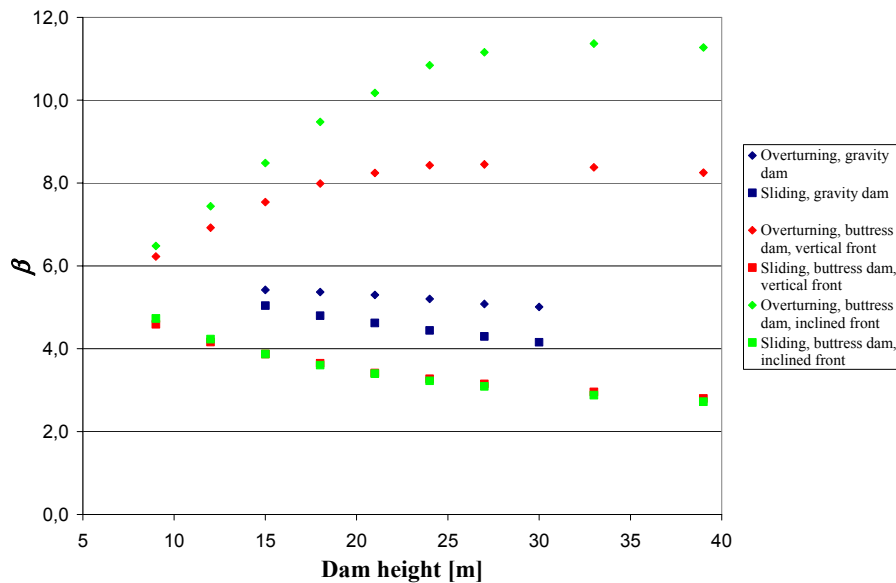


Figure 4-7 - β as function of dam height. Overturning and sliding of gravity dam, buttress dam with vertical front plate and buttress dam with inclined front plate.

4.4.2 Structural reliability in the dam safety in the near future

Until further development in this area states differently, the routine risk and safety assessment should preferably be carried on as presently done, using deterministic approach (safety factors). When a dam does not fulfil performance goals and a more detailed risk and safety assessment process is initiated the use of structural reliability analysis is advantageous. The use of object specific information in the analysis gives more exact information of the performance, resistance and actions and may be used to calculate the safety index of that specific structure. The process can be illustrated as shown in Figure 4-8, where, first, an assessment is performed based on the present design guidelines and, secondly, if the required safety level is not fulfilled, structural reliability analysis is used in the assessment. Comparison to a target safety index will then answer the question “is it safe enough?”. Questions regarding limit state formulation (failure modes) and probabilistic descriptions of loads have to be solved before it can be used in practice.

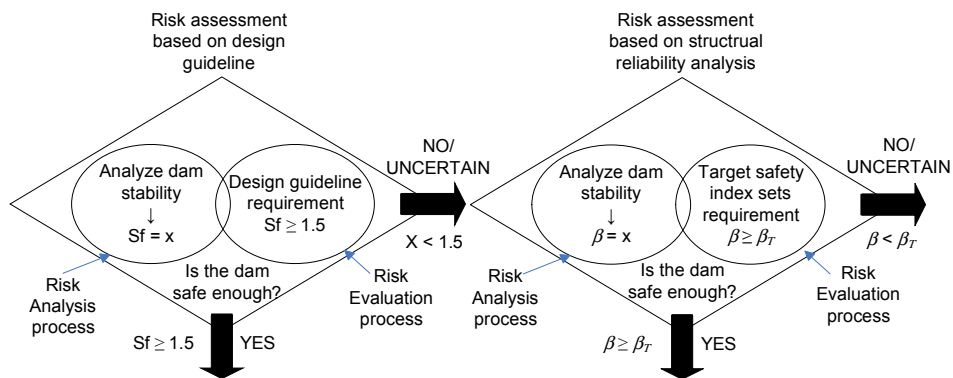


Figure 4-8 - Assessment procedure.

4.4.3 Structural reliability in the dam safety of tomorrow

When the use of structural reliability analysis in dam safety is sufficiently developed some different applications can be mentioned:

- Calibration of partial factors for design model based on partial factor-design.
- Design of more complex structures and structures where larger/smaller target safety (than according to design guideline) is required.
- Use in analysis of a specific dam. When safety according to the design guideline (deterministic/semi-probabilistic) is insufficient, use of monitoring

result, “proof-loading” (i.e. that a dam has survived for 40 years) etc can be used for thorough analyse of a structure.

- Input to quantitative risk analysis or assessment.
- Prioritization of remedial works
- Identify main sources of uncertainty (which loads are most important for an “unsafe” condition) in order to focus remedial works where it gives the best results.

4.5 Dam safety at Vattenfall

During the years 2002-2007 Vattenfall are upgrading and rebuilding approximately 40 dams to withstand floods with return period of about 10 000 years (flood calculation according to Flödeskommitténs riktlinjer). All the dams are designed for larger amount of water and the purpose is to increase the safety. In some cases dams will be rebuilt to increase the discharge capacity and in others the height of the dam crests will be increased to withstand larger water levels. Some dams will have a combination of both these improvements. In addition, measures to improve e.g. stability and erosion protection will be taken.

4.5.1 Risk management process

The dam safety work at Vattenfall is based on RIDAS, but a lot of additional improvements are also made. An example of the Dam Safety Management Process at Vattenfall is shown in Figure 4-9. Similar figures can be found in e.g. Hartford & Baecher (2004). The aim of risk management is to collect all questions related to dam safety and ensure that no important questions are forgotten. The three main parts are

- *Operation and Maintenance* - the normal operation of the facilities, the maintenance of emergency preparedness plans, the on-going monitoring and surveillance, and other basic maintenance work that is carried out at the facilities.
- *Overall Risk Management* – overall planning, prioritization of measures to be taken, follow-up, etc in order to have good and uniform dam safety.
- *Risk Management in Depth for a Particular Dam* – when simple measures are not adequate to correct deficiencies of a dam, a number of possible measures can be taken, and to choose the right action an in-depth risk management/analysis is performed for the specific dam.

In Figure 4-9 the diamond boxes are the risk assessment, as shown in Figure 4-10. The systematic risk assessment described previously has been used in a number of studies and will be further developed and used as standard procedure, especially concerning the in depth risk management of a particular dam.

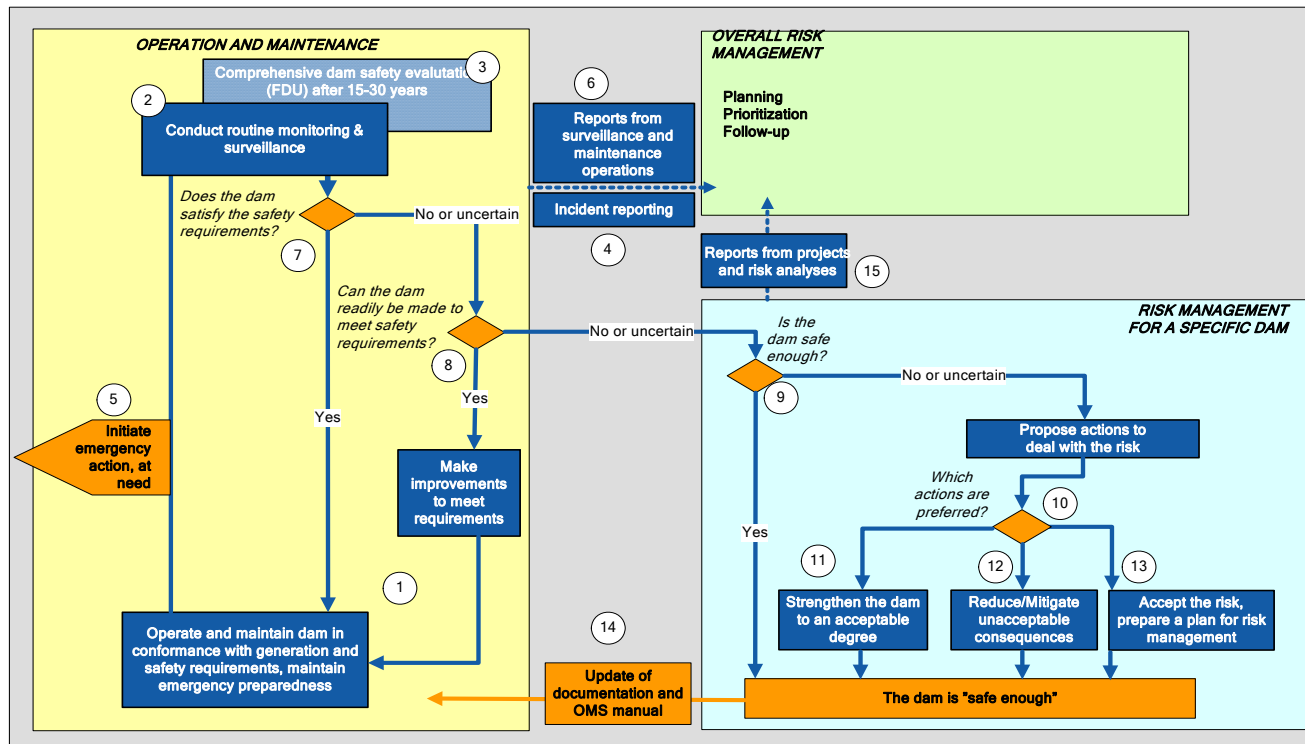


Figure 4-9 - Dam safety risk management process (Vattenfall AB, 2006, by courtesy of Vattenfall.)

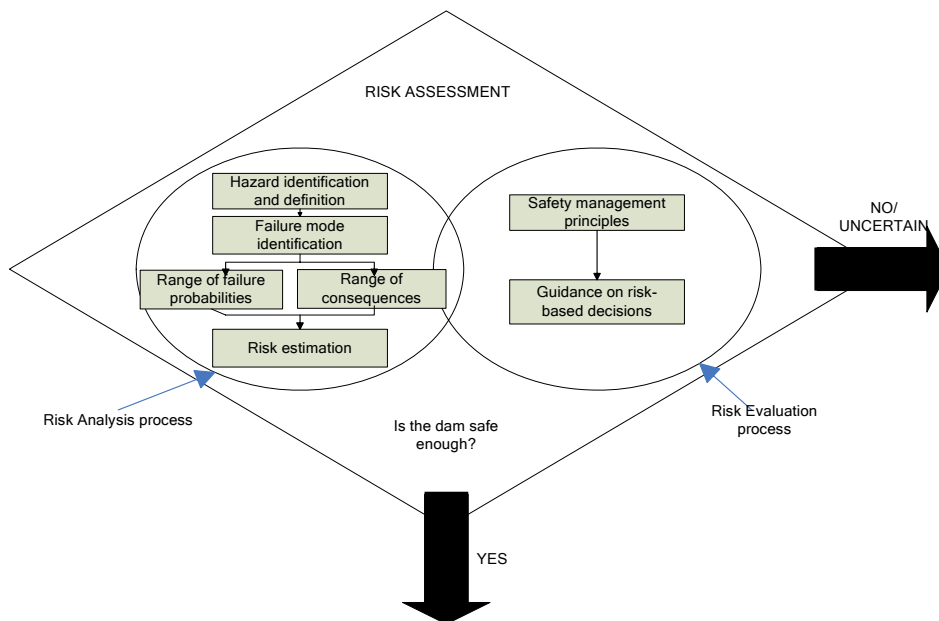


Figure 4-10 - Risk assessment (ICOLD, bulletin 130, 2005).

To achieve a good safety level throughout the entire dam portfolio, and focus resources on the dams where it is most urgent, a prioritisation system for known deficiencies is necessary. This is a vital part of the overall risk management and one of the major challenges at the time being is to develop this system to become fully operational.

4.5.1.1. Deficiencies and valuation

Deviations from specified level or function of features are divided into three groups; *physical deficiencies of the dam*, *deficiency in dam surveillance* and *deficiency in management, surveillance methods or working routines*. All of these are serious for dam safety. Deficiencies are found by inspections or monitoring.

Physical deficiencies are divided into reported and potential deficiencies. Examples on physical deficiencies are ability to retain or discharge water, e.g. leakage through a dam or insufficient discharge capacity. Each identified deviation is analysed with respect to dam safety based on four aspects linked together according to Figure 4-11 to give the *vulnerability index*. All criteria are represented by numbers between 1 and 5. The reason for the 1-5 scale is that deficiencies identified at the earlier Dam safety reviews (FDU) were given numbers from 1-5, which meant that already existing valuations was possible to use without re-work. The 1-5 rating is just a relative measure of safety and may be substituted by probabilities in the future. In the vulnerability index, rating 5 represents the most unfavourable event; large magnitude of deficiency, high criticality

4. Risk management and dam safety risk management

etc., and rating 1 represents the case of no magnitude of deficiency etc. The total vulnerability thus varies between 1 and 625. The aspects taken to consideration are:

- *Magnitude of the deficiency (M)* between performance capacity and desired capacity of the feature of interest, meaning that the capacity is compared to the capacity of a feature considered to be “safe” or “sufficient”. Here rating 1 is behaviour as desired and rating 5 complete or nearly complete loss of desired function. This is further described below.
- *Criticality of component or system (C)* of the feature. Rating 1 is a component with redundancy or a component not critical to the system while rating 5 is no redundancy of a critical component. In dam safety aspects many features are critical, e.g. gates and dams, as there exist no redundancy, resulting in 100% criticality.
- *Inability to detect and respond to deficiency (I)*. The ability to, in an emergency situation, detect and arrest the deficiency before it develops and leads to dangerous situations. When no measures are in place to prevent failure (interrupt started failure sequence) or mitigate the effects the “inability” is 100 %. Rating 1 corresponds to ability to detect and arrest while rating 5 means that no reliable method to detect and arrest the failure sequence is available.
- *Frequency of loading (F)*. Rating 1 corresponds to a loading frequency of approximately 1/1000 to 1/10000 years, while rating 5 is once or several times per year.

For each consequence class a *consequence index* is assigned. Combining the *vulnerability index* with the *consequence index* gives the *risk index*.

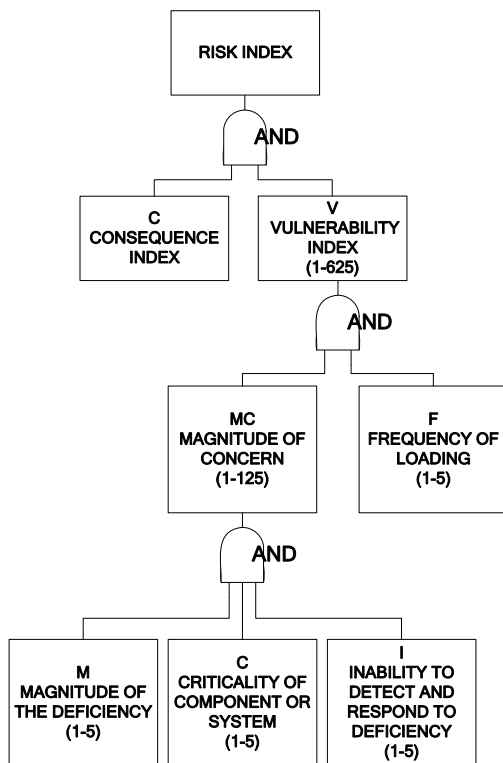


Figure 4-11 - Logic structure of risk index. (Vattenfall AB, 2006, courtesy of Vattenfall)

4.5.1.1.1. Magnitude of deficiency

The magnitude of deficiency can be illustrated as shown in Figure 4-12. The capacity can be described as a random variable due to inherent uncertainties in resisting factors, uncertainties in actual discharge capacity etc, and the demand can be described as a random variable due to uncertainties in loads, size of design flood etc. When the capacity is less than the demand, a deficiency exists.

Putting a rating on M is difficult and development is ongoing. A proposal on how to evaluate “magnitude of the deficiency” for stability of dams could be according to the following, where sf is the factor of safety. Other limits may be appropriate.

$sf > 1.5$	→ $M = 1$
$1.3 < sf < 1.5$	→ $M = 2$
$1.15 < sf < 1.3$	→ $M = 3$
$1.0 < sf < 1.15$	→ $M = 4$
$sf < 1.0$	→ $M = 5$

M could also be given a probabilistic interpretation and structural reliability analysis could be used to estimate it.

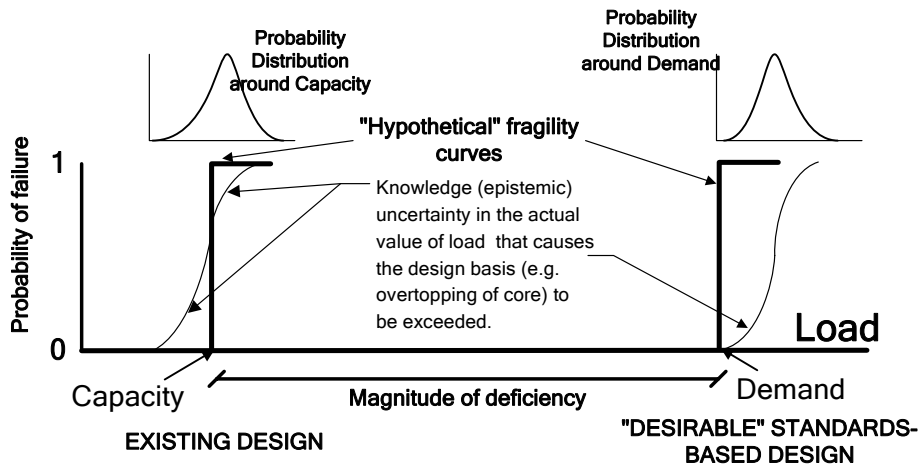


Figure 4-12 - Magnitude of deficiency(Vattenfall AB, 2006, by courtesy of Vattenfall).

4.5.1.1.2. Structural reliability analysis to determine magnitude of deficiency and frequency of stressing

When the present rating is used, the safety index calculated for a structure has to be compared to some “magnitude” indices. If the target safety is achieved, there exist no magnitude of deficiency, and M is 1. If the safety index is below the target safety M is 2 to 5.

If the safety factors shown above are used to determine M , it is possible to make a “translation” from M in terms of safety factor to M in terms of safety index. The procedure is similar to that used to calibrate target safety index. In short it is to:

- a) Define a “typical dam” that is safe according to RIDAS. Here the height was specified and the required width to fulfil the sliding and overturning stability requirements was calculated
- b) Perform a structural reliability analysis using basic variables. The result is a safety index.
- c) Define a dam with a lower safety factor according to RIDAS (e.g. 1.4 instead of 1.5 for overturning stability) and calculate the safety index with the same input parameters as in b) (except for the width of the that decreases).
- d) Go back to b) etc.

Figure 4-13 shows a possible relation between magnitude of deficiency, M , and safety index for concrete gravity dams of heights 5 to 40 m for the failure mode overturning.

The input used is uplift (normal distribution, $\mu = 1$ (linear distribution), $\sigma = 0.3$), ice load (normal distribution $\mu = 110$, $\sigma = 44$) and concrete density (lognormal, $\mu = 23$, $\sigma = 0.92$). The factor of safety and corresponding M is shown on the x-axis. The safety index and “translated” M for the “typical dam” is shown on the y-axis.

Now the safety index for a dam could be compared to the result and the following relation would be appropriate for the above assumptions and definition of M :

$sf > 1.5$	$\rightarrow 1 = M$	\rightarrow	$\beta > 4.6$	$(p_f < 2.1 \cdot 10^{-6})$
$1.3 < sf < 1.5$	$\rightarrow 2 = M$	\rightarrow	$2.6 < \beta < 4.6$	$(2.1 \cdot 10^{-6} < p_f < 0.0047)$
$1.15 < sf < 1.3$	$\rightarrow 3 = M$	\rightarrow	$1.5 < \beta < 2.6$	$(0.0047 < p_f < 0.0668)$
$1.0 < sf < 1.15$	$\rightarrow 4 = M$	\rightarrow	$0.5 < \beta < 1.5$	$(0.0668 < p_f < 0.3085)$
$sf < 1.0$	$\rightarrow 5 = M$	\rightarrow	$\beta < 0.5$	$(p_f > 0.3085)$

The results here should merely be treated as an example.

Also other values could be chosen for M , e.g. a system with uniform “steps”, like:

$(p_f < 2 \cdot 10^{-6})$	\rightarrow	$\beta > 4.6$
$(2 \cdot 10^{-6} < p_f < 9.8 \cdot 10^{-5})$	\rightarrow	$3.7 < \beta < 4.6$
$(9.8 \cdot 10^{-5} < p_f < 4.3 \cdot 10^{-3})$	\rightarrow	$2.6 < \beta < 3.7$
$(4.3 \cdot 10^{-3} < p_f < 0.2)$	\rightarrow	$0.85 < \beta < 2.6$
$(p_f > 0.2)$	\rightarrow	$\beta < 0.85$

The result of this assumption on M is also shown in Figure 4-13 (gray).

The choice has to be carefully prepared. The safety index corresponding to rating 5 here is likely too low as a probability of failure of 0.2 is very high.

For a dam structure the inability to detect and respond to deficiencies when it concerns structural failure can typically be assumed high. Failure of concrete dams can, as discussed earlier, be considered brittle and the result is little or no time to intervene in a failure sequence. The criticality is typically high as no redundant systems exist.

The structural reliability analysis, in general, gives a probability of failure for all loads. For concrete dams, however, as will be described in chapter 5.3, there are reasons to divide the water level (and so the hydrostatic pressure) into two parts, the first is constant and occur with an annual probability of approximately one (at retention water level) and the second occur with a low probability and is described by an exponential distribution (water above retention water level). This means that two analyses have to be made, one for water at retention water level, with a frequency of stressing of 5 and one for water above retention water level, with frequency of stressing less than 5 (depends on characteristics of the reservoir, operation etc).

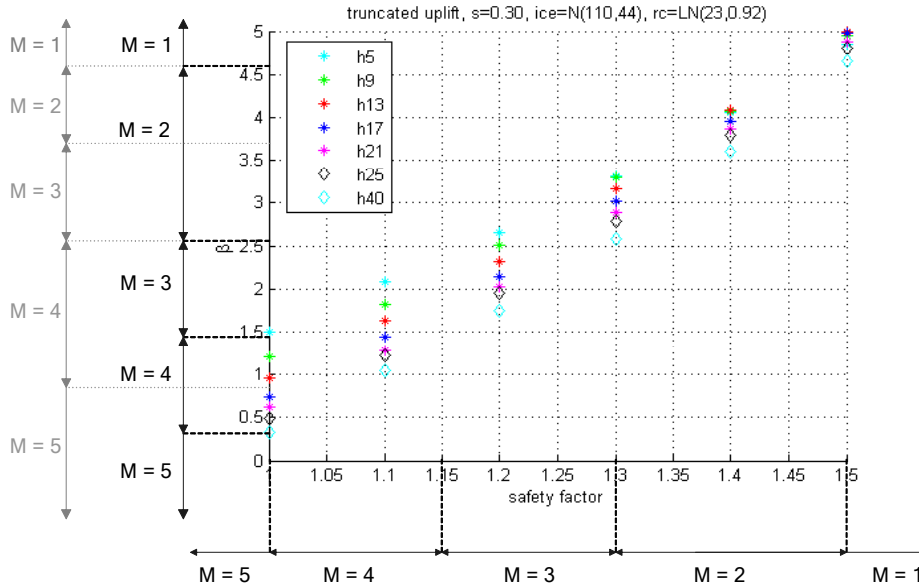


Figure 4-13 - Relation between safety factor and safety index, β , for triangular-shaped concrete gravity dams. Possible values for M .

4.5.1.2. Prioritization or risk reduction measures

Risk and vulnerability indices are useful tools to describe present status of deficiencies for a dam, plant, river system, or dam portfolio, and for follow-up on changes. It can also be used for prioritisation of strengthening measures, as dams with higher risk index should preferably be attended to before dams with lower risk index.

In future applications the actual risk index is also to be compared to allowed risk index to make decisions of rehabilitation and reinforcement. A hypothetical example of vulnerability index plotted versus consequence index is shown in Figure 4-14. Here the facilities in the upper right corner has the largest vulnerability and consequence and should therefore be attended to first. Consequences are often difficult to reduce and therefore the total risk is reduced by reduction of the vulnerability index. By back-tracing the vulnerability index-input, the largest contributors to the total vulnerability can be identified and attended to.

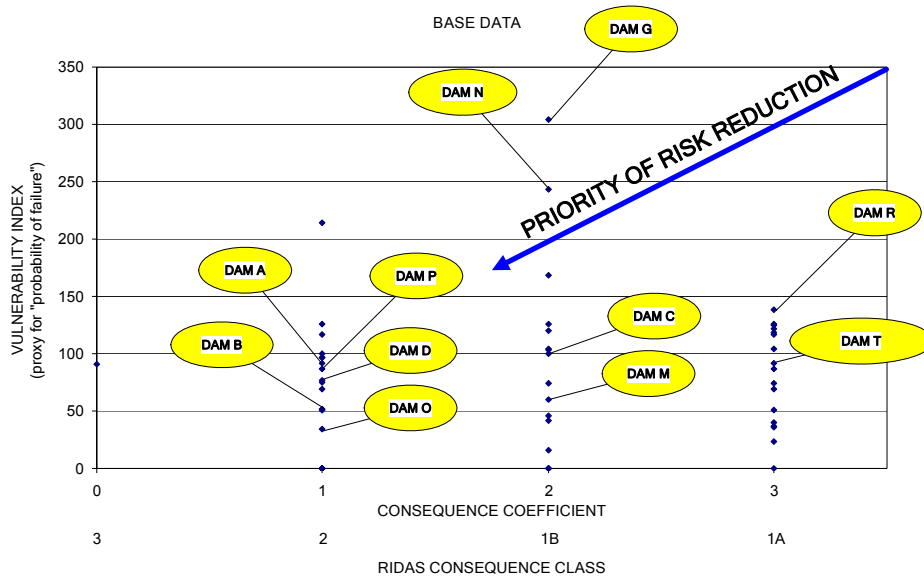


Figure 4-14 - Prioritization of risk reduction based on vulnerability index and consequence coefficient.

5. Random variables affecting dam stability

This chapter describes the main parameters contributing to the resistance of a concrete dam, as well as the main loads affecting the dam. Figure 5-1 shows a schematic concrete gravity dam with applied forces.

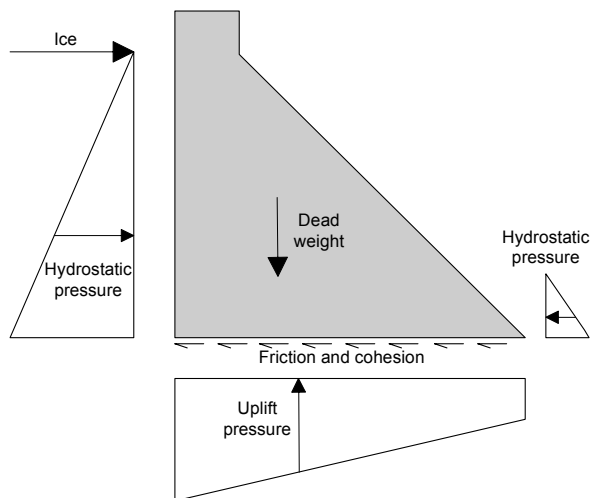


Figure 5-1 - Forces on gravity dam.

The outline of this chapter is

- Resistance
- Loads

The *resistance* can be described as the properties of the concrete and rock. For gravity dams the most important factor is the self-weight of the concrete and the shear strength of rock and concrete, but compressive and tensile strength is also of importance. For buttress dams substantial forces has to be withstood in the head and these factors are even more important. As focus in this thesis has been on the failure modes described in RIDAS TA (2003), overturning and sliding, the resistance chapter is limited to the discussion of

- Self weight
- Shear strength

Information on concrete strength can be found in e.g. JCSS (2001), Thelandersson (2004).

The *loads* discussed are

- Hydrostatic pressure

-
- Ice load
 - Uplift pressure

The largest focus during the work on this thesis has been on uplift; hence this is the most thorough section.

For each parameter the input into a structural reliability analysis is discussed for use in the example chapter.

5.1 Self-weight of concrete

The self-weight of a concrete dam is a function of the volume and density of concrete and both can be described as random variables, but it is generally difficult to specify them separately and the below values include both volume and density variability.

According to JCSS (2002) the uncertainty of the magnitude of variation in self-weight is normally small in comparison to other kinds of loads and the variability with time is normally negligible.

In JCSS the mean value of concrete density is set to 24 kN/m^3 . This is valid for concrete without reinforcement and with stable moisture content. In case of continuous drying under elevated temperature the stable volume weight after 50 days is $1.0\text{-}1.5 \text{ kN/m}^3$ lower. The coefficient of variation is 0.04. For large structures there also exist correlation between densities of two points depending on their separation. The variability of the weight density may be taken as

$COV \cdot \rho$

where ρ is the correlation coefficient. If other information is not available ρ may be taken as 0.85 for a large member and for a whole structure consisting of many members ρ may be taken as 0.7.

A gravity dam can be considered to be a large structure, and with this information the concrete density of a concrete gravity dam should be taken as

$\mu = 24 \text{ kN/m}^3$ and

$COV = 0.04 \cdot 0.85 = 0.034$

The weight density is assumed to have a Gaussian (normal) distribution.

According to Jeppsson (2003) NKB 36 gives a mean value between $23\text{-}25 \text{ kN/m}^3$ and $COV = 0.04$.

CIB (1989), which is the back-ground information to JCSS (2002), gives a mean value of 23.5 kN/m^3 and COV of 0.04 for concrete of compressive strength 20 MPa, and 24.5 kN/m^3 and $COV = 0.03$ for concrete of compressive strength 40 MPa.

In RIDAS the concrete density should be 23 kN/m^3 unless other values are proved by testing. It is not clear what this value represent (mean value, characteristic, other).

In the assessment of a concrete dam the above information (from e.g. JCSS) could be used as *a priori* information and samples from the structure could be used for updating to give the *a posteriori* information. The structural reliability analysis would then be based on the *posteriori* distribution.

It is important to note that for a concrete dam the volume can be difficult to determine. Design drawings does not provide good information and as-built drawings may also be inadequate, but must in most cases be relied upon. If large uncertainty exist or if the

structure is not likely to have dimensions according to the as-built drawings measuring by total station and drilling to find the rock level may be used. This important area should be further analysed.

Dams are built in a quite hostile climate, where the leaching of water or mechanical or chemical damage may reduce concrete volume or density. If uncertainties exist as to the status of the material properties they should be tested.

5.1.1 Distribution used

The normal distribution with $\mu = 24 \text{ kN/m}^3$ and $\text{COV} = 0.034$ is used. This may result in self weight of > 26 which is considered unlikely in reality, and if wanted the distribution can be truncated, meaning that values higher than e.g. 26 can not appear. In this case it is not considered necessary as this has only marginal effect on the rest of the distribution, and no effect on the lower tail, which is of largest interest.

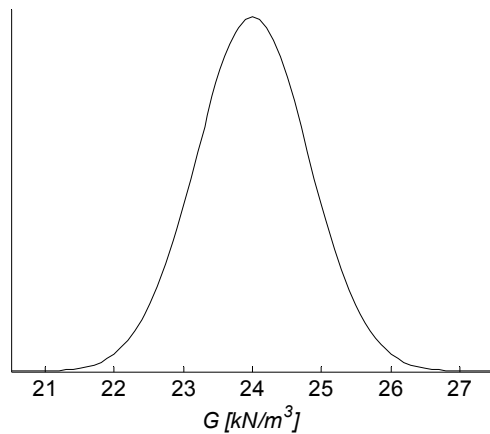


Figure 5-2 - distribution of self-weight, $\mu = 24$, $\text{COV} = 0.034$.

5.2 Shear strength

The sliding stability of concrete dams is significantly affected by the shear strength. This section is focused on shear strength of the concrete to rock interface and along lift joints in the dam body. Shear failure in the rock is not considered. In the first part of this section results summarised by Ruggeri et al (2004) and EPRI (1992) are reproduced as examples of shear strength received in tests.

In the second part the values for shear strength given in a Chinese standard are shown and translated to statistical distributions.

Last, the distributions used in the structural reliability analysis in this project are shown.

5.2.1 Ruggeri et al & EPRI

The most likely place for sliding to occur would be along relatively weak planar features such as concrete lift joints, unbounded concrete to rock contacts at the base of the dam, or along joints in the rock.

For the EPRI results all strength data were determined from cores taken from existing dams and the data apply only to the specific materials and the conditions under which they were tested. Weak concrete or rock layers could have strengths that are significantly lower than the values shown here.

The normal stresses beneath dams are usually low, and the friction angle is therefore relatively high, see section 2.2.1.1. According to EPRI for intact samples the Mohr envelope extends from the tension side of the normal stress axis into the compressive side. The intersection with the shear stress axis is the cohesion or inherent shear strength. The direct shear test requires at least some normal load so the cohesion cannot be determined directly, therefore in the EPRI-report results direct tensile data are included in the data plots to better define the cohesion.

Samples containing a plane of weakness are described as “bonded” if they are intact and as “un-bonded” if they are broken along the plane of weakness. Peak shear strength is determined during the shear tests, while residual strength determination is subjective as to when it occurs, as the laboratory data is not often as smooth as the curves shown in Figure 5-3. Table 5-1 shows the shear strength of lift joints and Table 5-2 the shear strength of the concrete to rock interface, from Ruggeri et al.

In the investigation by EPRI “best fit lines” are determined by linear regression and the lower bound lines were drawn by hand to include all data. Examples of best fit and lower bound line for peak shear strength of granite-to-concrete contacts is shown in Figure 5-4.

Table 5-1 summarize the shear strength for lift joints from tests (from Ruggeri et al, 2004 and EPRI, 1992). Table 5-2, Table 5-3 and Table 5-4 summarize the shear strength of the concrete to rock interface, from EPRI and Ruggeri et al.

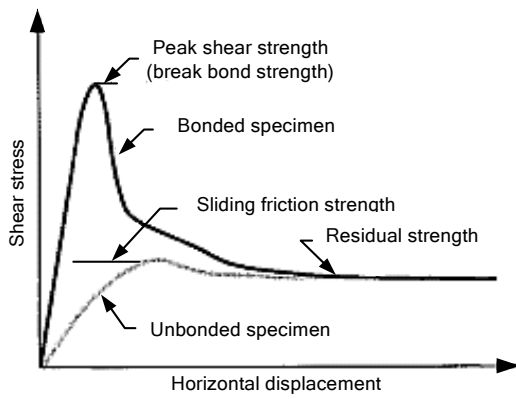


Figure 5-3 - Shear strength for bonded and unbonded samples. Ruggeri et al (2004).

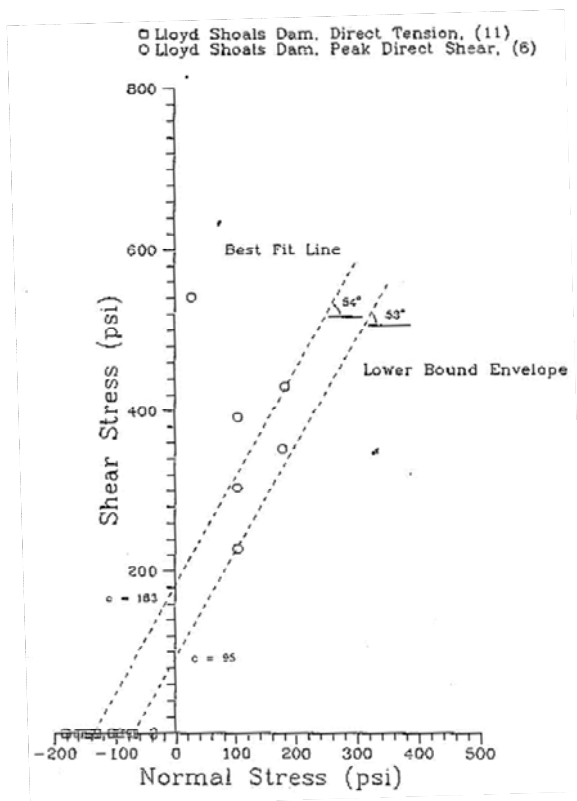


Figure 5-4 - Best fit & lower bound lines for granite to concrete interface. EPRI (1992).

Table 5-1 - Shear strength of lift joints.

	Procedure	Strength	Comments
EPRI	Data from 10 dams (built 1906-1973), 223 specimens were tested (69 bounded, 154 unbounded)	Peak strength Best fit line: $\phi = 57^\circ$, $c = 2.1$ MPa Lower bound: $\phi = 57^\circ$, $c = 1.0$ MPa Residual strength Best fit line: $\phi = 49^\circ$, $c = 0.5$ MPa Best fit line (bilinear): $\phi = 68^\circ$, $c = 0$ MPa for $\sigma < 0.3$ MPa $\phi = 49^\circ$, $c = 0.5$ MPa for $\sigma > 0.3$ MPa Lower bound: $\phi = 48^\circ$, $c = 0$ MPa	For un-bonded samples an apparent cohesion is the result of small, high angle asperities on the surfaces.
McLean and Pierce	Direct shear tests carried out on samples from USBR dams	Peak strength Best fit line: $\phi = 55^\circ$, $c = 2.4$ MPa Residual strength Best fit line: $\phi = 47^\circ$, $c = 0.6$ MPa	Bonded lift joints had a peak strength nearly identical to concrete ($\phi = 58^\circ$, $c = 2.5$ MPa)

Table 5-2 - Shear strength of concrete to rock interface.

	Procedure	Strength	Comments
Rocha	70 blocks of concrete (70x70x35cm) were cast at 6 dam sites on different types of rock	see Table 5-4 $\phi = 53-63^\circ$, $c = 0.1-0.7$ MPa	
Link		$\phi = 45-52^\circ$, $c = 0.1-3.0$ MPa	
Lo	Bonded (10 triaxial, 13 tri-axial extension and 45 direct tension tests) and un-bonded (38 tests, residual strength evaluated), samples from dams ageing 15-80 years. Normal stress range 0.1-1.4 MPa.	Peak strength Typical reported values: $\phi = 62^\circ$, $c = 2.2$ MPa Residual strength Reported values: $\phi = 32-39^\circ$, average 37°	The peak values were not too sensitive to the rock type. The concrete-rock contact is not necessarily the most critical failure surface.
EPRI	18 dams (built 1912-1965). Data also include two large scale in situ tests. Eight foundation rock types. 65 samples tested.	Peak strength, see table Table 5-3. best fit lines $\phi = 54-68^\circ$, $c = 1.3-1.9$ MPa lower bound lines $\phi = 53-68^\circ$, $c = 0.3-1.1$ MPa (for shale best fit $c = 0.1$ MPa and lower bound $c = 0$ MPa) Residual strength best fit lines $\phi = 24-39^\circ$, $c = 0-0.2$ MPa lower bound lines $\phi = 13-32^\circ$, $c = 0$ MPa	The measured cohesion for rocks (other than shale) is rather homogeneous, without large differences. The two large scale in situ tests were in the upper bound of data for both peak and residual strength.
ISMES	16 large scale specimens to evaluate influence of construction artefacts (extra bonding due to interposition of cement milk)		Peak strength was not strongly influenced by rock type, residual strength was. Lower peak strength when adhesive material (cement milk) was not used, residual strength was not.

Table 5-3 - Investigation by EPRI.

Contact Rock-type		Number of tests	Best fit			Lower bound	
			Cohesion [MPa]	Friction angle [°]	Correlation coefficient	Cohesion [MPa]	Friction angle [°]
Granite	Peak	6	1,26	54	0,84	0,66	53
	Residual	6	0,08	35	0,93	0	32
Granite gneiss	Peak	4	1,3	57	0,87	0,48	57
	Residual	4	0,03	34	0,99	0	31
Limestone - dolomite	Peak	9	1,92	68	0,49	1,14	68
	Residual	12	0,12	35	0,58	0	23
Phyllite	Peak	3	1,66	62	0,84	0,48	62
	Residual	5	0	39	0,89	-	-
Sandstone	Peak	15	1,79	65	0,8	0,34	65
	Residual	45	0,18	29	0,6	0	27
Shale	Peak	9	0,12	60	0,79	0	48
Shale laboratory	Residual	13	0	34	0,75	0	13
Siltstone	Residual	13	0,11	24	0,83	0	22

Table 5-4 - Investigation by Rocha.

Rock type/Dam	Number of tests	Cohesion [MPa]	Friction angle [°]
Altered Granite /Alto Rabagao	8	0.2	56
Shale/Bemposta	8	0.2	60-63
Shale/Valdecañas	3	0.4	62
Shale/Miranda	16	0.4-0.7	60-62
Shale/Alcantara	28	0.1	56
Sandstone/Cambambe	4	0.2	53

The above results can be summarised as:

- The strength of lift joints is significant with cohesion in the order of 1-2 MPa.
- The concrete to rock interface also experienced high cohesion and friction angles, and, as pointed out in Ruggeri et al, it is not necessarily the most critical failure surface. Where bonding is effective it can sustain high shear stresses leading to failure surface within the foundation rock, this is especially true for weak rock.
- Even small values of cohesion may provide a significant contribution to the tangential resistance. Interposition of cement milk between foundation rock and concrete cause “extra bonding” and give significant influence on cohesion.
- Many of the in situ cored concrete rock interfaces were found intact.
- The EPRI in situ tests were performed to account for large scale roughness present in the jointed rock surface and the influence of inclined bedding planes. Only two of five tests exhibited peak strength, for the others failure occurred along pre-existing planes of weakness. Those two belonged to the upper bound of the data. The correlation coefficient in Table 5-3 indicate the extent of relationship between shear stress and normal stress.
- Some of the best fit lines of the residual strength in the EPRI-report do not pass through the origin but show apparent cohesion, this is due to small, high-angle asperities on the surfaces being shared. If a test could be performed at zero normal stress (impossible), the opposing shear surfaces would tend to ride up the asperities and not shear them resulting in a very high friction angle and zero cohesion.

EPRI point out that use of site-specific strength based on laboratory tests of core samples can improve calculated stability since

- Site-specific strength are often greater than those based on empirical estimates and
- Site investigations associated with obtaining core samples reduces the uncertainty in the analysis and lower factors of safety may be justified.

Tests on small samples tend to overestimate the actual shear strengths.

5.2.2 Chinese standards

In China Electricity Council (2000), the Chinese standard for design of hydraulic structures in hydro power projects, design is performed based on the partial factor method.

“During the stage of feasibility study and bidding design of large projects, standard values of shearing rupture strength of interface between concrete dam body and

foundation rock, the bedrocks, soft weak structural plane and lift interface of roller compacted concrete shall be determined based on 0.2-fractile of the probability distribution results by field or indoor test. [...]. In the pre-feasibility study for large projects or in the design phase or medium projects, testing results of similar projects or the standard values described below could be adopted. The normal distribution will be taken as the distribution model of probability for shearing rupture resistance friction coefficient and the lognormal distribution will be taken as the shearing rupture resistance of cohesion”.

The “standard values” referred to above are shown in Table 5-5. From the information of distribution, mean value ($\mu_{f'R}$ and $\mu_{C'R}$) and characteristic values (f'_{Rk} and C'_{Rk}), COV and standard deviation, σ , has been calculated for the friction coefficient and variance, V , and COV for the cohesion.

Table 5-5 - shear strength parameters of concrete to rock interface. Standard values from Chinese design standards

Sorts of rock mass	Rock properties of dam foundation	Variation range of basic parameters of rock mass		Mean value and characteristic value of shearing rupture resistance for interface. Units for cohesion is MPa.				Parameters of normal distribution of friction coefficient			Parameters of log-normal distribution of cohesion		
				μ_{fR}	f_{Rk}	μ_{cR}	c'_{Rk}	μ	σ	COV	E	V	COV
I	Dense and sound. Distance between cracks >1 m. Magnetic rock, volcanic rock, abyssal (massive gneiss and chorismite) and massive thick layer sedimentary rock.		$R_b > 100$ MPa, $v_p > 5000$ m/s, $E_r > 2 \cdot 10^4$ MPa	1,50	-1,25	-1,50	-1,05	-1,50	0,30	0,20	1,50	0,295	
				1,30	1,08	1,30	0,91	1,30	0,26	0,20	1,30	0,221	0,362
II	Sound, weakly weathered massive rock with crack spaces 0,5 - 1m. E.g. Thick-layer sandstone, conglomerate, limestone without resorption, dolomite, quartzite, pyroclastic rock. The rock mass is stable except few local areas.		$R_b = 100 - 60$ MPa, $v_p = 5000 - 4000$ m/s, $E_r = (2,0-1,0) \cdot 10^4$ MPa	1,30	-1,08	-1,30	-0,91	-1,30	0,26	0,20	1,3	0,221	
				1,10	0,92	1,10	0,77	1,10	0,21	0,19	1,1	0,158	0,362
III	A rock mass of medium sound, poor completeness, weakly weathered massive and cyclopean structure. Crack spaces 0,3-0,5 m.	Mechanical properties are not even with great difference, and is under control of structural planes	$R_b = 60 - 30$ MPa, $v_p = 4000 - 3000$ m/s, $E_r = (1,0-0,5) \cdot 10^4$ MPa	1,1	-0,90	-1,10	-0,74	-1,10	0,21	0,19	1,1	0,158	
				0,9	0,73	0,70	0,47	0,9	0,20	0,22	0,7	0,078	0,4

5.2.3 Distributions used

Using the information from China Electricity Council (2000) the distribution for the friction angle (assuming normal distribution of the friction coefficient) becomes as shown in Figure 5-5 for the different types of rock in Table 5-5. Note that the friction angle is plotted, while the normal distribution is of the friction coefficient, hence the “strange” shape of the distribution. A lognormal distribution of the cohesion gives the distributions shown in Figure 5-6.

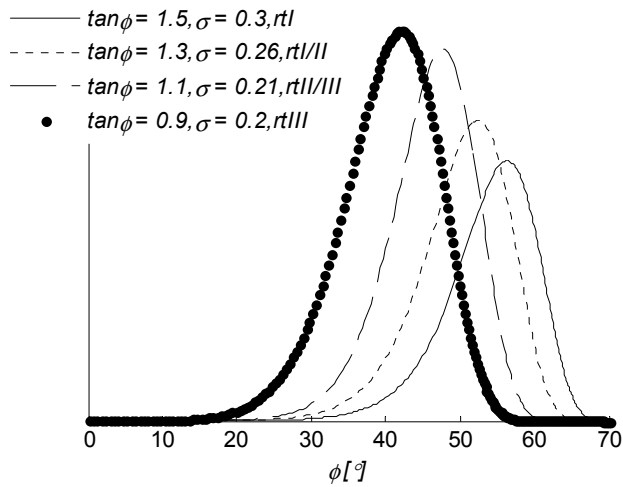


Figure 5-5 - Distribution of friction angle.

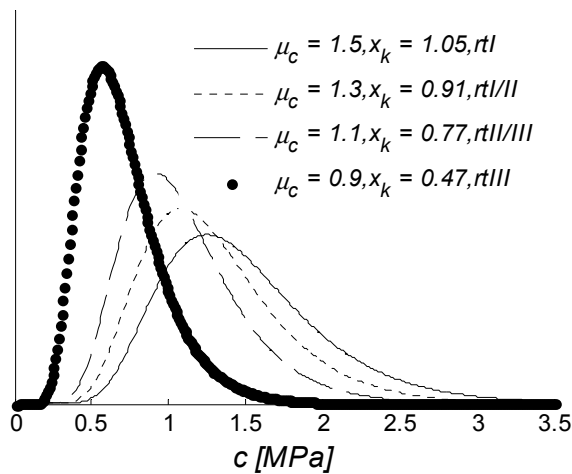


Figure 5-6 - Distribution of cohesion.

The information from Table 5-2 to Table 5-4 is more difficult to use for estimation of statistical distributions, and no attempt is done here. It can be noted that the peak strength values show quite high friction angles and are well represented by the distributions with $\mu_{\tan\phi} = 1.5$ and 1.3 , while the two other seems to be a bit too conservative (see Figure 5-5). The cohesion, as expected, shows much larger scatter, but as values as low as 0.2 MPa are noted the distribution giving the lowest cohesion ($\mu_c = 0.7$) is assumed. From the discussion of chapter 2.2.1.1 a correlation between friction coefficient and cohesion may be expected, where a high friction angle gives a low cohesion and a low friction angle gives a high cohesion (i.e. negative correlation). This has not been taken to account here and should be further investigated.

For safety assessment of an existing dam the friction angle and cohesion is difficult to estimate. The first step would be to characterize the rock and, based on past knowledge (if available) make a first assumption. Drilling cores and perform shear test would be the next step and from this the first assumption would be updated. Taking tests is expensive and it must be weighted against the associated benefit. The testing program should be carefully prepared, especially the number of tests needed to validate or falsify the assumed distribution.

5.3 Hydrostatic pressure

Any dam with a reservoir will be exposed to hydrostatic water pressure, determined by the head water level. The uplift pressure is also a function of the head water level. This section describes the characteristics of head water and suggest how to treat it in structural reliability analysis.

5.3.1 Flow in unregulated and regulated rivers

In unregulated rivers in the north part of Sweden the highest flow occurs in spring because of melting snow, while in the south part it occurs in autumn or winter because of large precipitation. In regulated rivers water is stored in reservoirs, either natural lakes or artificial ones built up by dams. The Swedish electrical energy production consists of about 45 percent hydropower, 45 percent nuclear power and about 10 percent from combined power and heating plants, wind and other. The consumption is highest in winter, autumn and spring and during these periods nuclear power is used to high extent, whereas the more flexible and adjustable hydropower is used as complement and in peak situations during the day. The reason is that hydropower, as water is stored in reservoirs, can be saved for periods of high demand and high energy prices. As high water levels (larger head) give higher utilisation water is kept as close to retention level as possible.

The result of storing water in the reservoirs is a more even water flow in the rivers than in unregulated river systems and in most cases lower peak flow. This is, however, not always the case since regulation can cause larger flows than the natural. The risk of large flows due to this increase in long periods of wet weather when reservoirs are filled and water must be discharged through several dams (Bergström, 1993).

For unregulated rivers the flow has an “inherent” randomness, resulting in aleatory uncertainty. The flow can be seen as a random process in time. To describe the flow models are used, which are themselves subject of epistemic uncertainty. Epistemic uncertainty is also called knowledge uncertainty and can be divided into model uncertainty, which has to do with the ability of a model to describe reality, and parameter uncertainty, which is the precision to which parameters can be described.

If, in theory, an infinite amount of data was available, the epistemic uncertainty could be eliminated and it would then be possible to describe the flow, but the aleatory uncertainty would still be present (for definition and use of aleatory and epistemic, see e.g. Hartford et al, 2004).

The situation in a regulated river is quite different. The runoff water from surroundings can still be described as a random process in time with an aleatory uncertainty, but the river flow is now also subject to other processes; water is saved for use in situations when it is needed resulting in more flow in cold weather (when the natural situation would result in precipitation as snow), less water during spring due to lower energy demand, etc. The result is that the flow in a regulated river can not fully be described as a random process in time and the uncertainty is thus not aleatory. Or, more correctly,

part of the uncertainty is aleatory but the greater part is assigned to the uncertainties of policy, of regulation etc that are largely influenced by humans and thus those uncertainties can be looked upon as a result of human factors.

The above description is true for “normal” situations. In case of extreme precipitation water flow can no longer be stored to great extent, as regulation of rivers reduce the ability of natural damping at high reservoir levels, and the result can be large floods that are not, or only partially, influenced by human activity. These situations are thus the result of more aleatory uncertainty, but due to the effect of regulation it is not the “same” aleatory uncertainty as for the natural flow.

5.3.2 Calculation of design flow

Where dam breach would cause loss in human lives or large economic or environmental damage the acceptable probability is very low, and return periods of 10 000 years are used for design floods. Calculation of the flow corresponding to this differ, however, between countries and regions, as there are, at present, no internationally accepted method for calculation of design flow in regulated rivers for large dams.

For most dam sites the statistical data of maximum yearly flood only extends for some 50 or 100 years, which is not sufficient to make a frequency analysis, as the tail, which is most important for extreme floods, is dependant on choice of distribution. In the USA federal governments therefore only accept extrapolation to return periods twice the observation period for data (Flödeskommittén, 1990).

There are different approaches to derive the design flood; methods based mainly on flow data or methods based mainly on rainfall data, such as the PMP. PMP (Probable Maximum Precipitation) is the “theoretically greatest depth of precipitation for a given duration that is physically possible over a given size storm area at a particular geographic location at a certain time of year”.

In many countries design floods for large dams are based on PMP used in a hydrological calculation model to estimate the PMF. PMF (Probable Maximum Flood) is the flow that can be expected from the worst combination of critical meteorological and hydrological conditions that can reasonably be expected in the region (ICOLD Bulletin 82, 1992). The PMP-concept is not useful in Sweden as it does not account for snowmelt, which significantly contributes to the largest floods.

In 1985 the Swedish Committee for Design Flood Determination (Flödeskommittén, 1990), was appointed to give new guidelines on the calculation of design floods for Swedish dams. The reason was that high floods during the summer and autumn of 1983 indicated that the discharge capacity of dams could be insufficient in case of extreme inflow and full reservoirs.

The design flood calculation for dams in risk class I (high consequence dams) proposed by the Committee is based on the HBV-model (a model taken out by SMHI (Swedish Meteorological and Hydrological Institute) in cooperation with the powerindustry) where a precipitation during 14 days (based on data of precipitation sequences from

1881-1988) over a 1000 km² area is combined with extreme snowmelt of a snowpack with return period of 30 years, a reservoir level corresponding to what might be expected at the time of year of interest and high amount of soil moisture (Bergström, 1993, Flödeskommittén, 1990). The committee estimate that a design flood calculated by this method have return periods that exceed 10 000 years, but probabilities can not be assessed more closely.

For dams in risk class II data from observed floods can be extrapolated to a longer return period (but not longer than 2-3 times the data) to give the design flood, which should be at least equal to the 100-year flood.

For a number of reasons; ecological, economical etc, head water for Swedish dams are kept between the minimum retention level and the retention water level which is the maximum level allowed. The water-rights court defines these levels and allowance for necessary violation has to be applied for in advance (or in extreme situations afterwards).

5.3.3 Treatment of headwater level

In a structural reliability analysis statistical distributions for loads and resistances are needed as input. From the above account it is obvious that this is not possible to attain for the flood, and hence for the head water level, but a method to deal with this in a structural reliability analysis is proposed. A risk class I facility should be able to discharge a design flood with a return period of approximately 10 000 years. In some cases the discharge facilities are capable of discharging this flow at retention level, but in others water levels above retention level has to be allowed to discharge sufficient amount of water.

The formulation of headwater in the structural reliability analysis is divided into two parts:

- Head water at retention level
- Head water above retention level

Figure 5-7 show the parameters used below.

Apart from extreme floods resulting in large headwater levels there are other events that could give rise to the same problems. These are also briefly discussed below.

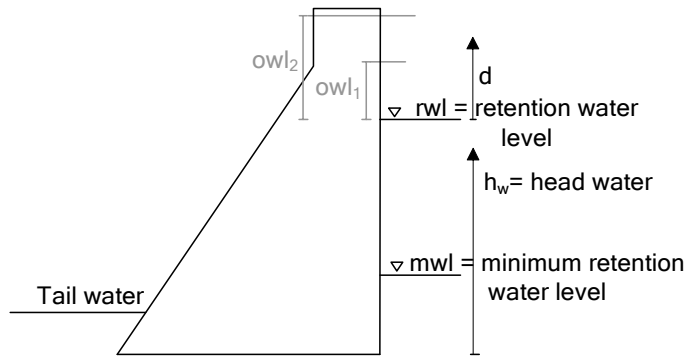


Figure 5-7 – Definition of parameters.

5.3.3.1. Head water at retention water level

Head water is assumed constant at retention water level with probability of occurrence of $p = 1 - P(h_w > rwl)$

where p is the probability of water at retention water level and $P(h_w > rwl)$ is the probability of exceeding retention water level. Calculation of the latter is shown below. In many cases the probability of exceeding retention water level is low and the probability of water at retention level can be approximated with one.

Headwater at retention water level is considered the “normal case”. Water levels below retention water level may occur, but as the statistical distribution should be based on annual maximum values, and it is likely to reach retention water level at least once in a year this possibility is conservatively neglected.

For this case ice is assumed present. If uplift pressure monitoring results are available, these can be used as input. If so, risk of drain clogging and grout curtain leaching has to be considered properly. The variation in uplift pressure distribution is not considered to be large as long as drains and grout function is proper.

5.3.3.2. Head water above retention water level

The water level *above* retention level is described by an exponential distribution and considered the exceptional case.

The exponential distribution has the general formulation

$$F(x) = \begin{cases} 1 - e^{-\lambda x} & \text{for } x \geq 0 \\ 0 & \text{for } x < 0 \end{cases} \quad \text{Eqn. 5-1}$$

In this case $x = 0$ would be water at retention water level and λ is a parameter of the exponential distribution.

For this case the exponential distribution describes only the water depth *above* retention water level.

With reference to Figure 5-7, h_w is the total water depth, rwl is the water retention level, d is water height above retention level and owl_1 is a known water level (measured from rwl) that occur with certain probability. hwl_1 is defined as owl_1+rwl . The exponential distribution of Eqn. 5-1 is, in this case, a function of d .

When the probability of exceeding retention level, $P(h_w > rwl)$, and the probability of exceeding another level above retention level, $P(h_w > hwl_1)$, are known the unknown parameter λ can be calculated.

We have

$$P(h_w > hwl_1) = P(d > owl_1) \cdot P(h_w > rwl) \quad \text{Eqn. 5-2}$$

which can be written

$$P(d > owl_1) = \frac{P(h_w > hwl_1)}{P(h_w > rwl)} \quad \text{Eqn. 5-3}$$

Since

$$P(d > owl_1) = 1 - P(d \leq owl_1) = 1 - F(owl_1) = 1 - (1 - e^{-\lambda \cdot owl_1}) = e^{-\lambda \cdot owl_1} \quad \text{Eqn. 5-4}$$

λ can be solved according to

$$\lambda = -\ln\left(\frac{P(h_w > hwl_1)}{P(h_w > rwl)}\right) / owl_1 \quad \text{Eqn. 5-5}$$

Another possibility is that the probability of exceeding retention level, $p_{hw>rwl}$, is not known but that another level owl_2 and the probability of exceeding this is, then

If $P(h_w > rwl)$ is unknown we now have two descriptions of λ which gives

$$\ln\left(\frac{P(h_w > hwl_1)}{P(h_w > rwl)}\right) / owl_1 = \ln\left(\frac{P(h_w > hwl_2)}{P(h_w > rwl)}\right) / owl_2 \Rightarrow$$

$$P(h_w > rwl) = \frac{P(h_w > hwl_1) - P(h_w > hwl_2)}{e^{\frac{owl_1}{owl_2}}}$$

and λ can again be calculated according to Eqn. 5-5.

For facilities in consequence class 1 and 2 (risk class I or II) the 100-year flood shall be possible to discharge with headwater at retention water level. In many cases the floods corresponding to the 1000-year flood, or even the 10 000-year flood, is possible to discharge at retention water level for risk class I facilities. It is necessary to determine

the exponential distribution of headwater that is to be applied in the structural reliability analysis for each facility, taking its specific characteristics into account.

Since the exponential distribution only describes the probability of reaching different headwater levels *above* retention water level the resulting safety index has to be compared to the adjusted target safety index (alternatively recalculated to the adjusted safety index), where the probability of headwater above retention water level is taken into account (mostly somewhere between 1/100 and 1/1000). The adjusted target safety index can be calculated according to equation 3-18 in chapter 3.

5.3.3.3. Operational or functional failures

Other types of events can give significant contribution to the overall risk, and sometimes be of larger importance than the extremely low-probability events such as the design flood. The reason is that they may be expected to occur more often. Examples are wrongful operation or failure function of gates at medium floods or loss of control. The probability of these events and perhaps even more so, their consequences in terms of water levels, are even more difficult to quantify than the extreme floods, but still has to be accounted for in a complete risk analysis.

Concerning operational loss of spillway gates, the probability of occurrence can be estimated from incident reports and by estimation from operation and maintenance staff. It must be remembered, however, that this information is from normal conditions, while the rate of failure functions might be higher in extreme weather conditions. The consequence in terms of higher headwater levels can then be judged based on number of gates, discharge capacity, etc for a specific flood.

When such information is available it is easily adopted in the structural reliability analysis, with calculations performed for the headwater level of interest and target safety index adjusted as in the case above.

The complete description of headwater in a structural reliability analysis is shown in Figure 5-8.

Attention is not given to operational and functional failures in this thesis.

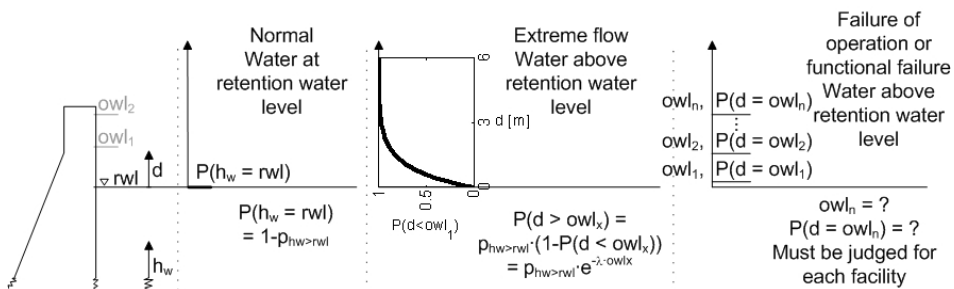


Figure 5-8 - Statistic description of headwater for normal operation, extreme floods and operational or functional failures.

5.3.4 Example

The Seitevare dam in Luleälven in Sweden has a discharge capacity at retention level of $896 \text{ m}^3/\text{s}$. Retention level is at + 477 m.

The regulated class II flood (100-year flood) is $420 \text{ m}^3/\text{s}$.

The design flood can be discharged if the water level rises to +478,8 m, i.e. 1.8 m above retention level. The design flood can be assumed to have a return period of 10 000 years.

The probability of exceeding retention level is not known and two assumptions will be investigated:

1. $p_{hw>rw} = \frac{1}{100}$, i.e. a very conservative assumption regarding the discharge capacity at retention level and the 100-year flood in the regulated river.

2. $p_{hw>rw} = \frac{1}{500}$, i.e. a less conservative assumption.

The first assumption gives $\lambda = 2.56$ and the second $\lambda = 1.66$. The associated exponential distributions for water above retention level are shown in Figure 5-9.

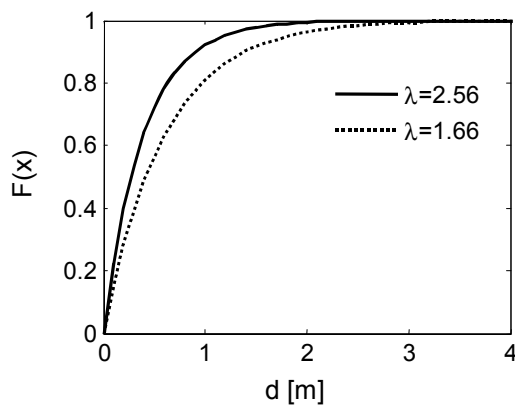


Figure 5-9 - Cumulative distribution function of exponential distributions.

5.4 Ice loads

This section gives only a brief summary of ice loads for the purpose of assigning a probability distribution for further calculations.

The magnitude of the ice load depends on the speed and magnitude of the ice movement towards a structure, as well as on the mechanical properties of the ice and extent of restraint from shores etc. The mechanical properties depend on, among other things;

- If it is sea ice, lake ice or river ice
- Formation development (primary/secondary ice, with or without snow, frazil or not etc)
- Extent of cracking

5.4.1 Reason for ice loads

Ice movement occur due to temperature changes, water level fluctuations, wind, currents etc. Three main reasons for ice loads can be distinguished:

- Ice loads due to cracking –freezing.

The underside of the ice is in contact with water and will have a temperature of 0° C. If the upper side of an ice cover is cooled, that part will contract, while the under side still has a temperature of 0° C and resumes its length. This gives rise to bending moment in the ice, but since it is floating on water bending is restricted and stresses will be released by the formation of deep cracks. Cracks will be filled by water, slurry or snow and the freezing, with volume increase, will cause pressures in the ice cover. If the temperature change is very slow the ice will deform viscously without formation of cracks (Bergdahl 1977a).

- Ice loads due to increasing temperature in the ice cover.

Ice, like any material, expands during heating. The heat expansion coefficient is about 5 times that for steel (Ekström, 2002) and a temperature increase of 20 ° C will cause a 1 km long ice sheet to expand about 1m (ICOLD bulletin 105, 1996). When the free expansion is restricted by restraint from structures or shoreline, stresses will develop in the ice and give rise to forces of considerable magnitude.

The force depends on rate of change of temperature in the ice, the coefficient of thermal expansion, rheology of the ice, the extent to which cracks have been filled, thickness of the ice cover, degree of restriction from shores, rate of change of weater conditions; wind speed, air temperature, solar radiation, depth of snow etc (Ekström, 2002). For pure thermal events the ice loads increase steadily during the period of increasing temperature, see Figure 5-10.

Ice loads generated by ice temperature increase in combination with water level changes.

Water level fluctuations in combination with thermal loads with distinct (but not excessive) water level changes, result in ice loads much larger and more variable than “pure” thermal ice loads (Comfort et al, 2003). Figure 5-11 show the steady increase of loads due to thermal changes and the spikes are due to water level changes.

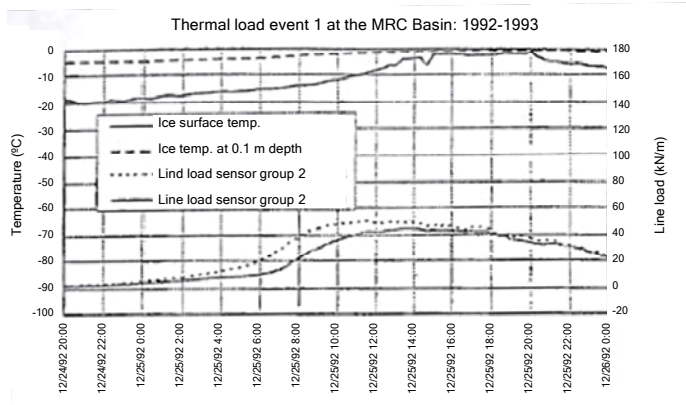


Figure 5-10 - Loads for pure thermal events. From Comfort et al (2003).

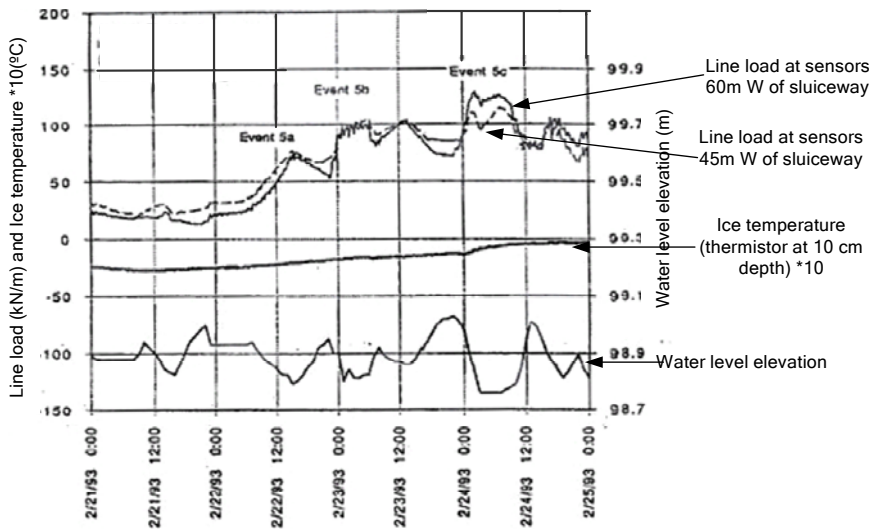


Figure 5-11 - Loads for combined thermal and water level changes. Comfort et al (2003)

Loads induced by increasing temperature are in general larger than that due to cracking and freezing and the discussion to follow is focused on this.

5.4.2 Creep

The ice strength is significantly lower in case of slow loading compared to quick loading. In case of slow movements the contact pressure is limited by creep (BYGG, 1985).

When strain rate is low, ice can creep indefinitely without breaking because of recrystallization. When subject to rapid deformation it becomes as breakable as glass and splits into small pieces (ICOLD bulletin 105).

The deformation of a loaded ice specimen can be divided into three separate parts; elastic deformation, elastic lag and creep. Figure 5-12 shows an idealized graph over the deformation following instantaneous loading and unloading of a sample. When loaded there appears elastic deformation, ϵ_e , which is completely recovered when the sample is unloaded. The elastic lag, ϵ_d , is recovered after some time, while the creep, ϵ_y , is permanent deformation.

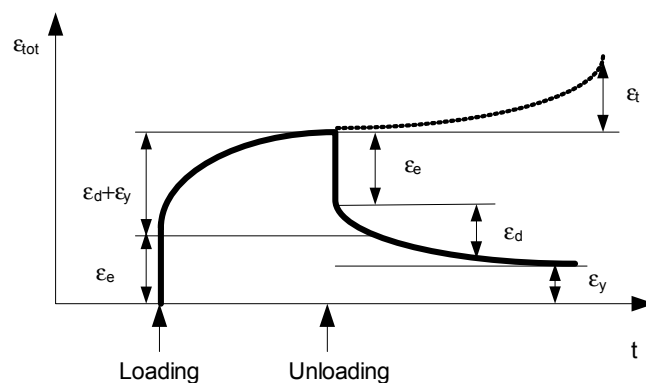


Figure 5-12 - Idealized deformation-time curve for ice body loaded and unloaded momentarily. After Ekström (2002) from Loset et al(1998).

Bergdahl (1977a) uses, with reference to other authors, a non-linear rheological model of ice deformations..

5.4.3 Time of peak loads

Ice loads can be produced in early season when there is no or little snow cover, but they tend to be low. Larger loads are produced in late winter due to extended heating periods (Comfort et al, 2003, ICOLD bulletin 105, 1996). Comfort et al (2003) found a strong relationship between thermal loads and the change in ice temperature area ΔA , see Figure 5-13 and Figure 5-14. They discovered that snowfalls contributed greatly to thermal loads by the insulation they added to the ice surface, causing rapid warming from the “bottom up”. Snowfalls initiated or contributed to 70 % of the thermal events

noted.

Long durations were required to cause large ice temperature changes and events with large ΔA tended to be of longer duration. When comparing events of the same ΔA but with different duration, lower loads were seen for the longer duration. This may be due to creep.

Larger ice thickness give larger ΔA and thus produce higher loads. There is less stress redistribution due to creep in thick ice which also give higher loads.

As summarized in Ekström (2002), Fransson & Cederwall (1984) found in field measurement of ice loads on bridge pillars that one of the most important load cases is flooding of cold ice due to water level increase. The water, with temperature of zero degree C, give quick heating of the ice cover with thermal expansion.

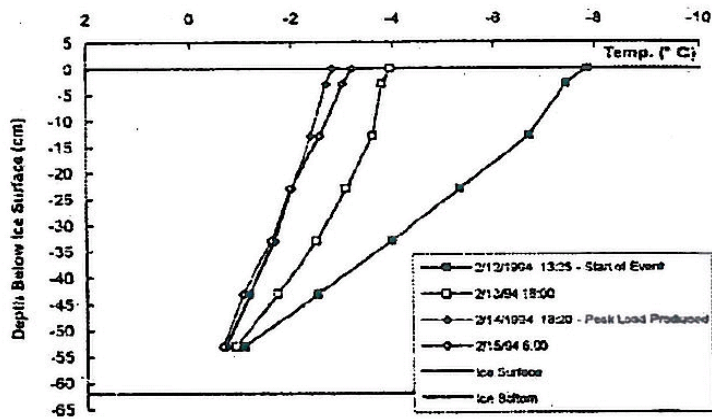


Figure 5-13 - Ice temperature profile changes for highest thermal load. From Comfort et al (2003).

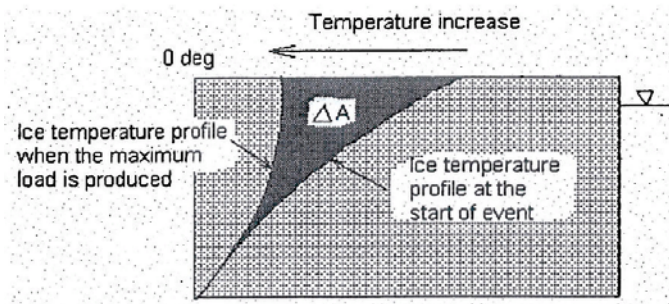


Figure 5-14 - Schematic picture of temperature profile changes. From Comfort et al (2003).

5.4.4 Other considerations

- The failure mode will have impact on the load. Izumiyama, Irani & Timco (1994) (summarized by Ekström, 2002) showed that high loading rate gave crushing of the ice, while low loading rate caused buckling of the ice.
- When the ice freeze to a structure, water level changes may also cause vertical forces (ICOLD bulletin 105).
- Thin structures will exhibit larger forces than wide.
- Flexible structures between rigid ones will exhibit lower loads. This is of importance for spillway gates.
- Structures with vertical sides will exhibit higher ice loads than those with sloping sides, as the ice may bend and “follow” the structure.
- Ice loads measured in situ are often smaller than those measured in laboratory, probably due to extensive cracking in the ice cover.

5.4.5 Testing and modelling

Løset et al (1998) (summarized by Ekström 2002) mention that laboratory tests, full-scale tests and theoretical modelling have to be combined to estimate the ice load on a structure.

5.4.5.1. Laboratory tests

Laboratory tests give important information of ice loads as the parameters affecting it can be controlled, but results are difficult to use for in situ ice.

Laboratory tests on small samples can not be used directly as the variable texture, thermal gradients, imperfections, impurities and biaxial state of stress of natural ice is largely varying (ICOLD bulletin 105, 1996).

Tests on small samples may give compressive strength of 5-10 MPa while in situ testing with natural blocks give 0.5-2 MPa (Ekström, 2002). Because of the anisotropy, with large crystals of varying orientation, imperfections and impurities, the mechanical properties vary significantly when testing in situ, even for blocks taken close to each other.

5.4.5.2. Field measurement

Field measurements could be thought to be the most reliable way to determine ice loads, but due to the nature of ice loads it is not (Løset et al, 1998, summarized by Ekström 2002). It is impossible to know all parameters of interest as they all vary at the same time, different failure modes affect each other and the result, it is extremely difficult to distinguish ice loads due to thermal events from those due to water level increase etc.

5.4.5.3. Theoretical modelling

Ekström (2002) and ICOLD bulletin 105 (1996) both refer to several modelling attempts. There are, according to Løset et al (1998) (summarized by Ekström 2002), no constitutive model that takes account of all parameters and can be used for numerical modelling.

Ashton (1986, according to Ekström, 2002) propose that a statistical analysis of ice loads is possible to perform by gathering data of ice characteristics and weather conditions and by performing numerical calculations of ice temperature and pressure based on rheological relationship. Bergdahl & Wernersson (1978) established a complete energy balance for the ice cover by using weather and ice data from 5 Swedish lakes. The weather parameters used were air temperature, extreme air temperature, wind speed, cloud cover, air vapour pressure. From weather information they calculated ice loads for a number of years and fitted statistical distributions to the results. They found that the normal or lognormal distribution was the best, but the series was too short for the method used and the results can therefore be questioned. Even so, this represents one of few (if any) attempts to describe ice loads as in terms of statistical distributions. Cox (summarized by Ekström, 2002) showed that the results from Bergdahl & Wernersson (1978) were conservative as it did not account for the stress distribution in the ice cover prior to the thermal event, and the parameters of the rheological model were a bit too conservative.

There are several more attempts to model ice loads, but as pointed out by Ashton (summarized by Ekström, 2002) they (including that by Bergdahl & Wernersson) give good approximations of thermal ice loads in an ice cover without cracks.

Ekström (2002) mention several attempts to model ice loads by Finit element models, combined finite element and finite difference models, linear fracture mechanics etc.

Comfort et al (2003) model the ice loads as

$$LL_{total} = LL_{residual} + \Delta LL_{thermal} + \Delta LL_{Water\ level} + \Delta LL_{contingency} \quad Eqn. 5-6$$

where LL_{total} is the total ice load, $LL_{residual}$ is the residual ice load, i.e. the ice load in the ice prior to the event, $\Delta LL_{thermal}$ is the “pure” thermal load, $\Delta LL_{Water\ level}$ is the ice load due to water level changes and $\Delta LL_{contingency}$ is a contingency to account for modelling errors and uncertainties. Equations for calculation of all loads are given in their paper. By use of long-term information of temperature, rain and snow etc, the thermal ice load on a dam can be calculated. Their model was derived on the basis of long time in situ monitoring.

5.4.6 Load values

From the above description it is obvious that ice loads is not an easy task to reliably describe.

In RIDAS TA (2003) the design ice loads is set to:

	Ice load [kN/m]	Ice thickness [m]
Sothern Sweden	50	0.6
North of southern Sweden, up to a line between Stockholm - Karlstad	100	0.6
North of a line between Stockholm - Karlstad	200	1.0

As design in RIDAS is based on safety factor, it is, however, not stated what those values represent. It is likely some kind of “maximum values”, but if they correspond to characteristic values (50 year return period) or something else is not known.

According to ICOLD bulletin 105 (1996) the Swedish design values are, just as former URSS and Norwegian design values, based on the work by Starosolsky (1979). This work has not been studied here. The design values given in ICOLD bulletin 105 (for Canada, USA, URSS, Norway, Sweden, Japan and China) are between 90-h (Norway) and 300-h (Siberia in URSS, China and by some Canadian/American standard). In this respect the Swedish values seem to be within the same bounds as are considered reasonable in other parts of the world as well.

According to Bergdahl & Wernersson (1978) the calculated ice loads for 100, 500 and 1000 return period was 480, 509 and 520 kN/m for Torne träsk and a Normal distribution. For Runn (in Dalarna) the values were 353, 381 and 392 kN/m. Those values are significantly higher than in RIDAS.

Comfort et al (2003) reported ice loads due to thermal events of up to 85 kN/m (McArthur Falls Dam) and for thermal events and water level changes the highest load measured was 374 kN/m (Seven Sisters Dam). The only information found where statistical distributions were presented was that by Bergdahl & Wernersson (1978) and results from a master thesis (Fredriksson & Persson, 2005). In the master thesis temperature data from 40 years was used to simulate temperature for a 1000 year period using the Autoregressive Moving Average model. Ice growth was then simulated with and without snow cover on the ice. Loads were calculated according to

$$P = E \cdot \Delta T \cdot h \cdot \alpha \quad \text{Eqn. 5-7}$$

Where E is the modulus of elasticity, ΔT is the temperature difference between the start and the end of an event, α is the heat expansion coefficient and h the ice thickness. The modulus of elasticity is very difficult to estimate. For short periods of loading $E = E_0 / 2$ was assumed and for long periods $E = E_0 / 4$ was used (due to creep). $E_0 = 6.5 \cdot (1 - 0.012 \cdot T_{average}) \cdot 10^9$ was used.

Ice loads were calculated for long and short time loads for ice with snow (the whole season) and without snow (the whole season). The result was fitted to Gumbel distributions.

The model to predict ice loads is perhaps too simplified to give accurate results of maximum ice loads, but the input data was from real temperature data and for this reason the coefficients of variation could be considered representative. The simulation resulted in COV ranging from 0.29 to 0.46 (8 values).

The modelling by Bergdahl & Wernersson (1978) give ice loads much higher than those received by others, but the procedure is thought to be valid. The high values are (according to Ashton, see Ekström 2002) thought to be the results of the modulus of elasticity being too high. The COV in Bergdahl ranged from 0.15 to 0.4.

5.4.7 Distribution used

It is extremely difficult to estimate a statistical distribution for ice loads as there is not sufficient data available and further research is needed. For this thesis a Normal distribution with characteristic value of 200 kN/m and COV = 0.46 was chosen.

This should not, for any reason, be considered anything that should be used in a real assessment situation. The basis for this choice is that

- 200 kN/m is the value used in RIDAS.
- Most countries use ice loads of around 200 kN/m (Ekström, 2002 and ICOLD bulletin 105, 1996)
- COV according to Bergdahl & Wernersson (1978) and Fredriksson & Persson (2005) was high (above 0.4).

The normal distribution used have the following properties:

$\mu = 103$ kN/m, $\sigma = 47.5$ kN/m and it is shown in Figure 5-15. As values below zero can not appear, the distribution should be truncated at zero or replaced with a lognormal distribution. Here truncation is chosen.

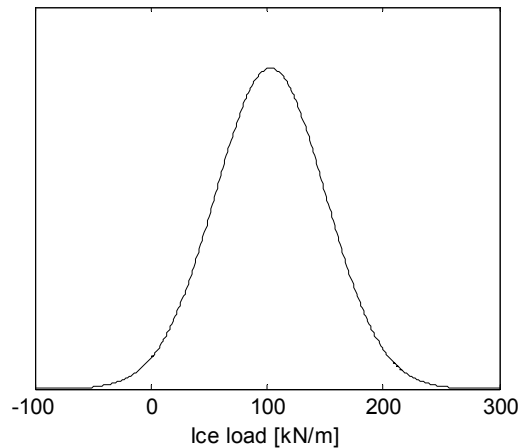


Figure 5-15 - Distribution of ice load, $\mu = 103$, $\sigma = 47.5$.

For the purpose of this thesis it is assumed that the ice loads above include both thermal loads and loads from any water level changes.

In future applications it seems wise to distinguish different cases for a specific dam, depending on the characteristics of operation and reservoir, related to the combination of thermal and water level fluctuations. The following is based on Comfort et al (2003).

- Steady drawdown. Broke the ice away from the dam and caused low loads.
- Large one-time drop or rise (i.e. more than ice thickness). Gave lower or no loads during the rest of the season.
- Large and frequent water level changes. Gave low loads as the water level changes inhibited the formation of a strong bond between ice and dam. Produced hinge-shaped ice cracks.
- Intermediate water level changes. Caused the highest ice loads because ice cracks and ice cover conditions that greatly resisted ice sheet movements were produced. Vertical cracks with a great deal of new ice growth.
- Small and slow water level changes. Ice loads were produced primarily by thermal events.

The type of water level fluctuation at the specific dam should be possible to use in the analysis of the ice loads. In this way conservative values would not have to be assumed for dams where it is not necessary to ensure stability of dams where higher ice loads are possible.

5.5 Uplift

5.5.1 State-of-the-art

Uplift is a general term to cover hydrostatic forces acting within a dam and its foundation, including interstitial or pore pressures (Thomas, 1976). It acts upon dams as the result of water in the reservoir percolating into the foundations or into the dam itself, pushing upwards, and thereby reducing the ability of the structure to resist horizontal hydrostatic pressure (Jackson, 2003). It is therefore of major importance for the stability of concrete dams, especially concrete gravity dams which rely solely upon the weight of the structure for stability. Even so, it was not known and accounted for until the late 19th or beginning of the 20th century (Foster, 1989a), and even then the cause of several dam failures due to ignorance or disregard (Jackson, 2003). Two factors directly affect the design of a dam and has been the subject of controversy for almost a century: the intensity of hydrostatic pressure at various points within or under the dam and the area upon which pressure acts (Thomas, 1976).

Uplift pressure is produced in a dam foundation by water flowing through fractures in the foundation rock. This water is under the pressure applied by the reservoir head at the heel of the dam and under the pressure applied by tail water at the toe. Between these points, the uplift pressure varies depending on the loads acting on the dam, the geology of the foundation rock, the type and extent of foundation treatment, and the operation of the foundation drainage system. (EPRI, 1992). Nowadays uplift is known to act over the whole base area, but when first accounted for it was only applied to as little as 10 %. (EPRI, 1992).

Uplift is difficult to quantify because it can only be measured at a limited number of points. It can vary widely depending on the foundation rock conditions and on the type and extent of foundation treatment (Grenoble et al, 1995).

The differences in opinion on the uplift magnitude arise over the effectiveness of uplift reduction methods, not only for normal loading conditions at which field measurements may be available, but also for extreme loading conditions when measurements are rarely available. The most common uplift reduction methods are excavation of cut-off trenches into the foundations, which can reduce the ability of water to seep under the structure, grouting of the foundation, which fills in cracks in the rock foundation and helps block the flow of water under the structure, and the placing of drainage pipes within the foundation and within the dam itself, which allows water to be carried through tunnels and dispersed downstream from the dam (Jackson, 2003). The level of disagreement rises considerably when theoretical base cracking is indicated by a conventional rigid body analysis, and the crack is determined to extend beyond the location of foundation drains (Foster, 1989b).

The following chapter is a literature review that will treat the basis for design assumptions, influence of uplift reduction methods, describe flow through rock and the impact of natural variations in temperature and due to reservoir level on uplift pressure.

As the focus in this thesis is mainly on concrete gravity dams and buttress dams in Sweden, the information on uplift given in this chapter is for those dams if not explicitly stated differently and loads not considered in Swedish requirements, such as earthquake loads, are not treated in this thesis.

5.5.1.1. Flow through soil

Groundwater flow may be either laminar or turbulent depending on permeability of the material and the hydraulic gradient. By use of Reynolds number it is possible to determine if the flow is laminar or turbulent. Reynolds number is a dimensionless number defined as

$$\text{Re} = \frac{\rho v_s L}{\mu} = \frac{v_s L}{\nu} \quad \text{Eqn. 5-8}$$

where ρ is the fluid density, v_s is the mean fluid velocity, L is the characteristic length (equal to $2r$ for a cylindrical pipe), μ is the dynamic fluid viscosity and ν is the kinematic fluid velocity. Transition from laminar to turbulent flow generally occur at $\text{Re} = 2000$.

In soil the size of pores is mostly small, leading to laminar flow. Pore channels are narrow and tortuous, of irregular cross section and complex in their interconnection, making it impossible to describe the flow through individual pores. In engineering problems this is, however, not necessary since it is the flow thorough a larger soil volume that is of interest. (Taylor, 1948)

Darcy demonstrated experimentally the law for flow through soil and Darcy's law is written as

$$Q = KA \frac{dh}{dl} \quad \text{Eqn. 5-9}$$

where Q is the rate of flow, K is the hydraulic conductivity, A is the cross-sectional area and dh/dl is the hydraulic gradient.

Hydraulic conductivity is a measure of the ability to transmit fluid. The hydraulic conductivity depends on the properties of the medium as well as the fluid.

In sedimentary formations grain-size characteristics are most important, as coarse-grained and well-sorted material will have high hydraulic conductivity as compared with fine-grained sediments.

The relation between hydraulic conductivity and properties of the medium and the fluid can be expressed as

$$K = \frac{cd_e^2 \gamma}{\mu} = \frac{k\gamma}{\mu} \tag{Eqn. 5-10}$$

where c is a dimensionless constant (shape factor), d_e is the effective diameter, μ is the viscosity, γ is the specific weight and k the permeability (Singhal & Gupta, 1999).

The permeability is independent of fluid properties and depends only on properties of the medium. The permeability is given by

$$k = \frac{\mu Q / A}{\gamma(dh / dl)} \text{ [darcy} = 10^{-5} \text{ ms}^{-1}] \tag{Eqn. 5-11}$$

Table 5-6 shows representative values of permeability and hydraulic conductivity for soil and rocks.

Table 5-6- Range of values of hydraulic conductivities (for water) and permeability for various types of geological materials from (Singhal & Gupta, 1999).

Hydraulic conductivity, K [m/s]	1	10 ⁻¹	10 ⁻²	10 ⁻³	10 ⁻⁴	10 ⁻⁵	10 ⁻⁶	10 ⁻⁷	10 ⁻⁸	10 ⁻⁹	10 ⁻¹⁰	10 ⁻¹¹	10 ⁻¹²	10 ⁻¹³	
Permeability, k [darcy]	10 ⁵	10 ⁴	10 ³	10 ²	10	1	10 ⁻¹	10 ⁻²	10 ⁻³	10 ⁻⁴	10 ⁻⁵	10 ⁻⁶	10 ⁻⁷	10 ⁻⁸	
Relative values	Very high			High		Moderate			Low			Very low			
Representative materials															
Unconsolidated deposits															
Gravel	←-----→														
Clean Sand	←-----→			←-----→											
Silty sand	←-----→		←-----→												
Clay till (often fractured)	←-----→	←-----→													
Rocks															
Shale & siltstone (unfractured)	←-----→											←-----→			
Shale & siltstone (fractured)	←-----→											←-----→			
Sandstone	←-----→											←-----→			
Sandstone (fractured)	←-----→				←-----→			←-----→							
Limestone & dolomite	←-----→											←-----→			
Karst limestone & dolomite	←-----→				←-----→										
Massive basalt	←-----→											←-----→			
Vesicular & fractured basalt	←-----→				←-----→										
Fractured & veathered crystalline rock	←-----→				←-----→										
Massie crystalline rock	←-----→											←-----→			

5.5.1.1.1. Flow nets and porous medium assumption

For the 2-dimensional flow through soil a graphical method based on Darcy's law and the equation of continuity ($Q_{section1} = Q_{section2}$ if no water is added or removed) can be used. The path which a particle of water follows in its course of seepage through a saturated soil mass is called *flow line*. The pressure head H is decreased from the water head at the start point to the water head at the end point and on each flow line there exist a point where the value of the pressure head equals h . An *equipotential line*, intersecting the points on each flow line with pressure h , can then be drawn..

The flow through pervious soil under a pile is shown in Figure 5-16. When the dam body is much more impermeable than the underground a flow net according to Figure 5-17 is received. Since the result is based on the assumption of a homogenous permeability, this is called the porous medium assumption.

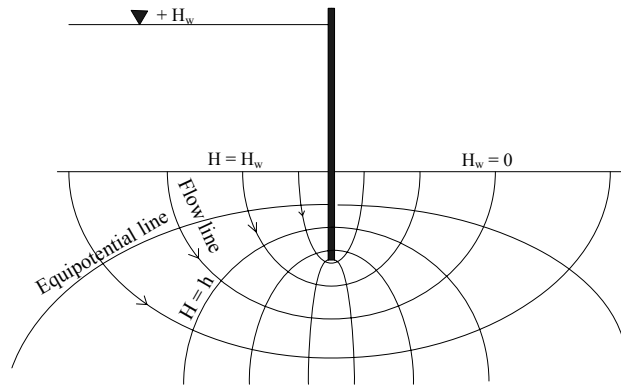


Figure 5-16 - Flow net under pile. After Taylor (1948).

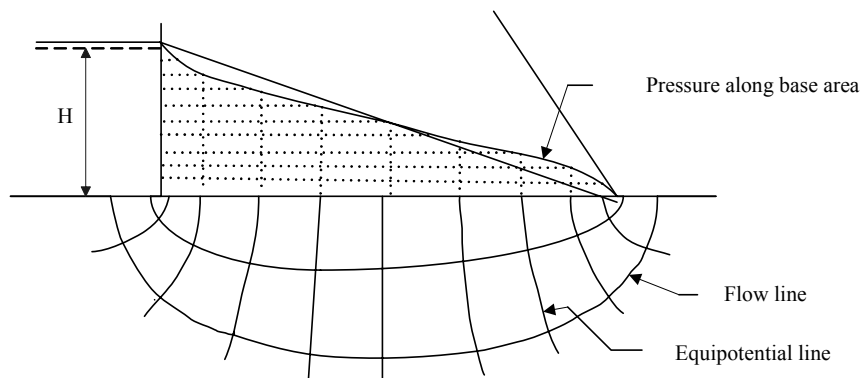


Figure 5-17 - Flow net and uplift under impervious dam. From Reinius (1962).

5.5.1.2. Uplift design assumptions

As the uplift pressure, acting on an impermeable dam body founded on soil of constant permeability, deviate insignificantly from a linear distribution, the design assumption for uplift pressure under dams is approximated by such; the uplift pressure at the upstream edge of a massive gravity dam is assumed to correspond to the upstream water

depth, and in the same way the uplift at the downstream edge corresponds to the downstream water level and the reduction in between is linear, see Figure 5-18.

If the permeability is non-uniform, as in fractured rocks, the uplift pressure distribution is not linear (Reinius, 1962). Even so, the linear assumption is generally applied in design and assessment all over the world (Ruggeri, 2001, RIDAS TA, 2003).

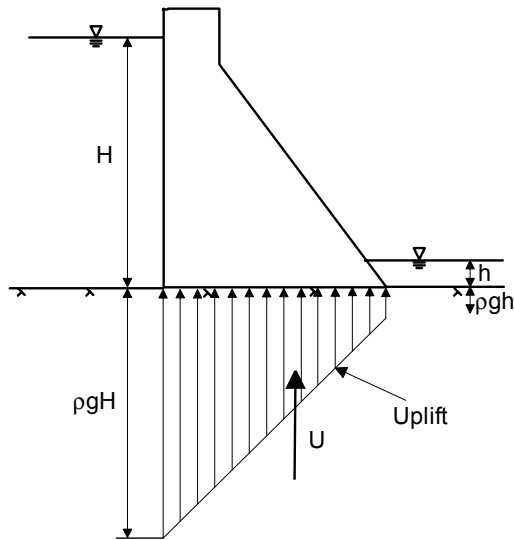


Figure 5-18 - Design assumption of uplift pressure distribution.

As uplift pressure significantly affects the stability, measures to reduce the uplift pressure are commonly used; the most important are drainage tunnels and grout curtains. Figure 5-19 shows the result of such measures. The effects of these methods have, however, often been overestimated. Especially the long-term effects of e.g. deterioration of grout curtain due to leaching or effectiveness of drainage being silted up, have been inadequately taken to consideration.

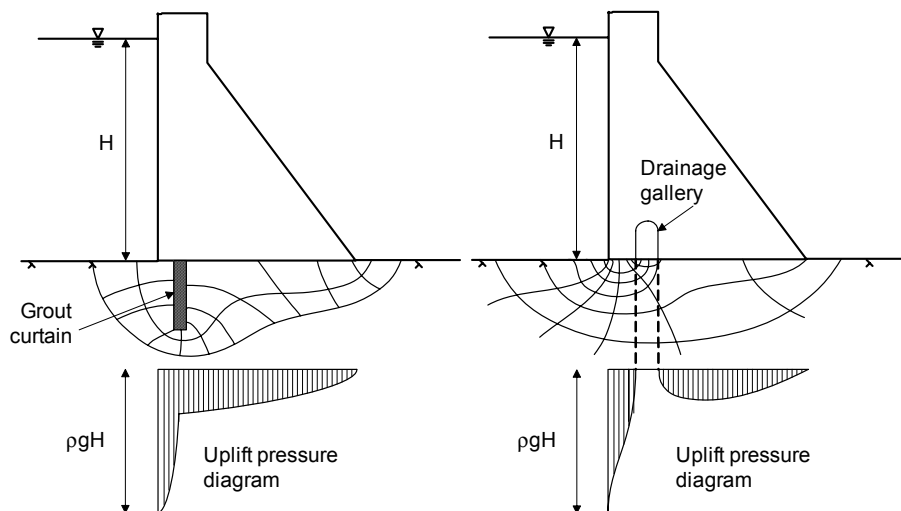


Figure 5-19 - Uplift reduction due to a) grout curtain and b) drainage gallery. After Reinius (1962).

5.5.1.2.1. Influence of drainage holes and tunnels

Drainage tunnel, inside the dam body or at the rock surface, and drainage holes (drains), drilled into the rock, gives a reduction of uplift. Drainage holes are, in essence, vertical large-aperture man-made joints, which provide a short, direct, highly permeable flow path to tailwater (EPRI, 1992). The water coming up in the drainage tunnel is then pumped or lead out of the dam body. The effectiveness depends on diameter of the holes, distances and drilling depths.

As a general design principle the uplift pressure is assumed linearly decreasing from upstream water level to 30 percent of the difference between upstream and downstream water level at the upstream edge of the drainage tunnel. The value 30 percent, however, is a rule of thumb and varies between countries and regions. From downstream edge of drainage tunnel, where the pressure is 30 percent of the difference between upstream and downstream water level the pressure is linearly decreasing to downstream water level at the downstream edge, see Figure 5-20 (in the figure the value 30 percent is replaced by the constant K_d). Drains can become filled with sediment or obstructed with minerals and cleaning is therefore necessary, but the uplift reduction may not be what is anticipated and in these cases re-drilling is effective to reduce uplift to original values. According to Amadi et al (Amadi et al, 1990) the drain effectiveness can be reduced because of head losses in the drain pipes. They describe that a decrease in drain diameter caused by a build-up of solid deposits can significantly reduce the effectiveness of drains with diameters less than 100 mm which intersect smooth cracks with large apertures. For drains with diameters larger than 100 mm, the increase in effectiveness with increase in drain diameter is small.

According to RIDAS (RIDAS TA, 2003) the function of drains should be regularly inspected and verified if the stability of the dam depends on proper function of the drainage holes and the importance of this is also confirmed by e.g. Amadi et al (1990), Amadi et al (1991) and Foster (1989b).

An inspection tunnel in the dam body (usually located higher in the dam body than a drainage tunnel), with vertical drainage holes drilled into the rock is assumed to reduce the uplift pressure to about 50 percent of the difference between upstream and downstream pressure at the position of the holes.

In Ruggeri et al (2001) results from four large investigations on uplift has been summarized:

- The results of all the four studies confirm that drainage is the single most effective means of reducing uplift pressure, providing a direct highly permeable path between the water bearing discontinuities and the tailwater.
- Examination of profiles of uplift pressure for gravity dams in one study (carried out by the Swiss Committee of Large Dams where 38 arch dams, 25 gravity dams, 3 arch-gravity dams and 4 buttress dams were investigated) showed a clear break in uplift directly behind the drainage line and low dispersion in uplift reduction, see Figure 5-21.
- In one study (EDF, France) measured uplift pressures in drained condition were compared with theoretical values for a perfectly drained condition and the conclusion was that the measured uplift pressures downstream of the drainage line (about 30 % of the reservoir head) were higher than the corresponding theoretical values.

In conventional design it is assumed that lack of compression at the upstream base of a gravity dam will result in full headwater pressure extending from the heel of the dam for the full length of the tension zone (Stelle et al, 1983) and uplift pressure can also cause the “crack” to expand (Amadi et al, 1990), but this assumption ignores the functioning of any system of drains. Stelle et al (1983) conclude that this assumption is not necessarily valid and that the uplift forces for the crack condition may, in fact, be closer to the forces acting according to the un-cracked condition, which was the case in the dam reported in their paper.

In conventional design it is also assumed that if the crack extends to the line of drains in the dam, the analysis must not take credit for any associated relief of pressure due to drains (Amadi et al, 1990).

A numerical solution by Amadi et al (1990) shows that a tapered crack gives higher uplift pressures compared with the case when it is assumed to be of uniform aperture.

The FERC criteria (according to Foster, 1989a) treat the measured drain effectiveness at the location of the drains. If the crack extends beyond the location of the drains and uplift measurements are available for the loading condition under study, then the

measured values can be used. If, however, uplift readings are not available then the drains are not assumed to be effective.

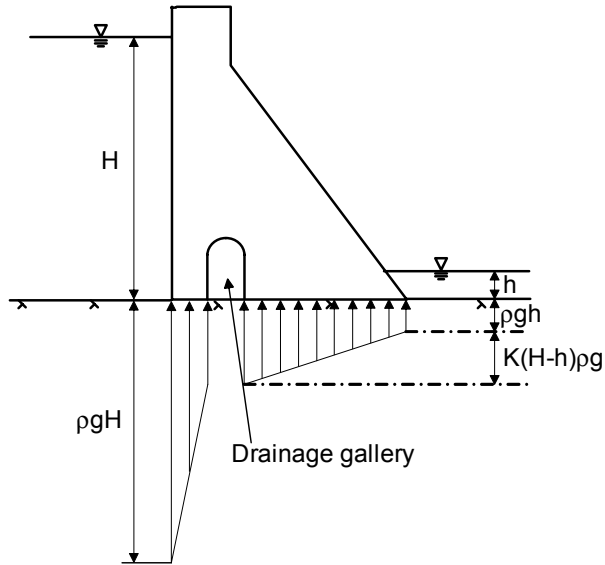


Figure 5-20 - Design assumption of uplift pressure, reduction due to drainage gallery. From Wiberg et al(2001).

SWISS GRAVITY DAMS

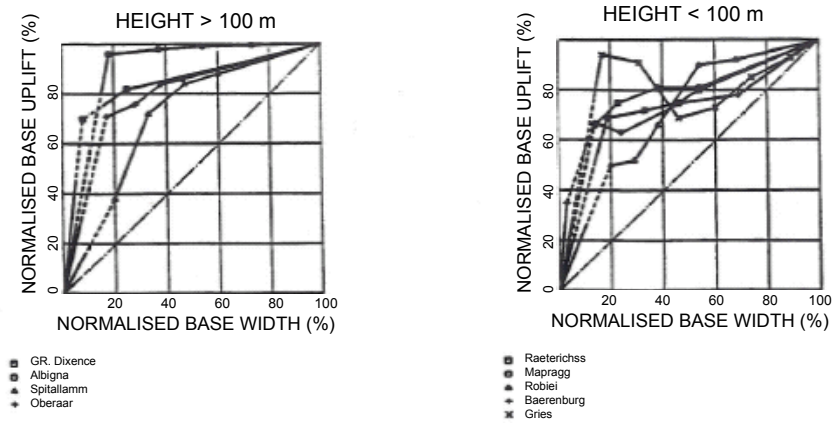


Figure 5-21 -Effect of drainage tunnel (Swiss study in Ruggeri et al, 2001).

5.5.1.2.2. Influence of grout curtains

Grout curtains at the upstream edge also reduce the uplift pressure. The grout curtain reduces the permeability of the foundation rock below the heel of the dam, thereby reducing the quantity of flow through the foundation and causing a large drop of head. According to design guidelines (i.e. RIDAS TA, 2003) a grout curtain can reduce the uplift pressure by about 50 percent, see Figure 5-22, but the effect will decrease with time as the curtain is leached. The effect of grout curtain assumed in design also differs between countries and regions. According to RIDAS TA (2003) the grout curtain may only be considered as extra safety measure unless the curtain is re-injected on regular basis (which in fact is not done very often).

In the report by Ruggeri et al (2001) the results show that "while it is agreed that a well-constructed grout curtain can reduce the amount of seepage through a dam foundation, the influence of the curtain on uplift pressures is still a topic of debate and this is confirmed by the results of these studies".

- Study 2 had not enough data to make quantitative statements on the effect of grout curtain.
- Study 3 (EPRI, USA, Uplift Pressures Under Concrete Dams) pointed out very variable situations, from excellent examples of grout curtain effectiveness to situations where the grout curtain had a negligible effect. Significant examples were also found of initially effective grout curtains later requiring remedial works. The conclusion was that in the absence of instrumentation to continuously prove the effectiveness it is not prudent to rely upon the curtain for significant uplift reduction.
- From study 1 (EDF, France, 31 dams) the effect of grout curtain could not be identified (probably shaded by the prevailing effect of drainage), thus confirming that it was not an important effect.
- From study 4 it was concluded that a single line grout curtains have no significant effect on uplift pressures, and this is also confirmed by Casagrande (1961). It was also stated that grouting is not generally successful as a remedial treatment for high pressures.

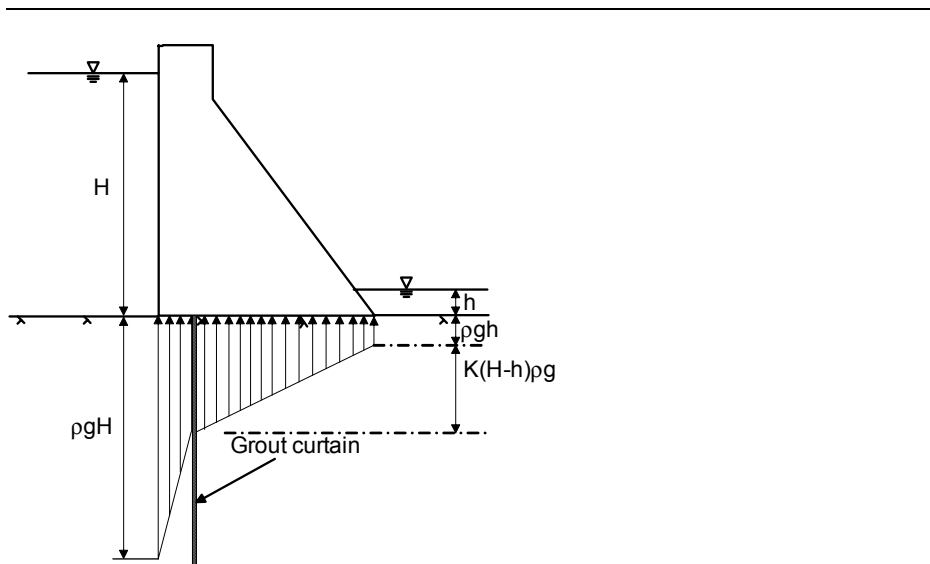


Figure 5-22 - Design assumption of uplift pressure, due to grout curtain from Wiberg et al (2001).

5.5.1.3. Water flow in rock and influence for dams on rock

Concrete dams, at least Swedish, are mostly founded on solid rock where the conditions are in fact different than for soil. In fractured hard rocks flow occur predominantly in main flow paths; along joints, fractures, shear zones, faults and other discontinuities, where the permeability is several orders of magnitudes larger than that for small cracks, which are in turn several orders of magnitude more permeable than the rock itself (which can in many cases be considered impervious) (Singhal & Gupta, 1999). For dense unfractured rock the permeability is usually very low, up to 10^{-11} m/s (0,001md). Fractures increase the permeability by several orders of magnitude, and can be up to 10^{-5} m/s. The conductivity decreases with depth (Singhal & Gupta, 1999).

In rock the flow rate depends on flow velocity, pore size and roughness of fractures and the transition between laminar and turbulent flow may occur at Re between approximately 100 and 2300 (Singhal & Gupta, 1999).

A number of factors, including stress, temperature, roughness, fracture geometry and intersection etc. control the groundwater or water flow through fractures. Fracture aperture and flow rate are directly interrelated, non-parallelism of walls lead to friction losses and normal compressive stress tends to close the fractures and reduce the hydraulic conductivity. Fracture permeability also reduces with increasing temperature due to thermal expansion in rock.

For hydrogeological purpose it is therefore important to understand and describe the structure of the rock mass. In a rock mass where the discontinuities are numerous, evenly distributed and small, the uplift pressure distribution is similar to that given by

the porous media idealisation and considered in design. Long (reproduced in Grenoble et al, 1995) showed that this idealisation is not correct unless the joint spacing is small and joints are highly interconnected in a joint network. Instead, the uplift pressure distribution is controlled by the length and relative permeability of the rock joints, which intersect to form the flow paths beneath the dam (Grenoble et al, 1995).

In EPRI (1992) the result of different aperture size on the uplift is shown, see Figure 5-23; flow through a small aperture will give rise to larger energy loss than flow through a large aperture and the result is that a joint starting out small and increasing will result in lower uplift than a large joint tapering under the dam. Unconnected joints may give rise to very high uplift pressure.

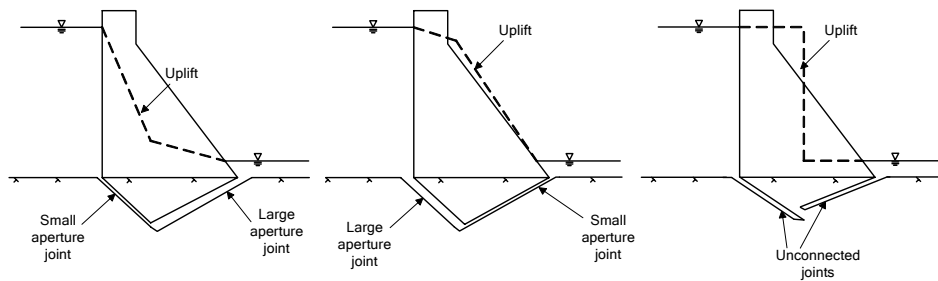


Figure 5-23 - Influence on uplift of joint aperture and interconnection (after EPRI, 1992).

5.5.1.3.1. Water flow in cracks

In the case of flow in rock joints it is common to consider the joint as composed of two smooth, parallel plates and the flow to be steady, single phase, laminar and incompressible. Under these conditions the hydraulic joint conductivity K can be written

$$K = \frac{\rho \cdot g}{\mu} \frac{e^2}{12} = \frac{g \cdot e^2}{12\nu} \quad \text{Eqn. 5-12}$$

where ρ is the fluid density, g is the gravitational acceleration, e is the hydraulic aperture, μ is the dynamic viscosity of the fluid and ν is the kinematic viscosity of the fluid. Darcy's law can be rearranged to the "cubic law"

$$Q = \frac{g}{\nu} \cdot \frac{w \cdot e^3}{12} i \quad \text{Eqn. 5-13}$$

where w is the width of the flow path and i is the dimensionless hydraulic gradient (Olsson & Barton, 2001, Olsson, 1998).

Natural rock joints are in reality not smooth and parallel. If the cubic law describes the relationship between joint flow rate and aperture, then the measured flow rate per hydraulic head unit versus the aperture data should plot as a straight line on a log-log

plot with a slope equal to three. Most laboratory experiments show a deviation from this, growing with increasing normal stress. The reason seems to be related to surface roughness, aperture, mating and stiffness. The cubic law seems to be valid only for very open joints or for joints with rather smooth surfaces. Therefore, when Darcy's law is applied to natural joints with rough surfaces, a correction factor has to be used, which accounts for deviations from the ideal conditions assumed in the parallel smooth plate theory. It has been shown that the hydraulic aperture is less than the mechanical (geometrical) aperture, E_g , by a factor that depends on the ratio of the mean value of the aperture to its standard deviation (Olsson & Barton, 2001, Olsson, 1998). According to Hakami (1995) the ratio

$$\frac{E_g}{e} = 1,1 - 1,7 \quad \text{Eqn. 5-14}$$

where E_g is the mean geometric (mechanical) aperture and Eqn. 5-14 is valid for $E_g = 100\text{-}500 \mu\text{m}$.

According to Olsson & Barton (2001) Barton (1982) proposed that the hydraulic aperture was related to the mechanical aperture by

$$e = \frac{E_g^2}{JRC^{2.5}} \quad \text{Eqn. 5-15}$$

where JRC is the joint roughness coefficient.

Results by Olsson & Barton (2001) show that both the ratio E_g/e and the hydraulic aperture e increase during increased shear displacement. The hydraulic aperture was coupled to the joint roughness coefficient (JRC) and the shear displacement, and by use of their results it is possible to calculate the changes of the hydraulic aperture during shearing and thus the hydraulic conductivity or transmissivity.

5.5.1.3.2. *Tapering of joints*

According to the cubic law, the quantity of flow through a rock joint is a function of the aperture of the joint and the roughness of the walls. A tapered joint can be illustrated as consisting of a series of progressively smaller pipes, and as the pipe diameter decreases, the slope of the pressure curve increases. Hence, the pressure distribution in a tapered joint is parabolic rather than linear (Grenoble et al, 1995). Figure 5-24 shows schematic pictures of uplift pressure distributions with tapering, widening and even-aperture joints.

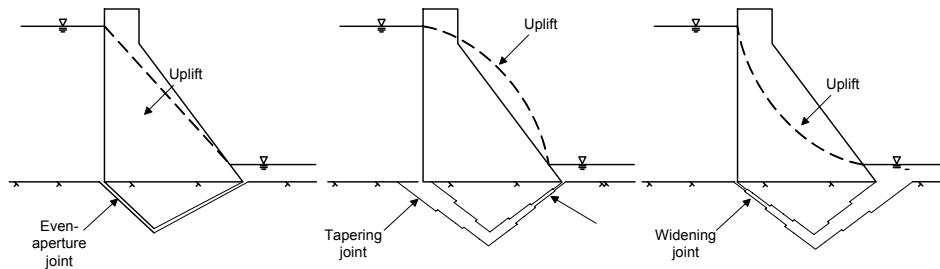


Figure 5-24 - Pressure distribution in tapered pipe.

As the loads on a dam change, the loads on the foundation also change and cause the joints in the foundation to open or close. Increase of headwater as well as changing temperature may both influence the uplift, as will be shown later in this chapter.

The variation in stress at the dam base, caused by increase in head or temperature changes, is on the order of a few MPa. Load changes of this magnitude will cause only small deformations in the rock joints. If the primary flow paths through the foundation consist of open mismatched joints these small deformations will have little or no effect on the permeability and uplift. If the flow path consists of tight, interlocking joints, the deformations can be large compared to the original aperture of the joints and the change in permeability will cause measurable changes in uplift (EPRI, 1992).

Grenoble et al.(1995) investigated the effect on seventeen dams; three dams clearly exhibited effects on foundation permeability changes due to changes in reservoir level, seven showed no apparent sensitivity to this and seven did not have a fluctuation large enough to make an evaluation. Four of the dams exhibited permeability changes caused by changes in temperature.

For a dam with linear relationship between headwater elevation and uplift pressure the result indicates that changes in reservoir level do not change the permeability of the foundation enough to measurably affect uplift. The joint deformations caused by changes in reservoir level and temperature are small in comparison to the large aperture of the stress-relief joints.

5.5.1.3.3. Influence of temperature changes

Uplift pressure varies throughout the year and is strongly affected by the environmental thermal variations. Guidicini & Andrade (1988) analysed measurement from 752 piezometers from eight dams in Brazil and found that seasonal cyclic variation was found in six dams and especially in the piezometers near the concrete/rock interface and close to the upstream face, where about 10 % of the piezometers showed this type of behaviour. It was present for both hollow concrete structures, such as buttress dams, and gravity dams, but more significant for the former.

The highest uplift pressure figures occurred during the coldest winter. Noteworthy is that the temperature variation was only 10-15 degrees Celsius, and always above zero.

According to Guidicini & Andrade (1988) the uplift pressure variation due to thermal oscillation is influenced by:

- *Volumetric variations in the concrete structures.* Thermal variations cause volumetric changes in dam concrete structures that are reflected at foundation level as changes in the tensions. It is not the daily thermal oscillation, but seasonal thermal oscillation, although smaller in range, that gives the most significant results due to persistent action.
- *Volumetric variations of the discontinuous rock medium.* Any rock mass presents volumetric changes with seasonal thermal oscillations through direct incidence of the sun radiation. The temperature variation in depth will depend on thermal conductivity characteristics of the medium. The daily oscillation only reaches the approximate depth of one meter, while seasonal thermal oscillation can be detected at depths down to 20-25 meters. Presence of water strongly influences the thermal conductivity of the medium. The part most sensitive to thermal variations are the first top meters where the most significant water percolation occur. A rock mass supporting a hydraulic structure is directly affected by thermal oscillations on the downstream side and indirectly on the upstream side. Nearby the upstream toe the discontinuities are very sensitive to volumetric variations, although the reservoir water mass reduces this effect, and small variations in hydraulic conductivity can cause considerable changes in the uplift pressure figure.
- *Influence of the water flow through the rock mass.* The water volume in a reservoir undergoes seasonal temperature oscillations. When water percolates through the rock mass the temperature drop or increase is transferred into the rock mass. Temperature drop widens the discontinuities due to volumetric contraction and temperature rise cause a decrease in width. This effect may occur not only in the concrete/rock interface but also deeper in the rock mass.
- *Variations in kinematic viscosity of the water.* A temperature drop cause an increase in the kinematic viscosity of the water, which hinders the flow.

The observed magnitude of increase in uplift pressure presented by Guidicini & Andrade (1988) was 23-45%. A time lag between low-peak of temperature and maximum uplift, where maximum uplift occurred up to two months after the lowest temperature, was observed.

According to Grenoble et al.(1995) deflection measurements typically show that the crest of the dam moves downstream in the fall and winter when the downstream face cools and contracts, and then moves upstream in the spring and summer when the downstream face warms and expands. These loads are transferred to the foundation and sub-horizontal joints near the heel will open in the winter and close near the toe. As a

result the foundation can be idealized as a tapered joint where the degree of taper increases in the winter and decreases in the summer.

In Bernstone and Westberg (to be published, see also Bernstone (2006)) uplift pressures under a spillway structure show increasing uplift during the cold periods, but here the maximum uplift seems to appear earlier in the season than that reported in Guidicini & Andrade, before the lowest temperatures, and time-lag is not present. The spillway section is shown in Figure 5-25 and the uplift pressure monitoring results in Figure 5-26.

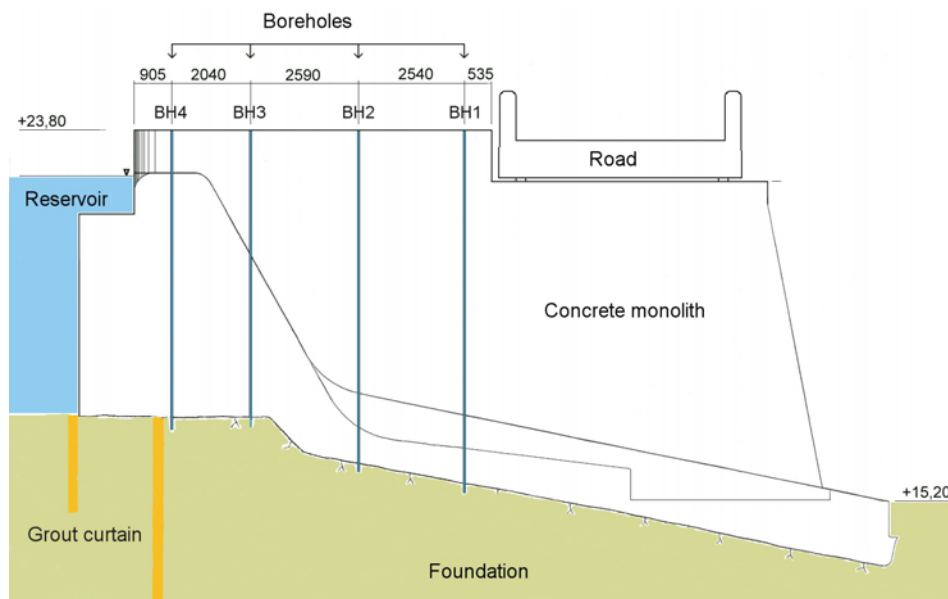


Figure 5-25 - Section of concrete monolith with installed TDR uplift pressure monitoring in BH1-4. From Bernstone & Westberg (to be published).

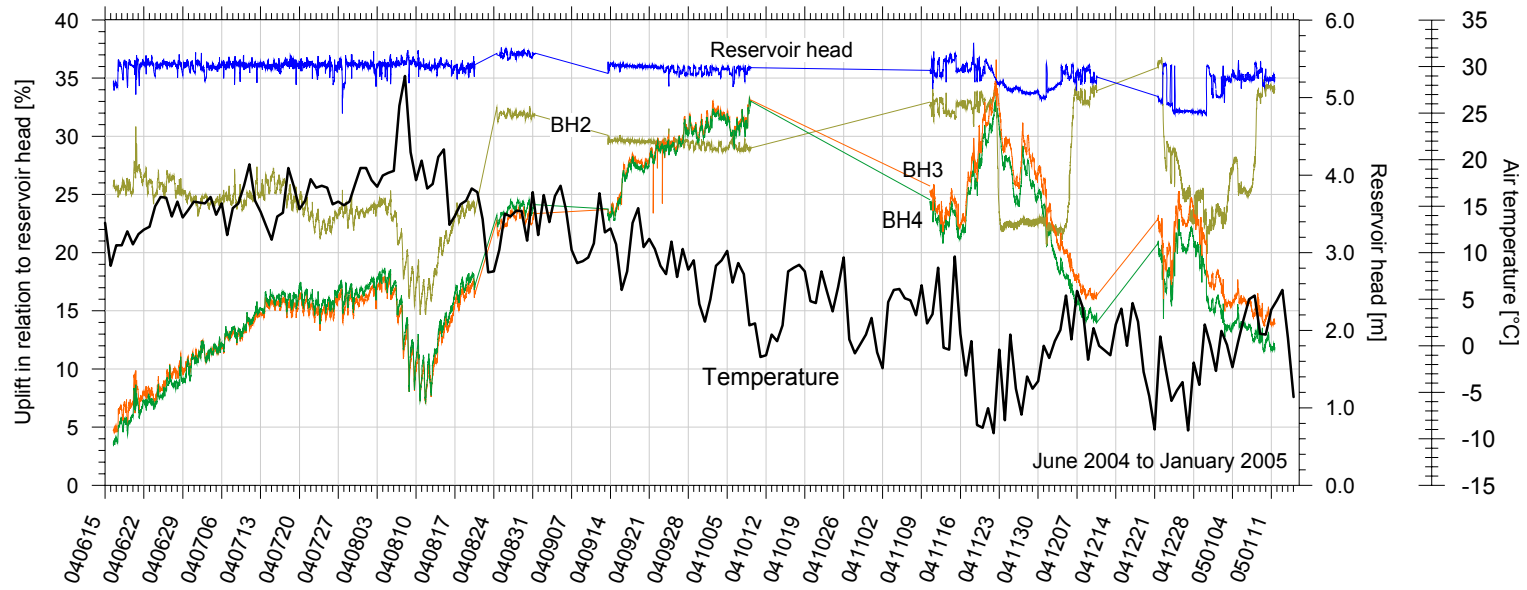


Figure 5-26 - Uplift pressure monitoring from Bernstone & Westberg (to be published).

5.5.1.3.4. *Influence of large reservoir head*

As uplift measurements are rarely available at high reservoir levels it is common practice (at least in the USA) to extrapolate the uplift from normal to high reservoir level as long as cracking (or no-compression) do not occur at the heel (Foster, 1989a). Since the relation between uplift and reservoir level is not always linear, as will be shown, this assumption can be questioned.

Grenoble et al (1995) performed a simple finite element analysis of a concrete gravity dam section for seasonal changes in headwater level and temperature and investigated how this affects the stress distribution along the base of the dam.

For rise of reservoir, the stress distribution changes from highly compressive at the heel to less compressive and at the toe it becomes more compressive with increasing head water level. Thus, as the reservoir rises, horizontal joints below the base of the dam open near the heel and close near the toe. The effect of a rise in reservoir level is that joints near the heel of the dam open and joints near the toe close. These deformations cause the permeability of the rock mass near the heel to increase and the permeability near the toe to decrease. Consequently, flow through the dam foundation can be simplistically viewed as flow through a tapered pipe. As the headwater level rises, the pipe becomes more tapered. Assuming that the joints do not deform will result in an un-conservative estimate of uplift pressure at higher headwater levels.

Figure 5-27 shows the result on uplift pressure; a tapered joint is subjected to different levels of headwater and as headwater rise the pipe tapers. Apparently the headwater rises cause the uplift pressure to change from a linear distribution to a curvilinear.

Grenoble et al (1995) show an example of a dam that exhibit curvilinear relationship between headwater level and uplift, see measurement data in Figure 5-28. Here the joints are tight, and the deformations caused by changes in headwater level are large in relation to the initial aperture of the joints. For a dam with linear relation between headwater level and uplift the joints are larger.

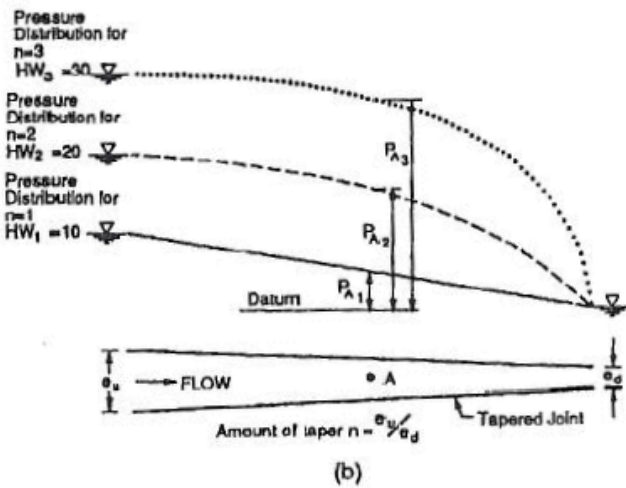


Figure 5-27 - Uplift pressure distribution caused by rise of headwater from HW1 - HW2 - HW3 (Grenoble et al, 1995).

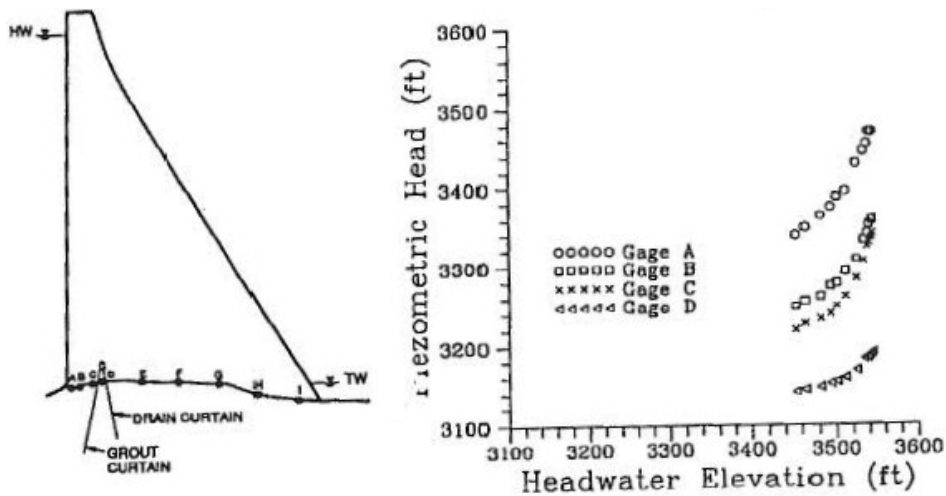


Figure 5-28 – Curvilinear relation between headwater level and uplift at Hungry Horse Dam. (from Grenoble et al, 1995).

Ruggeri et al (2001) mentions that the practise of assuming that uplift pressures vary linearly with headwater is not confirmed. In three of the investigations presented the variations (study 1 (EDF, France), 3 (EPRI, USA) and 4 (EPRI, USA)) were nonlinear.

- Study 3 showed that the increase in uplift pressure was not proportional to the rise in reservoir level, but somewhat less. The explanation was thought

to be the progressive closure of joints and other natural flow paths in the rock mass, that can be produced by increased compressive stresses produced by increased reservoir levels. This supports the validity and logic of extrapolating uplift pressures relative to head water levels as a reasonable conservative approach.

- Study 4 (among the authors Grenoble et al. (1995) referred to above) showed that uplift pressure (data from gravity dams) exhibited non-linear variations where uplift pressures increased more than reservoir level. This behaviour was associated to the variations of the permeability of a dam foundation when the joints of the foundation rock deform as the reservoir level changes. This was also confirmed by a finite element model. It appeared that only small aperture joints deform sufficiently to give rise to non-linear uplift response. Large aperture joints will probably not deform enough under the stress changes caused by headwater variations to create noticeable nonlinearity. Grouting may stiffen joints sufficiently to prevent tapering of joints and the resulting non-linear uplift. None of the gravity dams which had extensive consolidation grouting (grouting to prevent consolidation, i.e. not with primarily uplift reduction purpose) showed non-linear uplift. Dams which would be expected to have non-linear uplift would consequently be those with tight, un-grouted joints and large variations in reservoir level.
- In study 1 both increasing and decreasing gradients of uplift pressures were observed for increased headwater levels, in rare cases for the same dam.

Ruggeri et al (2001) concludes that it is essential to base the estimate of uplift pressure on measured pressures, because the actual uplift pressures can vary substantially from the assumption used in the design, and also underline that measured uplift pressures can exhibit high spatial variability. Ruggeri et al (2001) also recommend an extensive monitoring network to derive reliable uplift values for safety assessments from measured data, considering also that for gravity dams the safety assessment have to be carried out for independent monoliths. The possible variations of the measured relationship between external loads and uplift pressures must also be taken into account. In addition to possible slow and progressive variations (drifts), also the possibility of sudden variations related to the reaching of unusual or exceptional reservoir levels must be evaluated. Slow drifts can be associated to a slow variation in time of the permeabilities of the foundation. The opening of rock discontinuities can induce sudden and strong variations in uplift when the state of stress exceeds threshold values (more common for arch-gravity dams due to higher stress levels transmitted to the foundation). The extrapolation of measured uplift to higher water levels must therefore be based on a comprehensive understanding of the uplift under normal operating conditions and a thorough understanding of how reservoir level, foundation, geology and drainage affect the uplift pressures.

From Ruggeri et al (2001) it appeared that grouting may stiffen joints sufficiently to prevent tapering of joints and the resulting non-linear uplift. None of the gravity dams in the investigations referred to which had extensive consolidation grouting showed non-linear uplift.

The joint deformations caused by changes in the reservoir and thermal loads are not necessarily in phase and can amplify or offset each other. Consequently, the maximum uplift pressure may not occur when the reservoir level is highest. The time difference between the peak in reservoir level and the peak in uplift pressure has been misinterpreted as a time lag in the response of uplift pressures to changes in headwater (Grenoble et al, 1995).

Availability of drainage in case of large reservoir head

Since uplift pressure readings are generally only available at normal reservoir levels, drain effectiveness at reservoir elevations beyond those at which readings have been obtained cannot be predicted with any degree of confidence (Foster, 1989a). In the US the following factors are considered when the validity of extrapolation of drain efficiencies is determined:

- The percentage increase between the reservoir levels at which measurements are available and the level to which extrapolation is desired.
- The difference between the drain efficiency assumed in the design and the measured drain efficiency.
- Whether or not a theoretical crack propagates beyond the location of the drains during the loading conditions at which measurements are available.
- The degree of understanding of the geology of the foundation.
- The sensitivity of the sliding factor of safety to drain effectiveness assumptions.

5.5.1.4. Modelling water flow in rock mass

All evidence suggests that consistent modelling of flow and transport in fractured rock can hardly be done by treating it as a uniform or mildly non-uniform isotropic continuum. Instead, one must generally account for the highly erratic heterogeneity, directional dependence, dual or multi-component nature and multi-scale behaviour of fractured rocks. One way is to depict the rock as a network of discrete fractures (with permeable or impermeable matrix blocks) and another as a stochastic (single, dual or multiple) continuum. A third way is to combine these into a hybrid model of a stochastic continuum containing a relatively small number of, or statistical information about, discrete features (Neuman, 2005).

The spatial distribution of flow is very uneven in crystalline rock with inflowing water localized to a few unevenly spread spots. Only a fraction of all fractures are hydraulically important (Dverstorp, 1991). Conceptual models for crystalline rock environments are usually more complex than that for sedimentary rock. In uniform

granitic rock, fractures may be oriented in preferred directions according to magma emplacement and cooling, local deformation, regional deformation and erosional unloading (Delleur, 1999).

5.5.1.4.1. *Fracture network*

Modelling approaches to simulate flow and transport in fracture networks fall into one of three categories within the range of conceptual models for fractured rock (Delleur, 1999):

- Models based on equivalent porous medium treat the fractured porous rock as equivalent to a non-fractured continuum. Bulk parameters for the permeability of the rock mass are used, and the geometry of individual fractures or the rock matrix is not considered. This is a reasonable approach if fracturing is intense or the study domain is sufficiently large such that individual fractures have no influence on the overall flow systems (e.g. some regional systems of the scale of kilometres) (Delleur, 1999).
- The discrete fracture network (DFN) models describe the rock as a network of interconnected discrete fractures and such models may very closely represent the real structure of fractured rock. The crystalline rock mass contains deformation zones on a wide range of scales (micro-crack in the “intact rock”, individual visible joints, regional fault zones). The larger can be described deterministically, while the smaller require some kind of statistical representation. In the discrete fracture network concept, fracture orientation distribution for each fracture set is used together with spatial distribution of fractures (e.g. Poisson distribution) or models for statistical dependence among fractures, fracture size distribution (Stille et al, 2003)
- Double porosity models are used to attempt to bridge the gap between the simplifications of equivalent porous medium models and the details of the discrete fracture models by treating the fracture system and the porous matrix as two separate inter-related continua (Delleur, 1999).

5.5.1.4.2. *Stochastic continuum approach*

Laboratory and field measurements of hydraulic and transport parameters (such as permeability; specific storage; constitutive relations between saturation, capillary pressure and relative permeability; advective porosity; dispersivity) in porous media represent averages over many pores. The same is true about state variables such as pressure, saturation, concentration, flux and velocity. As these bulk or macroscopic quantities are defined at each point in space, adopting them implies that one ignores the complexities of the pore structure, replacing it by a fictitious continuum (Neuman, 2005).

The stochastic continuum concept is developed from the stochastic transport theory for an anisotropic porous medium (Dverstorp, 1991). This is also called the geostatistical approach. Blocks of constant properties (hydraulic conductivity and porosity) represent

the three-dimensional hydraulic conductivity field in the rock and the properties between blocks vary according to a specified covariance structure.

All that is required for such a continuum representation to be valid is that the quantities be measurable on a consistent “support” scale, which is large in comparison to a characteristic pore (or grain) scale and small in comparison to the flow or transport domain of interest. The support scale need not constitute a representative elementary volume (REV). Most commonly, one infers from packer tests hydraulic conductivities or permeability by treating the surrounding rock as a locally uniform (over the corresponding support volume) porous continuum. As the precise nature and size of a support volume associated with a packer test is difficult to ascertain it is common to quote results in terms of a nominal support scale equal to the length of the packed-off interval (this is valid at best for single-hole packer tests in which all measurements are confined to the fluid injection interval, not for fluid interference tests between boreholes or multiple test intervals within a single borehole). Permeabilities obtained in this manner tend to be highly erratic and sensitive to the length of the test interval (Neuman, 2005).

5.5.1.4.3. *Pros and cons for different approaches*

Some questions arise as to the applicability of the stochastic continuum-modelling concept for sparsely fractured rock. Another objection is that there is no (or weak) coupling between the flow geometry in the rock and the hydraulic properties in the model (Dverstorp, 1991). The spatial structure of fractures and fracture zones is not easily captured by a continuous representation. Instead they are better viewed as stochastic objects in space. (Stille et al, 2003)

Ando et al (2003) found that a high-resolution stochastic continuum model of flow and transport in fractured crystalline rock performed as well, and in some important ways better, than the DFN-based models of Cacas et al (see Ando et al). Neuman (2005) mention that at the Äspö Hard Rock Laboratory in Sweden a wide range of discrete and continuum models appear to have been capable of capturing key aspects of flow and transport in a fractured crystalline rock mass, including relatively simple models described by Dverstorp et al (see Neuman, 2005). According to Neuman some of the reasons for DFN models not being more competitive are:

- The ability to map discontinuities in the rock with available geological and geophysical tools tends to decrease as the scale of the discontinuity goes down
- Both surface and subsurface data are limited in that they provide much less information about fracture shapes and sizes than about densities and orientations, though all four parameters are equally important for the construction of realistic fracture network models.

Geology and geophysics alone do not provide any quantitative information about fracture apertures of the kind required to assess fracture flow and transport parameters purely on the basis of fracture-geometric data.

5.5.1.5. Cracking

Numerous papers describe the difficulties involved when determining the uplift pressure in cracks. As mentioned earlier, common practice is to assume that a non-compressive part of the dam body or foundation is cracked and that the pressure head at the mouth of the crack enters the whole length of the crack (Burec, 1987, Ferc, 2002, RIDAS TA, 2003).

Dewey et al (1994) use FE fracture mechanics to determine if the crack growth is stable or not and how far the crack propagates. They investigate four different uplift distribution models, and conclude that the stress intensity factor K_I is sensitive to uplift pressure model. Crack lengths in their model are sometimes longer than those determined by models compared (Federal Energy Regulatory Commission, US Army Corps of Engineers, US Bureau of Reclamation) since their analysis consider the stress concentration at the crack tip, while other models only consider the effective stress.

Amadei et al (1990) investigated crack properties and the influence on the uplift pressure distribution in case of high reservoir levels and found that

- Uplift increases with crack width and drain spacing.
- Cracks at the base of a dam are the most critical as far as uplift is concerned
- Drain effectiveness decreases as the crack aperture increases
- Drain effectiveness increases with crack roughness.
- Turbulence can exist near the entrance to the drains and between the drains and crack entrance at lower heads than what was expected. This phenomenon can produce higher uplift pressures in the crack and result in much lower drain effectiveness than if crack flow was purely laminar. Laminar flow assumption for a crack underestimates uplift.
- Drain effectiveness increases with reservoir head, but as turbulence develops, drain effectiveness drops drastically for drains with diameter less than 5 cm. For larger drain diameters turbulence does not seem to affect drain effectiveness.
- Tapered cracks always give higher uplift than cracks with constant aperture.
- Transient response of a crack can be neglected when estimating uplift because flood events are relatively slow (here it is thus assumed that a “time-lag” exists between head water rise and uplift pressure increase, but this is unlikely according to e.g. Ruggeri et al.).

5.5.2 Uplift modelling by geostatistical approach

To perform a structural reliability analysis it is necessary to have reliable input data and therefore a statistical distribution of uplift is needed. From the previous state-of-the-art

it is obvious that this is not an easy task to attain. Uplift monitoring results is, with few exceptions, only available at normal pool levels, and monitoring is only performed at a few points of the dam, rising questions regarding ability to reliably reflect reality. In the field of ground water flow of aquifers a large number of modelling attempts has been performed, but for uplift pressure distributions only one such has been found, that of Griffiths & Fenton (1993).

The uplift pressure distribution beneath a dam is dependent on the distribution of hydraulic conductivity; with low hydraulic conductivity close to the upstream side of the dam a drop in pressure will occur close to the upstream side, resulting in a low total uplift and moment of uplift. If, on the other hand, the hydraulic conductivity is large close to the upstream face and low further downstream the result will be high uplift under a large portion of the dam, resulting in larger total uplift and moment of uplift. This phenomenon can be compared to that of tapered joints shown in Figure 5-23. Thus it is the distribution of hydraulic conductivity beneath the dam that influences the uplift pressure distribution, and the absolute values of hydraulic conductivity are less important.

In this thesis a geostatistical approach has been used to simulate the hydraulic conductivity field and from this uplift pressure distribution has been derived by a finite element analysis. A large number of simulations has been performed to attain statistical distributions of uplift.

5.5.2.1. Geostatistics

Natural soils are highly variable in their properties and rarely homogenous. Soil properties do not vary randomly in space; rather such variation is gradual and follows a pattern that can be quantified using spatial correlation structures (Elkateb et al (2003). Toblers law (Schabenberger et al, 2002) states that “Everything is related to everything else, but near things are more related than distant things”, in other words we should expect relationships between spatially distributed quantities and the strength of the relationships is a function of their spatial separation. The spatial correlation is often expressed in terms of the variogram (see e.g. Cressie, 1993) or covariance function (Vanmarcke, 1977). To proceed with a statistical analysis of soil the main elements of soil spatial variability have to be identified, such as

- 1) Mean, coefficient of variation and probability distribution of soil data,
- 2) The spatial correlation structure,
- 3) The limit of spatial continuity and
- 4) The volume variance relationships.

5.5.2.1.1. Variogram and covariance function

The variogram is a measure of dissimilarity between two points in space separated by a distance h . The variogram is defined as

$$2\gamma(h) = \text{Var}[z(s) - z(s+h)] \tag{Eqn. 5-16}$$

where $z(s), z(s+h)$ are the values in point s and point $s+h$, h is the separation distance (or lag), $2\gamma(h)$ is the variogram value at separation distance h and $\text{Var}[\]$ is the variance operator (Cressie, 1993). The covariance function, on the other hand, is a measure of similarity between two points according to

$$C(h) = E(z(s) \cdot z(s+h)) - m^2 \tag{Eqn. 5-17}$$

where $C(h)$ is the value of the covariance function at separation distance h , $E[\]$ is the mean operator and m is the mean value of Z .

For second-order stationarity the variogram and covariance functions are correlated through

$$\gamma(h) = \sigma^2 - C(h) \tag{Eqn. 5-18}$$

Where σ^2 is the variance, Var .

Cressie (1993) argues that variogram estimation is preferred to covariance function estimation, since it is defined in cases when the covariance function is not.

Figure 5-29 shows the semivariogram ($\gamma(h)$) plotted against the separation distance. The sill is the value at which the semivariogram levels off corresponds to the variance. The spatial range is the separation distance at which the semivariogram reaches the sill and beyond this there is no, or insignificant, spatial correlation between data. There are several variogram models and the spherical model reaches the sill value at the specified range, while the exponential and Gaussian approach the sill asymptotically. Figure 5-29 shows the exponential and spherical models with the same variance (sill) and range (variance 16, range 12) and the exponential model with different variance, and range.

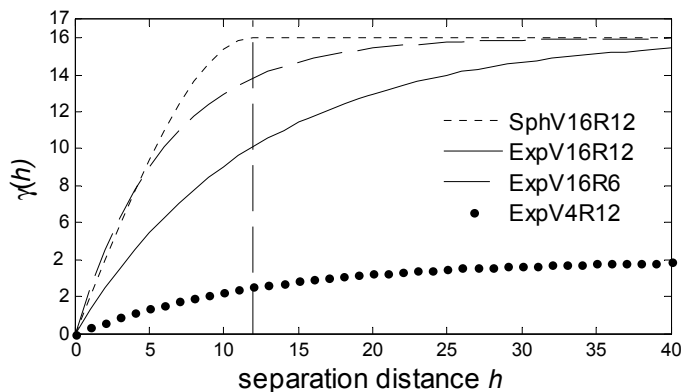


Figure 5-29 - Variograms of exponential and spherical model for different scale, variance and nugget.

5.5.2.2. Uplift simulation using geostatistics

The main idea herein is that a geostatistical approach can be used to describe the hydraulic conductivity field beneath the dam and then, for given boundary conditions, use a finite element solution to derive the uplift pressure. The reason to use a geostatistical approach for water flow in rocks is that there are main flow paths, and in case of high hydraulic conductivity in one point it is likely to find high hydraulic conductivity in a point close to this. Rocks can often be considered anisotropic, with large spatial range in one direction and small in the other (parallel and transverse to joints, respectively).

There are, however, some obvious objections to this approach:

- The geostatistical approach requires a continuum description of the rock mass. When the distances between discontinuities in the rock mass are long compared to the scale of interest, the rock mass can be considered as intact rock and modelled as a continuum. When the distances are short in relation to the scale of interest, the rock mass can be considered as heavily fractured and also be modelled as a continuum. At some intermediate scale, however, the rock mass is considered as a discontinuum material (Johansson, 2005). The continuum material is usually modelled as an isotropic or anisotropic material, while for discontinuum material the hydraulic properties are mainly governed by the discontinuities. The spatial distribution of flow is very uneven in crystalline rock with inflowing water localized to a few unevenly spread spots. Only a fraction of all fractures are hydraulically important (Dverstorp, 1991). The result is that the continuum approach is only valid in some cases, while in others a model with discrete cracks in an impervious material should be used.
- The range and variance of the hydraulic conductivity is unknown. According to hydrogeologist Follin (2006) the variance can be “any value” and the range is not feasible to assume.

In spite of this, a geostatistical approach is a way to describe possible uplift distributions and investigation of a number of different combinations of range and variance will increase the present state of knowledge. As mentioned above design is based on the assumption of linear uplift pressure distribution, and the literature treating uncertainties regarding this assumption is scarce or non-existent, and consequently any information of uncertainty is valuable even though it should be used with care.

5.5.2.2.1. *Simulation of hydraulic conductivity random field*

Using a geostatistical approach the hydraulic conductivity beneath a dam can be simulated as a random field. A set of spatial data $Z(x,y)$ is considered a realization of a random experiment and when mapped on to a surface a random field is obtained. A *variogram* can be used to define the extent of *spatial correlation* between the values in the data set. For each new experiment a new realization is obtained (Schabenberger et al 2002). Figure 5-30 show realizations of three random experiments. The first two with

the same variance, range and variogram model (a and b). When the *spatial range* is zero there exists no correlation between the values of Z at different locations and the result is a field where the values are completely random as that shown in c. In simple terms the variance and mean gives the properties of the statistical distribution of the hydraulic conductivity (large variance = wide distribution), whereas the spatial range gives information of the extent of spatial correlation.

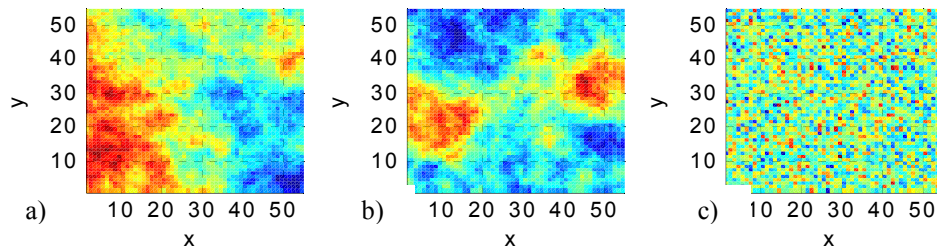


Figure 5-30 – three realizations of $Z(x,y)$.

For each realization of the hydraulic conductivity random field the uplift can be calculated by solving the differential equation for Darcy's law in two dimensions

$$\frac{\partial}{\partial x} \left(tK_{xx} \frac{\delta\phi}{\partial x} \right) + \frac{\partial}{\partial y} \left(tK_{yy} \frac{\delta\phi}{\partial y} \right) + tQ = 0 \quad \text{Eqn. 5-19}$$

where K_{xx} and K_{yy} is the hydraulic conductivity in x and y directions and Q the water volume supply per unit volume of the body and per unit time and t is the thickness of the underground section considered and for isotropic materials $K = K_{xx} = K_{yy}$.

As the stability of a concrete dam monolith is dependant on the total uplift force or total moment due to uplift this is what is interesting and the distribution of total uplift and moment will be investigated.

Input parameters

As mentioned above the input parameters are difficult to attain. From literature some examples are found of continuum descriptions of hydraulic conductivity fields.

- Follin (1992) performed numerical calculations of heterogeneity of groundwater flow and solute transport in hypothetical blocks of fractured hard rock in a “3m scale”. It must be pointed out that this was in fact for groundwater flow and solute transport in case of final disposal of radioactive waste and thus at a much larger scale than that for water flow beneath a dam. Follin uses a log-normal conductivity field of fractured hard rock as this, according to Follin, is well documented. Follin used
 - Mean of $Y = \ln(K)$, $\mu_Y = -16$ ($\Rightarrow K_G = 1.125 \cdot 10^{-7}$ m/s)
 - Standard deviation $\sigma_Y = 4$

-
- Correlation length $\lambda_y = (0, 6, 12)\text{m}$
 - Variogram function $\gamma(h) =$ isotropic and exponential.
 - Griffiths & Fenton (1993) used a local average subdivision (LAS) to generate realizations of a 2-dimensional random permeability field for a stochastic soil beneath a water retaining structure and solved the Laplace equation for flow by use of finite element analysis. Flow beneath the water retaining structure and uplift force in the contact between structure and soil was the result. The procedure used in this paper is similar, but performed for the base area of the dam, whereas the analysis by Griffiths & Fenton was for a vertical plane. According to the authors, field measurement has indicated that the probability distribution of hydraulic conductivity of soils is approximately log-normal (Griffiths & Fenton refer to Hoeksema & Kitanidis (1985) and Sudicky (1986)). Griffiths & Fenton used
 - mean permeability of $\mu_k = 10^{-5}\text{m/s}$
 - COV of the permeability was = 0.125, 0.25, 0.5, 1.0, 2.0, 4.0, 8.0 and 16.0
 - Scale of fluctuation (similar to range) was $\theta_k = 0.0, 1.0, 2.0, 4.0$ and 8.0.

Simulation procedure

Because of the difficulty to attain the “true” variance and range a number of combinations of range and variance was used the present case, see Table 5-7. In this table and further in this paper the combinations are denoted V16R12 for variance 16 and range 12. The mean($\ln(K)$) = -16 ($1.125 \cdot 10^{-7}$ m/s), is the same as that used by Follin (1992). The nugget (discontinuity at the origin, for further information see e.g. Cressie (1993)) is set to zero and an exponential variogram is used.

The simulation was performed in the computer software R (Hornik, 2006) with use of the package RandomFields (Schlatter, 2001), which simulate Gaussian random fields. The area was 20m·20m divided into $55 \cdot 55 = 3025$ elements. Apart from the simulations shown below the effect of drainage and grouting was tested for V16R12, the procedure is described below. The effect of anisotropic hydraulic conductivity field as well as uplift for buttress dams was also investigated.

Table 5-7 - Combinations of variance and range for simulations.

Range	Variance											
	0,0625	0,25	1	2,25	4	6,25	9	12,25	16	25	36	49
0												
2												
4												
6												
8												
10												
12												
16												
19												
22												

5.5.2.2.2. Finite element formulation

Darcy's law can be generalized to

$$\mathbf{q} = -\mathbf{D}\Delta\phi \quad \text{Eqn. 5-20}$$

where q is the volume flux vector, D the constitutive matrix for permeability (hydraulic conductivity) and ϕ is the piezometric head (Ottosen et al, 1992).

The so-called weak formulation of the two dimensional flow is

$$\int_A (\Delta v)^T t \mathbf{D} \Delta \phi dA = - \int_{Lh} v h t dL - \int_{Lg} v q_n t dL + \int_A v Q t dA \quad \text{Eqn. 5-21}$$

where v is any function, Lh is the boundary along which the pressure head $\phi = h$ and the flux q is unknown, while along the boundary Lg the flux is $q = g$ and the pressure head ϕ is unknown, Q is the water (flow) "supply" over the area and t is the thickness.

The FE formulation for the problem is now given by

$$\mathbf{K}\mathbf{a} = \mathbf{f} \quad \text{Eqn. 5-22}$$

where

$$\mathbf{K} = \int_A \mathbf{B}^T \mathbf{D} \mathbf{B} t dA$$

$$\mathbf{f} = \mathbf{f}_b + \mathbf{f}_1$$

$$\mathbf{f}_b = - \int_{Lh} \mathbf{N}^T h t dL - \int_{Lg} \mathbf{N}^T q_n t dL$$

$$\mathbf{f}_1 = \int_A \mathbf{N}^T Q t dA$$

where \mathbf{N} is the global shape function matrix

$$\mathbf{N} = [N_1 \ N_2 \ \dots \ N_n]$$

\mathbf{a} contains the pressure head at the nodal points in the entire body,

$$\mathbf{B} = \begin{bmatrix} \frac{\partial N_1}{\partial x} & \frac{\partial N_2}{\partial x} & \dots & \frac{\partial N_n}{\partial x} \\ \frac{\partial N_1}{\partial y} & \frac{\partial N_2}{\partial y} & \dots & \frac{\partial N_n}{\partial y} \end{bmatrix},$$

and \mathbf{f} is the force vector consisting of the boundary vector \mathbf{f}_b and the load vector \mathbf{f}_l . The boundary vector consists of known quantities of pressure head along the boundary Lh and flux along the boundary Lg . For the present problem the pressure head is known along the upstream and downstream boundaries and the flux along the sides, as shown in Figure 5-31. As no water supply is considered to exist anywhere over the area considered, the load vector \mathbf{f}_l becomes zero (Ottosen et al, 1992).

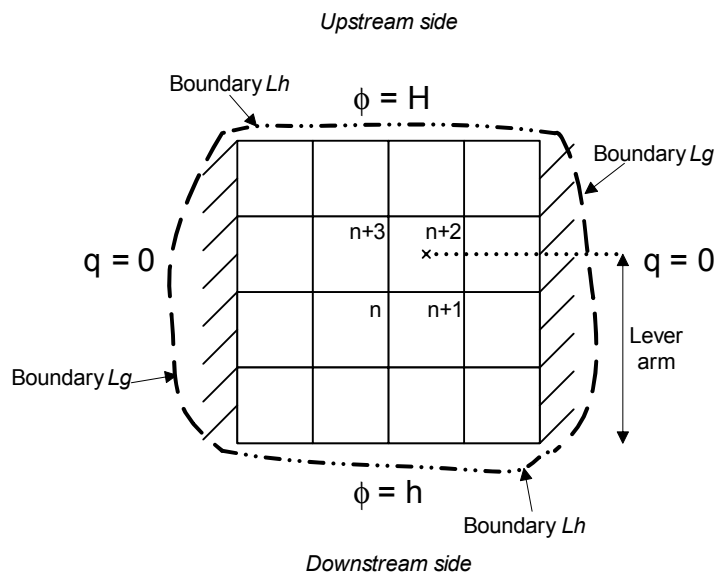


Figure 5-31 –Boundary conditions and node numbering of FEM-simulation.

The global stiffness matrix \mathbf{K} (and where relevant the global load vector \mathbf{f}) are obtained by integration over the entire region A . These integrations may be obtained as a summation of integrations over each element. In this way we are led to the expanded element stiffness matrix K_{ee} for element c given by

$$\mathbf{K}^{ee} = \int_{A_c} \mathbf{B}^e{}^T \mathbf{D}^e \mathbf{B}^e t dA \quad \text{Eqn. 5-23}$$

where A_c is the area of element c .

The global stiffness matrix is now given by

$$\mathbf{K} = \sum_{c=1}^{n_{el}} \mathbf{K}_c^{ee} \quad \text{Eqn. 5-24}$$

For a two-dimensional rectangular four node element (Melosh element)

$$\mathbf{B}^e = \frac{1}{4ab} \begin{bmatrix} y_3 - y_4 & y_3 - y_1 & y_2 - y_4 & y_1 - y_2 \\ x_1 - x_2 & x_1 - x_3 & x_2 - x_4 & x_3 - x_4 \end{bmatrix} \quad \text{Eqn. 5-25}$$

In the general case the hydraulic conductivity matrix \mathbf{D}^e is given by

$$\mathbf{D}^e = \begin{bmatrix} k_{xx} & k_{xy} \\ k_{yx} & k_{yy} \end{bmatrix} \quad \text{Eqn. 5-26}$$

while for isotropic materials, where the hydraulic conductivity is the same in all directions \mathbf{D}^e reduces to

$$\mathbf{D}^e = k \begin{bmatrix} 1 & 0 \\ 0 & 1 \end{bmatrix} \quad \text{Eqn. 5-27}$$

In the present case each element is considered to have an isotropic hydraulic conductivity. The conductivity field can, however, be anisotropic with different spatial range in different directions. Both isotropic and anisotropic conductivity fields have been investigated.

With all parts of the FE-formulation known, the vector \mathbf{a} , containing information of the pressure head at every node, can be calculated. This was performed in the computer software MATLAB (The Mathworks).

The uplift for each element was calculated as the mean of the pressure head in its four nodes. The contribution to the total moment of each element was calculated as the uplift for the element multiplied by its lever arm taken as the distance from the midpoint of the element to the “downstream” side. Node numbering, boundary conditions and definition of lever arm is shown in Figure 5-31.

In the simulation of drainage every 6th node was assumed to have the downstream water pressure h . When drainage is installed for dams it is recommended that the distance between the holes is 2-3 m and in this case every 6th node corresponds to approximately 2.2 m.

In the simulation of a grout curtain, all elements in two rows were assumed to have the hydraulic conductivity $2 \cdot 10^{-9}$ m/s. This is a quite rough assumption, since the grouting effect differ largely and can not be assumed this “perfect”, but the analysis give some idea of the effect of grouting as uplift prevention method.

For a buttress dam the uplift pressure distribution is assumed to exhibit a smaller variation since uplift is only active under the front plate and part of the column. A simulation of a buttress dam was performed, assuming downstream water level, h , on the boundaries shown in Figure 5-32.

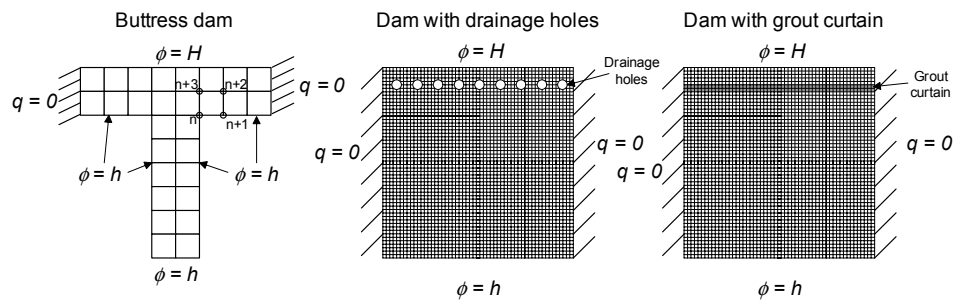


Figure 5-32 – Mesh and boundary conditions for buttress dam, dam with drains and dam with grout curtain.

5.5.2.3. Results

5.5.2.3.1. General representation

For the general case the uplift force, U , consists of two parts; the first, U_{tail} , is the uniform uplift force resulting from tail water (buoyancy force) and the second, U_L , the uplift force due to head water (difference between head and tail water). U_{tail} is constant, whereas U_L varies depending on hydraulic conductivity conditions beneath the dam. U_L is described as consisting of two parameters

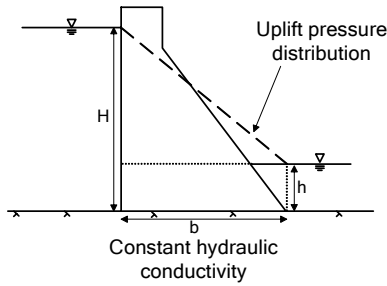
$$U_L = C \cdot u \tag{Eqn. 5-28}$$

where u is the uplift in the linear deterministic case and C a random variable. Due to physical constraints the uplift force can only vary within the bounds $0 < C < 2.0$ as shown in Figure 5-33. This is true for most cases with exceptions e.g. for complicated geological conditions with artesian pressures beneath the dam.

Similarly the moment of uplift is divided in two parts; the first consisting of the moment due to tail water, M_{tail} , (due to buoyant force) and the second, M_L , consisting of the moment resulting from uplift due to head water (difference between head and tail water). The second term consists of two parameters

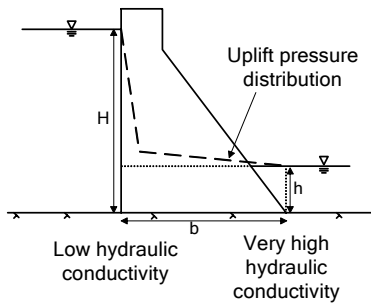
$$M_L = C_m \cdot m \tag{Eqn. 5-29}$$

where m is the moment in the linear case and C_m is a random variable that, as shown in Figure 5-33, varies within the bounds $0 < C_m < 1.5$. For every simulation U_L is normalized to u and the M_L to m .



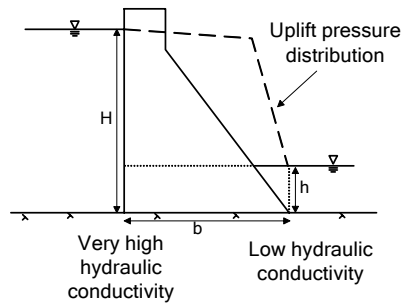
$$U = \rho g h b + \frac{\rho g (H - h) b}{2} = U_{tail} + u$$

$$M = \frac{\rho g h b^2}{2} + \frac{\rho g (H - h) b^2}{3} = M_{tail} + m$$



$$U_{\min} = \rho g h b + 0 = U_{tail} + 0$$

$$M_{\min} = \frac{\rho g h b^2}{2} + 0 = M_{tail} + 0$$



$$U = \rho g h b + \rho g (H - h) b = U_{tail} + u \cdot 2$$

$$M = \frac{\rho g h b^2}{2} + \frac{\rho g (H - h) b^2}{2} = M_{tail} + m \cdot 1,5$$

Figure 5-33 - Influence of physical restraints on uplift and moment.

For each combination of variance and range 1000 simulations were performed. For some combinations a larger number of simulations were performed (V9S2 – 6000, V16S12 – 6000 and V49S22 – 4000).

5.5.2.3.2. Results of simulations

The Beta-distribution is nonzero only on the interval $[a, b]$ and described by parameters r and t . The probability distribution function is given by

$$f_X(x) = \frac{\left(\frac{x-a}{b-a}\right)^{r-1} \left(1 - \frac{x-a}{b-a}\right)^{t-1}}{B(r,t)(b-a)}$$

Eqn. 5-30

where $B(\bullet)$ is the Beta function.

The Beta-distribution fitted the result of C_m and C well, some examples are shown together with the histograms of C and C_m in Figure 5-34. Figure 5-35 shows the resulting Beta-distributions for some combinations.

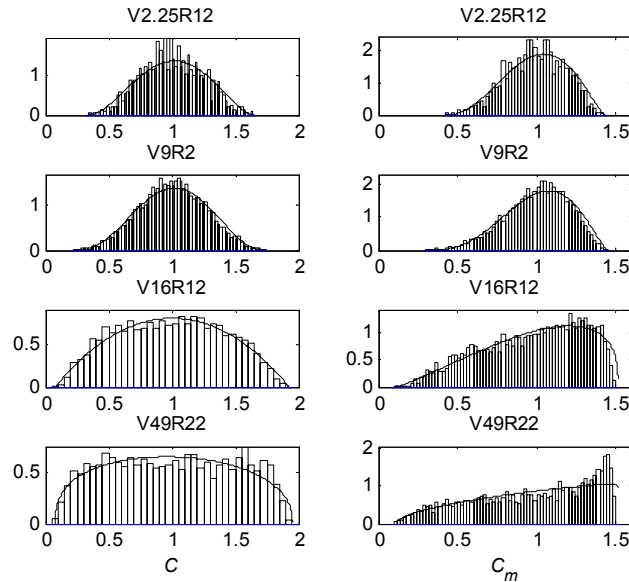


Figure 5-34 - Histograms and fitted beta distributions for C (to the left) and C_m (to the right).

As shown in Figure 5-35 the maximum uplift and moment, respectively, never actually reaches the maximum possible number (2 and 1.5), but come close to it for combinations with high variance and large scale. The model used (the refinement of the mesh sets the limit) can give values between 0.0185 and 1.9817 for uplift and between 0.0273 and 1.4997 for moment.

The uplift distributions are narrow and normal-like for small variance and small range and for increasing variance and range the distributions gets wider and more rectangular-shaped.

The moment distributions are also narrow and normal-like for small variance and range and for increasing variance and range the distributions become more triangular-shaped. Received parameters of the Beta-distributions below are shown in Appendix A1.

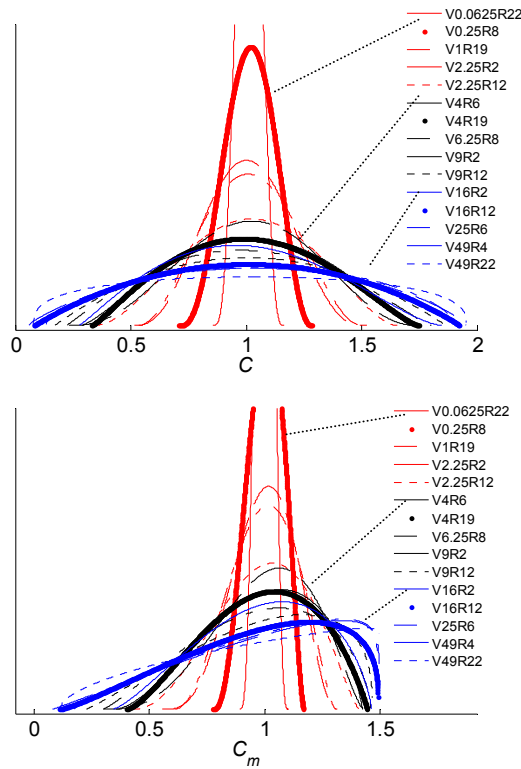


Figure 5-35 - Fitted Beta-distributions for uplift of all combinations (*V1S0* and *V12.25S0* not included). a) show distributions for *C* and b) for *C_m*.

5.5.2.3.3. Influence of assumption of range

Figure 5-36 show the influence of range on *C* and *C_m*, respectively. From these figures it is evident that the distributions of *C* and *C_m* are sensitive to ranges \leq approximately 4 m for the area investigated (20·20m).

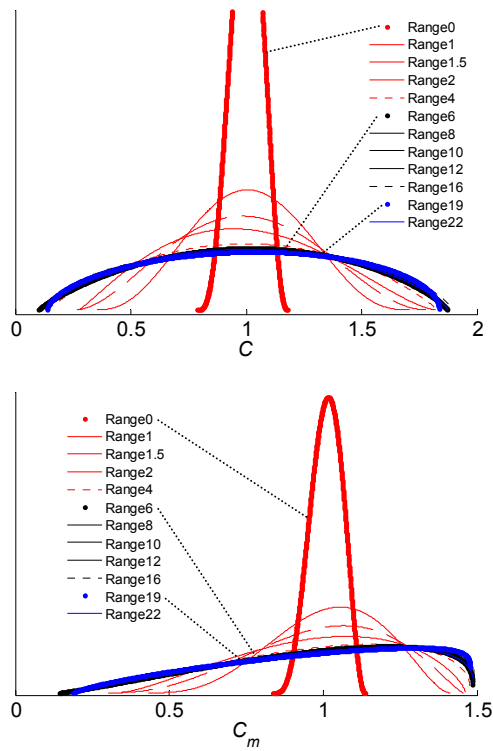


Figure 5-36 - Variance 16 and ranges 0-22 for a) C and b) C_m .

5.5.2.3.4. Influence of the assumption of variance

The influence of variance show similar behaviour as that of range, but the curves seem to become more rectangular and triangular shaped. The distributions of C and C_m seems to be sensitive to increasing variance for all variances tried, but less so for variances ≥ 36 (although the resolution of variance is not fine enough to make conclusions).

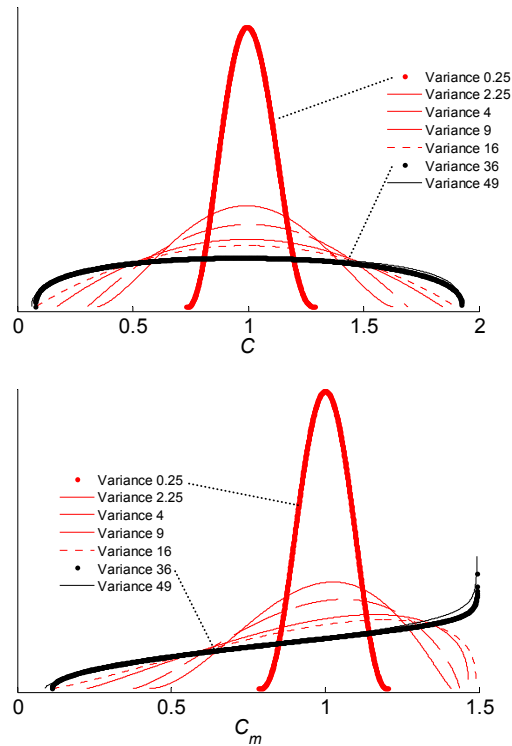


Figure 5-37 - Range 12 and variances 0.25 to 49 for a) uplift and b) moment.

5.5.2.3.5. Influence of drains and grouting

Drains have a large impact on the uplift pressure distribution, but the effect is largely dependant on the effectiveness of the drains.

In a comparison of uplift and stability analysis by three U.S. federal agencies (Ebeling et al, 2000), the definition of drain effectiveness of is compared. In the Swedish guidelines (RIDAS TA, 2003) only effective drains are mentioned, reduced efficiency is not dealt with. The U.S. Army Corps of Engineers (USACE), U.S.Bureau of Reclamation (USBR) and RIDAS assumptions are shown in Figure 5-38 (from Ebeling et al, 2000). The variables used in the figure are

H_d is the pressure head at the drains, E_d is the drain effectiveness, H is the head water level, h is the tail water level, x is the position of the drains, L is the length of the dam base and K_d is defined in the figure.

According to U.S. Army Corps of Engineers

$$H_d = K_d \left((H-h) \left(\frac{L-x}{L} \right) \right) + h$$

where $K_d = 1 - E_d$, $0 < K < 1.0$

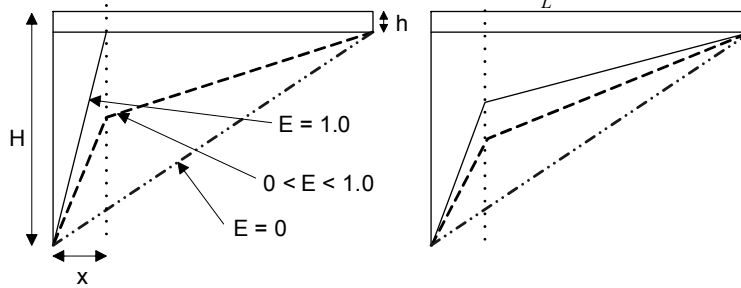
According to Bureau of Reclamation

$$H_d = (H-h) \cdot K_d + h$$

where $0 < E_d < 0.66$ and

$$K = 1 - E_d; 0.33 < K_d < 1.0$$

$$H_d^{\max} = \frac{(L-x)(H-h)}{L} + h$$



According to RIDAS

$$H_d = 0.3 \cdot (H-h) + h$$

for full effectiveness and

$$H_d = \frac{(L-x)(H-h)}{L} + h \quad \text{without drains}$$

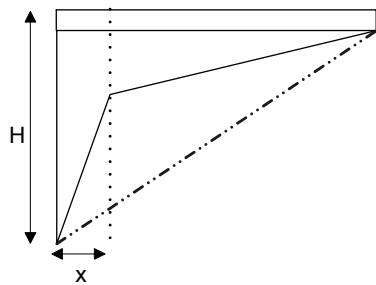


Figure 5-38 - Uplift pressure distribution as function of drain effectiveness. USBR, USACE and RIDAS assumptions.

The USBR assumption is “established from historic data”. Use of flow lines indicate that even if fully effective drains are used, these can not prevent but of course reduce, uplift downstream of the drains, see e.g. Reinius (1962). For this reason the USBR is considered more reliable than the USACE assumption. However, in the USBR calculation the drain location is not included and drain effectiveness of 67-100 % is automatically set to 67 % (since $0.33 < K_d < 1.0$). Therefore a calculation is proposed for H_d which include drain location and use a linear reduction for effectiveness, but where $0.33 < K_d < 1.0$ is still used.

This is

$$H_d = K_d \left((H - h) \left(\frac{L - x}{L} \right) \right) + h \quad \text{Eqn. 5-31}$$

where

$$K_d = 1 - 0.67 \cdot E_d$$

$$0 < E_d < 1.0$$

The simulations with drains was performed by introducing boundary conditions as shown in Figure 5-32b, where the pressure was given as input in the FE-analysis.

Figure 5-39 shows the uplift pressure distribution from one simulation for a dam with effective drains. The pressure drop along each line of elements is shown in a) and the uplift pressure distribution of the whole base area is shown in b). In this simulation the pressure head at the line of drains was assumed equal to that of the tail water which gives $E_d = 1.0$. This figure further validate the USBR and RIDAS assumption of uplift behind the line of drains.

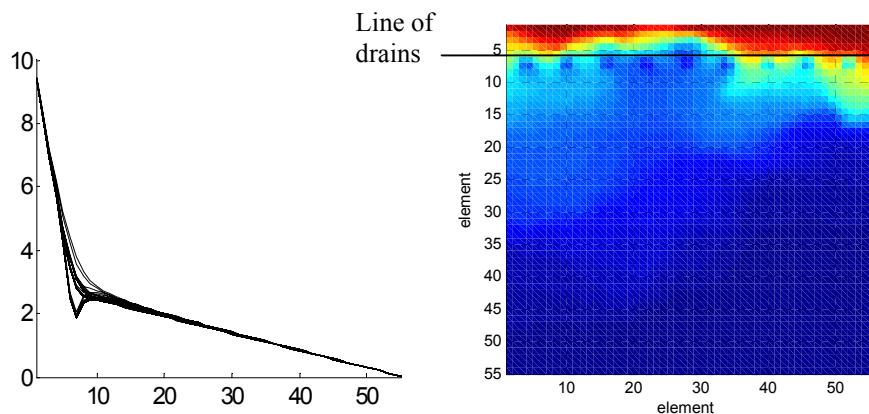


Figure 5-39 – Simulation results for dam with drains of effectiveness $E_d = 1.0$. a) pressure head along line of elements b) uplift pressure distribution of the whole base area.

The effect of drainage is shown in Figure 5-39b. This figure shows the uplift distribution for a typical simulation of V16R12. The drain holes are clearly visible.

H_d according to equation Eqn. 5-31 was used to normalize simulations of uplift and moment with drains of effectiveness 0, 0.18, 0.755 and 1.0 and the result is shown in Figure 5-40. The behaviour with drains is, as might be expected, quite different from that without. Drains effectively reduce uplift but for large effectiveness there is still a possibility of very high uplift if the hydraulic conductivity field is unfavourable. This is clearly visible in the figure as a significant tail towards high values. From Figure 5-40 it is also obvious that the design assumption used here is somewhat conservative for high

effectiveness (the mean value of received distributions is not 1), but this can be justified by the possibility of very high uplift due to the tail. The limit $0 < C < 2.0$ is still valid although higher values than 2 may be experienced for $E_d = 1.0$. Values slightly above 1.5 for C_m are obtained. As a conservative assumption of uplift with drains of known effectiveness the, uplift pressure distribution of Eqn. 5-31 can be combined with distributions of C and C_m received without drains.

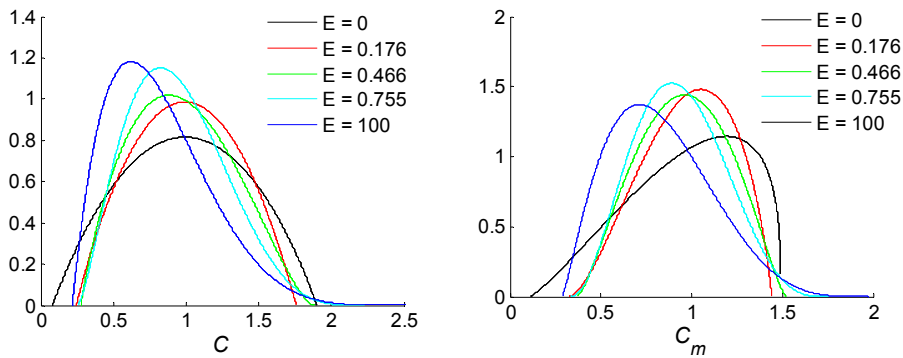


Figure 5-40 - Fitted distributions with drains a) uplift force and b) moment.

For the case where grout curtain is introduced the result is reduced uplift, but the effect is smaller and more uncertain than that for drains. Figure 5-41 a) show the uplift pressure distribution of the same hydraulic conductivity field as that used in Figure 5-39 (drains), while Figure 5-41 b) show another example of the uplift pressure distribution with grout curtain.

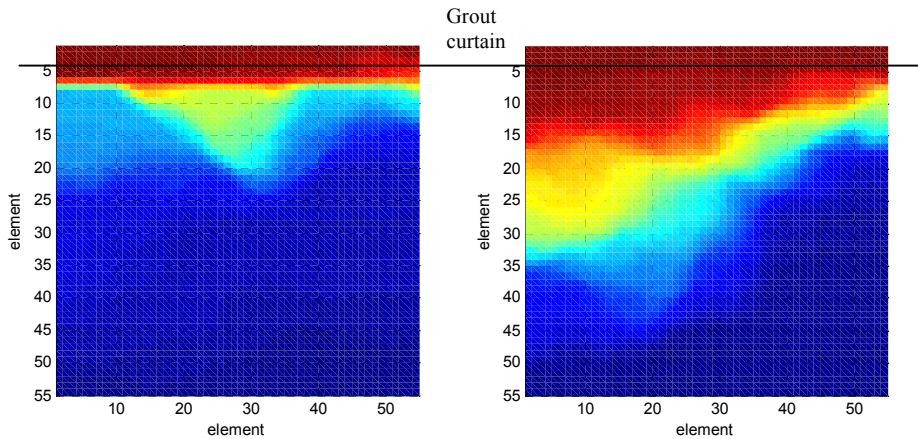


Figure 5-41 a and b) - Uplift pressure distribution with grout curtain for two cases.

The reason that the uplift pressure distribution is less influenced by grouting than drains is that the largest uplift pressure drop without drains occur in the area of lowest hydraulic conductivity. When there is an area downstream of the grouting with lower hydraulic conductivity than the grouted area itself, grouting has no effect on the uplift pressure distribution (but it does affect the flow through the foundation). With drains a “highly conductive joint” is introduced that connects directly to the downstream side and the hydraulic conductivity field is much less important.

In the simulation procedure used here the hydraulic conductivity in the areas that were assumed to be affected by the grouting were given a hydraulic conductivity of $2 \cdot 10^{-9}$ m/s. In some cases this resulted in a higher hydraulic conductivity than before grouting (unrealistic). A better simulation procedure should be used, e.g. where the elements in the grouted area are given a hydraulic conductivity of $2 \cdot 10^{-9}$ m/s if the value before was higher, while if the hydraulic conductivity was lower than this it should not be changed.

Since the assumption of grouting largely influences the result, and the procedure used here can be improved, it is not judged meaningful to compare the results with previous simulations. Histograms of C and C_m of the simulations with this assumption of grouting are shown in Figure 5-42 a) and b) (normalized to mean uplift without grout curtain) and it is obvious that the result is influenced by grouting but also that the scatter is very large.

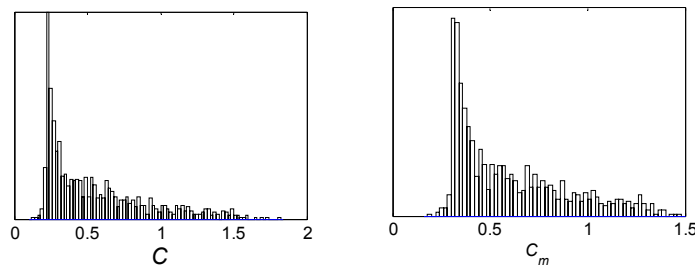


Figure 5-42 a and b) - Distribution of C and C_m with grout curtain.

5.5.2.3.6. Uplift pressure distribution for buttress dam

The expected uplift for a buttress dam would be approximately that shown in Figure 5-43a. It is not immediately obvious where the uplift pressure “ends” beneath the column, here this point is assumed to be $b/2$ behind the front plate (b is the thickness of the column), but this could be discussed. All histograms of uplift and moment for buttress dams are normalized to this assumption. For a buttress dam with thick column (here 6.6 m was assumed) the uplift under the column gives significant contribution to the total uplift (and moment), see Figure 5-44a, whereas for a thin column (here 2.2 m), see Figure 5-44b, the contribution of uplift beneath the column is insignificant. In Swedish guidelines, RIDAS TA (2006) it is recommended that uplift is disregarded beneath columns with thickness less than 2 m and these results support that assumption.

For buttress dams the limit $0 < C_m < 1.5$ is no longer valid, but will vary depending on thickness of front plate (t) and of column (b). Figure 5-43b show C_m as a function of t for different values of b . These limits are actually the parameters $[a,b]$ for the Beta distribution and r and t from equation Eqn. 5-30 could be combined with a new set of $[a,b]$ to fit the case of interest.

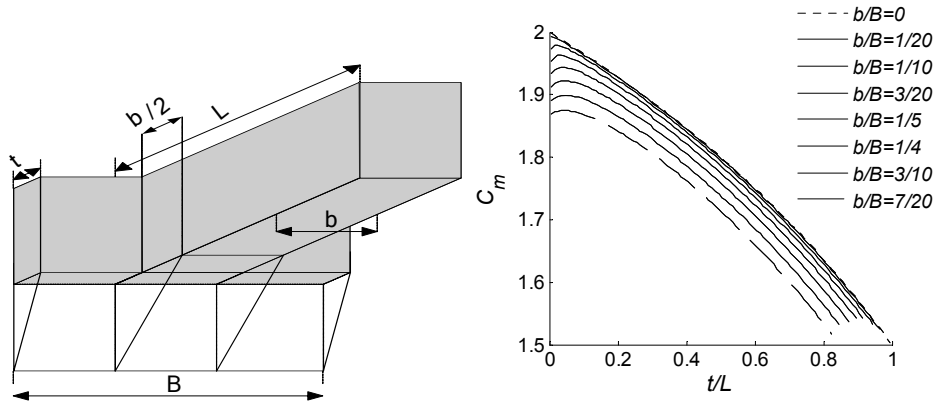


Figure 5-43 - a) uplift distribution assumed for buttress dam b) limits of C_m for varying t and b .

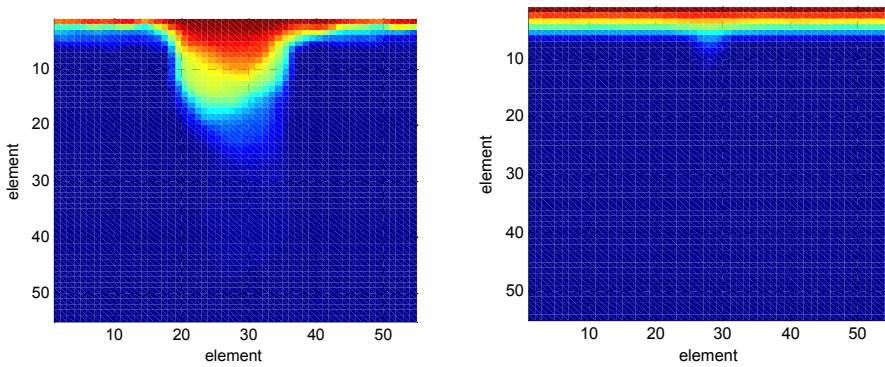


Figure 5-44 - Uplift pressure distribution beneath buttress dam a) for thick buttress dam and b) for thin buttress dam.

Figure 5-45 shows histograms and fitted Beta distributions of V16R12 and V16R4 for the thick buttress dam and V16R4 for the thin buttress dam explained above. The fitted distributions are also shown together with the Beta-distribution of V16R12 with limits $[0.11, 1.876]$ which are valid for a buttress dam with $b = 6.6$ m and $t = 2.2$ m and limits $[0.11, 1.9540]$ valid for $b = 2.2$ m.

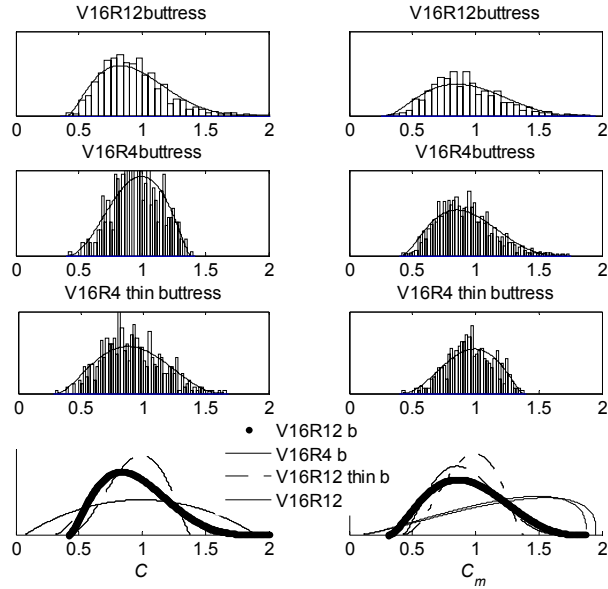


Figure 5-45 - Fitted Beta distributions of buttress dams.

5.5.2.3.7. Anisotropy

Fractures and joints in rock are more prone to one direction, and the assumption of isotropy is not necessarily correct. Simulations of anisotropic correlation structure is shown below, where the ranges are short in one direction and longer in the other. The

anisotropy is applied for variance 16 and the range matrix is $\begin{bmatrix} 0.25 & 0 \\ 0 & 2 \end{bmatrix}$ which basically

means that the range is $\frac{1}{0.25} = 4$ m in the direction transverse to the dam and $\frac{1}{2} = 0.5$ m

in the direction parallel to the dam length. For comparison the range matrix

$\begin{bmatrix} 2 & 0 \\ 0 & 0.25 \end{bmatrix}$ was also applied giving range 0.5 m in parallel direction and 4 m in

transverse direction (this is the field 90° to the first one).

If the anisotropy is not transverse or parallel, anisotropy can be applied according to

$$\begin{bmatrix} \sin \theta & \cos \theta \\ -\cos \theta & \sin \theta \end{bmatrix} \begin{bmatrix} 0.25 & 0 \\ 0 & 2 \end{bmatrix} \begin{bmatrix} \sin \theta & \cos \theta \\ -\cos \theta & \sin \theta \end{bmatrix}$$

where θ is the angle the anisotropic field, positive in the anti-clockwise direction. Angles of 30° and 60° are applied to the “transverse” field, giving range matrices

$$\begin{bmatrix} 0.69 & 0.75 \\ 0.75 & 1.56 \end{bmatrix} \text{ and } \begin{bmatrix} 1.56 & 0.75 \\ 0.75 & 0.69 \end{bmatrix}.$$

Figure 5-46 shows hydraulic conductivity fields and associated uplift pressure distributions of typical simulations.

Figure 5-47 shows fitted beta-distributions for uplift force and moment for 500-1000 simulations of the above four anisotropy assumptions. The fitted curve for V16R4 is also shown. The anisotropic case with larger range in the parallel direction gives higher uplift force and moment than the case with high range transverse to the dam. The results also indicate that the isotropic hydraulic conductivity field result in slightly higher uplift and moment than the worst anisotropic case, and the isotropic field might be considered a conservative assumption. If the anisotropic characteristics are known this should of course be used.

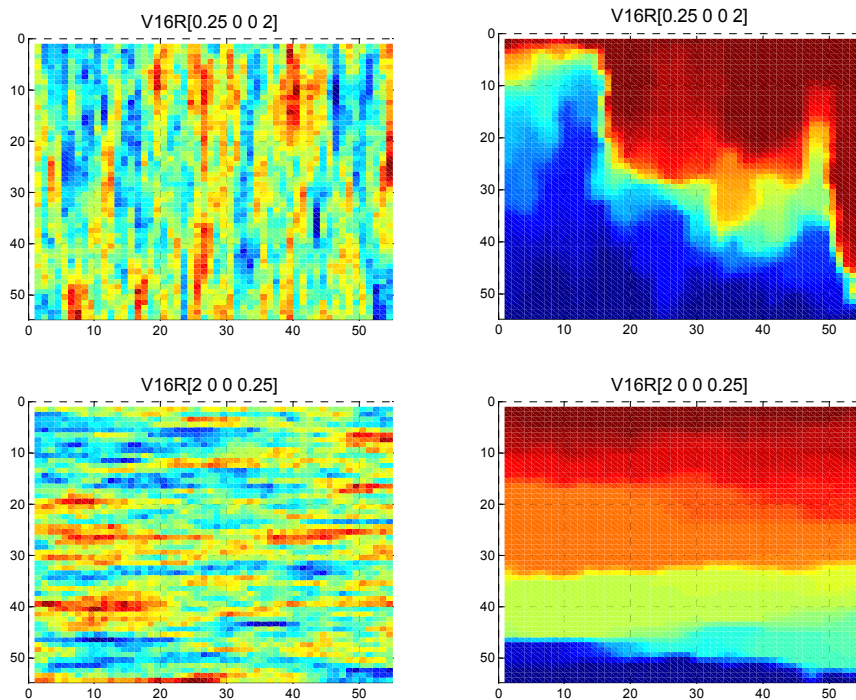


Figure 5-46 - Hydraulic conductivity fields and associated uplift distribution of anisotropic cases.

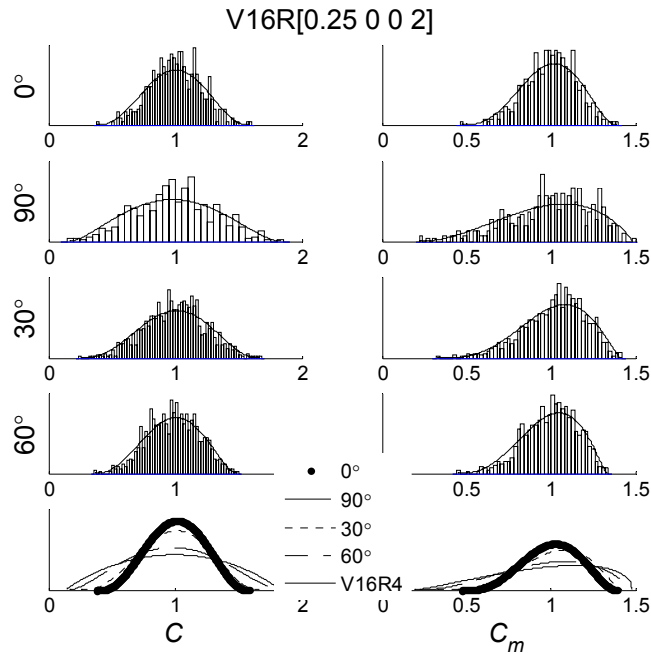


Figure 5-47 - Fitted distributions of C and C_m for anisotropic cases.

5.5.2.4. Discussion and conclusions of modelling

The results from the geostatistical approach include all uplift pressure distributions that can possibly be exhibited for that specific set of variance and range, and thus both “worst cases” and “favourable cases” are included in the statistical distributions of C and C_m . In this way deformations of dam or foundation in case of increasing pool levels or temperature changes are accounted for.

The Beta-distribution described by four parameters, r , t , a , b , fitted the simulation results well. The parameters are dependant on variance and range of the hydraulic conductivity field and the results are shown in Appendix A1.

There are difficulties connected to the input data, as hydraulic conductivity values, variances and range, are difficult to estimate, and for this approach to be useful the connection between assumptions in the model and reality has to be improved.

For concrete gravity dams with base area of other sizes than 20·20m², verification of the Beta-distributions is necessary. For larger areas it is likely that the distributions become narrower for a given variance and the opposite for smaller areas. The influence of range ceased for ranges > 4 in this investigation, but this value will also change for increasing or decreasing areas.

Uplift reduction by drains was shown effective, as could be expected. The uplift pressure distribution of drains assumed in design was shown to have quite good agreement with that received from simulation, which further validate the usefulness of this approach. As a conservative assumption the uplift pressure distribution assumed in design can be combined with the Beta-distribution of C (for the uplift force) or C_m (for the moment) received without drains. This does, however, not account for drains that fail to function. During extreme situations such as high floods and water levels above retention level drain efficiency should be treated with caution, if at all counted for. Influence of grout curtain is difficult to investigate due to the large uncertainty in hydraulic conductivity in the grouted regions.

For simulations of buttress dams significant uplift pressure was received under a thick column while there was almost no uplift pressure at all beneath a thin column. For buttress dams the upper and lower limits of C_m change (from 0-1.5 to 0-higher than 1.5) depending on thickness of front plate and column. A conservative assumption of uplift beneath a buttress dam is to use uplift force according to design and combine that with C obtained for a gravity dam and, similarly, combine moment according to design with C_m for a gravity dam but change the limits.

Anisotropy of rock characteristics can often be expected, e.g. fractures more prone to one direction might cause anisotropy of hydraulic conductivity. This was also investigated and the result shows that anisotropy has impact on the uplift pressure distribution, with the worst anisotropic case being that of fractures parallel to the dam length. This case was, however, not worse than the isotropic case (using the larger range), and thus Beta-distributions of the isotropic case can again be used as a conservative assumption.

It might be that the uplift pressure variations received are too high for normal pool levels, and in this case different variation of uplift is possible to consider for different situations. For normal pool levels the uplift pressure is possible to measure (although monitoring with high frequency over a long period of time is necessary) and the variation of this could be used for structural reliability analysis. For pool levels exceeding normal, as explained previously, measurement from normal pool levels are no longer valid and the Beta-distributions received from the geostatistical approach are a possible way to describe the variation.

The geostatistical approach can be questioned, mainly as the approach presuppose that the rock can be described by a statistical continuum, but for high values of V and R , the whole range of possible uplift pressure distributions are captured in the Beta-distribution. This might seem *ad hoc*, but is used as a strong argument for the use of this approach.

To perform a structural reliability analysis it is necessary to have reliable input data and for loads and resistance statistical distributions has to be known. The geostatistical approach is one possible way to obtain that for uplift pressure. To further increase the usefulness the following could be investigated:

- Can the geostatistical approach be combined with monitoring results?
- How can information from rock mapping and information of known fracture zones be used?
- How does larger/smaller areas affect the variance and range dependency?
- What is representative values of range and scale?
- How does a 3-dimensional random field affect the result?

5.5.3 Use of uplift monitoring

Uplift monitoring is performed at many dams, usually by piezometers, but there are other types of monitoring devices, e.g. TDR-monitoring, see Bernstone (2006) or Bernstone & Westberg (to be published).

The purpose of uplift monitoring is to

- Detect uplift pressures exceeding acceptable values
- Detect trends. Increasing (or perhaps also decreasing) trends indicate that changing processes take place.
- Verify function of drains and grout curtain
- Use as input in assessment.

The largest problems with use of uplift monitoring results as input in the assessment phase is that

- It can only be measured at a limited number of points, with the measured uplift only valid at that specific point,
- Measurement is rarely available at pool levels exceeding normal, while the uplift pressure increase with increasing pool levels can not immediately be assumed linear, see. e.g. Ruggeri et al (2001).

Due to this it is extremely difficult to describe the statistical distribution of uplift pressure. In a structural reliability analysis the statistical distributions shall be based on maximum annual loads.

Here it is suggested that results from uplift pressure monitoring could be used in the following way for **normal operation**:

- Continuous monitoring (at least daily measurement) is performed during a long period of time (a number of years). The mean of annual maximum of that bore hole is taken as E (maximum value each year) and the variance is taken as V (maximum value each year). The COV is given by \sqrt{V}/E .
- The question still arises; if measurement is only available at a few points we actually only know the uplift at those specific points, and not the whole pressure distribution. If an uplift pressure distribution is assumed (e.g. if

drainage is present the assumption would be a reduction behind the drains) and the uplift monitoring confirms this distribution (i.e. the maximum annual measured uplift is lower or close to that assumed), this assumption can be combined with the *COV* described above.

- Here it is assumed that the *COV*(maximum annual value) is generally not very large (but this has to be confirmed). This assumption is based on the knowledge that monitoring results follows a pattern of seasonal variation, and that increasing trends are seen as alarming indications of changing processes. If this is true the *COV* from monitoring at one dam could be used at another dam and the long period of monitoring (previous to analysis) is not necessary anymore.
- Continuous monitoring is necessary to detect changes, especially for dams where the safety index is low.

For exceptional cases monitoring results should not be used as they are measured for normal pool levels.

Figure 5-48 shows a section of the Seven Mile dam in Canada and the bore holes where uplift pressure monitoring is performed (Hole 88-10, 88-9 and 88-17). Figure 5-49 show uplift pressure measurement from the years 1993-1997. Measurement was performed several times each day. The seasonal oscillation discussed previously is visible, although there seems to be a time lag further downstream (the increase in uplift occur later in season the further downstream the measuring point is located). It should also be noted that pumping is taking place under the dam section, this is the reason for the low values of p_2 , bore hole 88-10 (where recorded piezometric uplift is actually less than the tailwater level).

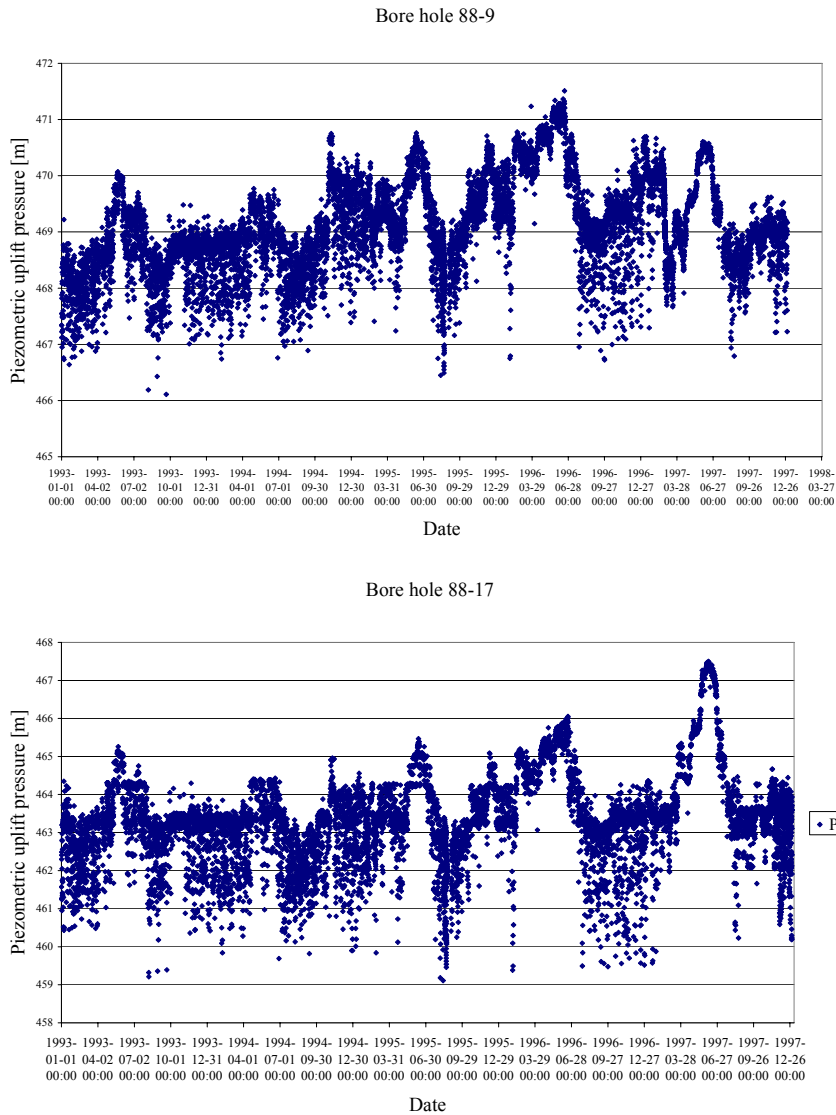


Figure 5-49 – Uplift measurement from Seven Mile Dam.

The monitoring from one bore hole at the Seven Mile dam has been analyzed. Tail water was assumed to be at + 464 m (according to drawing) and the monitoring results was reduced by 464 m. Taking out the maximum values each year for each bore hole gives 5 values/hole. This is used to calculate mean, standard deviation and COV for the maximum values of each hole. In this case pumping is taking place (obvious at P2), and

this might influence the reliability of the values, but the indication is that the *COV* is quite low if compared to that resulting from the simulations from the geostatistical approach discussed above. If the tail water level is lower than according to the drawing the mean value will increase and the *COV* will decrease.

Table 5-8 - Maximum annual values, standard deviation and *COV* of uplift monitoring data.

Bore hole	Maximum uplift [m]					Mean (maximum)	Stddev (maximum)	COV
	1993	1994	1995	1996	1997			
P1-88-10-P1	23,65	23,71	20,13	18,35	21,31	21,43	2,30	0,11
P1-88-10-P2	-1,72	-1,88	-2,38	-1,38	-2,08	-1,89	0,38	0,20
P1-88-10-P3	49,35	49,59	46,88	51,60	48,13	49,11	1,76	0,04

5.5.4 Distributions used

In case monitoring is undertaken the approach described above can be used for normal pool levels.

For higher pool levels the results from the geostatistical approach will be used. The true values of variance and range are presently unknown. According to Follin (1992) $V = 0.0625$ corresponds to an approximately homogeneous medium, and $V = 16$ to that observed for 3m packer tests in his thesis. As a rock foundation can rarely be considered as consisting of homogenous medium $V = 0.0625$ seems too low. According to Schabenberger (2002) the hydraulic conductivity of heavily fractured rock can be up to about 10 m/s while for massive low-porosity rocks it can be as low as 10^{-13} m/s, which corresponds to $\ln(K) = 2.3$ and $\ln(K) = -30$ respectively. For combinations with variance 49 about 3% of the results are outside of these bounds, suggesting that this large variance is not possible in reality. The range was shown to have little effect if the range assumed was > 4 m. In this project variance 16, range 12 is used. Parameters of the Beta-distribution are shown with associated mean value and standard deviation in Table 5-9. The distributions are shown in Figure 5-50.

Table 5-9 - Parameters of Beta distribution for V16R12.

	r	t	a	b	E	$V^{1/2}$	COV
C	1.96	1.95	0.08	1.90	0.99	0.41	0.41
C_m	2.22	1.33	0.11	1.49	0.97	0.31	0.32

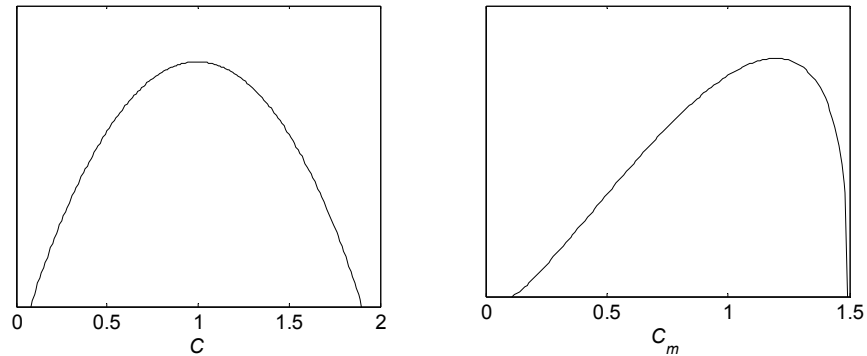


Figure 5-50 - distributions of C and C_m .

When monitoring is not available these distributions will be used for uplift at normal pool levels as well.

5.6 Conclusions of chapter

There are large difficulties involved in the formulation of resistance and load parameters. The self-weight has to be further analysed, especially how test results can be combined with the present information to give better estimates for a specific structure.

For description of the shear strength as well as the ice load a number of difficulties has to be confronted and solved.

One possible method for treatment of the head water level is proposed, where the water is assumed to be constant at retention water level most of the time, and only by some probability, given by specific characteristics of that particular reservoir and facility or dam, is it assumed to rise above this level. For water above retention level an exponential distribution is proposed.

As for uplift a geostatistical approach is used for simulation of possible uplift pressure distributions. The reference value is given by that assumed in design and the possible variation around this value is received. The results are thought possible to combine with exceptional situations where water levels are above retention water level. During normal operation it is likely that the variance of uplift is smaller than that received from the simulations, and when monitoring is performed variance (of annual maximum values) could be used as input instead. If monitoring is not performed the simulation results should probably be used.

The combination of different scenarios has not been treated yet, and here only some short but important notes are made:

- The maximum uplift pressure during normal operation is likely to occur in winter, as is the maximum ice load.

5. Random variables affecting dam stability

- High water levels, above retention water level, are likely to occur during spring or autumn.
- Ice loads tend to become higher due to moderate water level fluctuations, and if such are present, it should be accounted for.
- If exceptional water levels occur during winter this may also increase the ice load (if the water level elevation is not large enough to break the ice). In case this is likely to occur it should be accounted for, but as the highest probability of high water levels is during spring and autumn when there is no ice, it is in most cases not thought likely.

6. Examples

6.1 Example 1: Stability calculation of dividing wall in Ajaure spillway chute



Figure 6-1 - Ajaure spillway chute during discharge test.

6.1.1 Information about Ajaure

Ajaure dam is situated in the upper part of the river Umeälv, 4 km downstream from the Ajaure Lake and 30 km south of Tärnaby. It was constructed 1964-1966. The plant consists of a rock fill dam above the river line, underground power station embedded in the bedrock with the intake connected directly to the dam, tailrace tunnel with surge gallery and drainage canal, see Figure 6-2. The embankment dams are classified as high consequence dams, as the downstream effects of a dam break would be extensive. Failure of Ajaure dam under conditions of high reservoir levels in the river system has the potential to cause failure of all fourteen downstream dams and consequential damages all the way to Umeå on the coast of the Baltic sea.

The left embankment dam is approximately 360 m long with a maximum height of 47 m and the right is 100 m long.

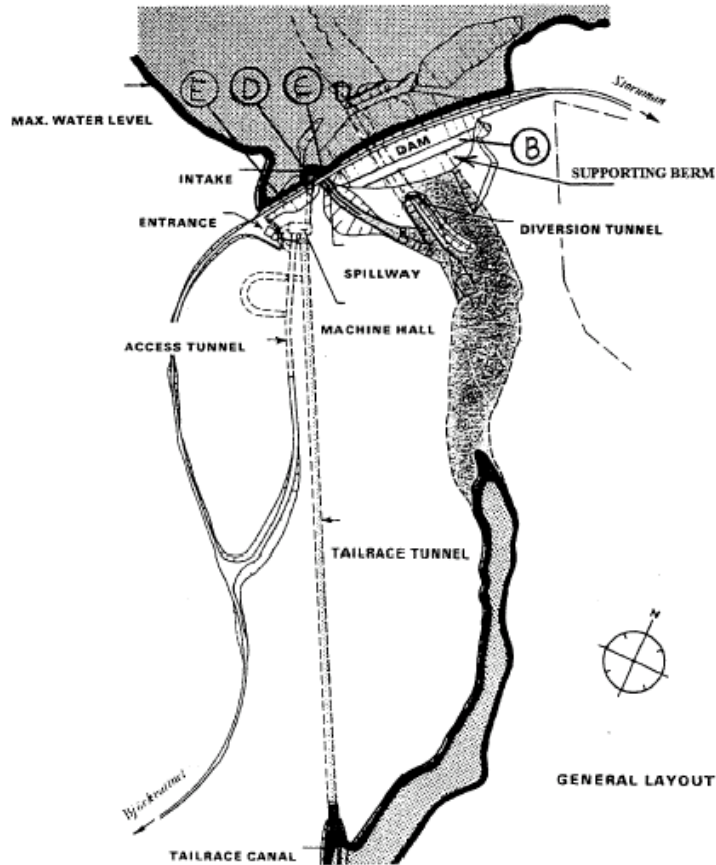


Figure 6-2- Plan showing the Ajaure hydropower plant.

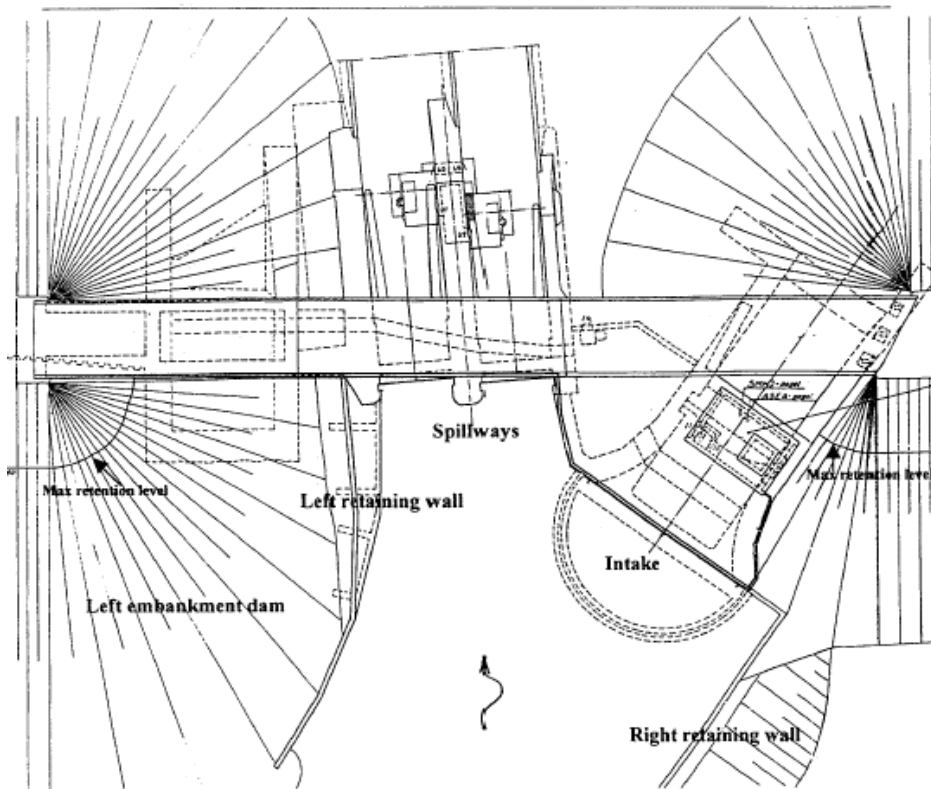


Figure 6-3 - Plan of the concrete structures.

The spillway and intake are concrete structures, see Figure 6-3. Before 2000 the spillway consisted of two bottom outlets. With water at reservoir retention level, + 440,5 m, the design discharge capacity was supposed to be 1020 m³/s, but in laboratory model tests in 1998 it was discovered that the actual discharge capacity was only 935 m³/s (Yang, 1998). According to “Flödeskommitténs riktlinjer” the design river discharge in Ajaure is 1340 m³/s. Modelling of the station was performed by Vattenfall Utveckling AB and measures were proposed and carried out to increase the discharge capacity at lowest possible cost. The following reconstructions are of interest in this report:

- The left spillway gate was reconstructed to a surface outlet
- The left and right walls of the spillway chute were raised to avoid water spilling over
- A concrete “wedge” (see Figure 6-4) was built on upper part at the left side of the dividing wall to give a more smooth transition section and a more

favourable state of flow. The wedge stretches from the middle column to section 0/200. Sections are shown in Figure 6-5.

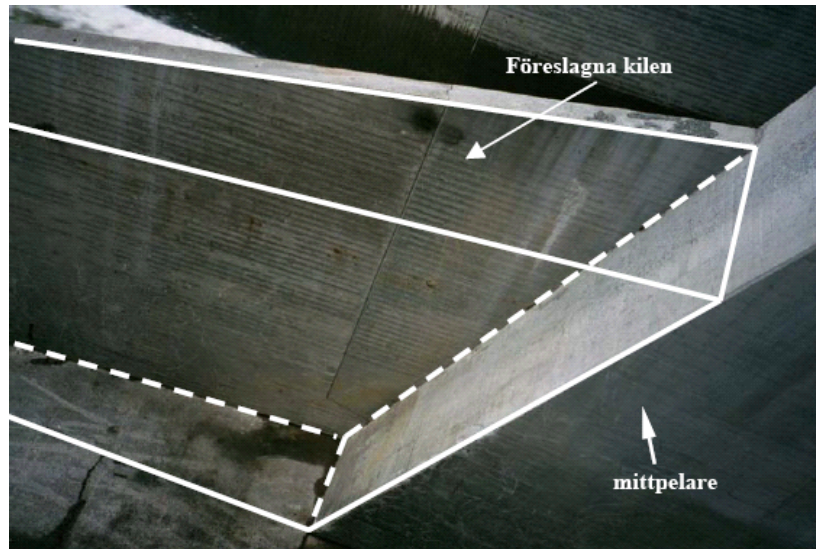


Figure 6-4 – Concrete wedge.

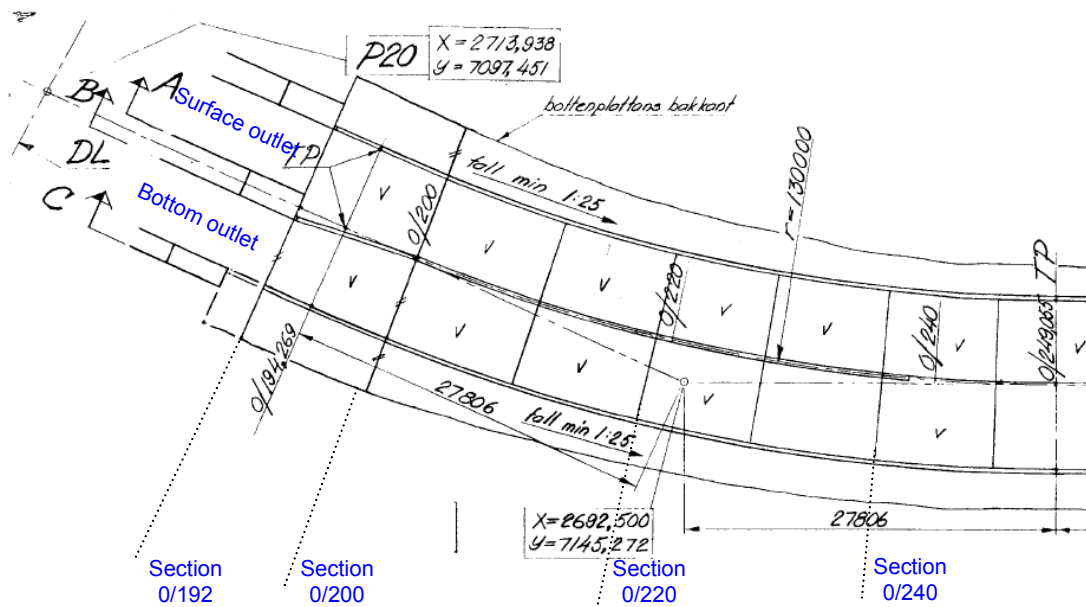


Figure 6-5 - Sections in canal.

After rebuilding of the left spillway gate, and with temporary raise of water level to 445,19 m (in front of intake building), the discharge capacity increased to 1340 m³/s. The discharge is larger in the left gate than the right. Figure 6-6 shows the spillway chute when water is discharged.



Figure 6-6 – Discharge of water.

6.1.2 Background of assessment

In 1998 Vattenfall decided to introduce the use of risk analysis in dam safety in Sweden by issuing two pilot studies on the Seitevare and Ajaure dams. The objective was to demonstrate methods to be applied for risk analysis on dams. The study of Ajaure dam was carried out by Swedpower in cooperation with BC Hydro International (Canada), which are recognised for their pioneering work in developing various approaches to characterising and managing risks posed by dams.

One observation from the risk analysis is that the dividing wall in the spillway chute is not designed for one-sided water pressures. No stability calculations or drawings were found for this wall and the stability is uncertain. According to operation staff at the plant, the wall was constructed for a difference in discharge between the two chute openings corresponding to 150 m³/s. According to the operating engineer this value can be exceeded “a little” in exceptionally dangerous situations.

A global fault tree in Figure 6-7 shows the different events that could lead to the scenario “down stream slope erosion of embankment dam during spill”. Erosion of the embankment dam could result in dam failure. One of the events observed that may lead

to this is that the dividing wall fail and get stuck in the chute and cause water spilling over the left (or right) wall, eroding the dam.

The Failure mode, effect and criticality analysis (FMECA) is shown in Figure 6-8. The dividing wall was given a vulnerability index of 240-500. This value is estimated based on known information and best guess, but since no stability calculations were found the magnitude of deficiency could be different.

The case of the dividing wall in Ajaure is a simple but illustrating example of when structural reliability analysis could be used in dam safety and how assessment could be performed and combined with knowledge of operation and past performance. The question that need answer is:

How big difference in discharge between the right and left gate is possible without endangering the dividing wall? Is 150 m³/s reasonable?

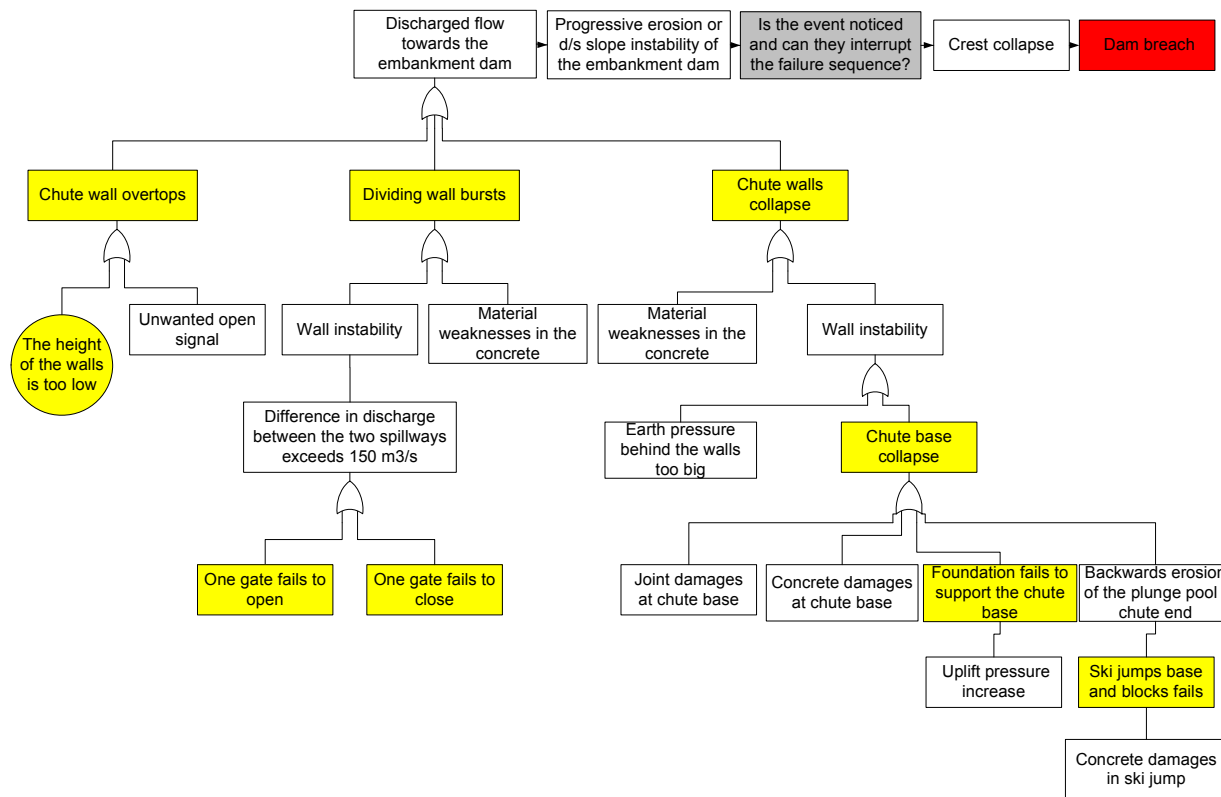


Figure 6-7 - Fault tree of Ajaure. Top event is discharge flow towards the embankment dam. (Vattenfall, 2000, by courtesy of Vattenfall).

SYSTEM AND SUBSYSTEM DETAILS					COMPONENT DETAILS			FAILURE MODES AND EFFECTS				CRITICALITY RATINGS (1 - 5)			FREQ. OF LOADING	VULNERABILITY INDEX	RECOMMENDATION		
SUB-SYSTEM L1	SUB-SYSTEM L2	SUB-SYSTEM L3	COMPONENT L1	COMPONENT L2	DESIGN FUNCTION	DESIGN/ PERFORMANCE PARAMETERS	PERFORMANCE DETAILS	FUNCTIONAL FAILURE MODES	IMMEDIATE EFFECTS	FAILURE SEQUENCE INTERRUPTION	ULTIMATE EFFECT	MAGNITUDE OF DEFICIENCY	CRITICALITY OF COMPONENT	INABILITY TO DETECT AND RESPOND	(1/year)	Product Range: 1-125			
DISCHARGE FACILITIES (1-3)	SPILLWAY STRUCTURE (1-3-1)	INLET TO SPILLWAY STRUCTURE (1-3-1-1)	Wing wall upstream the outlet (1-3-1-1-1)		Contribute to ensure a controlled inflow to spillways. Protect the embankment dams from erosion. Provide a safe connection between earth and concrete dam. Support the embankment dam's rip rap	No stability calculations exists. No records from measuring exists.	No weaknesses are noted by surveillance personnel.	Failure to convey the flow into the outlet.	Erosion starts in the embankment dam interface		N: Dam breach A: Dam breach P: N.a.								
		HEADWORKS OPENING SIZE, THE GATE'S LIFTING MECHANISM (1-3-1-2)	Headworks opening size (1-3-1-2-1)		P1: Discharge of flows up to the design flow	Capacities: 1020 m ³ /s, RL=MWL, 1130 m ³ /s, RL= lowest crest of the core; 1180 m ³ /s, RL= lowest crest	Only 935 m ³ /s discharge when the RL=MWL	Failure to discharge flows up to the design flow. The opening too small	The reservoir water level rises		(N) Dam breach (A) N.a (P) N.a								
								Failure to discharge flows up to the design flow. The opening is partly blocked by debris.	The reservoir water level rises		(N) Dam breach (A) Dam breach / incident. (P) Dam breach / incident								
								P1: To open the gate.	The gate opens with a speed of 0.5 r/minute	No leakage problem	The gate fails to open.	The reservoir water level rises	(A) Possibilities exists to open the gate by for example crane or help motor.	(N) Dam breach (A) Dam breach / incident. (P) N.a.					
		CHUTE (1-3-1-3)	Base+ foundation (1-3-1-3-1)	Foundation (1-3-1-3-1-2)	The gate's lifting mechanism (1-3-1-2-2)	P2: To stay open			The gate fails to stay open.	The reservoir water level rises	(A) Possibilities exists to open the gate by for example crane or help motor.	(N) Dam breach (A) Dam breach / incident. (P) N.a.							
									P3: Close the gate			The gate fails to close.	Continued discharge.		(N) Dam breach (A) N.a. (P) N.a.				
									P1: Support walls and protect the foundation.			The chute base fails to support the chute walls	The chute walls deforms and collapses		(N) Dam breach (A) N.a. (P) N.a.				
		CHUTE WALLS (1-3-1-3-2)	Retaining walls (1-3-1-3-2-1)	Dividing wall (1-3-1-3-2-2)		P1: Safe passage of discharge flow from headworks to skijump.			Failure to provide a safe passage of discharge flow from headworks to	Water flows in an uncontrolled direction.		(N) Dam breach (A) N.a. (P) N.a.							
									P1: To steer the water and improve the stream line of the discharging water	The difference in discharge between the two spillways should not be more than 150 m ³ /s.	Structural failure of the dividing wall.	The dividing wall breaks.		(N) Dam breach (A) N.a. (P) N.a.	4-5	4-5	3-4	5	240-625
		SKI JUMP (1-3-1-4)	Base and blocks (1-3-1-4-1)			P1: Discharge the water from the chute and spread it out over the plunge pool. Throw away the water from the chute and spread it out over the plunge pool			Concrete damages at the base.	Structural performance failure of the base / blocks.	Erosion of the plunge pool		(N) Dam breach (A) N.a. (P) N.a.						
P1: Dissipate the kinetic energy of the discharging water into heat and potential energy.										Ruled out									

Figure 6-8 - FMECA of Ajaure. Subsystem "discharge facilities". (Vattenfall, 2000, by courtesy of Vattenfall).

6.1.3 Calculation model and assumptions

The calculations are based on information from drawings and their compliance with the actual conditions has not been investigated. The condition of the structure has not been checked, but the last FDU/SEED report does not mention problems with the dividing wall. The drawings were found in the Dam archive.

According to Yang (2001) the wedge stretches from 0/190 to 0/200 but on drawings it looks to be only about 2000 mm long, therefore calculations are performed for sections 0/192 and 0/200. The dam safety co-ordinator of Ume river (Vattenfall Service Nord in Jan 2005) confirms that the wedge has been built, but thinks it is longer than 2 m (perhaps 10 m). Since this has not yet been confirmed by drawings the length 2 m is still assumed (worst case).

In section 0/200 the wall is 4 m high. The left part of the chute bottom is lower than the right, causing the dividing wall to stand on the right part, see Figure 6-9. From the left the wall is thus 4,65 m and from the right 4 m. This means that the water depth in the left canal will be 4,65 m and the wall itself is 4m, when the chute is filled to the crest of the wall. In section 0/192 the wall is 5,75 m high.

6.1.3.1. Loads

The spillway chute is curved to the left and this gives a centripetal force due to the water velocity. The worst load case with respect to the dividing wall is therefore water only on the left side, when the forces acting on the wall are the hydrostatic force and the centripetal force as shown in Figure 6-9. In reality there are also forces from uplift pressure and dead weight, but these are small in comparison to other forces and will therefore be left out of the analysis.

The curve of the canal results in more water on the right side of the left and right canal, respectively. This effect is not taken into consideration.

Water up to crest

For water up to crest the hydrostatic water pressure, p_0 , is given by

$$p_0 = \rho_w \cdot g \cdot h_w \quad \text{Eqn. 6-1}$$

Where h_w is the water depth as defined in Figure 6-9, ρ_w is the density of water. The centripetal pressure, c_p , is given by

$$c_p = \frac{m \cdot V_w^2}{r} \quad \text{Eqn. 6-2}$$

where V_w is water velocity, r is radius of curve of canal = 130 m, m is mass of water in the canal, $m = b_{canal} \cdot \rho_w$, $b_{canal} = 6.3$ m.

The moment of the loads are given by:

$$M_{hydro} = \frac{\rho_0 \cdot h_w^2}{6} \rho_0 \text{ according to Eqn. 6-1} \quad \text{Eqn. 6-3}$$

$$M_{centripetal} = \frac{c_p \cdot h_w^2}{2} \rho_w \text{ according to Eqn. 6-2} \quad \text{Eqn. 6-4}$$

The total moment is

$$M_{tot} = \frac{h_w^3 \cdot \rho_w \cdot g}{6} + \frac{h_w^2 \cdot \rho_w \cdot b_{canal} \cdot V_w^2}{2 \cdot r} \quad \text{Eqn. 6-5}$$

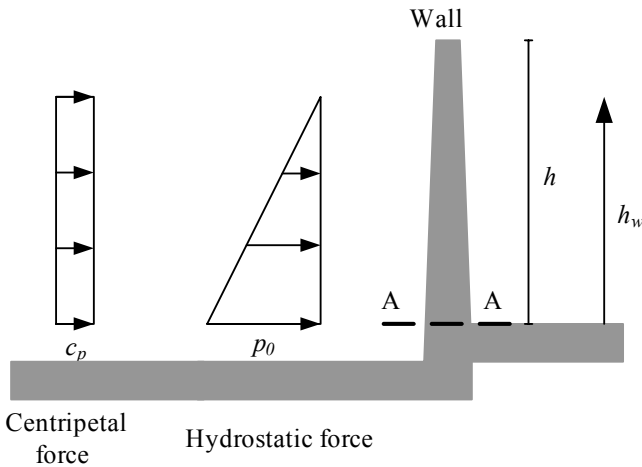


Figure 6-9 – Hydrostatic and centripetal force on wall.

Water above crest

If one gate is fully opened the water in the canal will spill over the crest of the wall to the adjacent canal. Since the gate opening velocity is approximately 0,5m/min, water will start spilling over the wall as soon as crest level is reached (as opposed to the theoretical case of instantaneous opening), causing a pressure from the adjacent side as well. It is very difficult, without actual model tests, to know the water depth in the adjacent canal, and for this reason this stabilizing effect has not been taken to account. The following calculation is based on the conservative assumption that the water level is above crest in the left canal and zero in the right one.

Water pressure will now be divided in two parts p_1 and p_2 :

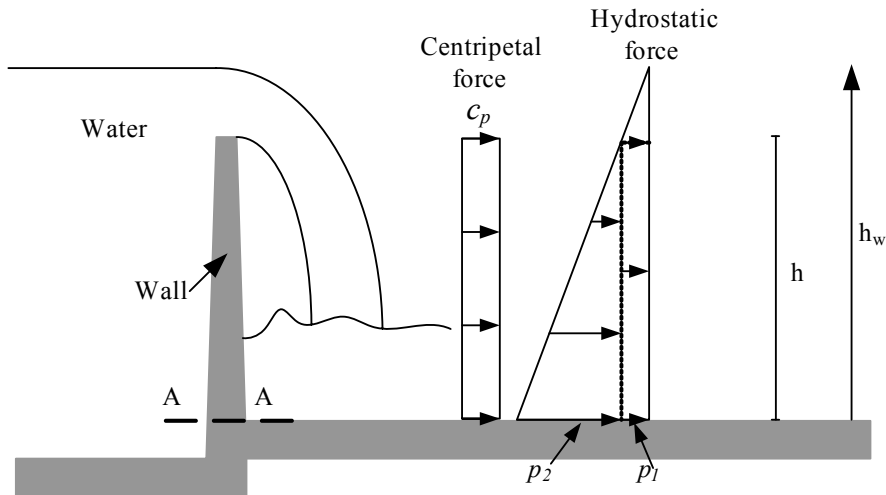


Figure 6-10 – Hydrostatic and centripetal force on wall when water level is above crest.

The centripetal pressure, c_p , is as before.

The hydrostatic water pressure is given by

$$\begin{aligned} p_1 &= \rho_w \cdot g \cdot (h_w - h) & \text{Eqn. 6-6} \\ p_2 &= \rho_w \cdot g \cdot h \end{aligned}$$

The total moment is thus given by

$$\begin{aligned} M_{tot} &= \frac{(p_1 + c_p) \cdot h_w^2}{2} + \frac{p_2 \cdot h^2}{6} = & \text{Eqn. 6-7} \\ h_w^2 &\left(\frac{\rho_w \cdot b_{canal} \cdot V_w^2}{2 \cdot r} + \frac{\rho_w \cdot g \cdot (h_w - h)}{2} \right) + \frac{h^3 \cdot \rho_w \cdot g}{6} \end{aligned}$$

6.1.3.2. Water depth and velocity in canal

In Yang (2001) the water levels, for discharge of 900-1340 m³/s, measured from the left and right crest respectively, are given. From drawings the heights of the walls were found, and the water depth in the left and right canal could be calculated for different discharge of water. It is not immediately possible to estimate the corresponding water depth adjacent to the wall in case only one gate is open, but the data in Table 6-1 will give some useful information.

Table 6-1 - Water depth in left and right canal for different discharge.

Section	Discharge [m ³ /s], both gates				
	900	1020	1100	1200	1340
0/190 Left	7,55	8,45	9,15	9,5	9,7
0/200 Left	6,05	6,55	7,2	7,65	8,85
0/190 Right	7,6	7,95	8,4	9,05	9,7
0/200 Right	7	7,3	7,4	7,6	9

In

Figure 6-11 water depth in different sections is normalized to the water depth in section 0/190 (gate). This diagram is, however, based only on large discharge and both gates open. The situation with smaller discharge and only one gate open is likely quite different. For more reliable results new model tests for smaller discharge would have to be performed. As water will start spilling over the crest in large discharge situations when only one gate is open, the results from Yang (2001) are considered to be on the safe side.

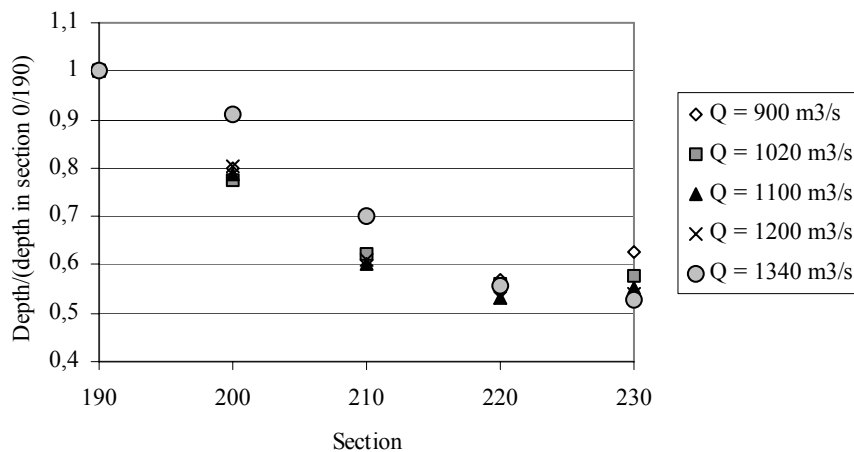


Figure 6-11 - Normalized water depth in different sections.

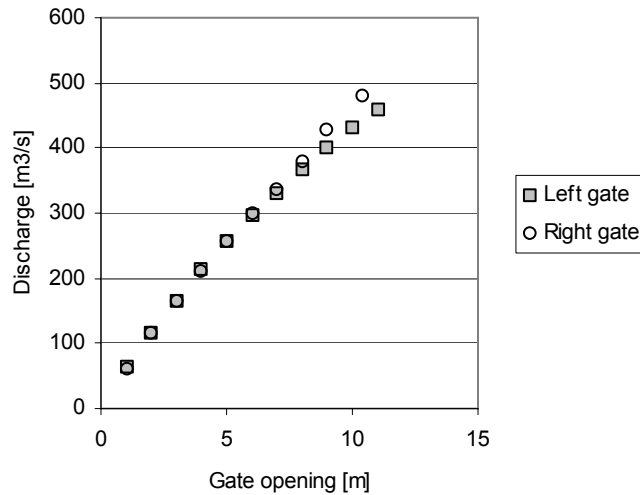


Figure 6-12 - Discharge at retention level as function of gate opening (one gate open).

Disregarding the water depth for $Q = 1340 \text{ m}^3/\text{s}$ it is obvious that the water depth in a certain section depends on the water depth in section 0/190 (and thus gate opening). The relation seems to be

$$D_{0/192} = 0.96 \cdot D_{0/190}$$

Eqn. 6-8

$$D_{0/200} = 0.8 \cdot D_{0/190}$$

From Yang (2000) discharge at retention level as a function of gate opening was received, see Figure 6-12.

These relations are used in further calculations to translate water depth in sections 0/192 and 0/200 to gate opening and discharge.

From $Q = A \cdot V_w$ the average water velocity is calculated. Since the velocity-profile is in reality as in the figure below the centripetal moment calculated is not exact, but gives a good approximation of the magnitude.



Velocity profile

$A = b_{canal} \cdot h_{water}$ where $b_{canal} = 6,3$ m. One value for each discharge is calculated, based on water depths on both left and right side, according to $V_w = \frac{Q}{A}$.

Table 6-2 - Velocity of water for different discharge.

Section	Velocity for discharge [m ³ /s]				
	900	1020	1100	1200	1340
0/190	9,4	9,9	9,9	10,3	11
0/200	10,9	11,7	12	12,5	11,9

In the structural reliability analysis a velocity of 11 m/s for section 0/192 and 12,5 m/s for section 0/200 has been used. The reason is that it makes the calculation easier and since the effect of centripetal force is only about 30 % of the hydrostatic force the effect of water velocity increase of 1 m/s gives only a small contribution. The calculation is on the safe side for relevant cases.

6.1.3.3. Material properties

The following material parameters were used:

6.1.3.4. Reinforcement

0/192

For 0/190,70 to 0/193,8 the reinforcement is 13 + 13 ϕ 25 c 240 giving

$$A_s = 26 \cdot \pi \cdot 25^2 / (4 \cdot 3,1) = 4117 \text{ mm}^2/\text{m}$$

0/200

The reinforcement from 0/196,9 to 0/200 is 11+11 ϕ 19 which gives

$$A_s = 22 \cdot \pi \cdot 19^2 / (4 \cdot 3,1) = 2012 \text{ mm}^2/\text{m}$$

From 0/200 to 0/204,35 it is 13+12 ϕ 19 which gives

$$A_s = 25 \cdot \pi \cdot 19^2 / (4 \cdot 4,35) = 1629 \text{ mm}^2/\text{m}$$

The lower value is used.

The reinforcement is Ks 40 S and according to BBK 94 (1995) this means the characteristic value of

$$f_{yk} = 380 \text{ MPa}$$

6.1.3.5. Concrete

The concrete is K 300, which according to BBK 94 (1995) corresponds to a characteristic value of

$$f_{ck} = 21,5 \text{ MPa}$$

From drawing in appendix of section 0/200 the base width of the wall is 500 mm.

6.1.4 Assessment according to RIDAS

The following text is taken from RIDAS (translated by author of this thesis):

“Design of concrete sections in dams shall be performed according to BBK 94, with alterations and additions as below.

[..]

Material properties shall be according to BBK 94 chapter 2.3-5. Safety class 3 shall be used, i.e. $\gamma_n = 1,2$.

Instead of the load values, load factors and load combinations stated in BBK 94, load values and load combinations according to § 3.3.2-3 above [in RIDAS] shall be used. To reach desired level of safety all forces in a section (moment, shear force and normal force) shall be multiplied with a partial coefficient called hydraulic factor, γ_h , when designing a concrete section.

[..]

in the table below γ_h for different “ultimate limit states” is given:

	γ_h normal load case	γ_h exceptional load case
Moment	1.50	1.25
Shear force	1.50	1.25
Normal force, tension	1.50	1.25
Normal force, compression	1.80	1.5

Accidental limit state

For accidents the hydraulic factor γ_h shall be 1.0.

Partial coefficients for load carrying capacity and safety class shall be according to BBK 94, i.e. $\eta\gamma_m = 1.2$ for concrete and $\eta\gamma_m = 1.0$ for reinforcement. The safety class is $\gamma_n = 1,0$. ”

6.1.4.1. Resistance of wall

Safety class 3 gives $\gamma_n = 1.2$. This gives

$$f_{st} = \frac{f_{yk}}{\eta \cdot \gamma_m \cdot \gamma_n} = \frac{f_{yk}}{1.1 \cdot 1.2} = 288 \text{ MPa} \quad \text{Eqn. 6-9}$$

$$f_{cc} = \frac{f_{cck}}{\eta \cdot \gamma_m \cdot \gamma_n} = \frac{f_{cck}}{1.5 \cdot 1.2} = 11.9 \text{ MPa} \quad \text{Eqn. 6-10}$$

The resistance was calculated by

$$M = 0,8 \cdot b_{sekt} \cdot x \cdot f_{cc} \cdot (d_e - 0,4x) \quad \text{Eqn. 6-11}$$

where b_{sekt} is the length of interest, in this case 1000 mm (since the calculation is per meter) and d_e is the distance from the compressed edge to the active reinforcement and

$$x = \frac{A_s \cdot f_{st}}{0,8 \cdot b_{sekt} \cdot f_{cc}}$$

6.1.4.2. Results

The wall will be subjected to the unfavourable loading condition only in situations when water has to be discharged and one gate fails to open or stay open.

The total moment is according to equation Eqn. 6-5 for water up to crest and according to Eqn. 6-7 for water above crest. This should be combined with the hydraulic factor, $\gamma_h = 1.25$. For both sections the water depth when the structure fails has been calculated. The results are shown in Table 6-3.

Table 6-3 - Calculation according to RIDAS.

Section	0/192	0/200
Resistance		
A_s [mm ² /m]	4117	1629
$M_{resistance}$ [kNm/m]	514	196
Loads		
Calculated water depth at failure [m]	5.77	3.92 (+0.65)
M_{hydro} [kNm/m]	314.4	98.6
$M_{centripetal}$ [kNm/m]	97.6 ¹	58.2 ²
M_{tot} [kNm/m]	412	170.8
$M_{tot} \cdot \gamma_h$ [kNm/m]	514	196
¹ $V_w = 11$ m/s		
² $V_w = 12,5$ m/s		

The wall is thus safe according to RIDAS for water levels slightly above crest (5.75m) in section 0/192 and for water levels slightly below crest (4.00 m) in section 0/200.

6.1.5 Structural reliability analysis

6.1.5.1. Target safety index

As noted in chapter 3 and 4 the choice of target safety index is not simple, but in this analysis it will be assumed according to BKR (2003), safety class 3 (highest), giving $\beta_T = 4.8$.

6.1.5.1.1. Update of target safety index with use of probability of occurrence

The calculated safety index should not be immediately compared to the target safety index from BKR (2003). The reason is that β_T is given per year, while in this case the loading condition will only appear when water has to be discharged at the same time as one gate is not possible to open (or when only one gate is opened). The probability of occurrence/year will be used to update the target reliability index.

Knowledge of operational experience and routines were used to make a very rough estimation of the probability of P(gate needing to be opened \cap failure to open). This

probability is then used to recalculate β_r . From inspection protocols and testing a more appropriate number of gate failures could be calculated, but this is not done here.

6.1.5.1.2. Operational experience

The following information was received from the operation staff in Storuman:

- During normal operation the reason for discharge are mostly: from 1990 and on there has been some years with rainy summers, some years with rainy autumns and some years when the snow has melted very fast, causing a great spring flood. On these occasions it is known in advance (from the meteorologists of SMHI) approximately when and how much water is coming, and therefore the operation can be planned in advance. However, Ajaure is a small and “fast” reservoir where the water level can rise quite quickly.
- In hydropower plants where there are problems with erosion downstream of the spillway chute the gate causing the least such problems is used firstly and other gates if necessary. In Ajaure there are no such problems, and thus no reason to only use one gate in normal discharge situations.
- There has been trouble with gates not opening on command from the Operation Central in Storuman (remote control), and therefore control and testing is quite frequent, especially during the times of year when high floods can be expected. According to operating engineer Jan Olofsson these problems have been quite frequent (during some time it was more usual that the remote control did not work than work), but reports in Conwide (reporting system) suggest it is taken care of (if necessary more checks will be made). In the case of remote control not working operating personnel on duty has to go to the dam and operate the gate manually. Problems with this are not known.
- When the gates are completely impossible to open, remote or locally, and it is necessary to open a mobile crane can be used. There are problems with this procedure, e.g. a steel loop has to be welded to the gate and the mobile crane has to have steady ground to stand on. Some dams are not designed for such a large concentrated load (posed by the heavy crane). The status of mobile crane use at Ajaure is not known.

Table 6-4 shows the number of days during the last 10 years that the gates have been discharging water. The first column shows the number of days the gates have been open at all, while the others show the number of days when the mean discharge over a 24 hour period have exceeded a certain level. Different levels of discharge was investigated. The probability of occurrence per year is based on the number of years when the discharge of interest had been experienced according to

$$P(\text{discharge}) = \frac{\text{Number of years of discharge} > \text{limit}}{\text{Number of years}} \quad \text{Eqn. 6-12}$$

Table 6-4 - Days of discharge/year 1995 - 2004.

Year	Days of discharge (mean discharge over day)								
	>0	>20	>100	>150	>200	>250	>300	>350	>400
1995	70	56	34	27	22	16	12	12	11
1996	20	13	6	5	3	2	0	0	0
1997	58	50	36	32	26	24	20	13	8
1998	69	60	41	26	19	15	5	3	0
1999	79	68	30	19	7	1	0	0	0
2000	175	169	38	22	15	13	2	0	0
2001	188	165	38	9	5	0	0	0	0
2002	82	60	31	15	5	3	0	0	0
2003	29	21	17	13	9	4	3	1	0
2004	57	38	19	15	13	11	5	4	3
Total no of days	827	700	290	183	124	89	47	33	22
no years of occurrence	10	10	10	10	10	9	6	5	3
probability of occurrence/year	1	1	1	1	1	0,9	0,6	0,5	0,3

Using operational experience to update β

The probability of gate opening necessary at the same time as the gate can not be opened is given by

$$P(A \cap B \cap C) = P(A) \cdot P(B) \cdot P(C) \quad \text{Eqn. 6-13}$$

where A is gate opening necessary (probability of occurrence of discharge > limit), B is remote control malfunctioning, C is local control inoperable. These three events can be assumed independent (perhaps loss of remote and local control is more probable in high-flood situations and perhaps loss of local control is somewhat related to loss of remote control, but this is disregarded).

The problem with remote control not working described above is serious, but the gates can still be operated locally. The dangerous case occur when local operation is

malfunctioning too. Assuming that remote control fails 9 times in 10 (very high) gives $P(B) = 0,9$ and assuming that local control fails 1 time in 10 (seems high) gives

$$P(C) = 0,1.$$

$$\text{Then } P(A \cap B \cap C) = P(A) \cdot 0,9 \cdot 0,1 = P(A) \cdot 0,09$$

According to eqn 3-18 in chapter 3 the safety index for a one-year period can be translated to another period according to

$$\Phi(\beta_n) = [\Phi(\beta)]^n$$

In this case we have $n = 1/p_{occurrence}$

$$\beta_T = 4.8 \text{ (From BKR, 2003).}$$

Table 6-5 shows the water depth, discharge, probability of occurrence of the discharge and the updated safety index.

Table 6-5 - target reliability for different water levels.

Discharge [m ³ /s]	Gate opening [m]	h _w in 0/192 [m]	h _w in 0/200 [m]	P(A)	p _{occurrence}	n	Updated β _T
< 250	< 5	< 4.8	< 4	1	1-0.09	11.1	4.29
250	5	4.8	4	0.9	0.9-0.09	12.35	4.27
300	6.13	5.88	4.9	0.6	0.6-0.09	18.52	4.18
350	7.26	6.97	5.81	0.5	0.5-0.09	22.22	4.14
400	8.38	8.04	6.7	0.3	0.3-0.09	37.0	4.02

6.1.5.2. Reliability analysis

The parameters used in the structural reliability analysis were:

Table 6-6 - Parameters in structural reliability analysis.

		Section 0/192	Section 0/200
Parameter	Distribution	Value (μ ; σ)	Value (μ ; σ)
A_s	Constant	4117 mm ²	1629 mm ²
f_{st}	Normal	(464 MPa; 30,4 MPa)	(464 MPa; 30,4 MPa)
f_{cc}	Lognormal	(34,3 MPa; 6,76 MPa)	(34,3 MPa; 6,76 MPa)
h	Constant	5,75 m	4 m
ρ_w	Constant	1000 kg/m ³	1000 kg/m ³
r	Constant	130 m	130 m
V_w	Constant	11 m/s	12,5 m/s
d_e	Normal	(478,5 mm; 12,5 mm)	(435,5 mm; 12,5 mm)

The derivation of f_{cc} (mean value and standard deviation) is described in Appendix A1.

f_{st} is taken from Carlsson et al (2006). The variation in cross sectional area of the reinforcement is included in the variation of strength Thelandersson (2004).

The effective depth, d_e , of concrete slabs cast in situ (which this wall can be considered to be) can be described as normal distributed variables with $\mu = -5$ mm and $\sigma = 12,5$ mm, in this case giving $\mu_{0/192} = 483,5 - 5 = 478,5$ mm and $\mu_{0/200} = 440,5 - 5 = 435,5$ mm.

The safety index calculation is performed by FORM (First Order Reliability Method) using the software COMREL (RCP, 1997).

The maximum gate opening, 10 m, gives water depths of approximately 9.6 and 8 m in sections 0/192 and 0/200 respectively (according to Eqn. 6-8). The maximum water depth calculated for is thus 9.7 m in section 0/192. In section 0/200 the ground is 0,65 m below the actual “wall foundation”, and for this reason the water levels up to 9 m is analyzed.

6.1.6 Results

According to RIDAS the wall could withstand water depths approximately equal the wall height. This corresponds to $\beta_{0/192} = 8,090$ and $\beta_{0/200} = 7,289$. For water levels above crest β decreases.

The diagrams of Figure 6-13 and Figure 6-14 show the actual calculated safety index as a function of water depth. The target safety, with respect taken to probability of occurrence of different gate openings, is also shown. The “meeting point” between those curves indicates the maximum allowable water depth in that section. The crest heights are also shown.

In section 0/200 the allowable water level is actually 0,65 m higher than that shown in the diagrams, as the canal ground is 0,65 m below the wall.

The wall is sufficient to withstand water levels of

0/192: 7,11 m

0/200: $4,83 + 0,65 = 5,48$ m

corresponding approximately to gate openings of 7,41 and 6,85 m and thus a discharge of 356 and 332 m³/s, respectively.

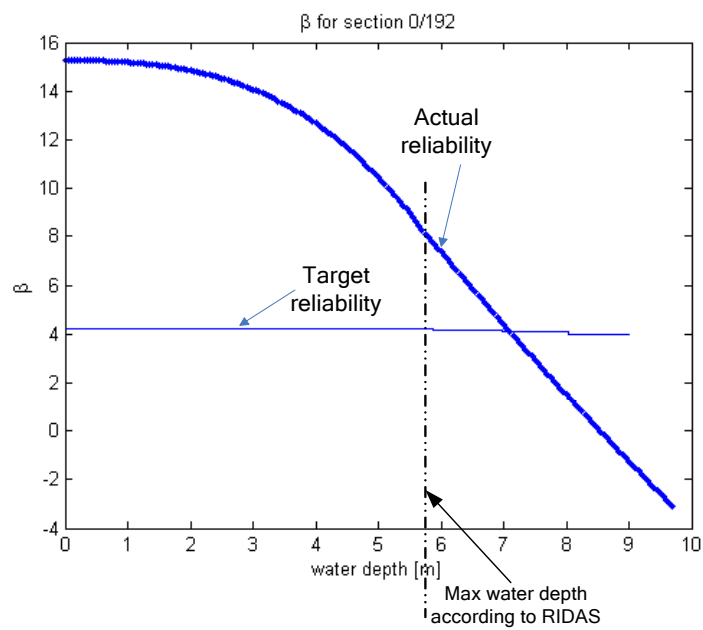


Figure 6-13 - β for section 0/192.

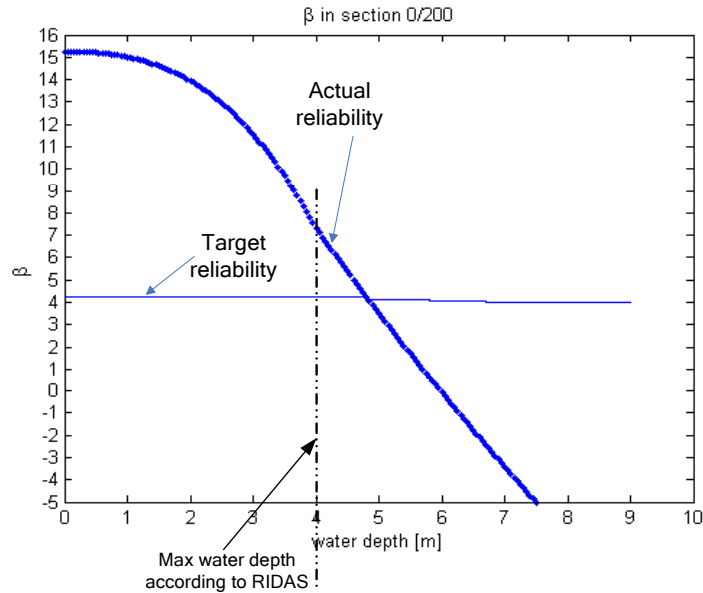


Figure 6-14 - b for section 0/200.

6.1.7 Cracking of concrete

It may be of interest to analyze the serviceability limit state, which in this case would be cracking of the concrete. As the major purpose of this thesis is to describe the ultimate limit state this is not given a through analysis, and only the limit state function for the serviceability limit state, input variables and results are given here. The literature used to define the input variables was Betonghandboken (1997), Carlsson et al. (2006) and EN 1992-1 (1991).

A reliability analysis was performed in the software COMREL (RCP, 1997). The limit state used was:

$$G = \frac{h_b^2 \cdot f_b}{6} - \frac{\rho_w \cdot g \cdot h_w^3}{6} - \frac{\rho_w \cdot b_{canal} \cdot V_w^2 \cdot h_w^2}{2 \cdot r} \leq 0 \quad \text{Eqn. 6-14}$$

The parameters were defined as:

Table 6-7 – Parameters used in structural reliability analysis of serviceability limit state.

Parameter	Distribution	0/192	0/200	[-]
f_b	Lognormal	$\mu = 2,94E6; \sigma = 0,88E6$		
ρ_w	Constant	1000		kg/m ³
g	Constant	9.82		m/s ²
r	Constant	130		m
b_{anal}	Constant	6.3		m
h_b	Normal	N (0,543;0,006)	N (0,497; 0,006)	m
h	Constant	5.75	4	m
V_w	Constant	11	12.5	m/s

Where f_b is tensile strength in bending, r is the radius of the canal and h_b is the width of the beam, which can be described as a normal distribution with $\mu = -3$ mm and $\sigma = 6$ mm.

A parameter study was performed for the water depth varying between 0 and wall crest level

The target safety index, β_{target} is set to 2.3, in accordance with BKR (2003). In this case we want to find the difference in water depth that will cause the wall to crack and hence the probability of gates to not open is of no importance. The update of β_T is performed as before.

Table 6-8 – Updating of β_T .

Discharge [m ³ /s]	Gate opening [m]	h_w in 0/192 [m]	h_w in 0/200 [m]	P(A)	n	Corresponding β
> 0	0	0	0	1	1	2.3
250	5	4.8	4	0.9	1.11	2.26
300	6.13	5.88	4.9	0.6	1.67	2.10
350	7.26	6.97	5.81	0.5	2	2.03
400	8.38	8.04	6.7	0.3	3.33	1.81

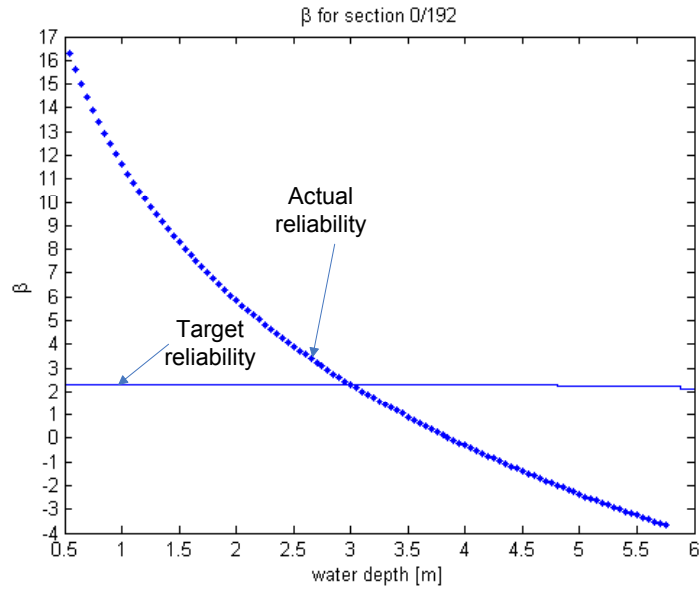


Figure 6-15 - Safety index β in section 0/192 for different water depth.

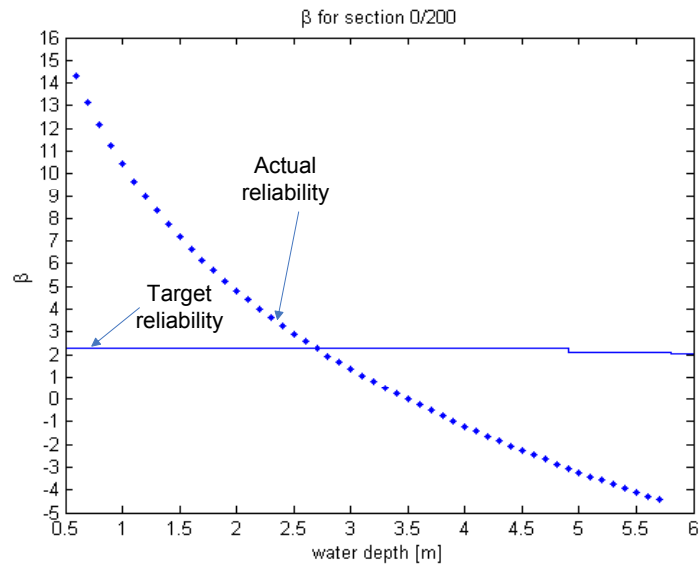


Figure 6-16 - Safety index β in section 0/200 for different water depth.

The maximum allowed water depth is thus

0/192: 3 m

0/200: $2,68 + 0,65 = 3,33$ m

corresponding to 3,13 and 4,16 m and thus a discharge of 166 and 212 m³/s respectively.

This discharge is, as mentioned earlier, only approximate and further tests would be needed to confirm the relation between water depth in different sections and gate opening and between gate opening and discharge.

6.1.8 Discussion and conclusions of example

The resistance according to RIDAS gave maximum water depths of 5.77 and 4.57 m in section 0/192 and 0/200. The reliability analysis, using the conservative assumption of water not spilling over the crest (giving no water on in the adjacent canal) and updating the target reliability index to account for probability of occurrence of the different water levels, gave maximum allowable water depths of $d_{0/192} = 7.11$ m and $d_{0/200} = 5.48$ m.

In the serviceability limit state water depths of 3 and 3,33 m can be allowed in section 0/192 and 0/200 respectively. The corresponding discharge is approximated to 166 m³/s. The recommendation is to use operational restrictions of 150 m³/s in discharge difference in normal situation to reduce the crack risk.

As the safety index was high the wall can be considered safe and the vulnerability index assigned before can now be reduced. The “magnitude of deficiency” was earlier 4-5, but can now be reduced to 1. The frequency of loading was previously 5 (occurring at least once every year), but as was shown in Table 6-5 the return period of the water levels of interest is in the order of 10 to 30 years, giving a frequency of stressing of 4. The total vulnerability index is thus reduced from 240-500 to 48-80.

This simple example illustrates the whole assessment strategy; a risk analysis identifies a (potential) weakness and structural reliability analysis is used in the “in depth analysis” and shows that the risk is not as high as expected and that the component is not critical. Resources can now be used elsewhere.

The explanation of the large difference in calculation according to RIDAS and that according to the reliability analysis in this case is some “strange” things in RIDAS. Forces and moments are to be calculated according to the global stability calculation, which is strange since for sectional design the actual design load case may be very different from the global case. Furthermore, and that of importance in this case, the “hydraulic factor” introduced to take care of uncertainties result in a heavy underestimation of the ultimate capacity. The combination of the partial factor design according to BKR and the safety factor-determination of design loads is an inconsistent handling of safety concepts. The result is that design is half-deterministic and half-semi-probabilistic. It would be much better to define the partial factors that are “special” for sectional design of dams and perform the sectional design in accordance with BKR.

6.2 Example 2: Reliability analysis of theoretical dam

This section is intended to show how a structural reliability analysis of a concrete dam is performed.

The first step is to have a dam to analyze. In this case a theoretical dam is chosen. The dam is designed to be safe according to RIDAS for overturning and sliding in the normal load case.

Figure 6-17 shows definitions of the loads acting on the dam and Table 6-9 shows the forces and moments (taken around the dam toe).

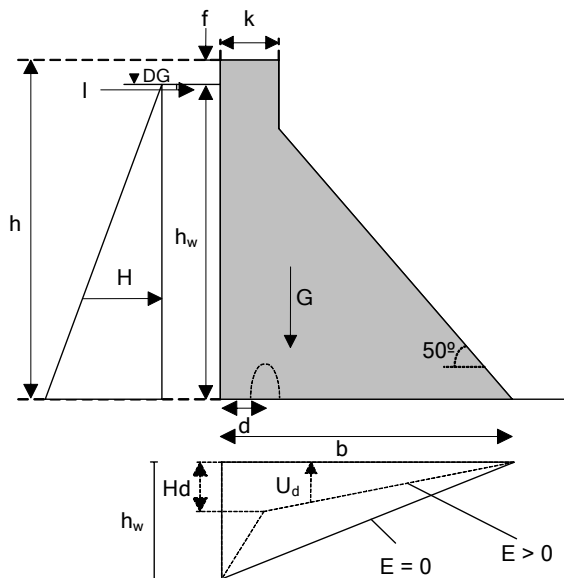


Figure 6-17 - Definition of loads acting on dam.

The uplift pressure at the drain position d is H_d , given in accordance with chapter 5.5 and as shown below. In this example tail water level is assumed to be zero.

$$H_d = K_d \left(h_w \left(\frac{b-d}{b} \right) \right)$$

$$K_d = 1 - 0.67 \cdot E_d$$

$$0 < E_d < 1.0$$

Table 6-9 - Forces and moments acting on the dam.

Parameter	Force, sliding failure	Moment (around dam toe), overturning failure
Self weight	$G = \left(k \cdot h + \frac{(b-k)^2 \cdot \tan 50}{2} \right) \cdot \rho_c$	$G_M = \left(k \cdot h \cdot \left(b - \frac{k}{2} \right) + \frac{(b-k)^3 \cdot \tan 50}{3} \right) \cdot \rho_c$
Ice load	$I = 200$	$I_M = 200 \cdot \left(h_w - \frac{1}{3} \right)$
Hydrostatic pressure	$H = \frac{h_w^2}{2} \cdot \rho_w$	$H_M = \frac{h_w^3}{6} \cdot \rho_w$
Uplift	$U_d = \left(\frac{b \cdot H_d}{2} + \frac{h_w \cdot d}{2} \right) \cdot \rho_w$	$U_{dM} = \left(\frac{b \cdot H_d}{3} \left(b - \frac{d}{2} \right) + \frac{d \cdot h_w}{2} \left(b - \frac{d}{3} \right) \right) \cdot \rho_w$

6.2.1 Stability according to RIDAS

The sliding stability can be written

$$\frac{R_H}{R_V} \leq \mu_{till} \quad \text{Eqn. 6-15}$$

where $R_H = I + H$ and $R_V = G - U$.

μ_{till} (assuming rock foundation) is 0.75 for the normal load case and 0.9 for the exceptional load case (frictional coefficient 1.0 and safety factor 1.35 and 1.1 respectively).

The overturning stability is

$$\frac{M_R}{M_S} \geq s \quad \text{Eqn. 6-16}$$

where $M_R = G_M$

and $M_S = I_M + H_M + U_M$

the safety factor s is 1.5 for the normal load case and 1.35 for the exceptional load case.

With the values in Table 6-10 the width, b , required to fulfil the above stability criterions are calculated, assuming drains of effectiveness 0 and drains of effectiveness 1. Results are shown in Table 6-11.

Table 6-10 - Values of parameters in stability calculations.

Parameter	Value	
ρ_c	23	kN/m ³
ρ_w	10	kN/m ³
k	5	m
f	1.9	m
h_w	23	m
h	24.9	m

Table 6-11 - Required width to fulfil stability criterions.

E_d	0	1
b_{over}	20.50	16.29
b_{slide}	20.49	16.41

6.2.2 Reliability analysis of dam

The input data used is that defined in chapter 5 and summarized in Table 6-12. Due to the large impact of the assumed cohesion also some other distributions than that described in chapter 5.2 was used, as shown in Table 6-12. Those distributions are also shown in Figure 6-18. For the hydrostatic water pressure, the exceptional load case is assumed according to the example shown in chapter 5.3 (hydrostatic water pressure), where the design flood (return period approximately 10 000 years) was assumed to be discharged with water 1.8 m above retention level. Two different assumptions of probability of exceeding the retention water level (1/100 and 1/500 per year) will be tested to show the impact of this on the result.

The uplift pressure is taken as the design assumption multiplied by a random variable (as in chapter 5.5). The random variable is C for uplift force and C_m for uplift moment. Physical restraints limit C and C_m to 0-2 and 0-1.5 respectively, as discussed in chapter 5.5. Regarding the uplift pressure several different approaches will be tested. The load cases analyzed here are:

1. C and C_m in accordance with the simulation results of chapter 5.5, shown in Table 6-13.
2. C and C_m assuming that uplift pressure monitoring has confirmed the design assumption and that the COV of annual maximum values is 0.2.
3. Exceptional load case. Uplift is Beta-distributed, $\lambda = 2.56$. No ice.
4. Exceptional load case. Uplift is Beta-distributed, $\lambda = 1.66$. No ice.
5. Assuming that the dam is designed for drains and that drains are in perfect condition ($E_d = 1$).
6. Assuming that the dam is designed for drains and that drains are completely clogged ($E_d = 0$).
7. Assuming that the dam is designed for drains and of an unknown state, $0 < E_d < 1$. E_d will be assumed to have a rectangular distribution (equal probability for any value between 0 and 1).

The limit state functions considered where, as discussed in chapter 2,

- Sliding, for which failure occur when

$$c \cdot A + (G - U \cdot C) \tan(\phi) - I - H \leq 0 \quad \text{Eqn. 6-17}$$

- Overturning, for which failure occur when

$$G_M - H_M - U_M \cdot C_m - I_M \leq 0 \quad \text{Eqn. 6-18}$$

Table 6-12 - Input parameters in the reliability analysis.

Parameter	Distribution	E	COV	$V^{1/2}$	
ρ_c	Normal	24	0.034	0.816	
$\tan(\phi)$	Normal	1.3	0,2	0.26	
c	Lognormal	0.7	0.4	0.28	
		0.7	1.0	0.7	
		0.7	0.57	0.4	
		0.4	1.0	0.4	
h_w (normal)	Constant	1	-	-	
h_w (exceptional)	Exponential	-	-	-	$\lambda = 2.56$ ($p_{h_w > r_{wl}} = 1/100$)
		-	-	-	$\lambda = 1.66$ ($p_{h_w > r_{wl}} = 1/500$)
I	Normal	103	0.461	47.5	

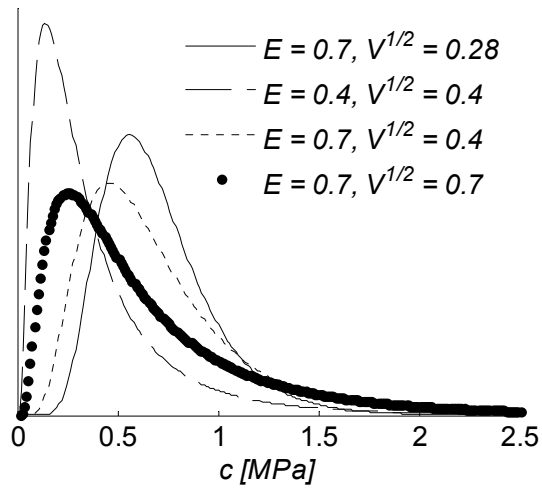


Figure 6-18 - Different assumptions of cohesion.

Table 6-13 - Parameters of the Beta-distribution.

	r	t	a	b
C	1,96	1,95	0,08	1,9
C_m	2,22	1,33	0,11	1,49

6.2.2.1. Results

Results of the reliability analysis are shown in Table 6-14. Diagrams of the α -variables (describing the influence of a specific variable on the resulting β) are shown in Figure 6-19 to Figure 6-27.

Table 6-14 - Results from the reliability analysis.

No	Load case	β_{over}	$\beta_{sliding}, c \in LogN$			
			(0.7; 0.28)	(0.7; 0.7)	(0.4; 0.4)	(0.7; 0.4)
1	Normal load case. Beta-distribution of uplift. $E_d = 0$	6.44	6.42	3.94	3.48	5.27
2	Normal load case. Uplift $\in N(1.0; 0.2)$ (monitoring results). $E_d = 0$	6.56	6.44	4.28		
3	Exceptional load case. Uplift Beta-distributet. $\lambda = 2.56$ ($p_{hw>rw1} = 1/100$). No ice.	5.09	6.42	3.92		
4	Exceptional load case. Uplift Beta-distributet. $\lambda = 1.66$ ($p_{hw>rw1} = 1/500$). No ice.	4.14	5.94	3.81		
5	Normal load case. Stability according to RIDAS relying on drains. Beta-distribution of uplift. $E_d = 1$.	8.3	6.05	4.11		
6	Normal load case. Stability according to RIDAS relying on drains. Beta-distribution of uplift. $E_d = 0$.	2.3	5.64	3.15		
7	Normal load case. Stability according to RIDAS relying on drains. Beta-distribution of uplift. $E_d \in Rect(0,1)$.	3.01	5.89	3.51		

6.2.2.1.1. Sensitivities in overturning case

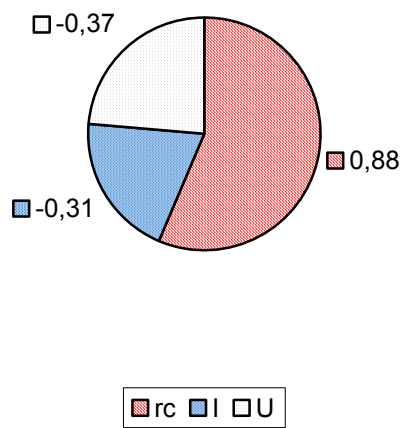


Figure 6-19- α :s of variables for load case 1

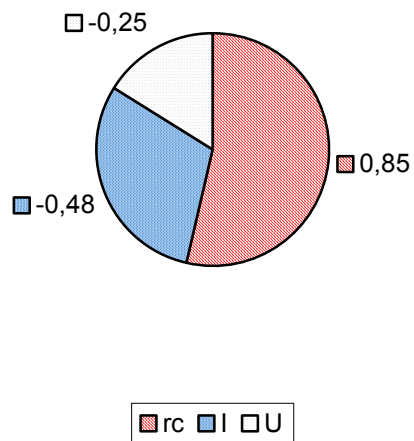


Figure 6-20 - α :s of variables for load case 5.

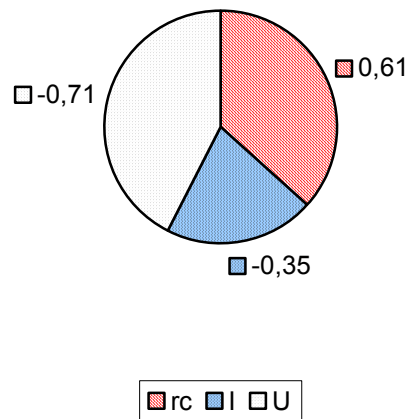


Figure 6-21 - α :s of variables for load case

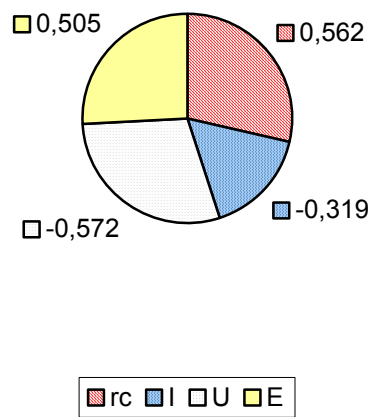


Figure 6-22 - α :s of variables for load case 7.

6.2.2.1.2. Sensitivities in sliding case

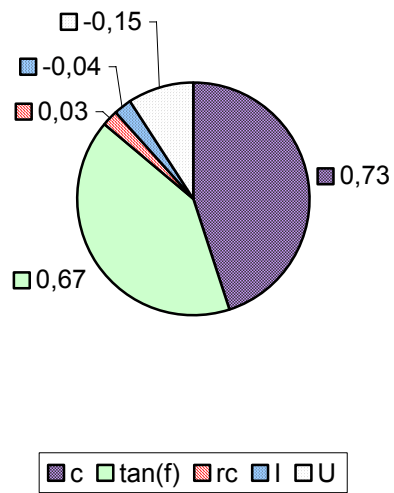


Figure 6-23 - α :s of load case 1. $c \in \text{LogN} (0.7;0.28)$.

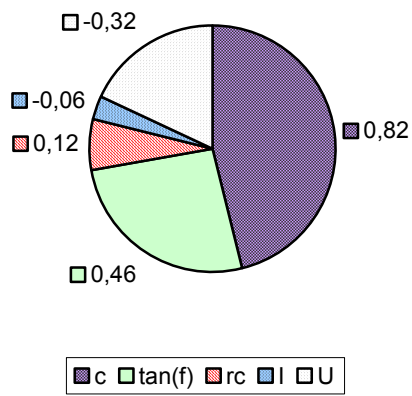


Figure 24 - α :s of load case 6. $c \in \text{LogN} (0.7;0.28)$

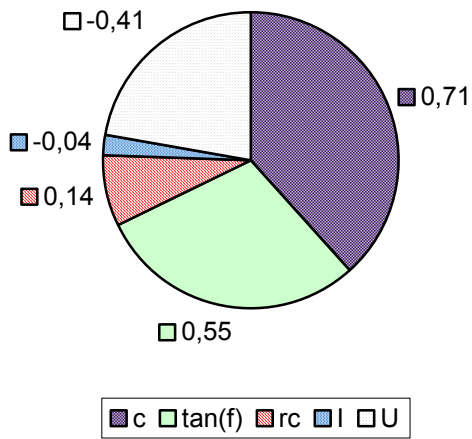


Figure 6-25- α :s of load case 1. $c \in \text{LogN} (0.7;0.7)$.

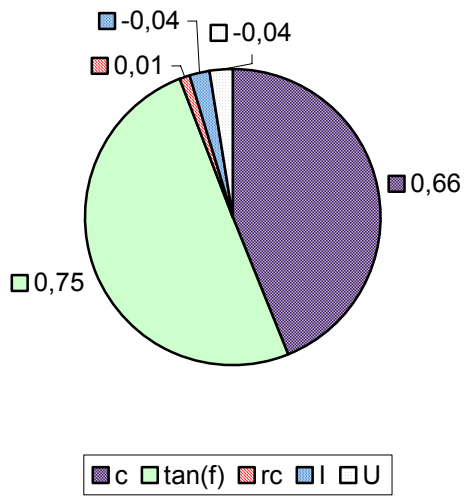


Figure 6-26 - α :s of load case 6. $c \in \text{LogN} (0.7;0.7)$

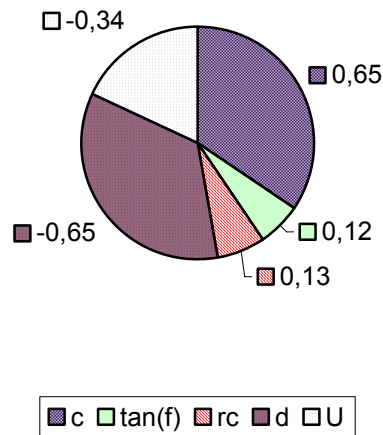
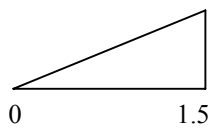


Figure 6-27 - α :s of load case 4, exceptional. $c \in \text{LogN}(0.7;0.7)$

6.2.3 Discussions and conclusion of example

6.2.3.1. Overturning

In the normal load case the sensitivity to the uplift pressure is quite low and the sensitivity is dominated by the uncertainties in the concrete density. An even worse random distribution of uplift than that used here is the triangular-shaped distribution. As noted in chapter 5.5 the Beta-distribution for large variance and scale in simulations rendered a triangular-shaped distribution. Using the distribution shown below as input gave $\beta = 6.2$. The worst uplift pressure would, however, be that the moment of uplift was 1.5. This gives $\beta = 5.7$.



A decrease in $E(\rho_c)$ to 23 with the same COV gave $\beta = 5.5$.

The exceptional load case has to be combined with the occurrence, in this case the probability of water levels above retention water level is 1/100 and 1/500 respectively. The updated safety index is calculated as in the previous example

$$\beta_{updated} = \Phi^{-1}\left(\left(\Phi(\beta)\right)^{p_{hw>rw}}\right)$$

Eqn. 6-19

to be

$$\beta_{up1/100} = 5.9 \text{ and } \beta_{up1/500} = 5.4.$$

When the dam is dependant on drains to fulfil safety requirements the following can be noted:

- The safety index in the case of effective drains is much higher than in the normal load case without drains (case 1 compared to case 4). The sensitivity to uplift is also lower (see Figure 6-20).
- When the drain effectiveness becomes 0 the uplift pressure increase from the reduced to full. With the geometry used here this gives an increase in moment of uplift with a factor of 2. In this case the sensitivity to uplift is higher and the result is a dramatic reduction of the safety index.

6.2.3.2. Sliding

Clearly the assumption of cohesion gives a huge impact on the result, as the sensitivity to cohesion is very high. If the cohesion is assumed to be zero β is reduced to 1.7.

In future applications it seems wise to treat the shear strength similar to the uplift pressure. The shear strength is affected by the whole base area and it seems unlikely (unless large displacements have occurred) that the whole area has cohesion zero. The area can be seen as a system of many small elements, each with a specific cohesion. If the shear strength of one element is exceeded the stress will be redistributed to other elements to a certain extent. In other words, the shear strength can be considered to function as a parallel system rather than a complete series system (which would fail when the weakest link does). The concrete to rock interface is, however, brittle which means that this redistribution can only be considered to a limited extent. With this background the cohesion can be assumed to exceed zero and the assumption of $E = 0.7$ and $V^{1/2} = 0.28$ is thus assumed reasonable.

The exceptional load case, updated as above, gives $\beta_{up1/100} = 7.1$ and $\beta_{up1/500} = 6.9$.

With effective drains the safety index is still high, but less than in the normal case.

Ineffective drains reduce the safety index but, as the sensitivity of uplift is low, this reduction is not very large.

If the cohesion has larger standard deviation, the safety index will be significantly reduced.

6.2.3.3. Conclusions of example

The difference in safety index when load case 1 and 5 (normal and $E_d = 1$) are compared is striking. In the overturning case the safety index is much higher for load case 5,

whereas in the sliding case it is slightly lower. This suggests that the design requirement is sensitive to load case. This is an unwanted situation and it may be due to the use of only one factor of safety.

This small example indicates, even though there is no target safety index to compare with, that the stability for the analyzed failure modes of a dam, which is safe according to today's requirements, is sufficient.

The analysis of the sensitivity factors indicates that the loads of largest importance for future research are *concrete density*, for which the assumed distributions according to JCSS (2002) has to be validated and procedures to incorporate test results has to be described, *cohesion* and *friction coefficient*. Ice loads is mainly of importance in the overturning case here, but it must be noted that for the sliding case the ice load has large impact for low dams. For a low dam the ice load is a large portion of the total horizontal force, whereas for a high dam it represents only a small portion.

6.3 Conclusions of chapter

The two examples here were both simple, but showed that

- Structural reliability can be used as a tool in the dam safety management process
- Today's design guidelines result in a number of "problems".
- The most important factors for further analysis are cohesion and friction coefficient, self weight and ice load.

7. Concluding remarks

7.1 General safety considerations

Safety is, and should be, given highest priority in dam engineering. The stability criteria, and thus safety, of concrete dams is based on safety factors, where one safety factor is used for each criterion. This type of design formulation was used for other types of structures as well, but during the 1970's and 1980's the partial factor format was introduced. This format takes into account the statistical variability of loads and resistance and the partial factors that are assigned to the different variables differ in size depending on the variability of the parameter. In this way the safety of structures becomes more uniform, and resources are likely to be spent more efficiently. There are still conservatism inherent in the partial factor format, and when complex structures are designed, or when safety assessment is performed for existing structures, use of reliability-based methods are advantageous. Reliability-based methodology offers the possibility of rational integration of information of a certain object and refinement of statistical descriptions of loads and resistances, e.g. based on monitoring and testing.

The safety format used today is deterministic and as such it only tells us that a dam is "safe" or "unsafe", but nothing of how safe, how un-safe etc. As was discovered in the 1970s the use of only one safety factor results in some structures to be much safer than others, when safety is given a probabilistic interpretation. The master thesis work by Ahlsén Farell & Holmberg (2007) indicates that the safety of dams is dependant on dam height, dam type and failure mode, which is exactly the situation we do not want.

We have to ask the question: how do we want our dams? The answer to this question is that we want them to be

- Safe "enough"
- Equally safe, the safety level for dams of a specified consequence class should be independent of dam height and dam type

If design and assessment should be based on the partial factor format some of the problems described above would be possible to "cure". Perhaps not entirely, as a partial factor based code is often made general to be applicable for a large number of structures. One further possibility is to base design and assessment directly on reliability based methodology. This means that statistical description of loads and resistance would have to be performed for each dam structure. It may be based on some general description, but would have to be adopted to every single structure, which is cumbersome and sometimes difficult. The advantage would be that all dam structures would have the "right" safety.

Development of the safety format has the possibility to give us:

- Different safety for different consequence classes. Target safety can be differentiated for different consequence classes, and if partial factors are used they can be related to different consequence class
- Uniform safety for each consequence class, independent of dam height, dam type and failure mode.

7.2 Conclusions

7.2.1 Target safety

For structural design according to BKR (2003), Eurocode (ENV-1990, 1991) and China Electricity Council (2000) a target safety index is defined. The result from a structural reliability analysis is then compared to this target value to evaluate if the structure is “safe enough”. For dams no such target value exists and if structural reliability analysis is to be used for assessment, design or development of new design guidelines based on partial factors, a target value must be defined. There are reasons to set the target safety index higher for new structures than for existing ones, as the relative cost of safety increase is small before the structure is built.

As dam safety activities to larger extent than other civil-engineering activities are affected by company or societal values, there are arguments that target safety values for dams should be based not only on that from other areas or calibration to existing practice, but also on tolerable risk criterions. This is a decision for politicians and society or, due to the strict responsibility, for the hydropower owners. It is not a decision to be made by engineers alone.

7.2.2 Failure modes definition

As noted in chapter 2 the overturning failure criterion may be questionable; does overturning really occur? USACE (2003) declare that sliding or overstressing will occur before overturning does. The sliding stability formulation in RIDAS (2000) does not, unlike design guidelines in many other countries, account for cohesion. There are, thus, reasons to look over the failure modes used in design, especially for use in reliability analysis and finite element analysis.

7.2.3 Loads and resistance

Statistical formulation of loads and resistances are all but easy. A promising approach on how to use geostatistical modelling to derive statistical distribution for uplift is shown. The uplift is described as a constant (derived from the linear uplift pressure distribution usually assumed in design) multiplied with a random variable (based on the simulations). This concept can and should be further developed, e.g. by investigating real rock properties and analyzing 3-D modelling of hydraulic conductivities. Even though there are questions to be solved this approach gives useful results.

The hydrostatic water pressure is a function of the headwater variation and it was shown that this can not easily be captured by a statistical description. Instead the headwater level was divided into two parts; normal pool levels, that occur with a probability close to one, and pool levels exceeding normal, described with an exponential distribution and occurring with a probability that is to be defined for the specific facility.

Cohesion was shown to have a huge impact on the sliding stability and statistical descriptions has to be further analysed. The same is true for the friction coefficient.

Ice loads have large impact on the overturning stability, especially when the uplift pressure is reduced due to drains. For sliding stability the ice load is important for low dams, but less so for higher ones.

The resistance of a concrete dam, at least to concrete gravity types, is highly dependant on the self weight as the stabilizing factor. The self weight used here is based on JCSS (2001) and has a low variability. It is recommended that further analysis, based on cores from concrete dams, is performed, and that Bayesian updating is performed to include test results.

7.2.4 General

The examples revealed that structural reliability analysis is useful as “in depth analysis” in dam safety management. They also revealed some problems with the present guideline; concerning inconsistent handling of safety concepts and different safety index for cases which are in fact the same.

Reliability based methodology fits into the dam safety risk management process and is possible to use for assessment of concrete dams.

To continue the safety factor design used today, referring to the fact that we do not know enough of resistances and loads to describe them statistically, is to choose ignoring the fact that the same is true about the design of today, only we do not see it!

7.3 Suggestions for further research

There are a number of areas where further research is needed or would be interesting:

- Failure modes and limit states definition
- Target safety
- How RIDAS assumptions affect the end result. It was seen in the examples that the inconsistency in use of safety concepts may result in structures that are “safe enough” to be considered “unsafe”. A master thesis referred to also demonstrate that the “safe” level is dependant on height of dams and the failure mode considered, resulting in a non-uniform safety level.
- Resistance parameters: friction and cohesion. Friction coefficient and cohesion parameters need further analysis. What would be representative distributions?

Can parameters be distinguished for different rock types? Can the shear strength be treated as consisting of a parallel system of many small elements?

- Load parameters: uplift, ice load, other loads. For uplift it would be of interest to further analyze the COV of annual maximum values and analyze the actual rock properties to give better estimate of modelling. For ice load a thorough investigation of statistical distributions is needed. The ice load should preferably be divided into different categories, depending on water level fluctuations and climate zone.
- Bayesian update of *a priori* information. Monitoring results and different types of measurement can be used to give better estimates of generic information. This is especially true for resistance parameters of existing structures.
- Failure in the rock mass. If the concrete to rock interface is strong in comparison to the rock mass (e.g. if fracture zones or weak planes exist), failure will occur in the rock mass.
- Analysis of real cases to "investigate" the real problems encountered in an assessment situation.
- Combination of different loads.

8. References

- Ahlsén Farell, L & Holmberg, J (2007). *Utvärdering av säkerhet för betongdammar*. Master thesis. Avd för Konstruktionsteknik. Lund University. TVBK-5150. ISSN 0349-4969. In Swedish.
- Ale, B.J.M. (2005). *Tolerable or Acceptable: A comparison of Risk Regulation in the United Kingdom and in the Netherlands*. Risk Analysis. 25 No.2 (2005) 231-241.
- Amadei, B. & Illagasekare, T. & Chinnaswamy, C. (1991) *Effect of crack uplift on concrete dam stability*. Conference on Research Needs in Dam Safety 1, 1991, New Delhi.
- Amadi, B., Illangasekare, T., Chinnaswamy, C. And Morris, D.I. (1990) *Reducing uplift pressures in concrete gravity dams*. Water Power & Dam construction, 1990.
- Ando, K., Kostner, A. & Neuman, S.P. (2003) *Stochastic continuum modelling of flow and transport in a crystalline rock mass: Fanay-Augères, France, revisited*. Hydrogeology Journal 11:521-535.
- De Araújo J. M., Awruch A.M. (1998). *Probabilistic finite element analysis of concrete gravity dams*. Advances in Engineering Software, vol 29 no 2 pp 97-104.
- Bandis, S., Lumsden, A.C. & Barton, N.R. (1981) *Experimental Studies of Scale Effects on the shear behaviour of rock joints*. Int. J. Rock. Mech., Min. Sci. & Geomech. Abstr. Vol 18 pp 1-21.
- BBK 94 (1995) *Boverkets handbok om betongkonstruktioner*. The Swedish National Board of Housing, Building and Planning.. In Swedish.
- Bergdahl, L & Wernersson, L (1978) *Calculated and expected thermal ice pressures in five Swedish lakes*. Department of Hydraulics, Chalmers University of Technology, Sweden. ISSN 0348-1069.
- Bergdahl, L. (1977a) *Physics of Ice and Snow as Affects thermal pressure*. Department of Hydraulics, Chalmers University of Technology, Sweden.
- Bergström, S. (1993) *Sveriges hydrologi – grundläggande hydrologiska förhållanden*. Norrköping: SMHI/Svenska Hydrologiska Rådet.
- Bernstone, C. (2006). *Automated performance monitoring of concrete dams*. Doctoral thesis. Engineering geology, Faculty of Engineering, Lund University. ISBN 91-628-6982-5.
- Bernstone, C. & Westberg, M. *Long term monitoring of uplift pressures in hydropower concrete structures based on TDR*. To be published.

Berntsson, S. (2001). *Dam safety and risk management*. Licentiate Thesis, Department of Civil and Environmental Engineering, Royal Institute of Technology, Stockholm, Sweden. ISSN: 1400-1292.

BKR (2003). Boverkets konstruktionsregler. ISBN 91-7147-740-3. ISSN 1100-0856.

Bureau of Reclamation (1987) *Design of Small Dams*.
http://www.usbr.gov/pmts/hydraulics_lab/pubs/manuals/SmallDams.pdf

BYGG, Handboken (1985). ISBN 91-38-06081-7

Canadian Dam Safety Association (1995) *Dam safety guidelines*.

Carlsson, F. (2002) *Reliability based assessment of bridges with short spans*. Division of Structural Engineering, Lund Institute of Technology, Lund University, Report TVBK-1025, ISSN 0349-4969.

Carlsson, F. (2006) *Modelling of traffic loads on bridges. Based on measurement of real traffic loads in Sweden*. Doctoral Thesis. Division of Structural Engineering, Lund Institute of Technology, Lund University, Report TVBK-1032. ISSN 0349-4969.

Carlsson, F., Thelandersson, S. (2006) *Probabilistisk modellering samt säkerhetsprinciper för befintliga broar*, Rapport TVBK-3052, Div. of Structural Engineering, Lund University, 164 p. In Swedish.

Casagrande, A. (1961) *Control of seepage through foundations and abutments of dams*. First Rankine lecture, 1961, p. 159-182.

Cederström, M. (2006) *Personal communication*.

China Electric Council (2000) *The Standards Compilation of Water Power in China*. China Electric Power Press, Beijing. ISBN 7-5083-0392-X.

CIB (1989) *Actions on structures. Self-weight loads*. Report by CIB Commission W81.

Comfort, G., Gong, Y., Liddiard, A. (2003). *Static ice loads on dams*. ICOLD congress, Montreal 2003.

Cressie, N.A.C. (1993) *Statistics for spatial data*. Revised edition. John Wiley & sons, USA. ISBN 0-471-00255-0.

Ekström, T (2002). *Isolaster mot hydrauliska konstruktioner. Inriktning mot betongdammar*. Elforsk rapport 02:03. In Swedish.

Elkateb, T., Chalaturnyk, R. & Robertson, P.K. (2003) *An overview of soil heterogeneity: quantification and implications on geotechnical field problems*. Can. Geotech. Journal, 40, (1-15).

ENV 1990. (2001) Eurocode – Basis of structural design. CEN, Brussels.

ENV 1992-1 (2002). *Eurocode 2: Design of concrete structures – Part 1: General rules for buildings*. CEN, Brussels.

EPRI – Electric Power Research Institute (1992). *Uplift Pressures, Shear Strengths, and Tensile Strengths for Stability Analysis of Concrete Gravity Dams. Volume 1. Final Report*. Stone and Webster Engineering Corporation, Denver, Colorado, USA. Report EPRI TR-100345

FEMA (2007) *Federal Guidelines for Dam Safety*
<http://www.fema.gov/hazard/damfailure/why.shtm> (2007-01-02)

FERC (2002) *Engineering Guidelines for the Evaluation of Hydropower Projects, Chapter III Gravity dams*. <http://www.ferc.gov/industries/hydropower/safety/guidelines/eng-guide.asp#skipnavsub>

Flödeskommittén (1990) *Riktlinjer för bestämning av dimensionerande flöden för dammanläggningar*. Slutrapport från Flödeskommittén. Statens Vattenfallsverk, Svenska Kraftverksföreningen & Sveriges Meteorologiska och Hydrologiska Institut. In Swedish.

Follin, S (1992). *Numerical calculations on heterogeneity of groundwater flow*. Doctoral thesis. Department of Land and Water Resources, Royal Institute of Technology, Sweden. TRITA-KUT 92:1066.

Follin, S. (2006). Personal communication.

Foster, J.L. (1989a) *Uplift under concrete dams on rocks*. Water Power, pp.322-331.

Foster, J.L. (1989b). *Uplift criteria for existing concrete gravity dams, past present and future*. Proceedings of the American Power Conference, pp. 766-771.

Fredriksson, M & Persson, J. (2005) *Modellering av extrema istryck - studie av Pajala och Frösön*. Master thesis. Avd för Konstruktionsteknik och Teknisk Vattenresurslära. Lunds Tekniska Högskola, Lund, Sweden. TVBK-5131. In Swedish.

Grenoble, B.A., Harris, C.W., Meisenheimer, J.K. and Morris, D.I.(1995) *Influence of rock joint deformations on uplift pressure in concrete gravity dam foundations: Field measurements and interpretation*. Fractured and Jointed Rock Masses, Myer, Cook, Goodman & Tsang (eds). 1995 Balkema, Rotterdam. ISBN 90 5410 591 7.

Griffiths, D.V. & Fenton, G.A. (1993) *Seepage beneath water retaining structures founded on spatially random soil*. Géotechnique 43, No. 4, 577-587.

Guidicini, G. & Andrade, R.M. (1988) *Seasonal uplift pressure in hydraulic structure foundation due to environmental thermal variations*. Rock Mechanics and Power Plants, Balkema, Rotterdam, ISBN 90 6191 8278, pp 467-471

Hakami, E. (1995) *Aperture distribution of rock joints*. PhD Thesis, Kungliga Tekniska högskolan, Stockholm, Sweden. ISBN 91-7170-835-9.

-
- Hansson, S.O. (2002). *Philosophical Perspectives on Risk*. Speech at conference Research in ethics and engineering, Delft university. www.infra.kth.se/~soh
- Hartford, D.N.D. & Baecher, G. B. (2004) *Risk and uncertainty in dam safety*. Tomas Telford Limited, Great Britain. ISBN: 0 7277 3270 6.
- Hartford, D.N.D. (2006) *On the harmonisation of qualitative and quantitative risk assessment arguments in safety decisions pertaining to earthfill dams*. Proceedings from ICOLD Congress, Barcelona, June 2006.
- Hasofer, A.M. & Lind, N.C (1973) *An exact and invariant first-order reliability format*. Solid mechanics division, University of Waterloo, Waterloo; Ontario, Canada. Paper No. 19, May 1973.
- Hornik (2006) *The R FAQ*. ISBN 3-900051-08-9. <http://CRAN.R-project.org/doc/FAQ/R-FAQ.html>
- HSE (2001) *Reducing risks, protecting people*. Health & Safety Executive, United Kingdom. ISBN 0 7176 2151 0.
- ICOLD (1987) Bulletin 59: Dam Safety guidelines.
- ICOLD Bulletin 82. (1992) *Selection of design flood*.
- ICOLD (1993) Bulletin 88: *Rock foundations for dams*. International Commission on large dams, Paris.
- ICOLD (1995) Bulletin 99: *Dam failures – statistical analysis*. International Commission on large dams, Paris.
- ICOLD bulletin 105 (1996). *Dams and related structures in cold climate*. Design guidelines and case studies.
- ICOLD (1997) Bulletin 109: *Dams less than thirty meters high*. International Commission on large dams, Paris.
- ICOLD (1998) Bulletin 111: *Dam-break flood analysis*. International Commission on large dams, Paris.
- ICOLD (2005) Bulletin 130: Risk Assessment in Dam Safety Management.
- IEC:1995 (1995) International standard 300-3-9. Part 3: application guide - Section 9: Risk analysis of technological systems. CEI 1995.
- IRGC (2006) *White paper on risk governance*. International risk governance council, Geneva. Printed Sept 2005, reprinted Jan 2006.
- Jackson, D.C. (2003) *It is a crime to design a dam without considering upward pressure: Engineers and uplift, 1890-1930*. In Darcy and Hydraulics, pp 220-232.
- JCSS (2001) *Probabilistic model code*. <http://www.jcss.ethz.ch/>

- Jeppsson, J. (2003) *Reliability –based assessment procedures for existing concrete structures*. Doctoral Thesis. Lund University, Division of Structural Engineering. Report TVBK-1026, Lund, Sweden.
- Johansson, F. (2005). *Stability analyses of large structures founded on rock – an introductory study*. Licentiate Thesis in Soil and Rock Mechanics. Stockholm, Sweden. ISSN 1650-951X.
- Kemikontoret (2001) *Riskhantering 3 – Tekniska riskanalyismetoder*. Kemikontoret, Stockholm. In Swedish.
- Kolluru R (1996): *Risk Assessment and Management Handbook*. McGraw-Hill Inc. New York.
- Ljungqvist, K. (2005) *A probabilistic approach to risk analysis. A comparison between undesirable indoor events and human sensitivity*. Doctoral thesis, Luleå University of Technology, Sweden. ISSN: 1402-1544.
- Melchers R.E. (2001) *Structural Reliability Analysis and Prediction*. Second Edition. John Wiley & Sons. ISBN 0-471-98771-9.
- Mill, O. (2001). *Dammsäkerhet i Sverige*. PM 2002-02-01. In Swedish.
- NKB 1995:02E (1995) *Basis of design of structures. Calibration of partial factors*. Nordic committee on Building Regulations. Monila Oy, Helsinki 1996. ISBN 951-53-0617-5.
- NKB 55E (1987) *Guidelines for loading and safety regulations for structural design*. Nordiska kommittén för byggbestämmelser. ISSN 0359-9981.
- Olsson, R. & Barton, N. (2001) *An improved model for hydromechanical coupling during shearing of rock joints*. International Journal of Rock Mechanics & Mining Science. 38, p 317-329.
- Olsson, R. (1998) *Mechanical and hydromechanical behaviour of hard rock joints*. Ph.D. thesis. Göteborg, Chalmers university of technology, Sweden. ISBN: 91-7107-748-1.
- Ottosen, N. & Petersson, H. (1992) *Introduction to the Finite Element Method*. Prentice Hall, Redwood Books, Trowbridge, Wiltshire, Great Britain. ISBN 0-13-473877-2.
- Ramsberg, J. (2000) *Comments on Bohnenblust and Slovic, and Vrijling, van Hengel and Houben*. Reliability engineering and system safety 67, p 205-209.
- RCP Consult (1997). STRUREL, *A Structural Reliability Analysis Program System*, COMREL & SYSREL Users Manual. RCP GmbH Barer Strasse 50, 80799 München, Germany.
- Reinius, E. (1962/1982) *Vattenbyggnad del 3 – Dambyggnader*. In Swedish.

RIDAS (1997, 2002) *Kraftföretagens riktlinjer för dammsäkerhet (Swedish Hydropower companies guidelines for dam safety)*. Svensk Energi. In Swedish.

RIDAS TA (2003, 2006). *Kraftföretagens riktlinjer för dammsäkerhet, tillämpningshänvisningar (Swedish Hydropower companies guidelines for dam safety, application guideline)*. Svensk Energi. In Swedish.

Ruggeri et al (2004) *Sliding stability of existing gravity dams – Final report*. ICOLD European Club. <http://cnpgeb.inag.pt/IcoldClub/index.htm> under working groups.

Ruggeri, G & European Working group (2001). *Uplift Pressures under Concrete Dams – Final report*. In *procs. From ICOLD European Symposium in Geiranger, 2001*. <http://cnpgeb.inag.pt/IcoldClub/index.htm> under working groups

Räddningsverket (1997) *Värdering av risk*. Statens räddningsverk, Karlstad, Risk- och miljöavdelningen, ISBN 91-88890-82-1.

Schabenberger, O. & Pierce, F.J. (2002) *Contemporary statistical data for the plant and soil sciences*. CRC Press LLC. ISBN 1-58488-111-9.

Schlather, M.(2001) *Simulation of stationary and isotropic random fields*. *_R-News_* *1*(2), 18-20.

Schneider, J. 1997) *Introduction to Safety and Reliability of Structures*. IABSE document, www.iabse.ethz.ch.

Singhal, B.B.S. & Gupta, R.P. (1999) *Applied Hydrogeology of Fractured Rocks*. Kluwer Academic Publishers, Netherlands. ISBN: 0-412-75830-X.

SS-EN 1050:1996. (1996) *Maskinsäkerhet – Principer för riskbedömning*. <http://www.sp.se/Electronics/RnD/projects/MaskinStandard/Standards/1050.htm>. In Swedish.

Stelle, W.W., Rubin, D.I. Buhac, J.H., Anderson, P.H. (1983). *New Role of Drainage Systems in Dam Stability*. *Journal of Energy Engineering* 3, (109), 181-191.

Stille, H., Andersson, J. & Olsson, L. (2003). *Information based design in rock engineering*. SveBeFo Rapport 61. ISSN 1104-1773.

Taylor, D.W. (1948) *Fundamentals of soil mechanics*. John Wiley & Sons, USA.

The MathWorks, Inc. *Matlab 7.3.0*. www.mathworks.com

Thelandersson, S. (2004). *Assessment of material property data for structural analysis of nuclear containments*. Report TVBK-3051, Division of Structural Engineering, Lund University, Sweden.

Thoft-Christensen P and Baker M J. (1982). *Structural Reliability and Theory and its Applications*. Springer-Verlag. Berlin, Heidelberg, New York.

- Thomas, H.H. (1976) *The engineering of large dams*. John Wiley & Sons, Great Britan. ISBN: 0-471-01528-8.
- U.S. Army Corps of Engineers (2003) *Gravity dam design – Engineering guideline*.
- U.S.Army Corps of Engineers (1994) *Engineering and design. Rock foundations*. EN 110-1-2908.
- Vanmarcke, E. H. (1977) *Probabilistic modelling of soil profiles*. Journal of Geotechnical Engineering Division, ASCE, 103, vol GT11.
- Vatn (1998) *A discussion of the acceptable risk problem*. Reliability Engineering and System Safety 61, p 11-19.
- Vattenfall AB (2006) *Handbok Dammsäkerhet*. Internal instruction. In Swedish.
- Vattenfall AB (2000). *Risk analysis Ajaure*. Internal report.
- Wiberg, U. , Engström, Å. & Eriksson, H. (2001) *Betongdammar: Kursmaterial i Dammar och dammsäkerhet vid KTH*, Stockholm. Kraftverksföreningen. In Swedish.
- Vrijling, J.K, van Hengel, W. & Houben, R.J.(1998) *Acceptable risk as a basis for design*. Reliability Engineering and System Safety (59) 141-150.
- Vrijling, J.K, van Hengel, W. & Houben, R.J. (2000) *Response to comments by J. Ramsberg on the paper Acceptable risk as a basis for design*. Reliability Engineering and System Safety. (67) 211-212.
- Vrouwenvelder, T., Lovegrove, R., Holicky, M., Tanner, P. & Canisius, G. (2001) *Risk assessment and risk communication in civil engineering*. Safety, Risk, reliability - trends in engineering. Malta 2001.
- Yang, J. *Ajaure Kraftsatation – modellförsök för bestämning av avbördningsförmåga*. Rapport US 98:29, 1998-12-20. Företagsintern rapport.
- Yang, J. *Ajaures utskovskanal – dimensioneringsunderlag vid dimensionerande flöde*. Rapport US 01:03, 2001-02-14. Företagsintern rapport.
- Yang, J. *Ombyggnad av Ajaures utskovskanal – dimensionering av utskovskanal & avbördning vid olika lucköppningar*. Rapport US 00:06, 2000-03-30. Företagsintern rapport.

Appendix A1

Table 1 - Parameters of Beta distributions.

		Uplift, C				Moment, C_m			
Variance	Range	r	t	a	b	r	t	a	b
0.0625	22	4,84	4,77	0,86	1,14	4,75	4,48	0,89	1,10
0.25	8	3,88	3,46	0,71	1,26	3,53	2,68	0,78	1,17
1	19	3,11	3,21	0,53	1,48	3,23	2,58	0,61	1,31
2.25	2	3,86	4,06	0,51	1,50	4,52	3,26	0,56	1,31
2.25	12	2,93	2,78	0,34	1,63	3,33	2,45	0,43	1,41
4	6	2,31	2,21	0,29	1,69	2,66	1,81	0,35	1,42
4	19	2,18	2,36	0,33	1,72	2,47	1,93	0,40	1,44
6.25	8	2,07	2,17	0,22	1,78	2,26	1,65	0,30	1,46
9	2	3,71	3,46	0,23	1,72	3,55	2,31	0,36	1,42
9	12	1,99	2,02	0,17	1,84	2,15	1,37	0,23	1,47
16	2	2,15	2,50	0,28	1,82	2,36	1,71	0,34	1,46
16	12	1,96	1,95	0,08	1,90	2,22	1,33	0,11	1,49
25	6	1,69	1,64	0,13	1,89	1,87	1,11	0,17	1,49
49	4	1,84	1,80	0,06	1,93	2,06	1,13	0,08	1,50
49	22	1,24	1,20	0,08	1,90	1,38	0,87	0,11	1,49

Appendix A2

Calculation of concrete compressive strength in Ajaure example.

In Ajaure concrete K300 was used. K300 corresponds to a mean **cube-compression** strength of $f_{cm,cube} = 39,8$ MPa, and $\sigma_{cm,cube} = 5,6$ MPa corresponding to a $Cov = 5,6/39,8 = 0,1761$ (from Carlsson et al (2006)).

To transform this value to **cylinder compressive strength** it is multiplied by 0,8.

To get the **in situ compressive strength** the cylinder compressive strength is multiplied by $\kappa = 0,85$.

κ has a coefficient of variation of 0,06

$$f_{cm,cylinder,is} = 0,80,85 \cdot 39,8 = 27,06 \text{ MPa}$$

The coefficient of variation is

$$COV_{fm,is} = \sqrt{0,1761^2 + 0,06^2} = 0,186$$

According to Carlsson et al (2006) the in situ compressive strength can be described as a log-normal distributed variable with parameters from the mean value and coefficient of variation.

The **in situ compressive strength with ageing included** is given from

$$\beta_{cc}(t) = \exp\left[s\left(1 - \frac{28}{t}\right)^{1/2}\right] = \exp\left[0,25 \cdot \left(1 - \frac{20}{(2004 - 1997)365}\right)^{1/2}\right] = 1,269$$

for $s = 0,25$ (normal and slow hardening concrete. This is not confirmed, but the most likely case).

gives $f_{cm}(t) = f_{cm,cyl} \cdot 1,269 = 34,3$.

$$COV_{\beta_{cc}} = \frac{0,3(\beta_{cc} - 1)}{\beta_{cc}} = \frac{0,3(1,269 - 1)}{1,269} = 0,0636$$